

**Histone methylation-mediated control  
for systemic priming and resistance  
in *Arabidopsis***

Inaugural-Dissertation

zur  
Erlangung des Doktorgrades  
der Mathematisch-Naturwissenschaftlichen Fakultät  
der Universität zu Köln

vorgelegt von  
**Eva-Maria Reimer-Michalski**  
aus Düren

**Köln 2015**



Die vorliegende Arbeit wurde am Max-Planck-Institut für Pflanzenzüchtungsforschung in Köln in der Abteilung für Pflanze-Mikroben Interaktionen (Direktor: Prof. Dr. Paul Schulze-Lefert) angefertigt.



MAX-PLANCK-GESELLSCHAFT



Max Planck Institute for  
Plant Breeding Research

Berichterstatter:

Prof. Dr. Paul Schulze-Lefert  
Prof. Dr. Ulf-Ingo Flüge  
Dr. Daniel Schubert

Prüfungsvorsitzende:

Prof. Dr. Ute Höcker

Tag der mündlichen Prüfung:

16.10.2014



## Publications

Saijo, Y. and Reimer-Michalski, E.-M. (2013): Epigenetic control of plant immunity.

In *Epigenetic Memory and Control in Plants*. Grafi Gideon and Ohad Nir (Eds).

Heidelberg, Springer (Signaling and Communication in Plants Vol. 18) pp 57-76.



# Table of Content

<b>Publications</b> .....	<b>V</b>
<b>Table of Content</b> .....	<b>VII</b>
<b>Abstract</b> .....	<b>XI</b>
<b>Zusammenfassung</b> .....	<b>XIII</b>
<b>1 Introduction</b> .....	<b>1</b>
1.1 The plant immune system.....	1
1.1.1 MAMP- and Effector-triggered immunity.....	2
1.1.2 Hormonal modulation of plant immunity.....	4
1.1.3 Systemic acquired resistance (SAR).....	5
1.1.4 Integration of immune signaling to the nucleus.....	9
1.2 Epigenetic control of the plant immune response.....	10
1.2.1 Chromatin remodeling and DNA methylation in plant immunity .....	11
1.2.2 Histone modifications correlated with a transcriptional control of gene expression .....	12
1.2.2.1 Histone modifications in plant immunity .....	16
1.3 Defense priming and underlying mechanisms in the plant immune response.....	17
1.4 Thesis aims .....	21
<b>2 Results</b> .....	<b>23</b>
2.1 Local Priming .....	23
2.1.1 Described histone marks on defense-related gene loci .....	23
2.1.2 Identification of local memory response candidate genes.....	24
2.1.3 Local memory response in trxG and PcG mutants .....	26
2.2 Systemic immunity .....	28
2.2.1 ETI- and MTI-induced transcriptional reprogramming and systemic priming .....	28
2.2.2 Duration of the systemic priming response .....	32
2.3 Identification of genes involved in the MTI- and ETI-induced systemic transcriptional reprogramming and priming response.....	34
2.3.1 RNA-Seq reveals qualitative and quantitative differences in the gene expression of MTI and ETI during SAR and the systemic priming response .....	34
2.3.2 The Top100 differentially expressed genes between MTI and ETI during SAR and the systemic priming response could be grouped into 12 clusters .....	37
2.3.3 Selected gene cluster provide new priming marker genes .....	40
2.3.4 Meta-expression analysis of SA-impact on systemic immunity.....	42
2.4 Elucidating the role for PcG- and trxG proteins in the systemic priming response .....	44

2.4.1	ATX1 and CLF are indispensable for the difference of the MTI- and ETI-induced systemic priming response .....	45
2.4.2	ATX1 and CLF exhibit a wild type-like local immune activation.....	47
2.4.3	Total levels of H3K4me3 and H3K27me3 do not significantly differ in systemic tissue upon local MTI or ETI activation .....	49
2.4.4	H3K4me3 and H3K27me3 are enriched on <i>PR1</i> upon ETI-induced systemic priming .....	51
<b>3</b>	<b>Discussion .....</b>	<b>55</b>
3.1	Identification and mechanisms of a local priming response .....	55
3.1.1	Several genes associated with defense execution carry H3K27me3 and H3K4me3 at high proportions .....	55
3.1.2	Selected local memory target genes are enriched with H3K27me3 prior to a transcriptional priming response .....	56
3.1.3	The local memory response requires functional PcG and trxG complexes .....	57
3.2	MTI and ETI induce divergent systemic priming responses .....	57
3.2.1	The systemic priming response exhibits a somatic memory .....	59
3.3	The systemic priming response represents a distinct phase of plant immunity.....	60
3.3.1	The Top100 significant differentially expressed genes are grouped into 12 clusters based on their expression patterns, providing MTI- and ETI-specific SAR and priming target genes .....	62
3.3.2	The SA-dependent systemic immune activation and priming response can be circumvented by ETI in a NPR1-dependent manner .....	65
3.4	The establishment and differentiation of an MTI- and ETI-induced systemic priming response is dependent on the presence of ATX1 and CLF in systemic tissue .....	68
3.4.1	H3K4me3 and H3K27me3 enrichment on <i>PR1</i> is specific for ETI-induced systemic priming .....	71
3.5	Conclusions and working model.....	75
<b>4</b>	<b>Materials and Methods .....</b>	<b>79</b>
4.1	Materials .....	79
4.1.1	Plant Material .....	79
4.1.2	Plant Pathogens .....	80
4.1.2.1	<i>Pseudomonas syringae (Pst)</i> .....	80
4.1.2.2	<i>Hyaloperonospora arabidopsidis (Hpa)</i> .....	80
4.1.3	Oligonucleotides .....	80
4.1.4	Chemicals.....	81
4.1.4.1	Antibiotics .....	81
4.1.4.2	Elicitor .....	81
4.1.4.3	Antibodies.....	82
4.1.5	Media, Buffers and Solutions.....	82
4.1.5.1	Media .....	82
4.1.5.2	Buffers and solutions .....	83
4.2	Methods .....	83

4.2.1	Cultivation of <i>Arabidopsis</i> plants .....	83
4.2.2	Maintenance of <i>Hyaloperonospora arabidopsidis</i> ( <i>Hpa</i> ) Noco2 .....	83
4.2.3	Elicitor-induced gene expression .....	83
4.2.4	MAMP-induced anthocyanin accumulation .....	84
4.2.5	Local memory response assay .....	84
4.2.6	Pathogen infection assays .....	84
4.2.6.1	Bacterial growth assay - <i>Pst</i> .....	84
4.2.6.2	Systemic assays .....	85
4.2.6.2.1	<i>Hpa</i> .....	85
4.2.6.2.2	<i>Psm</i> .....	85
4.2.6.3	Memory response assay in systemic leaves (Systemic priming) .....	85
4.2.6.4	Memory response assay in newly emerged leaves .....	86
4.2.7	Ion leakage measurement .....	86
4.2.8	Molecular biological methods .....	86
4.2.8.1	RNA extraction using TRI reagent .....	86
4.2.8.2	cDNA synthesis .....	86
4.2.8.3	Quantitative real-time PCR (qRT-PCR) .....	86
4.2.8.4	RNA-Seq .....	87
4.2.9	Biochemical methods .....	89
4.2.9.1	MAPK – protein lysis .....	89
4.2.9.2	SDS-PAGE for MAPK detection and total level of histone modifications .....	90
4.2.9.3	Western Blot .....	91
4.2.9.4	Chromatin Immunoprecipitation (ChIP) .....	92
4.2.9.4.1	qPCR of ChIP DNA samples .....	93
4.2.10	Statistics .....	94
<b>5</b>	<b>Supplementary information .....</b>	<b>95</b>
<b>6</b>	<b>Literature .....</b>	<b>117</b>
	<b>Abbreviations .....</b>	<b>139</b>
	<b>Danksagung .....</b>	<b>145</b>
	<b>Erklärung .....</b>	<b>147</b>



## Abstract

Plant immunity relies on two immune pathways: Recognition of so-called microbial-associated molecular patterns (MAMPs) and pathogen-derived effectors leads to MAMP-triggered immunity (MTI) and effector-triggered immunity (ETI), respectively. MTI and ETI both activate the release of systemic signals from the local challenged sites, and thereby enhance immunity in distal unchallenged cells, termed systemic acquired resistance (SAR). MTI and ETI activation entails extensive transcriptional reprogramming of a large set of defense-related genes in an appropriate timing and amplitude in local and systemic tissue. Following this, defense priming is conditioned via a process that appears to be under epigenetic control, where target defense-related genes are poised for a greater and/or faster activation upon second stimulation at lower fitness costs for the plant.

The results presented in this thesis indicate that systemic priming is greater in amplitude after ETI than after MTI. In correlation with previous studies, it was shown that the priming response further exhibits a somatic memory that is transferrable to newly emerged leaves. A RNA-Seq analysis of MTI-, ETI- and non-primed systemic leaves provides an inventory of SAR and systemic priming target genes, which can be classified into 12 clusters based on their expression patterns. Of note, MTI and ETI seem to influence partially different gene sets during systemic immunity. The MTI-ETI differences in the target genes become more prominent in the systemic priming response, which thus seems to represent a distinct phase of plant immunity. Salicylic acid (SA) as a central signaling component of SAR is inalienable, in both local and systemic leaves, for the establishment of SAR and mutants exhibiting a SAR-deficient phenotype are often defective in SA signaling. In this respect, this study could indicate that SA-dependence of systemic immune activation and priming response can be circumvented after ETI, but not after MTI. Interestingly, the transcriptional co-activator NPR1 as key-player of SA and SAR signaling seems to be indispensable for MTI- and ETI-induced systemic immunity and priming response. Additionally, I provide genetic evidence that a subset of the *Arabidopsis* histone modifiers, ATX1 and CLF, that act as part of the trithorax group (trxG) and Polycomb group (PcG) protein complexes, respectively, contribute to the systemic priming response and systemic pathogen resistance. ATX1 and CLF are associated with trimethylation of lysine 4 or 27 of histone H3 (H3K4me3, H3K27me3), respectively. Interestingly, they are dispensable for local defense activation, pointing to a role for H3K4me3 and H3K27me3 in systemic immunity and priming. The greater systemic immunity and priming response upon ETI is associated with an increase in H3K4me3 and H3K27me3 levels compared to MTI, at least on the locus for *PR1*, a SAR and priming target gene. In correlation with previous studies, it can be assumed that H3K4me3 serves as epigenetic memory for the ETI-specific priming response, whereas H3K27me3 is required for the full development of the associated priming response. On the other hand, MTI-induced systemic priming seems to be SA-dependent and is not correlated

with significant H3K4me3 and H3K27me3 enrichment on *PR1* associated with a lower gene expression and immunity level of MTI signaling compared to ETI.

In sum, the data presented in this work uncover novel mechanisms and differences in the regulation of systemic immunity and priming response, which involve specific histone modifications such as H3K4me3 and H3K27me3 and their corresponding histone methyltransferases ATX1 and CLF.

## Zusammenfassung

Die pflanzliche Immunabwehr beruht auf zwei Signalwegen: Zum Einen führt die Erkennung von pathogen-spezifischen hochkonservierten Molekülen („Microbial-associated molecular patterns“ – MAMPs) zur Aktivierung einer basalen Immunantwort („MAMP-triggered immunity – MTI) und zum Anderen löst die intrazelluläre indirekte oder direkte Erkennung von so genannten Effektoren, welche vom Pathogen in die Zelle eingebracht werden, eine zweiten Welle der Immunaktivierung aus („Effector-triggered immunity“ – ETI). Für beide Signalwege wurde gezeigt, dass diese nach Aktivierung einer lokaler Immunantwort die Freisetzung von Botenstoffen auslösen, welche zu einer erhöhten systemischen Immunität der Pflanze führen („systemic acquired resistance“ - SAR). Die Aktivierung von MTI und ETI geht einher mit einer umfassenden Veränderung der Genexpression in lokalem und systemischem Gewebe in einem zeitlichen und quantitativ kontrollierten Rahmen. Dabei ermöglicht ein Gen-Markierungsprozess, genannt „Priming“, eine schnellere und/oder stärkere Expression selektierter Gene um effektiv und zielgerichtet auf einen zweiten Stress-assoziierten Stimulus reagieren zu können, ohne die Kosten einer konstitutiv aktiven Immunabwehr. Dies ist unter anderem mit spezifischen Histonmodifikationen assoziiert, welche der Pflanze als ein transkriptionelles Gedächtnis dienen können.

Die Resultate der vorliegenden Arbeit deuten auf eine umfassende systemische Priming-Antwort, welche nach lokaler ETI Aktivierung höher ausfällt als nach lokaler MTI Aktivierung, als auch auf die Bedeutung von Histonmodifikationen in diesem Prozess hin. Es ist zudem möglich, die Priming-Antwort in neu entwickelten Blättern nachzuweisen, was ein somatisches Gedächtnis der Pflanze impliziert. Eine genomweite Transkriptionsanalyse in systemischen Blättern ermöglichte eine Unterteilung von SAR und/oder Priming-assoziierten Genen in Abhängigkeit der jeweiligen lokal induzierten Immunantwort. Interessanterweise beeinflusst die lokale MTI und ETI Aktivierung ein teilweise unterschiedliches Set an Genen während der systemischen Immunaktivierung. Dieser MTI-ETI spezifische Unterschied wird während der Priming-Antwort noch verstärkt, was auf die Abspaltung der Priming-assoziierten Immunaktivierung, neben der lokalen und systemischen, hindeutet. Frühere Arbeiten haben gezeigt, dass Salicylsäure (SA) als zentrales Signalmolekül unabdingbar ist für die Etablierung von SAR, sowohl in lokalem und als auch in systemischem Gewebe. Damit einhergehend korrelieren viele SAR-defiziente Phänotypen mit einem Defekt im SA Signalweg. Darauf Bezug nehmend konnte in dieser Arbeit Hinweise gewonnen werden, dass die SA Abhängigkeit der systemischen Immunaktivierung und Priming-Antwort nach lokaler ETI Aktivierung, aber nicht nach MTI Aktivierung, umgangen werden kann. Interessanterweise wird in beiden Fällen der zentrale Regulator SA-induzierter Immunantwort, NPR1, benötigt, welcher als transkriptioneller Co-Aktivatoren eine Schlüsselfigur während der Aktivierung von SAR und der Priming-Antwort einnimmt.

Die Histonmodifikationen der Trimethylierung von Lysine 4 oder 27 von Histone H3 (H3K4me3, H3K27me3) sind assoziiert mit den Histonmethyltransferasen, ATX1 und CLF, welche jeweils die katalytische Domäne der Trithorax- und Polycomb-Proteinkomplexe in *Arabidopsis* beinhalten. Anhand einer genetischen Fallanalyse konnte in dieser Arbeit gezeigt werden, dass CLF und ATX1 zur systemischen Immunaktivierung und Priming-Antwort beitragen. Hierbei ist anzumerken, dass ATX1 und CLF hauptsächlich im systemischen Gewebe benötigt werden, was auf die Bedeutung von H3K4me3 und H3K27me3 für die systemische Resistenz und Priming-Antwort hinweist. Die massive systemische Immunität und Priming-Antwort nach lokaler ETI Aktivierung geht einher mit einer für *PR1*, einem Markergen für SAR und Priming, erhöhten H3K4me3 und H3K27me3 Anreicherung. Dies führt in Korrelation mit früheren Arbeiten zu der Annahme, dass H3K4me3 als transkriptionelles Gedächtnis für die ETI-spezifische Priming-Antwort dient, während H3K27me3 für die volle systemische Immunität benötigt wird. Im Gegensatz dazu ist die MTI-induzierte Priming-Antwort nicht mit einem signifikant erhöhtem H3K4me3 und H3K27me3 Level assoziiert, was in Zusammenhang gebracht werden kann mit der schwächeren systemischen Genexpression und Immunität im Vergleich zu ETI.

Die Daten dieser Arbeit zeigen neue Mechanismen und Unterschiede in der Regulation der systemischen Immunität und Priming-Antwort auf, welche spezifische Histonmodifikationen und deren korrespondierenden Histonmethyltransferasen einschließt.

## 1 Introduction

Plants as sessile organisms are not able to escape by moving away from unfavorable abiotic stresses such as cold or water shortage, as well as biotic stresses including a wide range of harmful pathogens and pests, such as viruses, bacteria, fungi, oomycetes, nematodes and insect herbivores. Each of them is capable in exploiting of highly specific strategies to establish a close relationship with its host to promote their own growth and virulence. Plants, unlike animals, lack an adaptive immune system, which closely works together with the innate immune system and is characterized by specialized cell types like circulating B- and T-cells (Spoel and Dong 2012). Therefore, plants have evolved a broad range of defense mechanisms, which all are intended to prevent pathogen infection to avoid a disease outbreak. Those plant pathogens can cause devastating epidemics that affected the human civilization, for example the late blight Irish late potato famine of the 1840s caused by *Phytophthora infestans*. Plant diseases have great impact on the yield and quality of agricultural products with an estimated preharvesting loss of 15 % of the global crop production, resulting in large-scale economic, social and political implications (Strange and Scott 2005; Dangl et al. 2013). The full understanding of the plant immune system is therefore a prerequisite for effective and long lasting crop protection of the final goal to feed more humans from less agricultural available land.

### 1.1 The plant immune system

Plants, as well as animals, are surrounded and inhabited by numerous microbes of which some are commensally or symbiotic partners of the plant. Despite these beneficial microbes, several others enter the plant via natural openings like stomata, hydathodes or wounding or even penetrate and invade plant cells via specialized structures to feed from the nutrition-rich host. Depending on their lifestyle, plant pathogens can be divided in three classes: a) necrotrophs destroy the plant cell and feed on the released nutrients, b) biotrophs derive their nutrients from the living cell often using specialized structures like haustoria, and c) hemibiotrophs, which first rely on the living cell and during the course of infection kill the exhausted cell (Glazebrook 2005; Jones and Dangl 2006). Despite this, various non-adapted pathogens are not able to overcome the plants' defense responses resulting in non-host resistance (Thordal-Christensen 2003). Those phytopathogenic organisms that aim to infect a plant, first encounter an array of preformed barriers such as the cuticula or cell wall (Malinovskiy et al. 2014). But several pathogens succeed in breaking through this pre-invasive layer of defense, so that the plant needs to rely on the ability to distinguish self from non-self for the initiation of defense outputs. However, plants are able to selectively activate defense responses according to the pathogen

encountered. To this end, plants have evolved a multilayered cell-autonomous immune system relying on different classes of immune receptors that trigger an extraordinary set of defense mechanisms.

### 1.1.1 MAMP- and Effector-triggered immunity

The first layer of active plant defense is mediated at the plasma membrane by so-called pattern recognition receptors (PRRs), which are able to recognize evolutionary conserved microbial structures termed microbial-associated molecular patterns (MAMPs). MAMPs include components of the fungal cell wall such as chitin or bacterial lipopolysaccharides (LPS), peptidoglycans (PGN), elongation factor Tu (EF-Tu) or a subunit of flagellin (flg) (Felix et al. 1999; Zipfel et al. 2006; Segonzac and Zipfel 2011). MAMP perception is mediated by binding to their cognate receptor, such as the bioactive epitope flg22 of flagellin by the Leucine-rich repeat receptor-like protein kinase (LRR-RLK) FLAGELLIN SENSING 2 (FLS2) or elf18, the N-terminus of EF-Tu to EFR-TU RECEPTOR (EFR). Binding of these molecules to their receptors leads to the induction of MAMP-triggered immune responses (MTI), which aim to restrict or terminate the growth of pathogenic microbes (Felix et al. 1999; Kunze et al. 2004). MTI elicitation goes along with ion fluxes over the membrane ( $\text{Ca}^{2+}$ -spiking), production of reactive oxygen species (ROS), the activation of mitogen-activated protein kinases (MAPKs) and calcium-dependent protein kinases (CDPKs). These early (0-15 min) immune outputs are followed by later outputs (hours to days) such as hormone biosynthesis and signaling, as well as callose deposition, metabolic changes, production of antimicrobial compounds and extensive transcriptional reprogramming (Muthamilarasan and Prasad 2013; Macho and Zipfel 2014; Romeis and Herde 2014). The importance of MTI is demonstrated by the loss of FLS2 or EFR, which significantly reduces the basal immunity to infection of bacterial pathogens (Zipfel et al. 2004; Zipfel et al. 2006; Saijo et al. 2009). Recent studies suggest the requirement for a sustained signaling in effective MTI activation. An endoplasmatic-reticulum (ER) resident glucosidase II $\alpha$  mutant allele, *rsw3*, fails to develop a sustained transcriptional reprogramming upon elf18 treatment despite its wild type-like early immune activation (Lu et al. 2009).

It was postulated, that recognition of danger-associated molecular patterns (DAMPs), going along with changes in the cellular homeostasis, serves as amplification system for MTI. This is in accordance with the gene induction of the peptide precursor proteins PROPEP2 and PROPEP3 upon MAMP treatment, implementing a model of the cytoplasmic localized peptides being released into the apoplast by e.g. membrane disruption upon pathogen attack, where they could bind to their cognate plasma membrane localized receptors PEPR1 and PEPR2. Recent studies further indicate that PEPR-mediated signaling is required for maximal activation of FLS2- and EFR-triggered immunity as well as in systemic immunity (Huffaker and Ryan 2007; Fontana and Vance 2011; Yamaguchi and Huffaker 2011; Logemann et al. 2013; Tintor et al. 2013; Ross et al. 2014).

In order to promote their own virulence, phytopathogens either try to escape recognition or interfere and/or suppress the induced MTI responses. Phytopathogenic bacteria secrete effector molecules into the plant cell by membrane-penetration with their needle-like type III secretion system (TTSS), which aim to interfere or suppress MTI signaling resulting in effector-triggered susceptibility (ETS) (Jones and Dangl 2006; Cunnac et al. 2009). Contrary, oomycete and fungal pathogens use a highly specialized structure termed haustorium to deliver their effector proteins into the cell, serving also as exchange surface for nutrients and signaling components (Panstruga and Dodds 2009; Huckelhoven and Panstruga 2011).

One elegant strategy to counteract the mode of effectors is the evolvement of a second class of immune receptors, so-called resistance (R) proteins that reside inside the plant cell. Plants are able to directly or indirectly recognize the structure and mode of action of cognate pathogen effectors, which can be explained by the gene-for-gene model (Flor 1971) or by the guard model, where an accessory protein assists in the recognition, respectively (Dodds and Rathjen 2010). The major class of R-proteins is represented by nucleotide-binding leucine-rich repeat (NB-LRR) proteins, which can be further classified based on the N-terminal domain, namely the Toll/Interleukin-1 Receptor (TIR) or the coiled-coil (CC) domain (Jacob et al. 2013). Effector recognition leads to a strong and enhanced immune activation termed effector-triggered immunity (ETI), which often goes along with a localized programmed cell death called hypersensitive response (HR) (Levine et al. 1994; Greenberg and Yao 2004; Coll et al. 2011). Of note, new findings suggest that successful ETI is not invariably coupled to a HR to restrict pathogenic growth (Slootweg et al. 2010; Heidrich et al. 2011).

The identification of host targets of the bacterial TTSS is a subject of intense research in the field of phytopathology as a lesson for both sides, the bacteria virulence weapons and the plants signaling components such as bacterial phosphatases that inhibit MTI signal transduction by targeting PRRs or other downstream Serine/Threonine kinases (Gohre et al. 2008; Zeng et al. 2012; Macho et al. 2014). Effector proteins have been shown to interfere with MAPK signaling, SA (salicylate) synthesis, chloroplast components, vesicle trafficking, the tubulin network, and also to mimic transcription factors to modulate the host transcriptome for their advantage (Deslandes and Rivas 2012). Although several components of ETI are known to date, the signal transduction downstream of activated NB-LRR signaling remains poorly understood.

RPM1-interacting protein 4 (RIN4) of *Arabidopsis thaliana* (*Arabidopsis*) is a plasma membrane anchored protein and a key protein of plant immunity by mechanistically linking MTI, ETS and ETI responses. RIN4 was defined as negative regulator of MTI rendering in an excellent target of in total six effector proteins (Deslandes and Rivas 2012). RIN4 resides in a complex with the R-proteins RESISTANCE TO P. MACULICULA 1 (RPM1) and RESISTANT TO P. SYRINGAE 2 (RPS2), in which RPM1

perceives the phosphorylation of RIN4 induced by AvrB and AvrRpm1 via the RIN4-interacting receptor like kinase (RIPK). RPS2 recognizes the cleavage and degradation of RIN4 by AvrRpt2 (da Cunha et al. 2007; Chung et al. 2011; Spoel and Dong 2012). This interplay of two effectors illustrates the arms race of ETS and ETI as the cleavage of RIN4 by AvrRpt2 avoids RPM1-mediated recognition of RIN4 phosphorylation. These specific examples provide an insight in the mechanistic basis of effectors to modulate the plant immune system for their purpose.

MTI and ETI trigger a ROS burst, hormonal changes and transcriptional reprogramming with high similarity upon different MAMPs and effectors (Tao et al. 2003; Zipfel et al. 2006). Of note, these target genes undergo a faster, higher and/or prolonged expression pattern during ETI than MTI, whereas the differences between MTI and ETI in terms of the amplitude and kinetics rather than in the target gene choice *per se* could suggest that the signaling events and outputs of MTI are accelerated in R-gene mediated resistance (Tao et al. 2003; Caldo et al. 2004; Navarro et al. 2004; Tsuda and Katagiri 2010). These differences in the transcriptional reprogramming might arise as a direct consequence of the nuclear action of some signaling components (see 1.1.4). Studies by Tsuda et al. demonstrated that MTI and ETI use the plant immune system signaling sectors, defined as ROS, MAPKs and the plant hormone network (see 1.1.2), differentially in a way that synergistic relationships are evident in MTI and compensatory relationships between the sectors are dominant in ETI. Indeed, ETI activation can largely compensate the loss of the SA signaling sector by prolonged MAPK activation (Tsuda et al. 2013). Generally, ETI is therefore regarded to be more robust against perturbations caused by pathogens of the network sectors, whereas MTI is rather vulnerable.

New findings also start to integrate external influences such as light and temperature in the regulation of the plant immune system. It was shown, that the plant immune response differs with changing temperature favoring MTI at elevated and ETI at lower temperatures (Cheng et al. 2013). This is in accordance with the fact, that in several R-protein gain-of-function mutants the autoimmune phenotype is suppressed at higher temperatures (Hua 2013). In addition, recent publications point to a clock-dependent defense gene expression and susceptibility towards pathogens (Wang et al. 2011; Zhang et al. 2013a; Korneli et al. 2014).

In sum, MTI and ETI are highly interconnected and work in concert to confer a strong resistance against pathogen attack, not only in the affected tissue but also in yet unchallenged parts of the plant (Shah and Zeier 2013; Shah et al. 2014).

### **1.1.2 Hormonal modulation of plant immunity**

The described signaling processes are influenced and fine-tuned by a complex network of phytohormones, which are also indispensable for developmental processes as well as in the adaptation to abiotic stresses. They allow the plant to coordinate between different stresses in local and systemic

tissues (see 1.1.3) (Pieterse et al. 2012). In plant immunity the major players are SA, jasmonate (JA) and ethylene (ET), whereas several other plant hormones like abscisic acid (ABA), auxin, gibberellins and cytokinins are also involved (Pieterse et al. 2012). Of note, SA-dependent defense responses are regarded to be effective against biotrophic and hemibiotrophic pathogens, while JA and ET have been associated with defense execution against necrotrophic pathogens (Glazebrook 2005).

SA can be synthesized from chorismate by two pathways, which include on the one hand the key-enzymes PHENYLALANINE AMMONIA LYASE (PAL) or ISOCHORISMATE SYNTHASE 1/SALICYLIC ACID INDUCTION DEFICIENT 2 (ICS1/SID2) (Chen et al. 2009). MTI and ETI activation can both induce SA production via the SID2 pathway (Robert-Seilaniantz et al. 2011). MTI and TIR-NB-LRR-mediated ETI signaling relies thereby on ENHANCED DISEASE SUSCEPTIBILITY 1 (EDS1) and its interacting partner PHYTOALEXIN DEFICIENT 4 (PAD4) and SENESCENCE ASSOCIATED GENE 101 (SAG101), whereas CC-NB-LRR ETI activation requires NON-RACE-SPECIFIC DISEASE RESISTANCE (NDR1) (Aarts et al. 1998; Falk et al. 1999; Bernoux et al. 2011; Pieterse et al. 2012).

JA is synthesized for example upon necrotrophic pathogen attack or herbivory feeding via the oxylipin biosynthesis pathway using unsaturated membrane-derived fatty acids and its precursor 12-oxophytodienoic acid (OPDA) (Gfeller et al. 2010). Afterwards, JA can be metabolized to methyl jasmonate (MeJA) or conjugated to isoleucine resulting in the highly active JA-isoleucine (Fonseca et al. 2009). JA is also well established in having important roles in plant development like seed and flower development (Wasternack et al. 2013; Wasternack and Hause 2013).

ET as a gaseous hormone is regarded as the major constituent of the blend of defense signals that are released during the attack of various pathogenic organisms and as a modulator of plant immunity. It is acting positively and negatively on plant immunity depending on defense outputs (Broekaert et al. 2006; Merchante et al. 2013; Kim et al. 2014). For example, ET can potentiate the SA-response (Lawton et al. 1994; Clarke et al. 2000), whereas it also coordinates the defense response against necrotrophs together with JA (Leon-Reyes et al. 2009; Zhu et al. 2011).

There is a complex regulatory relationship between these hormone signaling sectors, which includes synergistic and antagonistic effects of SA, JA and ET. A well-documented relationship is the SA-JA antagonism, as SA signaling usually overrides JA action to force the plants immune activation to respond in an appropriate way to biotrophic attacks (Koornneef et al. 2008). This complex hormone-signaling network implies the ability to modulate the host immunity according to the type of pathogen encountered (Denance et al. 2013).

### **1.1.3 Systemic acquired resistance (SAR)**

Although plants possess a multilayered innate immune system, their immune response is not restricted to the local sites of pathogen attack, where a strong immune activation leads to the containment of

the pathogenic growth, but comprises a complex cell-to-cell communication network throughout the plant. This is correlated with the immunization of the rest of the plant including distal yet uninfected parts. The phenomenon was already reported in the early 1930s and later termed “systemic acquired resistance” (SAR) (Chester 1933b; Chester 1933a; Ross 1961b; Ross 1961a). This secondary immune response in the distal part of the plant, which can also be extended to the roots, is effective against a broad range of phytopathogenic organisms like viruses, fungi, oomycetes and bacteria. Furthermore, it is long lasting, even for the lifetime of a plant, and new findings suggest, that it can be transmitted to following generations (Sticher et al. 1997; Durrant and Dong 2004; Luna et al. 2012). Of note, resistance in distant tissue can also be enhanced by root-colonization of beneficial microbes and fungi, like plant-growth promoting rhizobacteria or mycorrhizal fungi (induced-systemic resistance, ISR) or after wounding by feeding insects (wound-induced resistance, WIR) (De Vos et al. 2006; van Loon et al. 2006; Pozo and Azcon-Aguilar 2007; Shores et al. 2010). WIR requires JA signaling (Sun et al. 2011), whereas ISR is commonly regulated by JA- and ET-dependent pathways and SAR triggered by e.g. bacteria is strongly associated with SA signaling (Fu and Dong 2013).

Irrespective of the nature of the trigger and the signal, effective long-distance communication is a prerequisite for effective broad spectrum immunity and early studies already suggested the need for an intact phloem, although it does not seem to be the exclusive way (Jenns and Kuc 1979; Guedes et al. 1980; Tuzun and Kuc 1985; Kiefer and Slusarenko 2003). The identification of the systemic signal(s) of SAR has challenged the scientific community for almost 60 years and is still under strong investigation. SAR-inducing compounds were isolated from phloem sap-enriched petiole exudates (Pex) of pathogen infected *Arabidopsis* leaves, which were shown to induce SAR in tomato, tobacco and wheat. Furthermore, they were proven to be protease sensitive, suggesting the involvement of proteins in the long distance signaling. The protein DEFECTIVE IN INDUCED RESISTANCE 1 (DIR1) was identified in the course of this study as being required for the accumulation and/or the systemic movement of SAR-inducing factors (Maldonado et al. 2002; Chaturvedi et al. 2008; Chaturvedi et al. 2012). Several primary and secondary plant metabolites like methyl salicylate (MeSA), abietane diterpenoid dehydroabietinal (DA), glycerol-3-phosphate (G3P), azelaic acid (AzA) and the lysine metabolite pipercolic acid (Pip) have been implemented in the signaling and enhancement of SAR (Jung et al. 2009; Chanda et al. 2011; Chaturvedi et al. 2012; Navarova et al. 2012). It seems to be rather an evolutionary advantage of the plant to feature a network of signals and use it flexibly depending on the nature of the SAR trigger and/or environmental cues such as the availability and duration of light (Griebel and Zeier 2008; Liu et al. 2011; Shah and Zeier 2013).

MTI- and ETI-activation, together with DAMP signaling, at local challenged sites triggers the release of an orchestra of systemic signals to induce an enhanced state of immunity in the distal part of the plant

(Mishina and Zeier 2007; Dempsey and Klessig 2012; Ross et al. 2014). This alarmed state of the distal part can also be induced by synthetic or unnatural compounds like acibenzolar-S-methyl (BTH) or  $\beta$ -amino butyric acid (BABA) (Katz et al. 1998; Zimmerli et al. 2000; Noutoshi et al. 2012; Gao et al. 2014). Despite the nature or the interplay of and with the regulatory components of the systemic signal(s), SA seems to play an important role in the development of SAR, although it was proven not to be the systemic signal *per se* (Vernooij et al. 1994a; Vernooij et al. 1994b), but was shown to accumulate in local infected tissue as well as in distal unchallenged parts (Mettraux et al. 1990; Fu and Dong 2013). *De novo* SA synthesis upon pathogen challenge proceeds via ICS1/SID2 and its accumulation is required in local and systemic leaves for SAR as demonstrated by the failure for SAR activation or inhibition of its biosynthesis genes and feedback-amplification loops, and on promoting its degradation (Mishina and Zeier 2006; Mishina and Zeier 2007; Attaran et al. 2009; Rietz et al. 2011; Chaturvedi et al. 2012). New findings connect the systemic SA accumulation and SAR-conferred resistance with the FLAVIN-DEPENDENT MONOOXYGENASE 1 (FMO1), which seems to be a critical regulator of SAR, functioning in an SA amplification loop downstream of Pip and upstream of SA, although the defined mode of action and the interaction with other SAR players is not fully explored to date (Mishina and Zeier 2006; Navarova et al. 2012; Shah and Zeier 2013; Shah et al. 2014).

The key-player of SA signaling and SAR is the transcriptional co-activator NON-EXPRESSER OF *PR* GENES 1/NON-INDUCIBLE IMMUNITY 1 (NPR1/NIM1), which has also been implemented in basal defense, ISR, ETI and in mediating the cross talk between JA and SA as well as other phytohormones (Pajerowska-Mukhtar et al. 2013). NPR1 resides in the cytosol in an oligomeric form, whereas rising SA concentration in the cell leads to redox changes resulting in the monomerisation of NPR1 associated with its nuclear localization (Kinkema et al. 2000; Mou et al. 2003). Numerous studies searching for “the” SA receptor converged on NPR1 and recently it was demonstrated that NPR1 is able to bind SA (Wu et al. 2012). Of note, another research group was unable to confirm SA binding by NPR1 in a non-equilibrium approach. Instead they found that the NPR1 orthologs NPR3 and NPR4 bind SA and thereby promote the SA-dependent interaction of phosphorylated NPR1 in the nucleus with the CUL3 ubiquitin ligase leading to a proteasomal degradation (Spoel and Dong 2008; Fu et al. 2012; Spoel and Dong 2012). A pathogen infection creates a SA gradient at the infection site and NPR1 contains programmed cell death (PCD) during ETI by favoring transcriptional reprogramming (Enyedi et al. 1992b; Enyedi et al. 1992a; Rate and Greenberg 2001). In the current model, the SA level is high enough in infected tissue for NPR3, with low SA binding affinity, to interact with NPR1 resulting degradation followed by PCD. In surrounding tissue, SA level is not high enough to promote NPR3-NPR1 interaction but at a level to disrupt NPR1-NPR4 interaction, with NPR4 having a high SA binding affinity. This results in the

accumulation of NPR1 promoting cell survival and resistance, whereas at low SA levels NPR4 promotes the NPR1 degradation (Fu et al. 2012).

NPR1 targets genes downstream of SA or SA-independent signals, such as the classical SAR (and SA) marker gene *PATHOGENESIS-RELATED 1 (PR1)* and other antimicrobial PR proteins, as well as genes involved in protein folding and secretion (Sticher et al. 1997; Wang et al. 2005; van Loon et al. 2006). A nuclear pool of NPR1 works cooperatively with the transcription factors TGA2, TGA5 and TGA6. TGA2 is regarded as transcriptional repressor, whereas TGA5 and 6 work as positive regulators (Jakoby et al. 2002; Zhang et al. 2003b; Kesarwani et al. 2007; Shearer et al. 2012). NPR1 is further recruited to target gene promoters by an unknown mechanism leading to the assembly of the RNA Pol II initiation complex and subsequent activation of transcription (Mukhtar et al. 2009). This NPR1 pool might then be phosphorylated by a kinase attached to RNA Pol II required for the CUL3-based E3 ligase protein complex degradation. Degradation of NPR1 following target gene activation allows fresh NPR1 to initiate the next round of transcription (Mukhtar et al. 2009; Spoel et al. 2009; Fu and Dong 2013). In addition to TGA transcription factors, NIM1-INTERACTING 1 (NIMIN-1), NIMIN-2 and NIMIN-3 were identified as NPR1 interactors, likely playing a negative role in NPR1-dependent gene regulation in a ternary NPR1-TGA-NIMIN complex, although the mechanisms remain unclear to date (Weigel et al. 2001; Weigel et al. 2005). Another negative regulatory protein SUPPRESSOR OF NPR1, INDUCIBLE 1 (SNI1) was identified in a genetic screen to define mutants that induce *PR1* expression in the *npr1* background. In *sni1 npr1* plants an NPR1-independent activation of *PR1* is detectable, which seems to be correlated with SA-induced DNA damage associated with facilitated gene induction as the *sni1* phenotype is suppressed in DNA damaging sensor mutants normally negatively regulated by SNI1. In the presence of NPR1, SNI1 dampens basal and induced *PR1* expression, which seems to be correlated with histone modifications (see below) (Li et al. 1999; Mosher et al. 2006; Durrant et al. 2007; Yan et al. 2013). New findings integrate also Mediator (MED), a multiprotein complex, into the transcriptional regulation during SAR and plant immunity. Mediator can work, depending on the composition of the associated proteins, as transcriptional co-repressor or -activator (Kidd et al. 2011; An and Mou 2013). MED16 was identified as an essential SAR component downstream of SA and positively regulating the NPR1 protein accumulation (Canet et al. 2012; Zhang et al. 2012). More recently, the Elongator complex subunit 2 (ELP2), an epigenetic regulator, was identified to interact genetically with NPR1 to promote pathogen-induced chromatin remodeling leading to transcriptional changes (Pajerowska-Mukhtar et al. 2013; Wang et al. 2013). The extraordinary group of WRKY transcription factors also implicates a role of gene regulation during SAR in correlation with NPR1 supported by the overrepresented number of W-boxes, the *cis*-element for WRKYs, in the promoters of SAR-related

genes, including *ICS1*, *NPR1* and *PR1* (Maleck et al. 2000; Wildermuth et al. 2001; Pandey and Somssich 2009).

#### 1.1.4 Integration of immune signaling to the nucleus

An efficient immune response of the plants against pathogenic infections relies on the ability to rapidly couple pathogen recognition to downstream signaling responses. Following this line, plant immunity requires highly dynamic outputs including several organelles and signaling events. It has been estimated, that upon pathogen infection roughly 25 % of the *Arabidopsis* genes undergo transcriptional changes, which indicates the presence of a fast and flexible but also a tight control of gene expression to avoid unnecessary immune activation (Maleck et al. 2000; Tao et al. 2003).

Protein phosphorylation provides a fast and dynamic link from the first pathogen recognition via the activation of PRRs and their co-receptors (MTI) and the intracellular recognition of specific effectors (ETI) to the gene transcription machineries in the nucleus (Tena et al. 2011). The MAPK cascade, including the well-studied MPK6 and MPK3, provides one direct link between immune activation and transcriptional outputs, favoring them as targets of several effector proteins (Fiil et al. 2009; Pitzschke et al. 2009). In mammals, it was demonstrated that MAPK activation upon different stimuli could result in direct phosphorylation of histone H3 in correlation with subsequent transcriptional reprogramming (Clayton and Mahadevan 2003). In *Arabidopsis*, it was shown that histone H3 and the histone variant H2A.Z can be phosphorylated by MPK6 and MPK3, indicating that MAPKs could provide a link between immune signaling and chromatin modulation (Asai et al. 2002; Feilner et al. 2005; Fiil et al. 2009).

Another key mechanism for signal integration into the nucleus seems to be provided by the nucleocytoplasmic shuttling of signaling components and transcription factors including effector proteins (Meier and Somers 2011; Heidrich et al. 2012). An emerging number of NB-LRR receptors require their nuclear localization for distinct outputs of their immune execution, as shown for the barley CC-NB-LRR receptor MLA1 or the *Arabidopsis* TIR-NB-LRR receptor RESISTANCE TO *P. SYRINGAE* 4 (RPS4). They are important for the resistance against the fungus *Blumeria graminis* f. sp. *hordei* or *Pseudomonas syringae* pv. *tomato* (*Pst*) carrying the avirulence gene *AvrRps4*, respectively (Garcia et al. 2010; Heidrich et al. 2011; Maekawa et al. 2012). It was shown that the barley MLA1 receptor is fully functional in partially immunocompromised *Arabidopsis* plants and that MLA1-dependent sustained transcript accumulation is associated with its nuclear localization upon pathogen trigger (Maekawa et al. 2012). The effector *AvrRps4* is recognized by RPS4, which relies on EDS1 that acts in a complex consisting of PAD4 and SAG101 (Wiermer et al. 2005). The nucleo-cytoplasmic shuttling of EDS1 together with RPS4 and *AvrRps4* is needed for distinct immunity-related outputs, the cytoplasmic cell death induction and nuclear transcriptional activation of defense genes (Bhattacharjee et al. 2011; Heidrich et al. 2011; Buscaill and Rivas 2014). RPS4 works closely together

with RESISTANT TO RALSTONIA SOLANACEARUM 1 (RRS1-R) as TIR-NBB-LRR for full resistance against *Pst* AvrRps4. RRS1-R possesses a C-terminal WRKY transcription factor DNA binding domain, implying that important RPS4/RRS1-R recognition and signaling events occur at the nuclear chromatin (Heidrich et al. 2013). RPS4 was also shown to interact with SUPPRESSOR OF *npr1-1* CONSTITUTIVE 1 (SNC1), a TIR-NB-LRR protein that binds to the co-repressor TOPLESS-RELATED 1 (TPR1), and thereby leads to immune activation by inactivation of negative immune regulators via chromatin remodeling (Bhattacharjee et al. 2011). In line with this, genetic studies revealed the requirement of the nuclear pore complex in pathogen resistance for proper nuclear accumulation of SNC1, EDS1 and NPR1 (Cheng et al. 2009). This demonstrates the functional significance of the accessibility of the nuclear compartment and the transcriptional machinery for immune regulators (Garcia and Parker 2009). In sum, the aforementioned selected examples provide evidence for the connection of signal perception and transcriptional regulation of the defense-related transcriptome, and predict the need for mechanisms that can rapidly and flexibly reprogram the expression of a bunch of gene sets at once.

### **1.2 Epigenetic control of the plant immune response**

Epigenetic changes define a set of heritable, but potentially reversible alterations in gene expression, which occur without a change in DNA sequences. These alterations can be induced spontaneously, by abiotic and biotic environmental factors or in response to the expression of other genes (Pien and Grossniklaus 2007). In eukaryotic cells nuclear DNA is associated with core histones and other chromosomal proteins to form chromatin. The smallest packaging unit of chromatin is provided by the nucleosome consisting of two copies of histone H2A, H2B, H3 and H4 wrapped by 146 base pairs (bp) of DNA. RNA and non-histone proteins are also important functional components of the chromatin (Zhang and Reinberg 2001). The accessibility of the transcriptional machinery to DNA is dependent on the nucleosome positioning and chromatin architecture. Generally it can be said, that condensed heterochromatic regions are silenced, whereas loosened euchromatic regions often carry transcribed genes (Berr et al. 2012). The structure and function of chromatin can be regulated by multiple epigenetic mechanisms including DNA methylation, ATP-dependent chromatin remodeling, placement of histone variants, noncoding RNA and histone modifications. The N-terminal tails of the core histones are subjected to various posttranslational modifications including ubiquitination, phosphorylation, glycosylation, ribosylation, sumoylation, acetylation and methylation. The histone code hypothesis predicts that these specifically placed covalent modifications might provide further specificity for reader proteins that bind those marks interpreting the code into functional outcomes. The hypothesis further suggests the presence of “writer” proteins dedicated in placing the specific mark, whereas

“eraser” proteins dynamically remove it (Kouzarides 2007b; Kouzarides 2007a; Pien and Grossniklaus 2007; Sang et al. 2009; Badeaux and Shi 2013).

The role of histone modifications, histone replacement and ATP-dependent chromatin-remodeling in the control of rapid, reversible and heritable gene expression patterns is well established in the regulation of developmental processes, such as flowering time control and organ development (Berr et al. 2011). The involvement of these mechanisms in the control of the defense-related transcriptome has only gained interest in the last six to seven years meaning to provide only a mosaic-like structure of knowledge.

### 1.2.1 Chromatin remodeling and DNA methylation in plant immunity

In *Arabidopsis*, 40 different genes have been identified to date, which are annotated to encode the components of the ATP-dependent chromatin remodeling complexes. These complexes can be divided into five subfamilies based on their ATPase subunits: a) SWI/SNF, b) ISWI, c) NURD/Mi-2/CHD, d) INO80 and e) SWR1. They commonly use the ATP hydrolysis energy to remodel the chromatin structure by moving histone octamers, weaken histone-DNA interaction or incorporation of defined histone variants (Clapier and Cairns 2009; Alvarez et al. 2010; Gentry and Hennig 2014). In unstressed *Arabidopsis* plants, it was shown that disruption of the SWR-like complex, containing PHOTOPERIOD-INDEPENDENT EARLY FLOWERING 1 (PIE1), causes upregulation of several defense-related SA-dependent genes, spontaneous cell death and enhanced resistance against *Pst* DC3000. PIE1 was shown to be required for the deposition of the non-canonical histone mark H2A.Z associated with maintenance of transcription-repressive chromatin, avoiding precocious immune activation in the absence of pathogens (Deal et al. 2007; March-Diaz et al. 2008). Depending on the context or cell-type, H2A.Z can function as transcriptional repressor or activator as shown for the *FLOWERING LOCUS C* (*FLC*), which controls the transition from vegetative growth to flowering by repressing flowering when active (Deal et al. 2007; Lazaro et al. 2008).

Genetic evidence further demonstrated an involvement of the ATP-remodeling complexes in the regulation of SA-based immunity to pathogens. Mutants of *SPLAYED* (*SYD*), *BRAHMA* (*BRM*) and *DECREASED DNA METHYLATION 1* (*DDM1*) exhibit an enhanced expression of SA-responsive genes and basal immunity to biotroph and hemibiotroph pathogens. *SYD* and *BRM* have partially overlapping function, but distinct target gene sets reflected by the fact that in pathogen challenged *syd* and in non-elicited *brm* plants a hyperactivation of SA-responsive genes, including *PR1*, was detectable, whereas the defined mode of action remains open (Bezhani et al. 2007; Walley et al. 2008). It would also be interesting to explore how and if microbial pathogens use diverse strategies to suppress plant immunity, since the conserved chromatin-remodeling complexes provide valuable targets to subvert plant immunity (Ma et al. 2011).

Genetic characterization suggests the need of DDM1 to maintain DNA methylation along the genome (Jeddeloh et al. 1999). The sum of several epigenetic and genetic alterations in the hypomethylated mutant cumulate in dwarfism, curled leaves and EDS1-dependent enhanced disease resistance correlating with the de-repression of several NB-LRR genes from the *RECOGNITION OF PERONOSPORA PARASITICA 5 (RPP5)* locus (Yi and Richards 2007; Yi and Richards 2009). In the absence of DDM1, a duplication event occurred between several clustered NB-LRRs within the *RPP5* locus that increased the copy number *SNC1*, which was originally identified in a suppressor screen of *npr1*. The gain-of-function allele *snc1* rescues the SA-signaling deficient *npr1* mutation (Zhang et al. 2003a; Yi and Richards 2009). Comparative and phylogenetic studies revealed that several NB-LRR genes reside in clusters as a consequence of tandem gene duplication events (Baumgarten et al. 2003; Meyers et al. 2003). Thus, DDM1 seems to stabilize the genomic region, while avoiding misexpression, which might allow the plant to accommodate highly related but variant repeat sequences.

DNA methyltransferases were also shown to be an important component in the regulation and maintenance of gene expression and silencing (Milutinovic et al. 2003; Kim and Zilberman 2014). DNA cytosine methylation can occur on symmetric (CpG and CpNpG) or asymmetric sites (CpNpN). In *Arabidopsis* DOMAINS REARRANGED METHYLASE 1 (DRM1) and DRM2 are responsible for *de novo* methylation, DNA METHYLTRANSFERASE 1 (MET1) is required for the maintenance of symmetric cytosine methylation and CHROMOMETHYLASE 3 (CMT3) for CpNpG methylation patterning (Cao and Jacobsen 2002a; Cao and Jacobsen 2002b; Cao et al. 2003). DNA methylation profiling of *Arabidopsis* plants exposed to bacterial pathogen or upon SA treatment showed that differentially methylated cytosines were enriched in gene-rich, but depleted in gene-poor regions. This suggests a role of these methylation changes in the transcriptional control. Of note, the symmetric and asymmetric methylation patterns were altered similarly upon avirulent and virulent bacterial challenges, as well as after SA application, but the CpNpN methylation differs upon ETI induction. In line with this, several defense-related genes are deregulated and antibacterial immunity is enhanced in *met1-3* and *drm1 drm2 cmt3* hypomethylation mutants (Downen et al. 2012). It is therefore conceivable, that the DNA methylation changes contribute to the activity or integrity of genes, resulting in differences in their expression. Whether the DNA methylation changes are also transmitted through generations or erased under certain conditions needs to be proven in further studies (Alvarez et al. 2010).

### **1.2.2 Histone modifications correlated with a transcriptional control of gene expression**

In general, histone modifications associated with active (transcription-permissive) chromatin include histone H3, which can be mono-, di- or tri-methylated on lysine (K) 4 (H3K4me1, H3K4me2 or H3K4me3, respectively), H3K36me3, or acetylated on histone H3 and H4 (H3ac and H4ac). Transcription-repressive histone marks include H3K9me1, H3K9me2, H3K9me3, H3K27me1,

H3K27me2 or H3K27me3 (Fuchs et al. 2006; Kouzarides 2007a; Roudier et al. 2009; Liu et al. 2010). New findings suggest the presence of different combinations/patterns of histone modifications, which define the chromatin structure and transcriptional competence of target loci. This comprehensive view of different epigenome mapping studies includes eleven histone modifications, while the first chromatin state (CS1) corresponds to transcriptional active genes enriched with H3K4me3 and H3K36me3. CS2 and CS3 correspond to repressive chromatin, whereas H3K27me3-marked CS2 is mainly associated with repressed genes and CS3 with H3K9me2 and H4K20me1 corresponds to heterochromatin formation and silenced transposable elements. CS4 does not carry any prevalent mark and is correlated with weakly expressed genes and intergenic regions (Roudier et al. 2011). This suggests that the functional outcome of the histone modification is connected to the presence of other histone marks as well as the position of these modifications with respect to the gene structure and genomic context (Roudier et al. 2009; Roudier et al. 2011; Schwammle et al. 2014).

Histone acetylation on lysine residues neutralizes the positive charge of lysine thus loosening the association of histones and DNA, which relieves the DNA from its condensate state. This provides a direct platform for transcriptional activation, whereas lysine methylation often creates binding sites for other proteins with specific effect on the chromatin and is regarded as more stable (Francis et al. 2004; Pray-Grant et al. 2005; Sims et al. 2007; Eskeland et al. 2010; Berr et al. 2011).

The major subclass of lysine-specific histone methyltransferases (HMT) involves Su[*var*]3-9, Enhancer of Zeste, Trithorax (SET) with 37 members annotated in *Arabidopsis* (Hennig and Derkacheva 2009; Thorstensen et al. 2011). Those HMT catalyze mono-, di- or trimethylation of different lysine residues on H3 and/or H4. Two prominent H3 modifications are H3K27me3 and H3K4me3, which are strongly correlated with transcriptional repression or activation and with the Polycomb group (PcG) protein complex Polycomb Repressive Complex 2 (PRC2) and the trithorax group (trxG) complex(es), respectively (Sang et al. 2009; Margueron and Reinberg 2011). This is in accordance to *Drosophila melanogaster* (*Drosophila*) and human, where it is known that both, PcG and trxG proteins, form high order complexes, which antagonistically repress and maintain the expression of developmental genes, respectively (Simon and Tamkun 2002; Schuettengruber et al. 2007; Schwartz and Pirrotta 2007; Alvarez-Venegas 2010).

The four core PcG complex subunits of PRC2 in *Drosophila* are defined as Enhancer of Zeste (E(z)) harbouring the SET domain, Extra Sex Combs (Esc), Suppressor of Zeste (Su(z)) and Nucleosome remodelling factor 55 (N55) of which homolog subunits exist in human and *Arabidopsis* that have evolved into small families. In human the E(z) homologs Enhancer of Zeste (EZH) 1, 2; the Esc homologs Embryonic Ectoderm Development (Eed) 1, 2, 3, 4; the Su(z) homolog Suppressor of Zeste 12 (SUZ12); and the N55 homologs Retinoblastoma binding protein (RbAp) 46, 48 exist. In *Arabidopsis* the E(z)

homologs MEDEA (MEA), CURLY LEAF (CLF) and SWINGER (SWN); the ESC homolog FERTILIZATION INDEPENDENT ENDOSPERM (FIE); the Su(z)12 homologs EMBRYONIC FLOWER (EMF), FERTILIZATION INDEPENDENT SEEDS 2 (FIS2), VERNALIZATION 2 (VRN2); and the N55 homologs MULTICOPY SUPPRESSOR OF IRA 1-5 (MSI1-5) are present (Liu et al. 2010; Jeong et al. 2011) (Figure 1). Molecular and genetic evidence suggest, that the encoded proteins form at least three distinct complexes harbouring different paralogs of the E(z) and Su(z)12 protein families that co-exist in *Arabidopsis* and control several developmental programs like gametogenesis, fertilization, seed development, vegetative development, flower transition and organogenesis (Schubert et al. 2005; Kohler and Aichinger 2010; Butenko and Ohad 2011; Holec and Berger 2012; Molitor and Shen 2013). The core component of the PRC2 is the SET domain harboured in CLF, SWN and MEA, whereas CLF and SWN have partially redundant function and MEA is endosperm specific. Of note, the H3K27 trimethylation starts from a nucleation site, which is linked to a PcG-recruiting region. Subsequently, the H3K27me3 spreads to flanking regions as the PRC2 recognizes its own target modification and is further activated by binding to H3K27me3 (Goodrich et al. 1997; Chanvivattana et al. 2004; Schubert et al. 2006; Farrona et al. 2008; Yang et al. 2014).

In order to maintain a stable repression of gene expression during mitosis and development, the H3K27me3 mark alone is not sufficient. Studies in *Arabidopsis* support the presence of functional homologs of the *Drosophila* PRC1 complex that recognize the H3K27me3 mark and mono-ubiquitinate histone H2A (H2Aub1), which is correlated with stable silencing, although the full identity and mode of action of PRC1 has not been established yet and ubiquitination-independent mechanisms are also present (Turck et al. 2007; Bratzel et al. 2010; Molitor and Shen 2013; Calonje 2014).

The trxG protein complexes do not display a grade of conservation as PcG protein complexes (Figure 1). One trxG complex of *Drosophila* with similarity to human and *Arabidopsis* consist of Trithorax (Trx); host cell factor 1 (HCF1); dumpy 30 (DPY30); retinoblastoma-binding protein 5 (RbBP5); Absent, small, or homeotic-like (Ash2L); WD40 Repeat domain 5 (WDR5) and Menin. In human mixed-lineage leukemia (MLL) 1-3 proteins are similar to Trx, but the complex composition differs regarding its subunit male absent on the first (MOF) (Schuettengruber et al. 2007; Alvarez-Venegas 2010; Schuettengruber et al. 2011). The first identified trxG protein in *Arabidopsis* was HOMOLOG OF TRITHORAX 1 (ATX1) as a plant counterpart of the Trx and MLL1 proteins. ATX1, Trx and MLL1 are capable of H3K4 trimethylation, whereas recently WDR5a, RBL and ASH2R have been described to participate in the complex formation (Alvarez-Venegas et al. 2003; Pien et al. 2008; Saleh et al. 2008a; Alvarez-Venegas 2010; Ding et al. 2011b). Of note, the *Arabidopsis* genome encodes five ATX1-like (ATX1-5) and seven ATX-related (ATXR1-7) proteins, with different target genes, methylase and tissue specificity, whereas to date the exact composition of the *Arabidopsis* trxG complex(es) and its

evolutionary counterparts are unknown (Baumbusch et al. 2001; Pontvianne et al. 2010; Thorstensen et al. 2011).

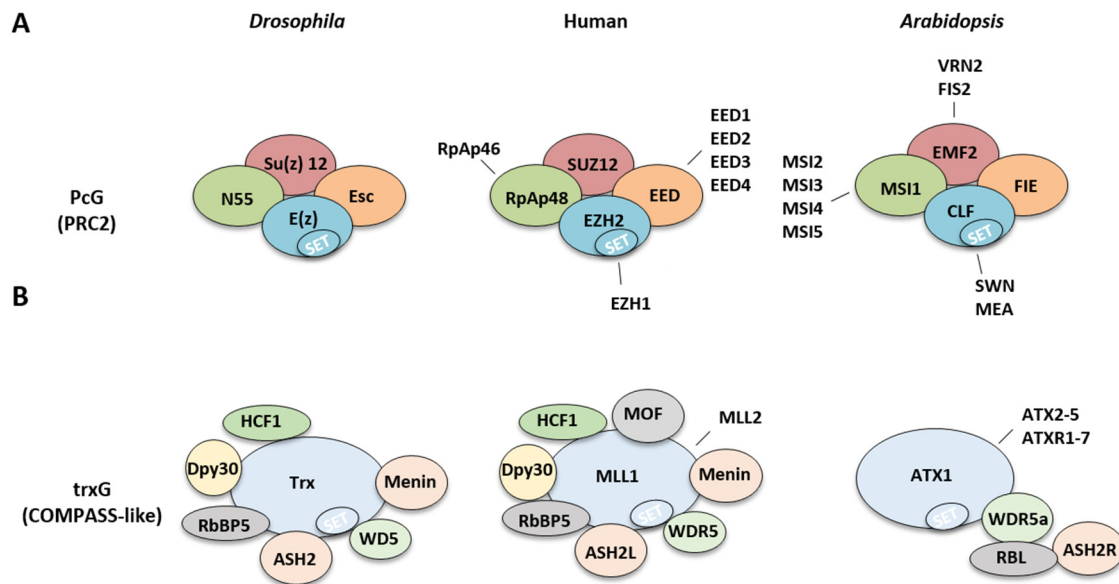


**Figure 1: Schematic illustration of the PcG and trxG complex core components in *Drosophila*, human and *Arabidopsis*.**

(A) The PRC2 complex in *Drosophila* consists of Enhancer of Zeste (E(z)) harbouring the HMT catalytic SET domain, Extra Sex Combs (Esc), Suppressor of Zeste (Su(z)) and Nucleosome remodelling factor 55 (N55). In human and *Arabidopsis*, the PRC2 components have evolved into families that are interchangeable to form distinct complexes. **Human:** Enhancer of Zeste (EZH) 1, 2; Embryonic Ectoderm Development (Eed) 1, 2, 3, 4; Suppressor of Zeste 12 (SUZ12); Retinoblastoma binding protein (RpAp) 46, 48. **Arabidopsis:** MEDEA (MEA), CURLY LEAF (CLF), SWINGER (SWN); FERTILIZATION INDEPENDENT ENDOSPERM (FIE); EMBRYONIC FLOWER (EMF), FERTILIZATION INDEPENDENT SEEDS 2 (FIS2), VERNALIZATION 2 (VRN2); MULTICOPY SUPPRESSOR OF IRA 1-5 (MSI1-5). Homologues proteins are depicted in same colors.

(B) One trxG complex of *Drosophila* with highest similarity to human and *Arabidopsis* consist of Trithorax (Trx), host cell factor 1 (HCF1); dumpy 30 (DPY30); retinoblastoma-binding protein 5 (RbBP5); Absent, small, or homeotic-like (Ash2L); WD40 Repeat domain 5 (WDR5) and Menin. In **human** mixed-lineage leukemia (MLL) 1-3 proteins are similar to Trx, but the complex composition differs regarding its subunit male absent on the first (MOF). In **Arabidopsis** ATX1 has highest similarity to Trx and MLL1. The COMPASS-like complex containing ATX1 seems to inhabit WDR5a, RBL and ASH2R. Furthermore, ATX1-like 2-5 (ATX1-5) and ATX-related 1-7 (ATXR1-7) proteins are present, but the exact composition of the complex(es) is unknown. Homologues proteins are depicted in same colors.

Although comprehensive studies of trxG proteins are practically lacking behind the studies of PRC2 in *Arabidopsis*, ATX1, ATX2 and ATXR7 have been implemented in the flowering time control as necessary for a proper expression of *FLC* (Pien et al. 2008; Tamada et al. 2009; Deal and Henikoff 2011a). Contrary to its role in development, ATX1 binds phosphatidylinositol 5-phosphate (PI5P) upon environmental stresses such as high salinity or hyperosmosis and is required for dehydration stress responses via ABA-dependent and ABA-independent pathways.

In addition, ATX1 serves to recruit the pre-initiation complex, including the TATA-box binding protein and RNA Pol II, to its target gene promoters. Upon transcription initiation, the phosphorylated form of RNA Pol II at Serine 5 (Ser5) clears the promoter and shifts to the transcriptional starting site to recruit ATX1 in a second event for H3K4 trimethylation. This implies that ATX1 affects the transcription of

target genes by a mechanism distinct from its H3K4 trimethylation activity that is further correlated with effective transcriptional elongation. H3K4me3 level generally show a positive correlation with transcription rates and the occupancy of the activated RNA Pol II phosphorylated at Ser5 (Alvarez-Venegas et al. 2006; Ndamukong et al. 2010; Ding et al. 2011a; Ding et al. 2012b; Fromm and Avramova 2014).

Although the role of H3K4me3 and H3K27me3 is emerging, it remains elusive how PcG and trxG protein complexes are recruited to their target genes in *Arabidopsis*, whereas in *Drosophila* they bind to a conserved Polycomb- and Trithorax responsive element, PRE and TRE, respectively (Schwartz and Pirrotta 2007; Alvarez-Venegas 2010; Schuettengruber et al. 2011). One possible mechanism of recruitment could be provided by non-coding RNAs (ncRNA), transcribed from the respective loci, as demonstrated for *FLC* in *Arabidopsis*, by the interaction with transcription factors and/or the chromatin structure *per se* (Schuettengruber et al. 2007; Swiezewski et al. 2007; Kanhere et al. 2010; Heo and Sung 2011; Klose et al. 2013). A dynamic transcriptional regulation might also require specific demethylation of histone marks as reported in animals (Verrier et al. 2011). In *Arabidopsis*, FLOWERING LOCUS D (FLD) is associated with demethylation of *FLC*, RELATIVE OF EARLY FLOWERING 6 (REF6) acts as H3K27me3 demethylase, and JM14 is described as H3K4 demethylase (Shi et al. 2004; Lu et al. 2010; Lu et al. 2011).

### 1.2.2.1 Histone modifications in plant immunity

Several studies implement a control of the defense-related transcriptome by histone modifications, whereas the full picture of the underlying mechanism remains elusive. A suppressor screen for *Arabidopsis* lesion mimic mutants identified *accelerated cell death 11 (acd11)* as SET DOMAIN GROUP 8 (SDG8), a H3K36 methylase, that is required for basal expression of *RPM1*, RPM1-mediated ETI and basal immunity to bacterial infection (Palma et al. 2010; De-La-Pena et al. 2012). In addition, SDG8 also seems to play a role in the transcriptional activation of JA/ET-related genes against the necrotrophic fungus *Alternaria brassicola* by H3K36 trimethylation of a subset of these defense-related genes (Berr et al. 2010). However, SDG8 displays multi-catalytic activity for H3K36me2/me3 and H3K4me3. In *sdg8* plants, the H3K4me2 and H3K4me3 levels on *PR1* upon pathogen challenge are also altered, which seems to enhance susceptibility towards *Pst* (Cazonelli et al. 2009; Grini et al. 2009; De-La-Pena et al. 2012). Future studies will need to clarify whether SDG8 directly catalyzes all these H3 methylations.

Recent findings also suggest a role of H2Bub1, which is generally associated with gene activation, in the immune response to the necrotrophic pathogen *Botrytis cinerea* together with the Mediator subunit MED21 (Dhawan et al. 2009). In line with their first study, the authors provided further evidence that *SNC1* and *RPP4* show enhanced H2Bub1 level upon infection with *Pst* DC3000, suggesting a mechanism to modulate immune responses in plants (Zou et al. 2014).

Loss of ATXR7, which seems to require the collaboration with MODIFIER OF SNC1.9 (MOS9), enhances susceptibility towards the oomycete *Hyaloperonospora arabidopsidis* (*Hpa*), which was associated with reduced H3K4me3 levels on the R-genes *RPP4* and *SNC1* (Xia et al. 2013). This already indicates the multilayered regulation of one gene by methylation and ubiquitination.

Interestingly, ATX1 seems to be required for the proper immune response modulation, as *atx1* shows reduced basal resistance and impaired expression of a high proportion of defense-related genes, like *PR1*. Transcriptional activation of *WRKY70*, which is important for the balanced JA-SA crosstalk towards the SA branch upon pathogen challenge, is correlated with direct ATX1 binding and ATX1-dependent H3K4me3 signatures to *WRKY70*. In contrast, ATX1 binding was not detected on *PR1*, suggesting that ATX1 confers its resistance effects as the sum of indirect consequences such as modulation of transcriptional control of putative *PR1*-regulating transcription factors (Alvarez-Venegas et al. 2007). Increased H3K4me3, together with H3ac, was detected on *PR1* in non-elicited *sni1* plants, which also seems to account for the NPR1-independent recovery of *PR1* expression in *sni1 npr1* plants. Interestingly, this elevation of histone marks also occurs 48 h after BTH treatment, suggesting that the increase follows the transcriptional activation to keep the chromatin in an active state for the recruitment of further reader proteins (Li et al. 1999; Mosher et al. 2006; Sims and Reinberg 2006; Sims et al. 2006). In addition, it was shown that ELP2 genetically interacts with NPR1. ELP2 regulates the kinetics of pathogen-induced transcriptional reprogramming, maintains histone acetylation levels in several defense genes and impacts the pathogen-induced dynamic DNA methylation changes (Wang et al. 2013).

To counterbalance, the HISTONE DEACETYLASE 19 (HDA19) is recruited to several *PR* loci, such as *PR1* and *PR2*, to ensure basal expression of defense genes in unchallenged conditions, as well as their proper induction to avoid overstimulation during defense responses as a general transcriptional control mechanism (Wang et al. 2010; Choi et al. 2012). This holds true not only for the model plant *Arabidopsis*, but also for the important crop plant *Oryza sativa* indicating that demethylation and -acetylation are required to positively and negatively regulate the defense-related transcriptome (Ding et al. 2012a; Li et al. 2013).

### **1.3 Defense priming and underlying mechanisms in the plant immune response**

Priming is described as a physiological state that enables stress-exposed plants to alter their cellular, biochemical and/or transcriptional outputs in a way to encounter subsequent abiotic or biotic stresses of a similar nature with faster and/or higher responses depicting a kind of memory (Conrath 2011; Sani et al. 2013; Thellier and Luttge 2013; Liu et al. 2014). Each defense induction forces the plant to balance its energy sources away from growth, decreasing the fitness of the plant. Priming allows the plant to

elevate its immunization status without detrimental constant immune activation, leading to an optimized fitness where growth and defense are appropriately prioritized in response to both environmental and developmental cues (van Hulten et al. 2006; Alcazar et al. 2011; Huot et al. 2014). This phenomenon was not only described for plants, but also characterized for the innate immune system of vertebrates termed “trained immunity”. This implies similar underlying mechanism(s) despite the presence of the adaptive immune system (Netea et al. 2011; Quintin et al. 2014).

Defense priming in plants can be induced by MAMPs, DAMPs, effectors, wounding, and treatment with natural or synthetic compounds (Conrath 2011; Pastor et al. 2012). The secondary faster and/or stronger immune activation is not solely limited to the site of the first encounter, but also transmitted to unchallenged parts of the plant resulting in systemic plant immunity. This holds true for several types of systemic immunity as SAR, ISR and WIR. ISR and WIR prime JA- and ET-dependent pathways and genes against herbivory and necrotrophs attacks, whereas SAR is connected with the potentiation of SA-associated mechanisms (Durrant and Dong 2004; Jung et al. 2012; Pieterse et al. 2012). The potentiation of SAR by plant derived compounds, such as SA, thiamine, riboflavin, or synthetic substances like BTH and BABA, is used for crop plants in field applications since several years, but the underlying molecular mechanisms remained fairly unexplored (Katz et al. 1998; Thulke and Conrath 1998; Ahn et al. 2007; Beckers and Conrath 2007). In the last years, several causative mechanisms, such as induced metabolic changes, callose deposition, ROS signaling, non-coding RNA, RNA quality control mechanisms and RNA-directed DNA methylation (RdDM), the accumulation of transcription factors and signaling proteins as well as chromatin modifications have been proposed (Luna et al. 2012; Pastor et al. 2012; Pastor et al. 2013b).

MAPKs function downstream of receptors in plant immunity and amplify the signal towards intracellular responses, providing strong candidates for priming mediators (Meng and Zhang 2013). In *Arabidopsis*, a flg22 stimulated MAPK cascade is composed out of MEKK1, MEK4/5 and MPK6/3, of which activation lead to gene induction of for example *WRKY29* (Asai et al. 2002). Beckers et al. demonstrated that chemical- or pathogen-induced priming in local tissue results in the increased accumulation of MPK6/3 at the protein and mRNA levels in systemic tissue. Of note, these kinases are held in an inactive state in primed cells providing a platform for faster and higher signal amplification. After systemic priming response induction, more of these proteins are activated compared to non-primed plants correlated to an enhanced defense gene induction. This priming event was fully dependent on NPR1 for which an accumulation of transcriptional active monomers in systemic tissue upon local pathogen attack was also reported, suggesting that MPK6/3 and NPR1 could confer long-lasting resistance to subsequent pathogen attack (Mou et al. 2003; Beckers et al. 2009). A similar

mechanism was reported for enhanced expression of SA-regulatory transcription factors such as WRKYs, which accumulate upon BTH treatment (Van der Ent et al. 2009).

Recent studies suggest the importance of secondary metabolites in promoting an enhanced immune activation in the priming response. Upon local pathogen attack, azelaic acid is transported throughout the plant conferring local and systemic immunity. It primes the plant to accumulate higher SA levels upon infection than non-primed plants, although the biochemical mechanisms remain elusive (Jung et al. 2009). Priming is further characterized at the molecular level by a potentiated biosynthesis and accumulation of the secondary metabolite Pip, which is critical for SAR priming. Moreover, the Pip biosynthesis gene *AGD2-LIKE DEFENSE RESPONSE PROTEIN 1 (ALD1)*, *FMO1* and *PR1* show potentiation for a priming response (Navarova et al. 2012; Shah and Zeier 2013).

Histone modifications and histone replacement, as mentioned above, have been considered as a molecular basis for priming of SAR-related genes. They can provide a long-lasting change in gene responsiveness compared to the accumulation of signaling proteins with limited turnover time (Pastor et al. 2012). The induction of JA/ET-inducible defense related genes upon pathogen challenge or JA treatment goes along with an increase of H3K36me3 at gene promoters mediated by SDG8 (van den Burg and Takken 2009; Berr et al. 2010). Recently, Singh et al. showed that repetitive exposures to mild environmental stresses induce the enrichment of open chromatin marks such as H3K4me3 and H3K9K14ac and the RNA Pol II on MTI-responsive genes in a manner correlated with a primed state of immunity, which lead to enhanced immune activation upon subsequent pathogen challenge. This observed phenomenon was impaired in the *histone acetyltransferase 1-1 (hac1-1)* providing a mechanistic link between the primed state and epigenetic modifications (Singh et al. 2014a). It is of great interest to understand how these histone modifications are integrated in the establishment of an immune memory.

A recent study demonstrates a correlation between systemic priming of SA-inducible WRKYs transcription factors and changes of several histone modifications at their promoters. Upon BTH or pathogen challenge in local leaves, permissive histone marks like H3K4me3, H3K4me2, and acetylation of H3K9, H4K5, H4K8 and H4K12 were found on *WRKY29*, *WRKY6* and *WRKY53* in systemic tissue. H3K4me3 and H3K4me2 were elevated for all WRKYs tested, and especially H4K5ac, H4K8ac and H4K12ac on *WRKY29* upon the priming response stimulation by water infiltration of primed compared to non-primed plants. Interestingly, some of these marks were already found on the gene promoter prior to a second stimulation, suggesting that an histone-based memory underlies defense priming, although the responsible histone modifying enzymes are not known yet (Jaskiewicz et al. 2011). Recently, the requirement of FLD for SAR development and systemic priming was demonstrated, correlated with demethylation in the flowering time control (He et al. 2003; Yu et al. 2011). Contrary,

FLD was required for H3K4me2 and H3K14ac enrichment on *WRKY6* and *WRKY29*, suggesting an indirect effect of FLD by inhibiting negative regulators (Singh et al. 2013; Singh et al. 2014b). Of note, all these described priming events were abolished in *npr1* plants, suggesting a general requirement for NPR1 in the priming response.

These induced priming states raise the question of duration and heritability on target defense-related genes and cellular changes. A trans-generational memory regarding a stress adaptation was reported for abiotic stresses and for biotic cues, albeit in mainly descriptive studies, supporting the existence of such a memory (Chinnusamy and Zhu 2009; Holeski et al. 2012; Slaughter et al. 2012). A recent study in *Arabidopsis* shows that primed states for defense-related genes and immune responses after challenges with a hemibiotrophic pathogen can be transmitted to the following generation along with an increase of H3K9ac and H3K27me3 on SA- and JA-inducible priming genes, respectively. The preference of SA over JA is fully dependent on NPR1. Moreover, trans-generational SAR occurs in non-primed *drm1 drm2 cmt3* plants, which exhibit a reduction of non-CG methylation, raising the possibility that hypomethylation also facilitates the heritability, correlated with the presence of functional RNA-directed DNA methylation machinery (Luna et al. 2012; Luna and Ton 2012; Rasmann et al. 2012). Carefully designed experiments will clarify in the future, whether transgenerational defense priming is solely based on changes on the chromatin level rather than stress-induced genetic changes that may interfere with chromatin organization as recently suggested by Yan et al. (Pecinka and Mittelsten Scheid 2012; Yan et al. 2013).

The full understanding of the complex network underlying SAR and the systemic priming response will challenge the scientific community in multiple ways. This will provide important principles in the generation of future crop plants and/or modern pesticides with higher yields and less fitness costs, due to wisely modulated immune responses.

## 1.4 Thesis aims

Numerous studies have indicated the presence of a process known as priming, which causes defense-related genes to remain in a poised state, presumably after a transient transcriptional upregulation, upon the perception of pathogen-related signals. This phenomenon can be regarded as an immune memory. Such memorized genes are activated at faster and/or to higher levels upon a secondary pathogen encounter. In agreement with this, the initially activated genes are competent for increased expression upon second stimulation, which is designated priming response (Conrath 2011; Berr et al. 2012). A clear advantage of defense priming is the sustained enhancement of host immunity at lower fitness costs, compared to direct immune activation (van Hulten et al. 2006). Recent publications implemented alterations of histone modifications at priming target genes as stable immune memory compared to metabolic changes, yet the underlying mechanism(s) and epigenetic modifier(s) involved remain fairly unexplored (Jaskiewicz et al. 2011; Liu et al. 2014; Singh et al. 2014a).

In line with this, I aimed to shed light on the questions: Do histone modifications play a role in the control of defense-related transcriptome in local and systemic immunity, and if so, are histone modifications associated with memories of transcriptional reprogramming? Are there differences in the MTI- and ETI-triggered systemic priming responses? In addition, which histone modifier(s) are associated with an epigenetic regulation of priming?

As a first step, I analyzed whether defense-related marker genes carry specific histone marks, namely H3K4me3 and H3K27me3 that are associated with a transcriptional memory of gene expression, and then investigated the relevance of these marks in the control of the defense-related transcriptome. The established systemic priming assay on selected defense marker genes could provide insights into the differences of MTI- and ETI-induced systemic immunity, which were subsequently strengthened with the global RNA-Seq studies. These findings could further allocate SAR and the systemic priming response in connection with separate marker gene sets. Moreover, I aimed to determine the significance of ATX1 and CLF as trxG and PcG protein complex members, respectively, in systemic immunity and priming response. This was accomplished by ChIP qPCR analysis of H3K4me3 and H3K27me3 on *PR1*, as a SAR and priming marker gene, in systemic tissue upon local MTI and ETI activation.



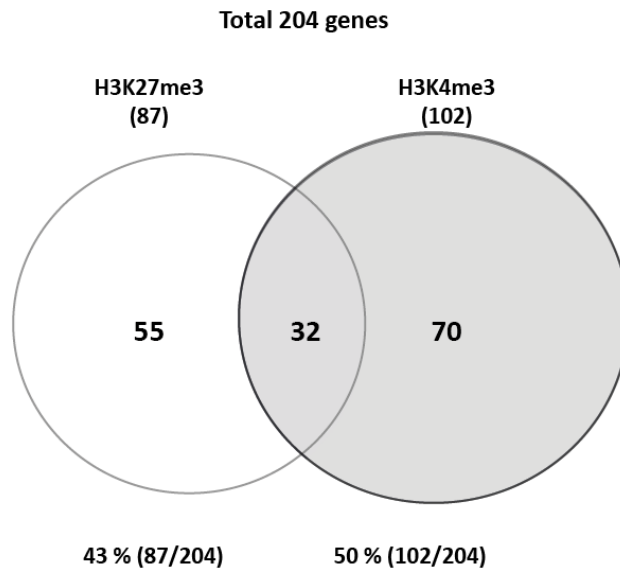
## 2 Results

### 2.1 Local Priming

#### 2.1.1 Described histone marks on defense-related gene loci

The work of our group suggests the presence of different phases during MTI activation in *Arabidopsis*, including a sustained transcriptional reprogramming phase that is important for effective immunity. In *rsw3*, an ER-localized glucosidase II  $\alpha$ -subunit allele, sustained transcriptional reprogramming upon MAMP treatment failed to activate host immunity despite the wild type-like co-activation of early MAMP outputs like ROS production, MAPK activation and initial transcriptional upregulation of defense marker genes (Lu et al. 2009; Tintor et al. 2013; Ross et al. 2014). This could lead to the assumption that target genes of the sustained transcriptional reprogramming are closely associated with defense execution. Using a transcriptome analysis of *rsw3* upon elf18 treatment, several target genes of a sustained PRR signaling, including *PR1*, could be defined (Ross et al., unpublished). Using 204 of these genes, which were significantly more than 2-fold less expressed 10 h after elf18 treatment in *rsw3* compared to wild type plants (Supplementary Table 1), an *in silico* approach using a public available database was performed to evaluate the histone mark occurrence of H3K4me3 and H3K27me3 on these genes (Figure 2).

A genome-wide chromatin immunoprecipitation (ChIP) experiment demonstrated that ca. 17 % of all annotated *Arabidopsis* genes are H3K27me3 and ca. 50 % are H3K4me3 positive in non-elicited 10-day-old wild type seedlings (Zhang et al. 2007; Zhang et al. 2009). The two histone marks are supposed to work antagonistically and to be deposited by the PcG and trxG protein complexes (He et al. 2011). Of note, the 204 selected genes carry the histone marks H3K27me3 and H3K4me3, associated with transcriptional repression and activation, respectively, with 43 % and 50 % indicating a high representation of H3K27me3 on the selected genes (Figure 2). This could be statistically confirmed by testing the null-hypothesis that the observed distribution (methylated vs. unmethylated) does not differ between the expected (published) distribution (methylated vs. unmethylated) using a Chi-squared test. The null-hypothesis is rejected for H3K27me3 (p-value <  $2.2e^{-16}$ ) and accepted for H3K4me3 (p-value = 0.1633).



Genes which are downregulated in *rsw3* (> 2-fold;  $p < 0.05$ ) compared to WT upon elf18 for 10 h.

**Figure 2: *In silico* analysis for H3K27me3 and H3K4me3 on defense-related genes in non-elicited *Arabidopsis* seedlings.**

The Venn diagram indicates the number of *Arabidopsis* genes carrying H3K27me3 and/or H3K4me3 out of 204 genes that are up-regulated in a late MTI phase in wild type but not in *rsw3* plants (Ross et al., unpublished). Further *in silico* comparative analysis suggests their close association with defense execution in diverse plant-pathogen interactions. The database referred was publicly available at the Jacobsen Lab, USA (Zhang et al. 2007; Zhang et al. 2009).

### 2.1.2 Identification of local memory response candidate genes

To monitor a potential transcriptional memory response in terms of an enhanced and/or faster gene activation after a secondary pathogenic stimulus, a robust and reliable assay method needed to be established.

To this end, five-day-old wild type seedlings were pretreated for 48 h with a saturated flg22 concentration of 0.5  $\mu$ M (= primed) or kept in MAMP-free media (= non-primed). The seedlings were then incubated for 72 h in MAMP-free media to ensure, that initial gene activation could return to basal levels before retreatment with 10 nM flg22, which is typically below the threshold for the induction of these genes. The expression of the selected candidate genes *WRKY29*, *PROPEP3*, *PROPEP2* and *PR1*, as defined MAMP-induced genes (see 1.1, 1.3), was assessed by quantitative real-time (qRT)-PCR regarding a memory response in wild type seedlings upon the retreatment with 10 nM flg22.

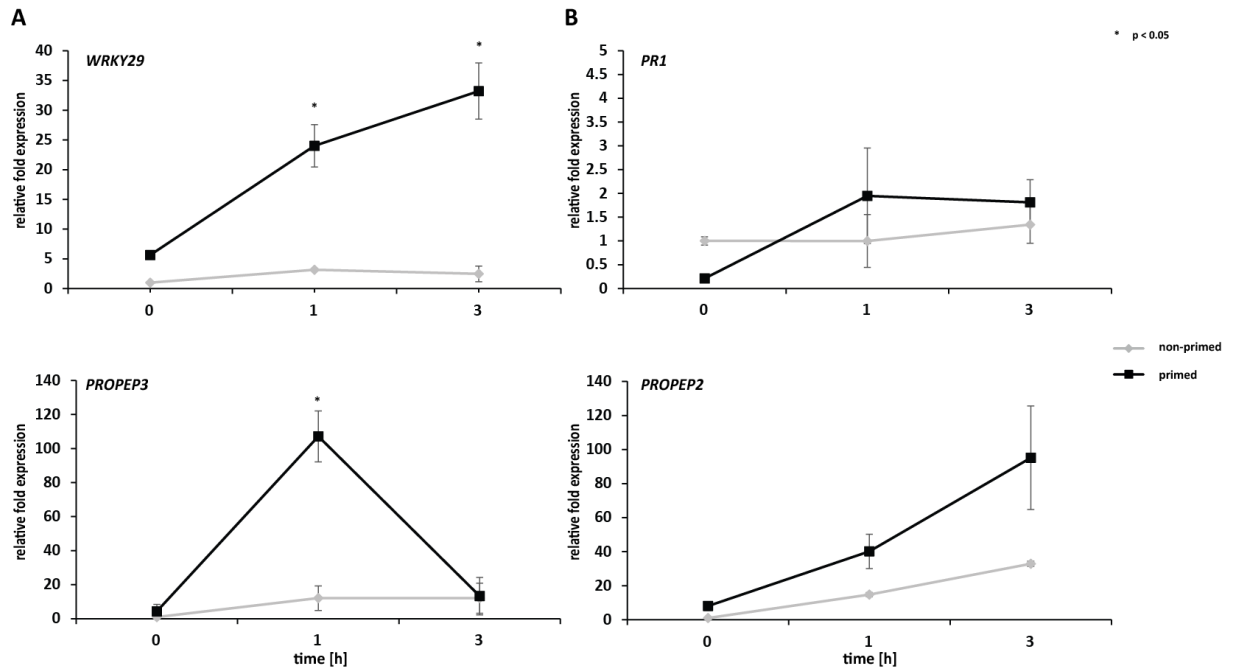


**Figure 3: Gene expression analysis of local memory response candidate genes.**

Five-day-old WT seedlings were treated for 48 h with 0.5  $\mu\text{M}$  flg22 (primed) or kept in MAMP-free media (non-primed). The seedlings were then incubated for 72 h in MAMP-free media before retreatment with flg22. The expression of defense-related marker and candidate genes (A) *WRKY29*, *PROPEP3* and (B) *PR1*, *PROPEP2* was assessed by qRT-PCR regarding a memory response during the retreatment with 10 nM flg22. Fold changes were calculated relative to non-primed samples at 0 h and normalized against the endogenous reference gene *At4g26410*. Error bars represent standard error (SE;  $n=2$ ) of two biological replicates with four technical replicates each, respectively. For *PR1* one biological replicate is shown. Error bars represent here standard deviation (SD;  $n=4$ ) or four technical replicates. P-value of  $p < 0.05$ , indicated by asterisk, was calculated using Student's t-test comparing expression at 1 h and 3 h of primed and non-primed samples. The corresponding *fls2* control is shown as Supplementary Figure 2.

Figure 3A shows the results of the memory response assay for the two candidate genes *WRKY29* and *PROPEP3*. If these genes were targeted by the aforementioned memory response, a faster and/or higher gene expression in primed compared to non-primed samples would be expected. Indeed, a significant higher expression was detected in primed seedlings after the retreatment for both genes. Unexpectedly, the retreatment with 10 nM flg22 activated these genes in non-primed seedlings albeit to a lesser degree. The further analyses on the memory response candidate genes *PR1* and *PROPEP2* displayed no significant differences in gene expression between primed and non-primed seedlings (Figure 3B). It should be noted, that *WRKY29* and *PROPEP3* are among the 204 selected genes enriched with H3K27me<sub>3</sub>, but not H3K4me<sub>3</sub>, in untreated wild type seedlings, whereas *PROPEP2* and *PR1* are not among those genes for either histone mark (Supplementary Table 1; Figure 2). As assumed, *WRKY29* and *PR1*, as representatives for primed and non-primed genes, showed induction during the initial MAMP treatment (Supplementary Figure 1). The data analysis also revealed that it is suitable to assess a memory response for *WRKY29* up to 3 h after the retreatment according to a robustly

observable difference regarding the expression between primed and non-primed samples. In sum, *WRKY29* was chosen as marker gene for local priming studies.

It was further assessed how durable the local memory response is. To this end, seedlings were cultivated for 144 h instead of 72 h after the initial MTI activation in the absence of MAMPs. Indeed, the priming response of *WRKY29* was still detectable, indicating the stability of the induced memory response (Supplementary Figure 3A). I also tested whether memory setting occurs upon elf18 treatment (Kunze et al. 2004). The obtained data confirmed that both elf18 and flg22 pre-treatments confer a memory, which allows faster and/or greater activation of the target genes tested (Supplementary Figure 3B). Interestingly, the gene expression levels of *FLS2*, encoding the cognate flg22 receptor (Gomez-Gomez and Boller 2000; Chinchilla et al. 2006), was increased in flg22-primed seedlings, pointing towards a possible role for an elevation in the steady-state levels of the receptor in priming (Supplementary Figure 3C).

### **2.1.3 Local memory response in *trxG* and *PcG* mutants**

To assess whether histone modifications mediated by *trxG* and *PcG* protein complexes, namely H3K4me3 and H3M37me3, could play a role in the regulation of a priming response, possible alterations in *atx1* and *clf* mutant plants were tested in the local memory response assay.

For both, *ATX1* and *CLF*, an involvement in the transcriptional memory of gene expression was described, although it was correlated with developmental and abiotic stress responses (Alvarez-Venegas et al. 2003; Alvarez-Venegas et al. 2006; Pien et al. 2008; Shafiq et al. 2014). *ATX1* plays also a role in orchestrating different branches of the plant immune system by directly targeting *WRKY70* function at the cross road of the JA- and SA-pathway (Alvarez-Venegas et al. 2007).

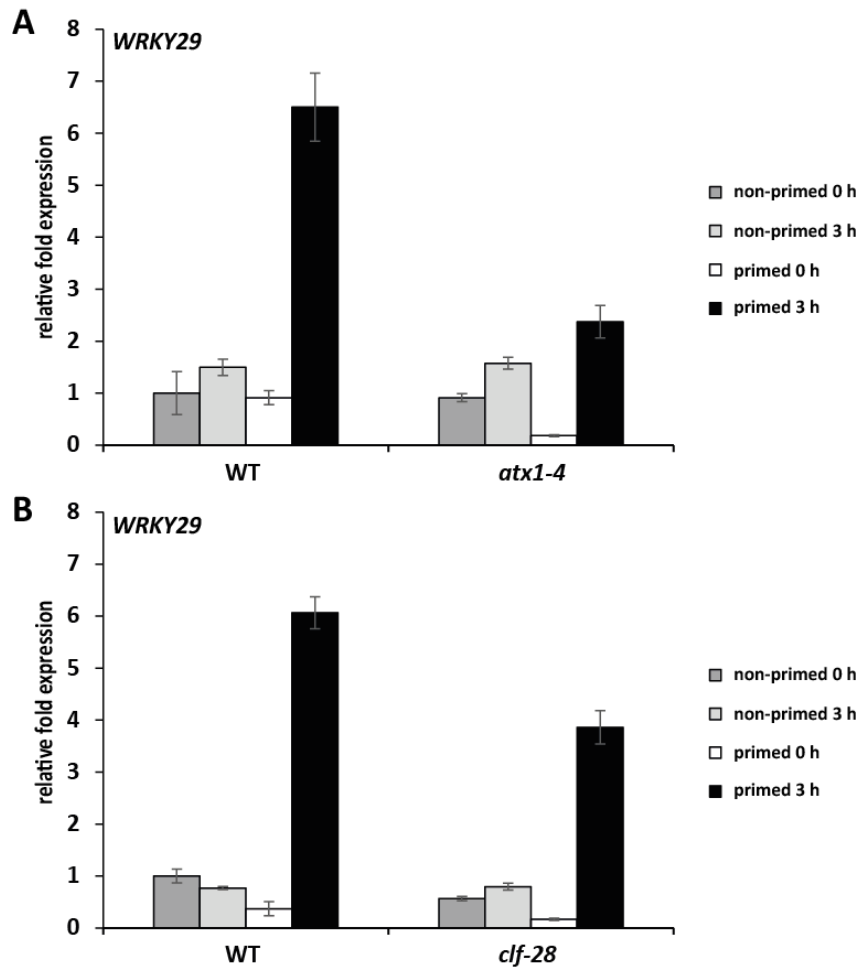


**Figure 4: Local memory response analysis of *trxG* and PcG mutants by using qRT-PCR.**

Five-day-old seedlings were treated for 48 h with 0.5  $\mu$ M flg22 (primed) or kept in MAMP-free media (non-primed) followed by incubation for 72 h in MAMP-free media before retreatment. The gene expression of *WRKY29* was analysed by qRT-PCR before (0 h) and 3 h after the retreatment with 10 nM flg22 in (A) WT and *atx1-4* and (B) WT and *clf-28* primed and non-primed seedlings. Fold changes were calculated relative to non-primed WT samples at 0 h and normalized against the endogenous reference gene *At4g26410*. Error bars represent standard deviation (SD; n=4) of four technical replicates each, respectively. Experiment was repeated three times with similar results.

As shown in Figure 4, *atx1-4* and *clf-28* mutants are reduced in their capability to mount a local priming response. Interestingly, those mutants show a wild type-like MAPK activation, anthocyanin suppression and *WRKY29* gene expression level upon flg22 treatment. MPK6, MPK3 and MPK4 activation was tested before, 5 and 15 minutes after MAMP application as an early MAMP signaling output in *atx1-4* and *clf-28* (Supplementary Figure 4) (Asai et al. 2002; Pitzschke et al. 2009). Suppression of anthocyanin accumulation under high sucrose stress upon MAMP treatment was correlated with immune activation (Lu et al. 2009; Saijo et al. 2009; Serrano et al. 2012; Tintor et al. 2013). Again a wild type-like pattern was observed although the lack in *clf-28* plants for sucrose-induced anthocyanin accumulation hampered me to test MAMP-induced anthocyanin suppression in this mutant (Supplementary Figure 5). Furthermore, the qRT-PCR studies of the local priming target gene *WRKY29* demonstrated a transcript profile similar to wild type (Supplementary Figure 6),

indicating that *atx1-4* and *clf-28* plants are defective in the memory setting despite their initial wild type-like immune activation. This could suggest a possible role for H3K4me3 and H3K27me3 that are supposed to be deposited by ATX1 and CLF, respectively, as markers for a memory of the aforementioned gene activation during or after the initial saturated MAMP treatment.

## 2.2 Systemic immunity

Plants, which have been already exposed to a stress, can alter their biochemical, cellular and/or transcriptional responses, possibly as a prerequisite for subsequent stress responses of a similar nature. This not only holds true for abiotic stresses but also for biotic ones (Baldwin et al. 1996; Goh et al. 2003; Ton et al. 2005; Bruce et al. 2007; Conrath 2011; Navarova et al. 2012). Thus, the second part of the study focusses on the impact of pathogenic induced alarmed state of distal parts of the plant upon local immune activation. This process, known as priming, causes defense related genes to remain in a poised state upon an presumably initial transcriptional upregulation, whereas such poised, or memorized genes are supposed to get activated faster and/or to a higher level in primed plants than in non-primed plants upon second stimulation (Conrath 2011). The transcriptional reprogramming upon MTI or ETI activation uses a largely overlapping set of genes with a faster, greater, and/or prolonged expression during ETI compared to MTI (Tao et al. 2003; Caldo et al. 2004; Tsuda and Katagiri 2010). For both, MTI and ETI activation at local challenged sites triggers the release of systemic signals to induce an enhanced state of immunity in distal parts of the plant (SAR) (Mishina and Zeier 2007; Dempsey and Klessig 2012). It was postulated that these differences in transcriptional reprogramming result also in divergent systemic priming responses upon secondary challenges.

### 2.2.1 ETI- and MTI-induced transcriptional reprogramming and systemic priming

In order to reveal the underlying molecular mechanisms of the potential differences in the MTI- and ETI-induced priming responses, mature plants grown in soil, instead of sterile seedlings grown in liquid culture were used. To trigger a sufficient MTI response, *Pst*  $\Delta$ *hrpS*, defective in its TTSS and therefore mostly representing a collection of MAMPs, was used (Roine et al. 1997; Wei et al. 2000). On the other hand, *Pst AvrRpm1* infection of *Arabidopsis* leads to a strong ETI induction via the resistance protein RPM1 (Bisgrove et al. 1994; Tian et al. 2003; Heidrich et al. 2012). To compensate for the reduced ability of *Pst*  $\Delta$ *hrpS* to multiply *in planta*, a ten-fold higher inoculum density than for *Pst AvrRpm1* was used.

In order to reveal differences during the MTI- and ETI-induced transcriptional reprogramming the gene expression of *PR1*, a SA-based immunity marker gene, was monitored (Uknes et al. 1992; Durrant and

Dong 2004), in local (expanded rosette leaves in the lower layer of the plant) and systemic (young expanded rosette leaves in the upper layer of the plant) leaves upon local pathogen infection.

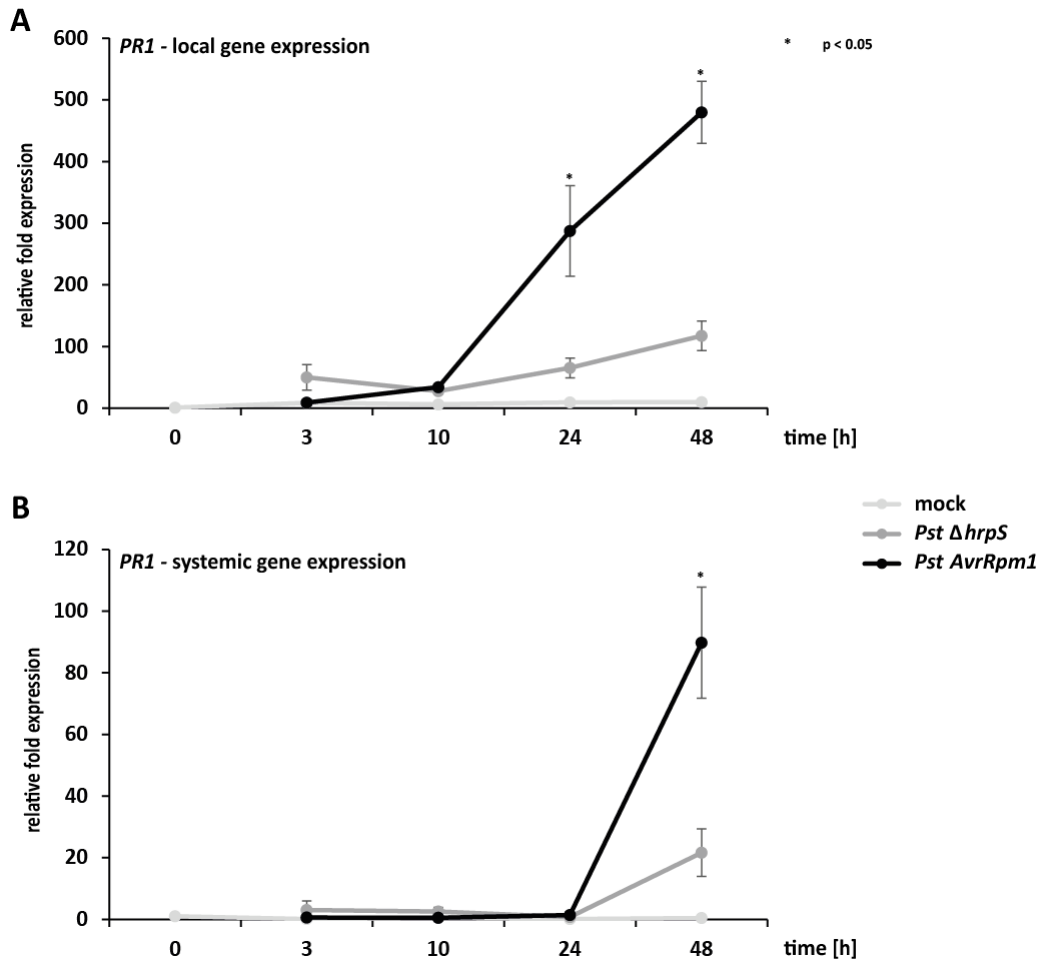


**Figure 5: MTI- and ETI-induced transcriptional reprogramming in local and systemic tissue.**

Four-week-old WT plants were syringe-infiltrated in three well-expanded local leaves with 10 mM  $MgCl_2$  (mock),  $1 \times 10^8$  cfu/ml *Pst*  $\Delta$ *hrpS* or  $1 \times 10^6$  cfu/ml *Pst* *AvrRpm1*. At indicated time points, *PR1* transcript abundance was measured by qRT-PCR in local (A) and systemic tissue (B). Fold changes were calculated relative to mock samples at 0 h and normalized against the endogenous reference gene *At4g26410*. Error bars represent standard error (SE;  $n=2$ ) of two biological replicates with three technical replicates each, respectively. P-value of  $p < 0.05$ , indicated by asterisk, was calculated using Student's t-test comparing the gene expression of *PR1* after ETI activation with that after MTI.

The transcript profiles of *PR1* in Figure 5A show an enhanced gene expression in local leaves upon ETI induction compared to MTI that started to differ at 10 hours post inoculation (hpi). This difference is further strengthened up to 48 hpi. In systemic tissue, the aforementioned enhanced *PR1* expression peaks at 48 hpi (Figure 5B). These data suggest that the expected transcriptional differences in local and systemic tissue were detectable between MTI and ETI under these settings, going along with the previously published enhancement of defense-related transcriptional reprogramming in ETI compared

to MTI (Tsuda and Katagiri 2010). This encouraged me to unravel possible differences between MTI and ETI in terms of the systemic priming response.

Based on the results presented for Figure 5, I further focused on the 48 hpi time point for the secondary treatment of systemic leaves, as it was also used for detecting systemic priming responses in previous studies (Mosher et al. 2006; Jaskiewicz et al. 2011; Navarova et al. 2012). For this purpose, local leaves of *Arabidopsis* wild type plants were syringe-infiltrated with *Pst*  $\Delta$ *hrpS*, *Pst* *AvrRpm1* or 10 mM MgCl<sub>2</sub> (as mock control). At 48 hpi, the local challenged leaves were removed and systemic leaves were infiltrated with water for which it was shown to trigger a sufficient priming response (Beckers et al. 2009; Jaskiewicz et al. 2011). The water infiltration ensured also a more uniform cellular response rather than a pathogen treatment as secondary challenge (Wright and Beattie 2004; Beckers et al. 2009). *PR1* was chosen as the initial systemic priming response marker gene, as it was described to exhibit a priming response under similar conditions (Mosher et al. 2006; Alvarez-Venegas et al. 2007; Jaskiewicz et al. 2011), whereas priming responsiveness is defined such that primed plants show sensitized gene expression profile upon secondary treatment compared to non-primed plants.

To this end, the dynamics of the marker gene *PR1* were monitored in systemic leaves upon secondary treatment up to 24 h.

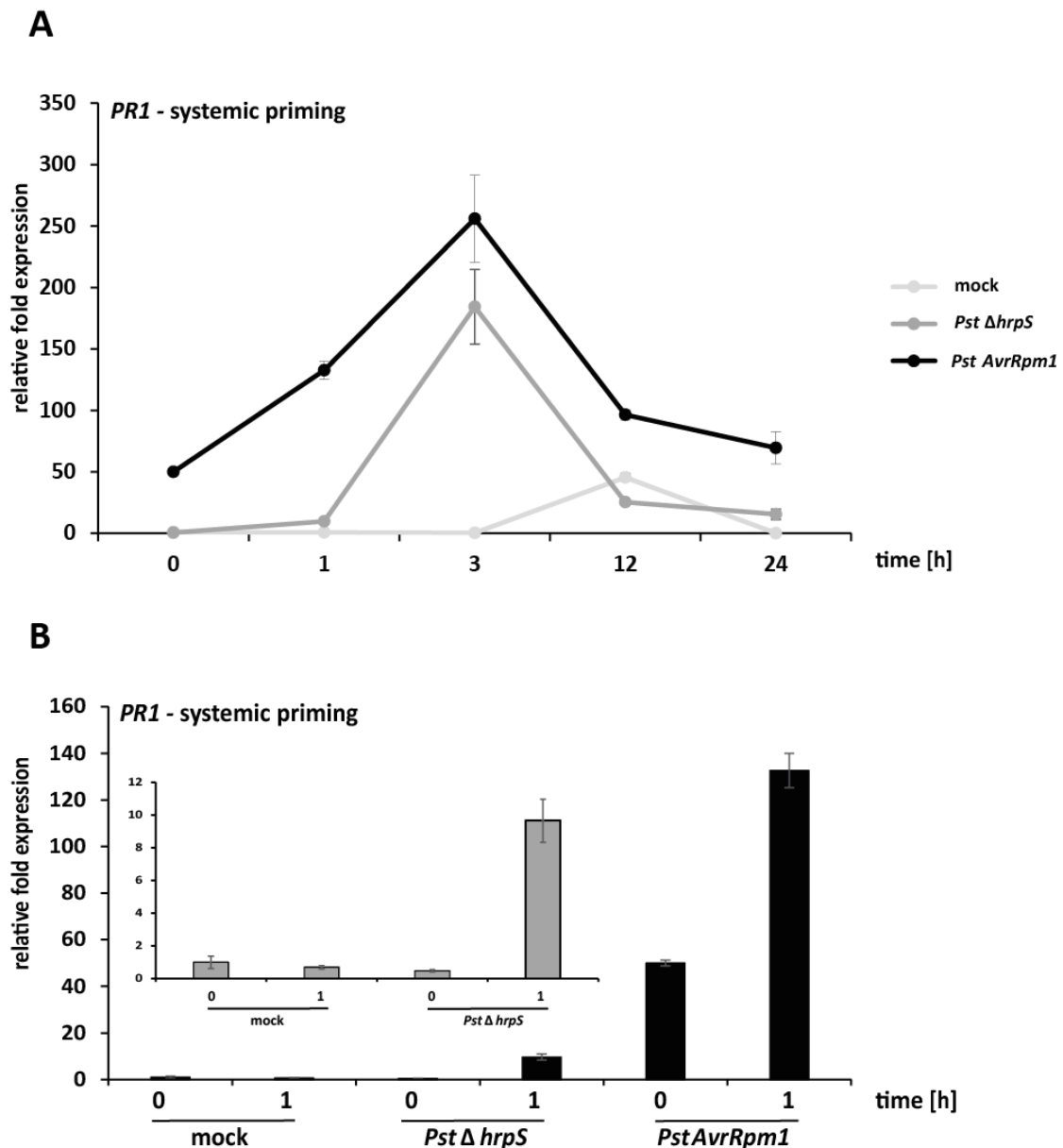


**Figure 6: MTI- and ETI-induced systemic priming response.**

(A) Four-week-old WT plants were syringe-infiltrated in three well-expanded local leaves with 10 mM MgCl<sub>2</sub> (mock), 1x10<sup>8</sup> cfu/ml *Pst ΔhrpS* or 1x10<sup>6</sup> cfu/ml *Pst AvrRpm1*. At 48 hpi, local infiltrated leaves were removed and systemic leaves infiltrated with water. At the indicated time points, *PR1* transcript abundance was measured by qRT-PCR. Fold changes were calculated relative to mock samples at 0 h and normalized against the endogenous reference gene At4g26410. Error bars represent standard deviation (SD; n=3) of one biological replicate with three technical replicates, respectively. Experiment was repeated three times with similar results.

(B) The respective expression values of 0 h and 1 h were extracted from (A). The grey bars represent a magnification of the results obtained for *Pst ΔhrpS*. Experiment was repeated three times with similar results.

Figure 6A illustrates that the ETI-induced systemic priming response is enhanced compared to MTI after water infiltration retreatment. The expression of *PR1* peaks at 3 h of the systemic priming response and gets attenuated thereafter. This finding can be explained that is detrimental for the plant with high fitness cost by having constitutive enhanced immune activation (van Hulten et al. 2006).

Therefore it is important to tightly regulate such costly immune activations. Interestingly, the difference between MTI- and ETI-induced systemic priming response was detectable 1 h after the secondary challenge with water (Figure 6B).

Of note, the expression levels of *PR1* were already higher in systemic tissue 48 h after ETI activation compared to MTI (Figure 5). Along with this, earlier studies suggested that ETI is more powerful in SAR than MTI (Mishina and Zeier 2007; Truman et al. 2007).

Using *Pseudomonas syringae* pv. *maculicola* (*Psm*) as secondary infection on systemic leaves 48 h after local MTI and ETI activation demonstrates that the MTI- and ETI-induced differences in the systemic priming response are not solely due to an artifact of the water infiltration (Supplementary Figure 15). Additionally, I tested whether the observed systemic priming response signature was specific for the infection with *Pst AvrRpm1* or a general effect, traceable with different ETI-inducing *Pst* strains. Initially, the pathogenic growth and gene activation of *PR1* in local tissue was tested to exclude possible differences of the systemic priming response are due to a diverse local immune activation. The bacterial growth of *Pst AvrRpm1*, *Pst AvrRps4* and *Pst AvrRpt2* (Jones and Dangl 2006; Heidrich et al. 2012) *Pst ΔhrpS* and the virulent strain *Pst* DC3000 (Thilmony et al. 2006) was monitored at 48 hpi in local leaves. The *Pst* strains expressing specific Avr-genes were essentially indistinguishable from each other in their growth and induction for local *PR1* expression, whereas the virulent strain *Pst* DC3000 multiplied to a higher extent (Supplementary Figure 7A and B) (Zheng et al. 2012). *Pst ΔhrpS* grew significantly less than the aforementioned strains. *Pst AvrRpm1*, *Pst AvrRpt2* and *Pst* DC3000 did not provoke a strong gene induction prior to the priming response, whereas *Pst AvrRps4* exhibits elevated *PR1* induction at all-time points tested compared to mock (Supplementary Figure 7C). Based on these results, *Pst AvrRpm1* was selected as the ETI trigger and *Pst ΔhrpS* as the MTI trigger.

### 2.2.2 Duration of the systemic priming response

As mentioned above, the systemic resistance response can allow a broad spectrum of resistance against a wide range of phytopathogenic organisms. This phenomenon is already known since the early 1960s (Ross 1961a; Ross 1961b) and prompted me to test on newly emerged tissue of the same plant after local immune activation how long the systemic priming response lasts under my conditions. Recent studies show the transmittance of an immune memory to following generations of pathogen exposed parental plants. Such trans-generational SAR was transmitted over one stress-free generation after infection with *Hyaloperonospora arabidopsidis* (*Hpa*) or *Pst* DC3000 going along with changes on an epigenetic level of gene regulation (Luna et al. 2012; Pastor et al. 2012).

For this purpose it was tested, whether even newly emerged leaves (leaves not present at the stage of priming setting) show a memory response after local immune activation. To this end, plants were infected with *Pst* DC3000 or 10 mM MgCl<sub>2</sub> (as mock control) on local leaves and one week later newly

emerged leaves were tested, regarding their priming potential by assessing the gene expression of *PR1* and, another defense-related marker gene, *WRKY29*.

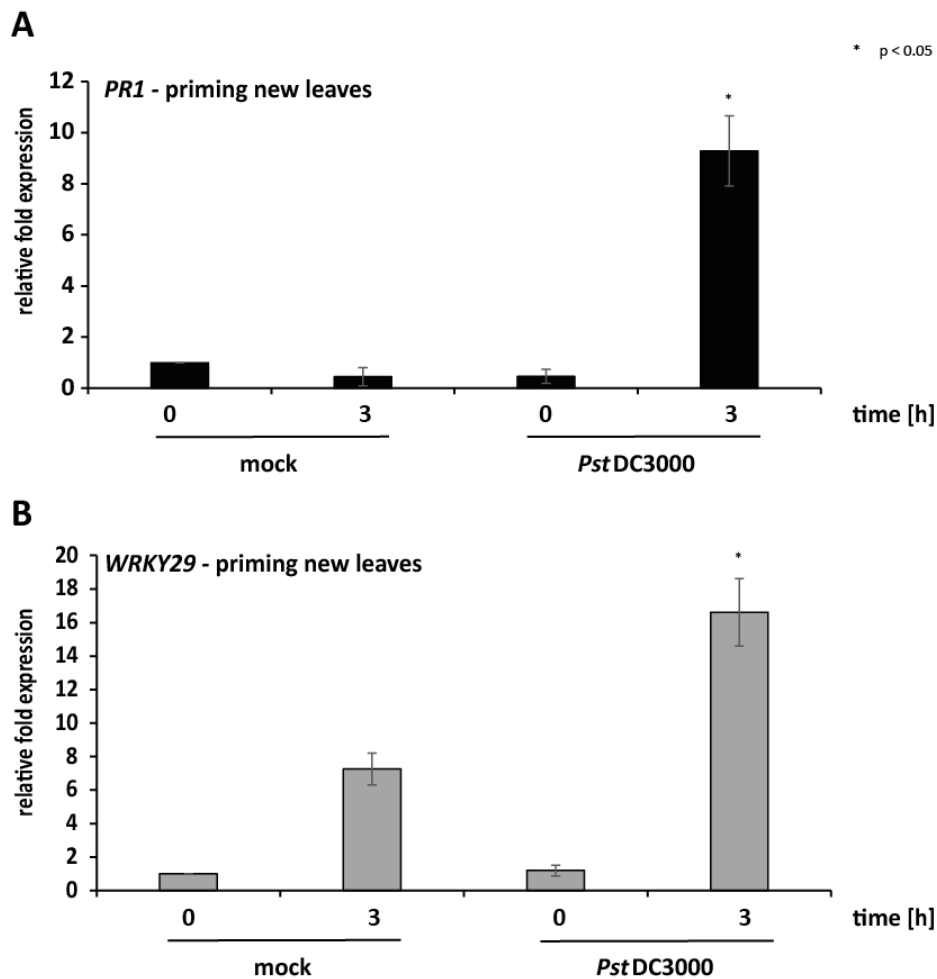


**Figure 7: Priming response assay in newly emerged leaves.**

Four-week-old WT plants were syringe-infiltrated with  $1 \times 10^6$  cfu/ml *Pst* DC3000 or 10 mM  $MgCl_2$  (mock). At 48 hpi the local leaves were removed and young leaves present at this growth stage were marked to distinguish those from newly emerged leaves. Seven days later, three newly emerged leaves were syringe-infiltrated with 1 nM flg22. Before (0 h) and 3 h after infiltration with 1 nM flg22, *PR1* (A) and *WRKY29* (B) transcript abundance was measured by qRT-PCR. Fold changes were calculated relative to mock samples at 0 h and normalized against the endogenous reference gene At4g26410. Error bars represent standard error (SE;  $n=2$ ) of two biological replicates with three technical replicates each, respectively. P-value of  $p < 0.05$ , indicated by asterisk, was calculated using Student's t-test comparing the gene expression 3 h after secondary stress treatment of primed vs. unprimed plants.

As illustrated in Figure 7, the *Pst* DC3000-priming response was stably transmitted to newly emerged leaves for both tested genes, *PR1* and *WRKY29*, compared to non-primed plants. A subsequent characterization of this phenomenon will reveal possible underlying mechanisms for an epigenetic memory of the plant as aforementioned.

## **2.3 Identification of genes involved in the MTI- and ETI-induced systemic transcriptional reprogramming and priming response**

The outputs of the immune activation are similar between MTI and ETI as recent publications demonstrate overlapping gene sets during transcriptional reprogramming (Tao et al. 2003; Navarro et al. 2004; Zipfel et al. 2006). Despite this high similarity of MTI and ETI signaling, emerging evidence also suggests differences in the use of signaling and transcriptional components, such as MPK6 and MPK3. They show a prolonged activation upon ETI to bypass the loss of the SA sector (Tsuda et al. 2013). Local MTI and ETI activation can trigger SAR in distal parts of the plant with overlapping principles (Mishina and Zeier 2007; Jing et al. 2011). This includes the use of SAR immune signals like SA and systemic expression of SAR marker like the *PR* genes (Navarova et al. 2012; Gruner et al. 2013). The identification of a general priming mechanism detectable in seedlings by using flg22 as a representative MAMP and the identification of differences between the MTI- and ETI-induced systemic transcriptional reprogramming, prompted me to perform a genome wide analysis using RNA sequencing (RNA-Seq). This analysis aimed to identify an inventory of genes associated with the differences in MTI- and ETI-induced systemic transcriptional reprogramming and priming.

### **2.3.1 RNA-Seq reveals qualitative and quantitative differences in the gene expression of MTI and ETI during SAR and the systemic priming response**

Four-week-old *Arabidopsis* wild type plants were infiltrated in local leaves with *Pst*  $\Delta$ *hrpS*, *Pst* *AvrRpm1* or 10 mM MgCl<sub>2</sub> (as mock control) of three biological replicates and systemic leaves were harvested at 48 hpi. This sample corresponds to the 0 h time point in the RNA-Seq experiment and represents the systemic status of gene expression after local immune activation (= SAR). To further assess genome wide transcriptional changes during the priming response, another three sets of plants were water-infiltrated in systemic leaves 48 h after the local immune activation and harvested 1 hpi (= priming response). The 1 h time point was chosen based on the findings presented in Figure 6 and the assumption that later time points results might mask the fast priming response genes by side effects going along with cell collapse related gene expression pattern caused by the water infiltration (Kohler et al. 2002; Beckers et al. 2009; Jaskiewicz et al. 2011). Furthermore, the analysis of systemic tissue 48 h after the local induction of MTI and ETI would allow a correlation with published studies, whereas the second time point 1 h after the elicitation of a systemic priming response could give new insights into the coordination and pattern of the systemic priming response, which was not explored previously.

The first raw data analyses showed that the aimed 10.000.000 reads per sample were reached by most of the samples. For some even more reads could be generated, but for six samples less reads were

gained (Table 1). Of note, around 90 % of the reads could be mapped onto the *Arabidopsis* genome with one outlier (mock 0 h, replicate II). Here, an extraordinary high number of sequenced reads was obtained of which only 50 % could be assembled on the template genome. Careful analysis of this sample revealed contamination of foreign non-*Arabidopsis* genomic information. After subtraction of these sequences, the remaining ones were aligned to *Arabidopsis* with around 90 % coverage, which was then used for further analyses (Supplementary Figure 8A).

**Table 1: Number of sequenced and aligned reads.**

	Replicate	mock		<i>Pst ΔhrpS</i>		<i>Pst AvrRpm1</i>	
		0 h	1 h	0 h	1 h	0 h	1 h
<b>sequenced reads</b>	I	8.741.202	12.847.762	9.711.684	9.560.356	9.256.313	9.789.865
	II	41.934.785	24.111.645	7.058.954	8.504.654	6.721.292	7.386.773
	III	5.715.823	9.304.403	6.825.523	8.868.948	28.474.062	7.107.818
<b>aligned reads</b>	I	7.814.488	11.999.233	9.168.014	8.976.616	8.558.729	8.620.102
	II	22.164.116	22.288.293	6.529.702	7.933.783	5.991.849	6.930.219
	III	5.389.010	8.690.249	6.303.173	8.283.223	26.955.483	6.765.530

The multi-dimensional scaling (MDS) plot demonstrates that the samples obtained at 0 h and 1 h cluster together. Furthermore, at 0 h the control sample can be subdivided from the pathogen-induced tissue samples, which is in accordance with the findings of other aforementioned studies. Interestingly, at 1 h the clustering of the genes assigned to the three treatments got further split up, now having a clear separation in systemic priming-associated transcriptional reprogramming of *Pst ΔhrpS* (= MTI) and *Pst AvrRpm1* (= ETI) (Supplementary Figure 8).

Subsequently, the gene set profiles were obtained at both time points by comparing *Pst ΔhrpS* vs. mock and *Pst AvrRpm1* vs. mock. To further assess these gene sets, the number of MTI- and ETI-specific differentially expressed genes of the 0 h and 1 h time point with a  $\log_2FC$  of more than 1 were extracted, respectively, and illustrated in a Venn diagram.

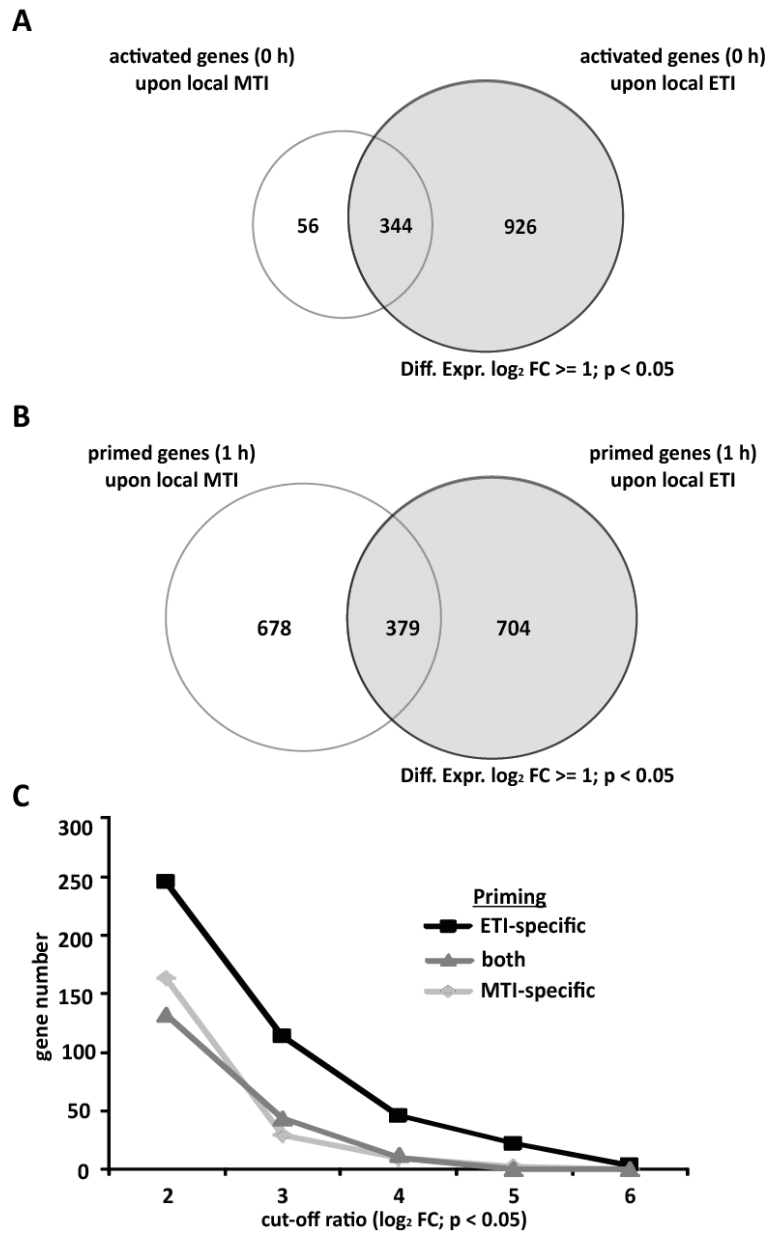


**Figure 8: MTI- and ETI-specific differentially expressed genes during SAR and systemic priming.**

(A) Venn Diagram showing the number of genes in systemic tissue (0 h) being differentially expressed compared to mock with  $\log_2 FC \geq 1$  and  $p < 0.05$  at 48 h after local MTI or ETI activation.

(B) Venn Diagram showing the number of genes in systemic tissue 1 h after water infiltration being differentially expressed compared to mock with  $\log_2 FC \geq 1$  and  $p < 0.05$  at 48 h after local MTI or ETI activation.

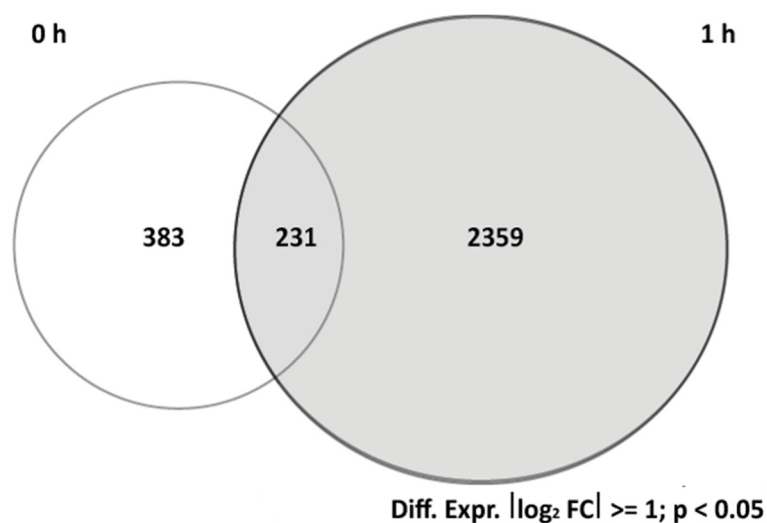
(C) Number of differentially expressed genes after water stimulation in a manner specific to MTI or ETI or common to the two with an increasing cut-off ratio.

Figure 8A clearly indicates that a higher proportion of genes were upregulated upon local ETI activation than after MTI in accordance with the aforementioned findings, indicating that ETI induces a stronger SAR response than MTI. This observed difference was erased at the 1 h time point during the systemic priming response as almost equal numbers of genes were differentially upregulated (Figure 8B).

Both figures indicate, that there are quantitative differences between MTI and ETI in the systemic priming target gene sets, which is further supported by the results shown in Figure 8C. Here, an

increasing cut-off ratio regarding the  $\log_2FC$  of genes differentially expressed at 1 h was applied. It can be concluded from this analysis, that ETI is more powerful in the systemic priming response than MTI and that the commonly used gene set is dependent on both MTI and ETI. Additionally, the Venn diagrams also demonstrates differences in the target gene sets used at 0 h and 1 h.

The unexpected high number of qualitative differently used genes at 0 h and 1 h was further assessed by comparing the number of genes, which were differentially expressed at 0 h and 1 h between mock vs. *Pst ΔhrpS* and mock vs. *Pst AvrRpm1*, respectively. These numbers obtained from 0 h and 1 h were then compared regarding their significant difference between MTI and ETI. The Venn diagram in Figure 9 shows the summary of this analysis.



**Figure 9: Venn diagram illustrating the number of genes with significant differences between MTI and ETI during SAR and the systemic priming response.**

Venn diagram analysis showing the number of gene sets identified as significantly different between MTI and ETI at 0 h and 1 h considering a cut-off of  $\log_2 FC \geq 1$  and  $\log_2 FC \leq -1$  with a p-value of 0.05.

As clearly demonstrated, more genes are differentially expressed between MTI and ETI at 1 h in the systemic priming response as during SAR (at 0 h), which supports the aforementioned findings of the MDS plot (Supplementary Figure 8B). In sum it can be said, that MTI and ETI use different gene sets during systemic immunity, which becomes more prominent in the systemic priming response.

### **2.3.2 The Top100 differentially expressed genes between MTI and ETI during SAR and the systemic priming response could be grouped into 12 clusters**

After the identification of a larger subset of differentially regulated genes between MTI and ETI during the systemic priming response, also a layer of functionality was added to the RNA-Seq analysis to provide further insights and new priming marker genes. To this end, the Top100 most significant differentially expressed genes for each comparison, mock vs. *Pst ΔhrpS* and mock vs. *Pst AvrRpm1* at 0 h and 1 h, were extracted, respectively. The union of these gene sets was then visualized in a heatmap

by clustering the genes according to their expression pattern with  $\log_2FC \geq 1$  and  $\log_2FC \leq -1$  with a p-value of  $p < 0.05$ , which yielded 12 clusters (Figure 10).

The corresponding trace plot (Supplementary Figure 9) further supports the cluster differences for the two time points and treatments. Of note, *PR1* was also found in this analysis in cluster XI (Figure 10) and the expression pattern was corresponding to the aforementioned observed expression profile by qRT-PCR during SAR and the systemic priming response after local MTI and ETI elicitation (Supplementary Figure 10A, Figure 6).

*CHALCONE SYNTHASE (CHS)*, which is present in cluster IX, encodes the first essential enzyme for the flavonoid synthesis and is shown to be downregulated upon MAMP application (Figure 10) (Saijo et al. 2009; Serrano et al. 2012). Interestingly, it mirrors the expression pattern of *PR1* of being less expressed during the ETI-induced priming response. This illustrates, that the RNA-Seq data also reveals several downregulated or less expressed genes, which is in accordance to the findings that a large proportion of such genes in the distal unchallenged tissue upon local immune activation is associated with cell wall remodeling, biosynthesis of secondary metabolites or the JA pathway. With this mechanism, the plant might redirect its energy sources towards anti-(hemi)biotrophic defense response (Gruner et al. 2013). This assumption was validated e.g. for cluster I, which showed a large proportion of genes being downregulated during SAR and an significant enrichment of gene ontology (GO) terms associated with JA and several biosynthetic processes (Supplementary Figure 12A).

During this study I focused on the identification of new systemic priming genes associated with an upregulation of the respective gene. Such a gene can be used as a biomarker for a successfully primed plant without or with a minimum level of defense gene expression during the priming process to ensure low fitness costs for the plant by mounting a higher gene expression during secondary immune activation.

A priming positive gene was defined as a) not being upregulated during SAR, either upon local MTI- or ETI-elicitation and exhibiting enhanced gene expression during the defense-induced priming response and b) being upregulated during SAR and illustrating an further enhanced gene transcription profile during the priming response, indispensable if MTI- or ETI-specifically and being higher expressed in an ETI-specific manner than MTI. According to the heatmap and trace plot visualization this holds true for cluster V and VI for a) and for cluster XI and XII for b).

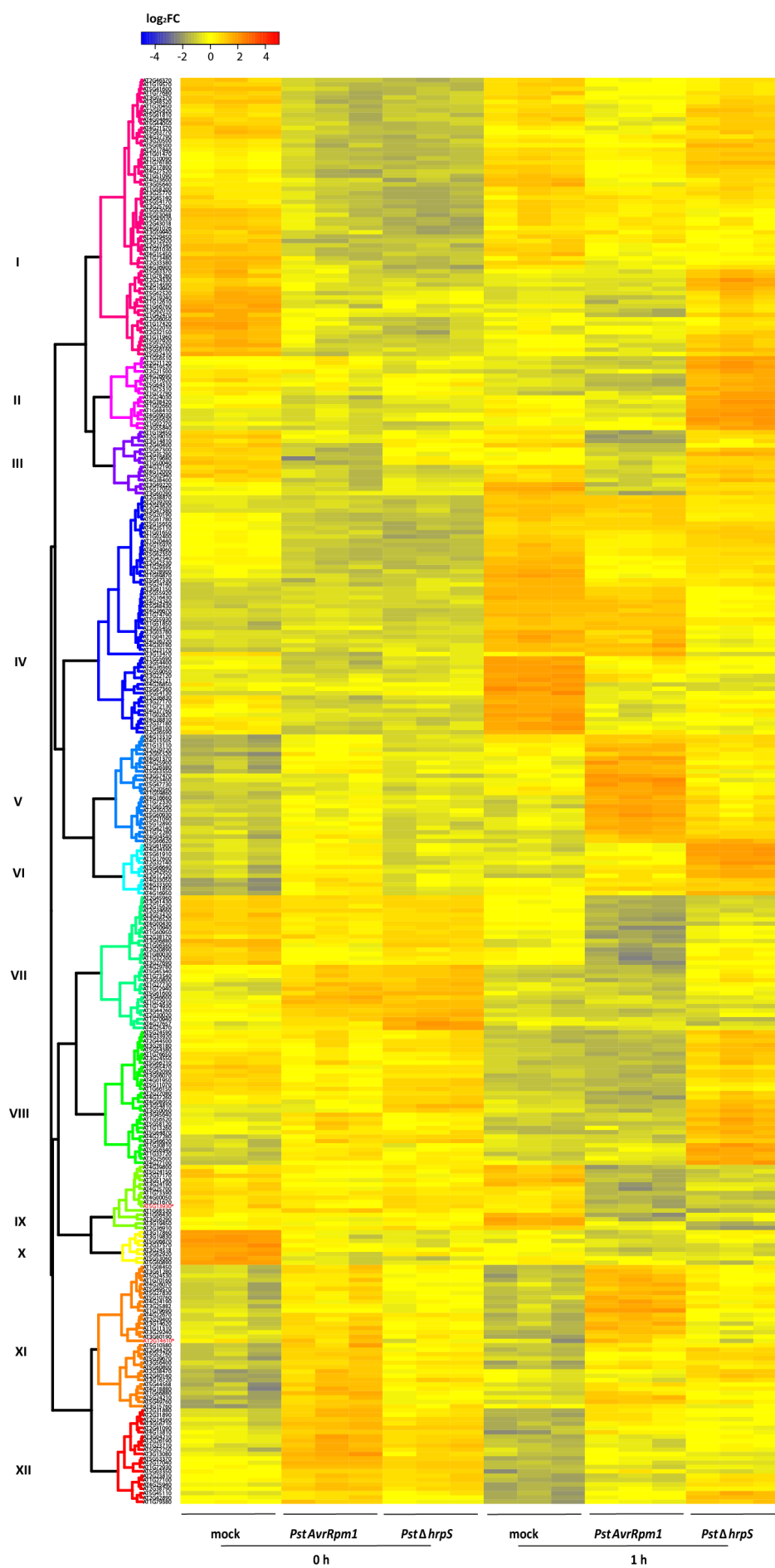


**Figure 10: Heatmap of the Top100 differentially expressed genes at 0 h and 1 h upon local MTI and ETI activation.**

The Top100 most significant genes for each comparison, mock vs *Pst ΔhrpS* and mock vs *Pst AvrRpm1* at 0 h and 1 h, respectively, were extracted and the union gene set was used for heatmap visualization. Genes were clustered according to their expression pattern  $\log_2FC \geq 1$  and  $\log_2FC \leq -1$  with a p-value of  $p < 0.05$  using complete linkage hierarchical clustering with the Pearson correlation as distance measure. Cutting the obtained dendrogram at height 1 yielded 12 clusters of expression patterns. Each column represents one biological replicate. The color code of the heatmap indicates the up- or downregulation of gene expression as indicated in the legend on top. Indicated with red letters is the expression of *CHS* (At5g13930) and *PR1* (At2g14610).

Interestingly, the functional gene categorization by GO term analysis of all genes included in the heatmap revealed no clear association with a specific GO, which points to the divergent regulation of the plants gene expression upon stress exposure (Supplementary Figure 11). In order to reveal new priming target genes, it was decided to perform the subsequent analysis with selected clusters based on their expression pattern and GO term assignment.

Not for all clusters significant GO terms could be found and for several the response to abiotic stimuli, water or wounding was prominent, probably entailed by the syringe-infiltration of the pathogen in local leaves or the water infiltration as priming stimulus in systemic leaves. Interestingly, cluster VI and XI are significantly enriched with GO terms assigned to defense response and immune system (Supplementary Figure 12GC). Cluster V and XII did not show a significant GO term association, but they display an interesting expression pattern. Cluster V genes were less expressed during SAR (= 0 h) at all conditions and get solely higher expressed during the ETI-induced priming response. A similar tendency was observed for cluster VI, but for the MTI-priming response. Cluster XI and XII were chosen based on the fact that the genes were less induced or not expressed in the mock treated systemic and priming samples, but upregulated upon pathogen treatment at 0 h and 1 h by being higher expressed in the priming response (Figure 10).

### 2.3.3 Selected gene cluster provide new priming marker genes

These findings encouraged me to evaluate selected marker genes for each cluster during systemic immune activation and during the priming response. To this end, local leaves of wild type plants were syringe-infiltrated with 10 mM  $MgCl_2$  (as mock control), *Pst ΔhrpS* or *Pst AvrRpm1*. The gene expression pattern of selected marker genes was assessed in systemic tissue by qRT-PCR before (SAR, = 0 h) or upon secondary treatment (priming response, = 1 h) in a time course to rule out that the observed gene expression pattern rely on timing differences of the MTI- and ETI-induced gene expression.

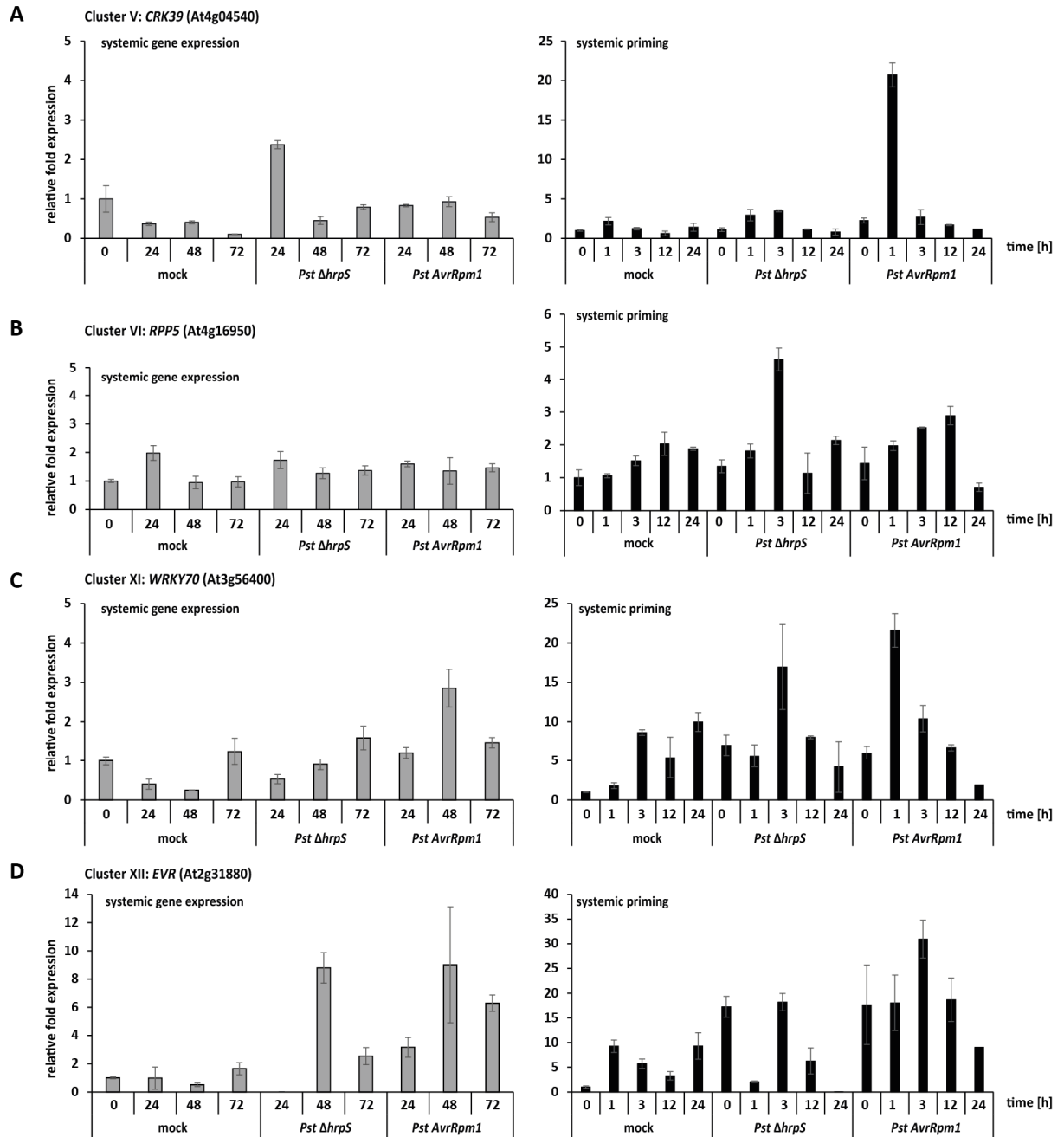


**Figure 11: Marker gene analysis of cluster V, VI, XI and XII.**

Four-week-old WT plants were syringe-infiltrated in three well-expanded local leaves with 10 mM  $MgCl_2$  (mock),  $1 \times 10^8$  cfu/ml *Pst ΔhrpS* or  $1 \times 10^6$  cfu/ml *Pst AvrRpm1*. Systemic gene expression was assessed by harvesting systemic leaves at the indicated time points after local infection (left column). For systemic priming response (right column), at 48 hpi local infiltrated leaves were removed and systemic leaves infiltrated with water. At the indicated time points leaf tissues were harvested and transcript abundance was measured by qRT-PCR for *CRK39* (A), *RPP5* (B), *WRKY70* (C) and *EVR* (D). Fold changes are calculated relative to mock WT samples at 0 h and normalized against the endogenous reference gene At4g26410. Error bars represent standard deviation (SD; n=3) of one biological replicate with three technical replicates.

For cluster V, the gene *CYSTEINE-RICH RLK 39* (*CRK39*) was chosen. *CRK39* belongs to the family of RLKs containing cysteine-rich repeats in their extracellular domain and it was shown to be induced upon pathogen infection. For some family members of *CRK39*, namely *CRK5*, 6, 10 and 11 a role in the

regulation of hypersensitive cell death was reported (Du and Chen 2000; Chen et al. 2003; Chen et al. 2004). The transcript profile of *CRK39* in systemic tissue showed no clear elevated expression, whereas the gene was specifically induced during the ETI-induced systemic priming response. This is in agreement with the aforementioned expression profile observed in the RNA-Seq results (Figure 11).

Cluster VI genes were associated with defense execution and contains also immune-related genes like *BONZAI 1 (BON1)* (Zou et al. 2014). As marker gene for this cluster *RECOGNITION OF PERONOSPORA PARASITICA 5 (RPP5)* was selected (van der Biezen et al. 2002; Bailey et al. 2011; Wang et al. 2011), which showed an MTI-priming specific enhanced gene expression without being transcribed during SAR (Figure 11B).

Cluster XI genes also correlated with defense response (Supplementary Figure 12G) and encode numerous defense-responsive genes like *WRKY33*, *NIM1-INTERACTING 2 (NIMIN2)*, *PR1* and *WRKY70* (Li et al. 2004; Alvarez-Venegas et al. 2007; Logemann et al. 2013; Shim et al. 2013). The gene expression of *WRKY70* resembles the expression pattern seen for *PR1* by being higher expressed in systemic tissue after ETI-induction than MTI, which is the same for the ETI- and MTI-induced systemic priming response (Figure 11C).

In cluster XII, beside the *NONEXPRESSER OF PATHOGENESIS-RELATED 3 (NPR3)* gene as SA-receptor (Fu et al. 2012), the gene *EVERSHED (EVR)* was assigned, for which recent publications raised an involvement in plant defense (Liebrand et al. 2013; Zhang et al. 2013b; Liebrand et al. 2014). *EVR* was upregulated during pathogen-induced SAR compared to mock in a similar way as in local MTI- and ETI-elicitation and displayed an enhanced ETI-induced systemic priming response (Figure 11D).

In sum, no obvious differences in the timing of the MTI- and ETI-induced systemic gene expression and priming response was detectable during the time course. This validates on the one hand the aforementioned RNA-Seq results and on the other hand the ability of the priming response in the usage of different sets of genes.

### **2.3.4 Meta-expression analysis of SA-impact on systemic immunity**

SA as central signaling component is inalienable for the establishment of SAR in both local and systemic leaves and mutants exhibiting a SAR-deficient phenotype are often defective in SA signaling (Durrant and Dong 2004). To this end, the genes defined in the four different clusters were cross-referenced with public available transcriptome database by an *in silico* approach using Genevestigator V3 (Hruz et al. 2008).

Interestingly, comparing the selected genes of the four defined clusters with the respective transcriptome data revealed that the majority of the clustered genes were induced upon SA treatment in wild type plants and not expressed or downregulated in the *npr1* and *sid2* mutants. Of note,

inoculation with an avirulent ETI-inducing *Pst* strain could overcome the SA-dependency in *sid2* mutant plants (Figure 12).

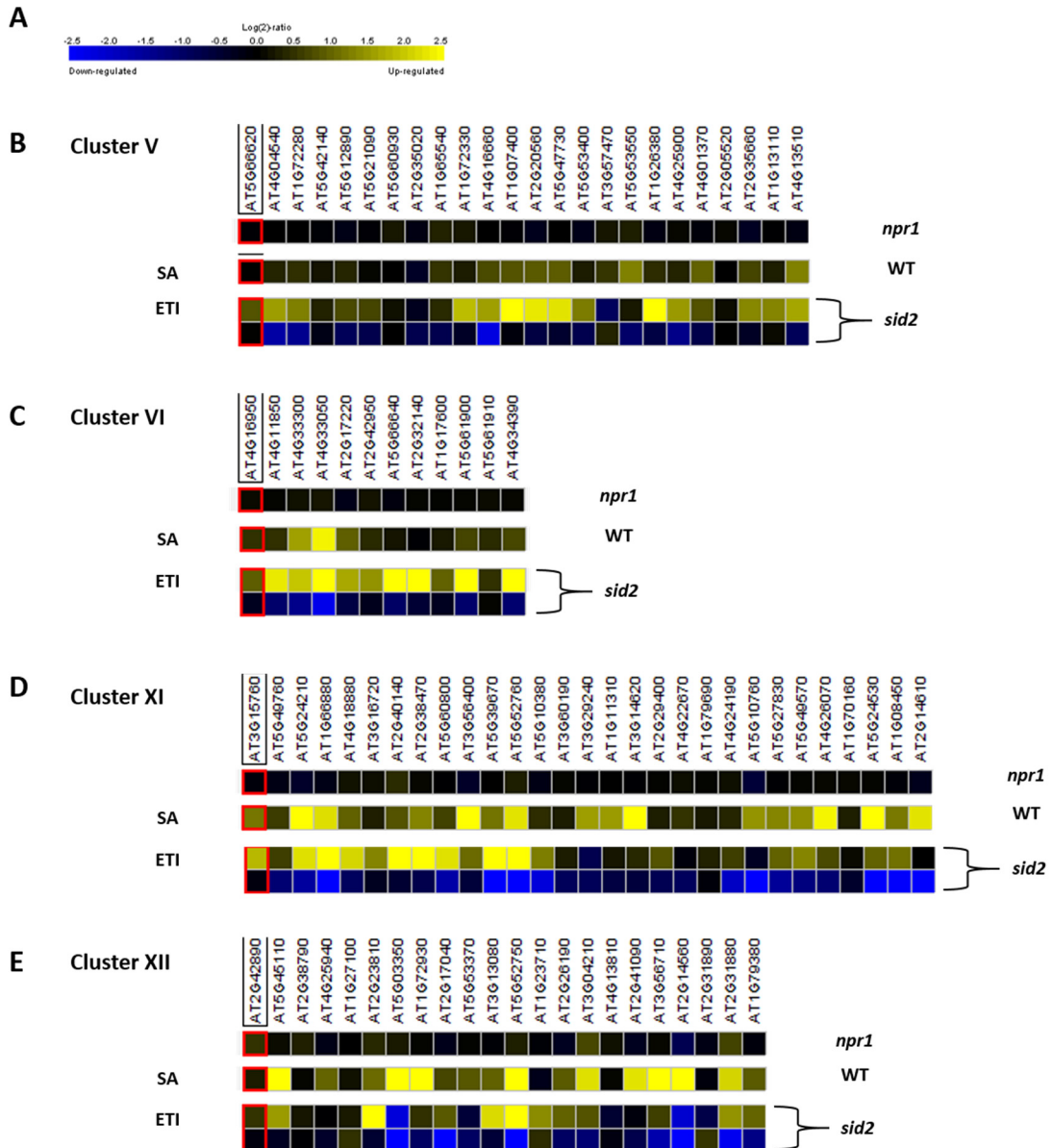


**Figure 12: Genevestigator analysis of cluster V, VI, XI and XII.**

Relative expression analysis of genes from cluster V (B), VI (C); XI (D) and XII (E) upon SA and avirulent pathogen (ETI) treatment in WT and mutant plants using Genevestigator V3 (Hruz et al. 2008). Relative gene expression is represented in color-coding from blue (downregulated) to yellow (upregulated) as depicted in (A).

These findings could be cross-referenced with obtained qRT-PCR data for *PR1*, indicating the NPR1-dependency of SAR and the systemic priming response for both MTI and ETI, but also the ability of ETI to circumvent the loss of SA in *sid2* (Supplementary Figure 13). The qRT-PCR results are supported by findings that SAR also occurs upon local ETI- and prolonged MAPK activation in *sid2* plants (Y. Wang, personal communication). Further experiments will clarify the spatial and temporal requirement of SA during MTI- and ETI-induced systemic immunity and priming response.

Taken together, it can be hypothesized that genes involved in SAR and the priming response require NPR1 for the proper systemic activation and priming of defenses, whereas SA is most likely indispensable for systemic immune activation and priming response after MTI, but dispensable after ETI.

### **2.4 Elucidating the role for PcG- and trxG proteins in the systemic priming response**

The identification of several SAR- and priming response related genes by the RNA-Seq analysis, including those that show MTI and ETI specificity, support the idea of a global regulation of a larger gene set in order to prepare the naïve tissue for further immune activation. This goes along with a memory of the first mode of activation, whether it was MTI or ETI. These aspects of the systemic priming response predict the need for mechanisms that enables fast and flexible regulation for the expression of a larger gene set in a similar manner. This also implies the possibility of a memory of gene expression transmitted by a yet unknown mechanism from local challenged sites to the distal part of the plant. One effective way to meet such requirements could be achieved by dynamic changes of chromatin modifications on specific gene loci. During this study, I focused on specific histone modification changes that are known to be correlated with a transcriptional memory of gene expression such as H3K4me3 and H3K27me3 as mentioned in 2.1 (Zhang and Reinberg 2001; Fuchs et al. 2006; Kouzarides 2007a; Zhang 2008; Roudier et al. 2009; Berr et al. 2011).

To get a first hint for a possible involvement of specific histone modifiers in the systemic immune and priming response, it was tested whether *atx1-4*, *atx1-2*, *clf-28* and *swn-7* were impaired in SAR using *Hpa* as systemic immune trigger upon local SAR induction. The experiment clearly showed a failure of these mutants to develop a full SAR response and a reduced basal immunity in systemic leaves except *swn-7* (Supplementary Figure 14). Interestingly, the *swn-7* mutant showed a more wild type-like pattern, which is in agreement with the redundant function of CLF and SWN during plant development (Chanvivattana et al. 2004; He et al. 2012).

Thus, it was tested whether ATX1 and CLF play a role in the systemic priming response and in the differentiation of MTI- and ETI-induced priming. This would add one link between stress responses, histone modifications and the potential causative players for it.

### 2.4.1 ATX1 and CLF are indispensable for the difference of the MTI- and ETI-induced systemic priming response

In order to assess a possible involvement of ATX1 and CLF in the regulation of a systemic priming response, it was tested whether *atx1* and *clf* plants were impaired in systemic immunity. To this end, wild type, *atx1-4*, *atx1-2*, *clf-28* and *npr1* as SAR-deficient plant (Kohler et al. 2002; Durrant and Dong 2004), were syringe-infiltrated in local leaves with 10 mM MgCl<sub>2</sub> (as mock control, M), *Pst*  $\Delta$ *hrpS* (H) or *Pst* *AvrRpm1* (R). Two days later the systemic leaves were infected with *Psm* and the bacterial growth in systemic tissue was evaluated.

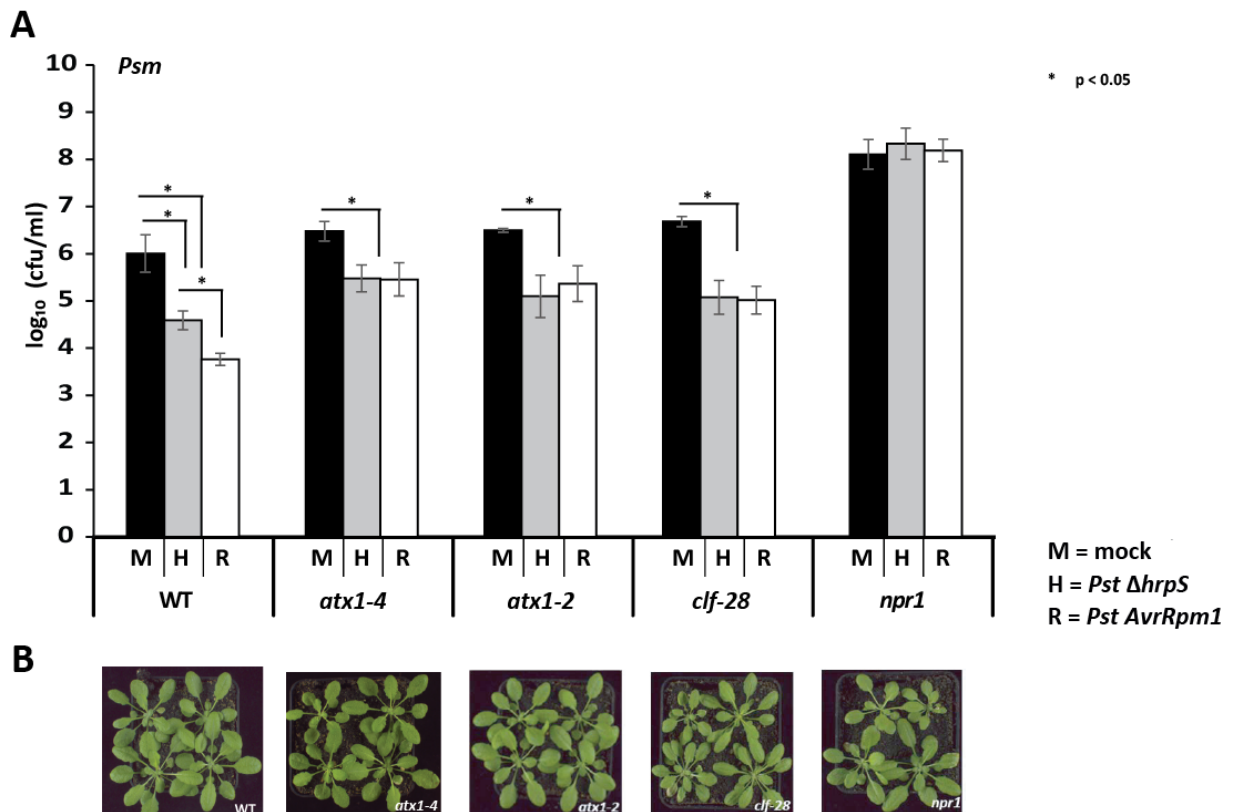


**Figure 13: MTI- and ETI-induced systemic immunity assay using *Psm*.**

(A) Four-week-old plants were syringe-infiltrated in three well-expanded local leaves with 10 mM MgCl<sub>2</sub> (mock, M), 1x10<sup>8</sup> cfu/ml *Pst*  $\Delta$ *hrpS* (H) or 1x10<sup>6</sup> cfu/ml *Pst* *AvrRpm1* (R). At 48 hpi systemic leaves were syringe-infiltrated with 1x10<sup>4</sup> cfu/ml *Psm*. Three days later, *Psm* was re-isolated and the bacterial growth evaluated. Error bars represent standard error (SE; n=4) of four biological replicates with six technical replicates each, respectively. P-value, indicated by asterisk, was calculated using Student's t-test.

(B) Morphological appearance of 4-week-old plants grown under short day conditions.

As mentioned above, ETI activation is capable of inducing a stronger immune activation compared to MTI (Tsuda and Katagiri 2010). This was also detectable in wild type plants in a systemic immune response, where local MTI activation leads to a reduced bacterial growth of *Psm* of more than one log<sub>10</sub> difference. This was further dampened after ETI activation for additional 1.5 log<sub>10</sub> units, so that ETI alone is capable of decreasing the bacterial growth threefold (Figure 13A). As expected, *npr1* was not able to mount systemic immunity (Durrant and Dong 2004).

Of high interest was the finding that *atx1* and *clf-28* were able to exhibit a reduction of pathogen growth upon immune activation albeit the fact that they show a slightly lowered basal resistance. Furthermore, they fail to show the quantitative differences between MTI- and ETI-induced systemic immunity compared to wild type plants (Figure 13A). So it can be concluded that ETI causes a more efficient systemic immunity than MTI in an ATX1- and CLF-dependent manner.

To underline these findings, the systemic priming response of *PR1* was monitored in systemic leaves before and after water infiltration upon local MTI and ETI activation. In accordance with the observed systemic immune activation pattern, the systemic priming response assay revealed a similar trend. Again, *PR1* was shown to be differentially activated upon MTI- and ETI-induced priming as shown in Figure 6 and dependent on NPR1 (Figure 12). In *atx1-4* and *clf-28* a significantly reduced priming response was detectable after ETI-priming induction similar to the one observed after MTI-priming in wild type plants (Figure 14). This corresponds also to the level of immune activation in the *Psm* SAR assay (Figure 13), which together strengthens the hypothesis that functional trxG and PcG protein complexes are required to differentiate between MTI and ETI priming.

To cross-reference the priming output with a natural secondary infection of systemic tissue, *Psm* was also used as another second stimulus in the systemic priming assay (modified after (Navarova et al. 2012)). The results validated the aforementioned conclusions regarding the role for ATX1 and CLF obtained with the assay using water infiltration as a priming response trigger (Supplementary Figure 15).

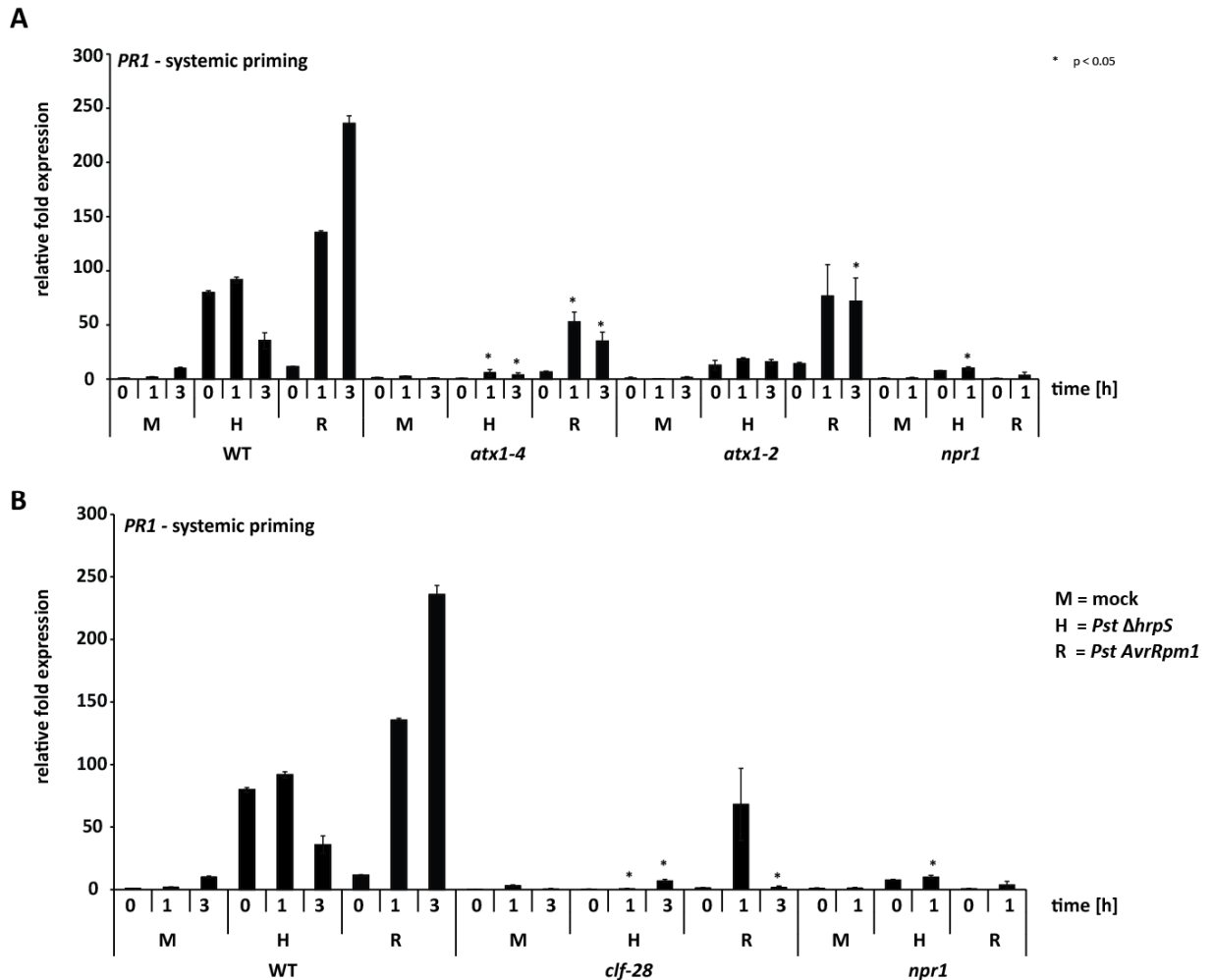


**Figure 14: Systemic priming response assay in *trxG* and *PcG* mutant plants.**

Four-week-old plants were syringe-infiltrated in three well-expanded local leaves with 10 mM  $MgCl_2$  (mock, M),  $1 \times 10^8$  cfu/ml *Pst ΔhrpS* (H) or  $1 \times 10^6$  cfu/ml *Pst AvrRpm1* (R). At 48 hpi infiltrated leaves were removed and systemic leaves infiltrated with water. At the indicated time points, *PR1* transcript abundance was measured by qRT-PCR in WT, *atx1-4*, *atx1-2* and *npr1* (A) and in WT, *clf-28* and *npr1* (B). Fold changes are calculated relative to mock WT samples at 0 h and normalized against the endogenous reference gene *At4g26410*. Error bars represent standard error (SE; n=2) of two biological replicates with three technical replicates each, respectively. P-value of  $p < 0.05$  indicated by asterisk, was calculated using Student's t-test comparing gene expression at 1 hpi and 3 hpi, respectively, for *atx1-4*, *atx1-2*, *clf-28* and *npr1* to the respective WT expression.

#### 2.4.2 ATX1 and CLF exhibit a wild type-like local immune activation

The aforementioned findings encouraged me to test whether local and/or systemic responses are impaired in the histone modifier mutants. This could gain insight into where the histone modifiers act during systemic immunity and priming response (Fu and Dong 2013).

To test this, the local immune activation capability of wild type, *atx1-4*, *atx1-2*, *clf-28* and *npr1* plants was determined by measuring the bacterial growth of *Pst ΔhrpS* and *Pst AvrRpm1* in local leaves at 48 hpi.

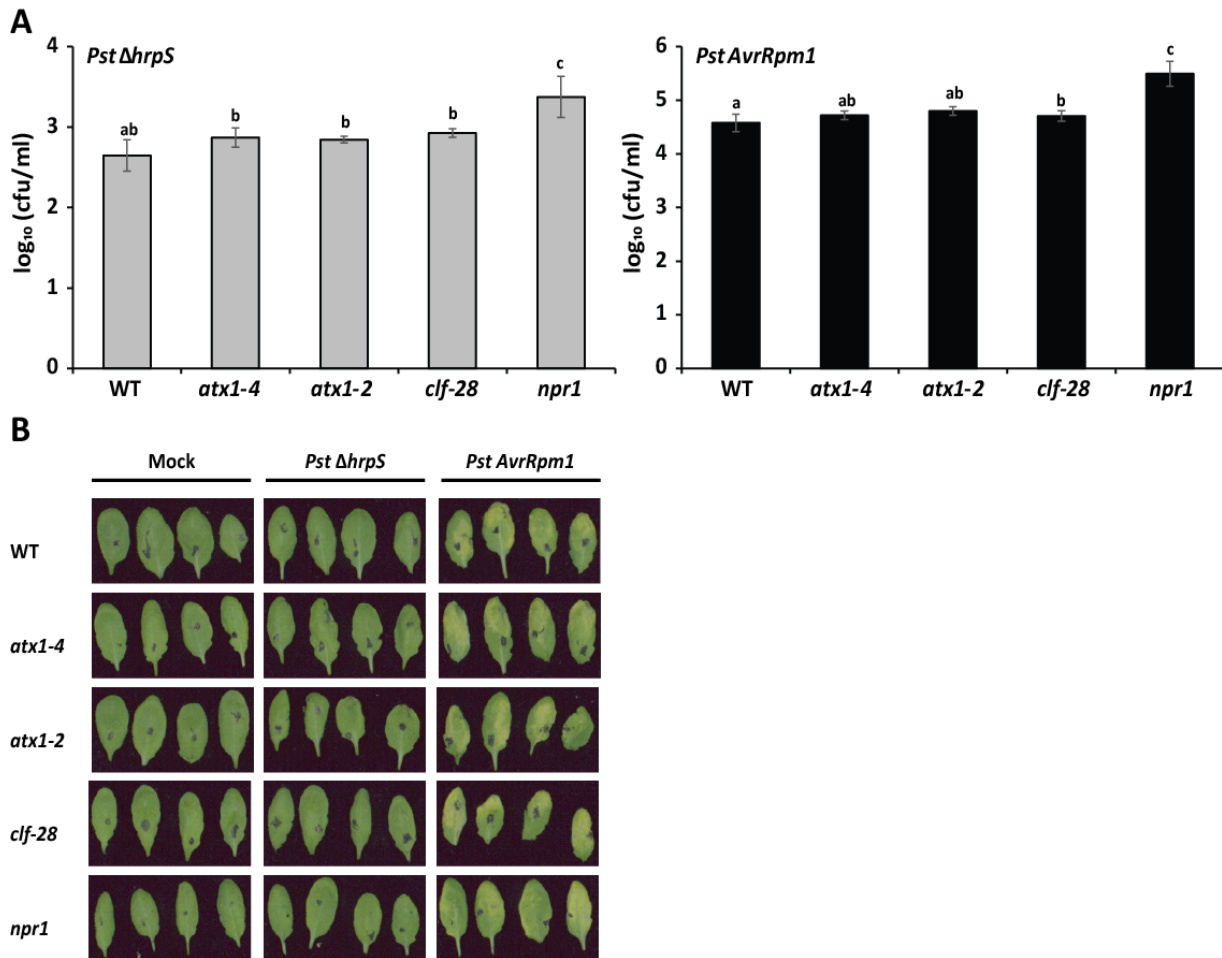


**Figure 15: Local immune response in *trxG* and PcG mutant plants.**

(A) Four-week-old plants were syringe-infiltrated in three well-expanded local leaves with  $1 \times 10^8$  cfu/ml *Pst ΔhrpS* or  $1 \times 10^6$  cfu/ml *Pst AvrRpm1*. At 48 hpi, bacteria were re-isolated and the bacterial growth was evaluated. Significant effects were identified by analysis of variance (ANOVA) and post hoc testing using Tukey contrasts. Statistical significance was defined as  $p < 0.05$  and indicated by different letters (a, b, c). Error bars represent standard error (SE:  $n=4$ ) of four biological replicates with six technical replicates each, respectively.

(B) Macroscopic appearance of disease symptoms of local leaves at 48 h post infiltration with 10 mM  $MgCl_2$  (mock),  $1 \times 10^8$  cfu/ml *Pst ΔhrpS* or  $1 \times 10^6$  cfu/ml *Pst AvrRpm1*. Four representative leaves of one biological replicate are shown. Experiment was repeated four times with similar results (see (A)).

As shown in Figure 15A, the bacterial growth in local leaves was not significantly different between the wild type and mutants after inoculation with *Pst ΔhrpS* and *Pst AvrRpm1* in the histone modifier mutant plants *atx1-4*, *atx1-2* and *clf-28*. Of note, *npr1* displayed lowered local resistance, along with the failure to develop systemic immunity and priming response (Figure 14A). These conclusions were further strengthened by the macroscopic disease symptoms appearance, where no obvious differences were visible in the development of HR upon ETI elicitation (Figure 15B).

The finding that ETI-associated local immune response in *atx1* and *clf* mutant plants is similar to wild type responses is in good agreement with the fact that RPM1-induced cell death, the hypersensitive response in infected tissues, is not altered in the tested *trxG* and PcG protein mutants as quantified by electrolyte leakage measurement (Supplementary Figure 16).

### 2.4.3 Total levels of H3K4me3 and H3K27me3 do not significantly differ in systemic tissue upon local MTI or ETI activation

Genetic evidence identified a requirement of ATX1 and CLF for the differentiation between the MTI- and ETI-induced systemic priming responses, despite a wild type-like immune activation at the pathogen challenged sites in *atx1* and *clf-28* mutant plants. This is in accordance with studies demonstrating the tissue- and developmental specificity for trxG and PcG protein complexes (Alvarez-Venegas and Avramova 2005; Saleh et al. 2008a; Saleh et al. 2008b; Farrona et al. 2011). PcG and trxG complexes and their catalytic subunits are supposed to be capable of the deposition of histone marks, H3K27me3 and H3K4me3, at their target chromatin loci, thereby playing complementary roles in silencing and activation of therein (Alvarez et al. 2010).

In order to reveal possible changes of H3K4me3 and/or H3K27me3 in systemic tissue upon local MTI or ETI activation, the total protein levels of these marks were assessed by SDS-PAGE and western blot analysis. To this end, chromatin extracts obtained from systemic leaves 48 h after the inoculation with 10 mM MgCl<sub>2</sub> (as mock control, M), *Pst ΔhrpS* (H) or *Pst AvrRpm1* (R) was used to enrich the histone protein signals. As the general protein levels were not detectable by e.g. the Bradford method (Bradford 1976) an equal volume of protein extracts on the tissue amount basis was loaded on the gel for each sample. The signals obtained from each sample after probing the membrane with H3K4me3 and H3K27me3 specific antibodies were then calculated relative to the signal obtained from the H3 specific antibody, which allowed me to obtain the presented relative values.

## Results

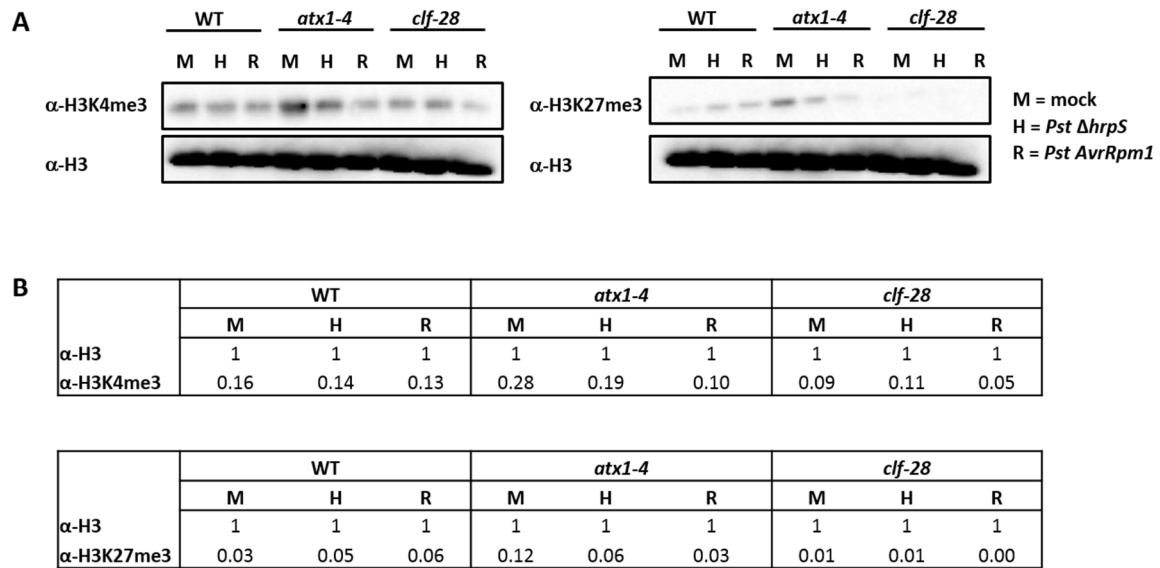


**Figure 16: Histone mark survey of H3K4me3 and H3K27me3 in systemic leaves of WT, *atx1-4* and *clf-28* upon local MTI- and ETI-activation.**

(A) Four-week-old plants were syringe-infiltrated in three well-expanded local leaves with 10 mM MgCl<sub>2</sub> (mock, M), 1x10<sup>8</sup> cfu/ml *Pst ΔhrpS* (H) or 1x10<sup>6</sup> cfu/ml *Pst AvrRpm1* (R). At 48 hpi systemic leaves were harvested and chromatin extracted. Chromatin extract was subjected to SDS-PAGE and western blot analysis probing the membrane with α-H3K4me3, α-H3K27me3 and α-H3, detecting the unmodified C-terminal part of H3. One representative result is depicted.

(B) Relative protein abundance of H3K4me3 and H3K27me3 to H3, (set as 1), respectively.

Replicates are depicted in Supplementary Figure 17.

The quantification results indicate that the levels of H3K4me3 were not significantly different between M, H and R in WT when comparing both replicates (Figure 16, Supplementary Figure 17). A decrease of H3K4me3 in the order of M > H > R in *atx1-4* was detected, although there is no severe loss of H3K4me3 in this mutant, which might be explained by the redundancy between five ATX and seven ATXR proteins in *Arabidopsis*, of which some were shown to exhibit H3K4 methyltransferase activity. Those proteins might compensate for the loss of ATX1 in the total H3K4me3 levels (Figure 16) (Baumbusch et al. 2001; Pontvianne et al. 2010). In *clf-28* plants, a slight decrease of H3K4me3 levels was detected compared to those in wild type plants (Figure 16B).

H3K27me3 levels were also not highly different between the control treatment, MTI and ETI in wild type as indicated in the western blot and relative quantification. Although a slight decrease of H3K27me3 in the order of M > H > R was detectable in systemic tissue of *atx1* plants (Figure 16). The total H3K27me3 levels were strongly reduced in the *clf-28* mutant contrary to published results, which claim that CLF is mainly responsible for the deposition of H3K27me3 in differentiated cells, although it has largely overlapping function with SWN, so that only in the absence of both CLF and SWN H3K27me3 is virtually non-detectable (Farrona et al. 2011; Lafos et al. 2011; He et al. 2012) and (T. Zografou, PhD Thesis, 2013). Of note, the total protein level was already reduced of these samples, which might explain the failure to detect a reduced H3K27me3 level in *clf-28* by western blot.

In sum, it was shown that the total levels of H3K4me3 and H3K27me3 do not significantly differ in systemic tissue of wild type plants between the different local immune triggers. This implies a more defined mechanism that changes histone modifications on specific gene loci, which might be important for the proper MTI- and ETI-induced systemic priming responses and the differences between them.

#### **2.4.4 H3K4me3 and H3K27me3 are enriched on *PR1* upon ETI-induced systemic priming**

Previous studies demonstrated that *PR1* shows enhanced H3K4me3 levels upon treatment with the SA analogue BTH (Mosher et al. 2006). H3K4me3 was also found to be enriched on several promoters of *WRKY* transcription factor-encoding genes upon pathogen challenges and BTH treatment, correlated with a systemic priming response. This mark was further enhanced after secondary systemic immune activation (Jaskiewicz et al. 2011).

The aforementioned findings that no significant changes of H3K4me3 and H3K27me3 were detectable in wild type plants at the total protein level in MTI- and ETI-primed systemic tissue encouraged me to test whether specific changes on the priming target gene *PR1* could be detected, since this marker gene shows a differentially priming response upon MTI and ETI activation in systemic tissue. It was tested whether MTI or ETI priming can cause a particular histone mark composition, as a possible basis for the priming response. The levels of H3K4me3 and H3K37me3 occurrence were determined from three different amplicons distributed over the *PR1* loci relative to the respective INPUT, followed by a normalization with the signal obtained from the DNA immunoprecipitated with  $\alpha$ -H3 for each sample (Figure 17) (Haring et al. 2007). This can incorporate possible differences in the nucleosome occupancy at these amplicons, which can be changed during transcription or repression (Henikoff and Shilatifard 2011).

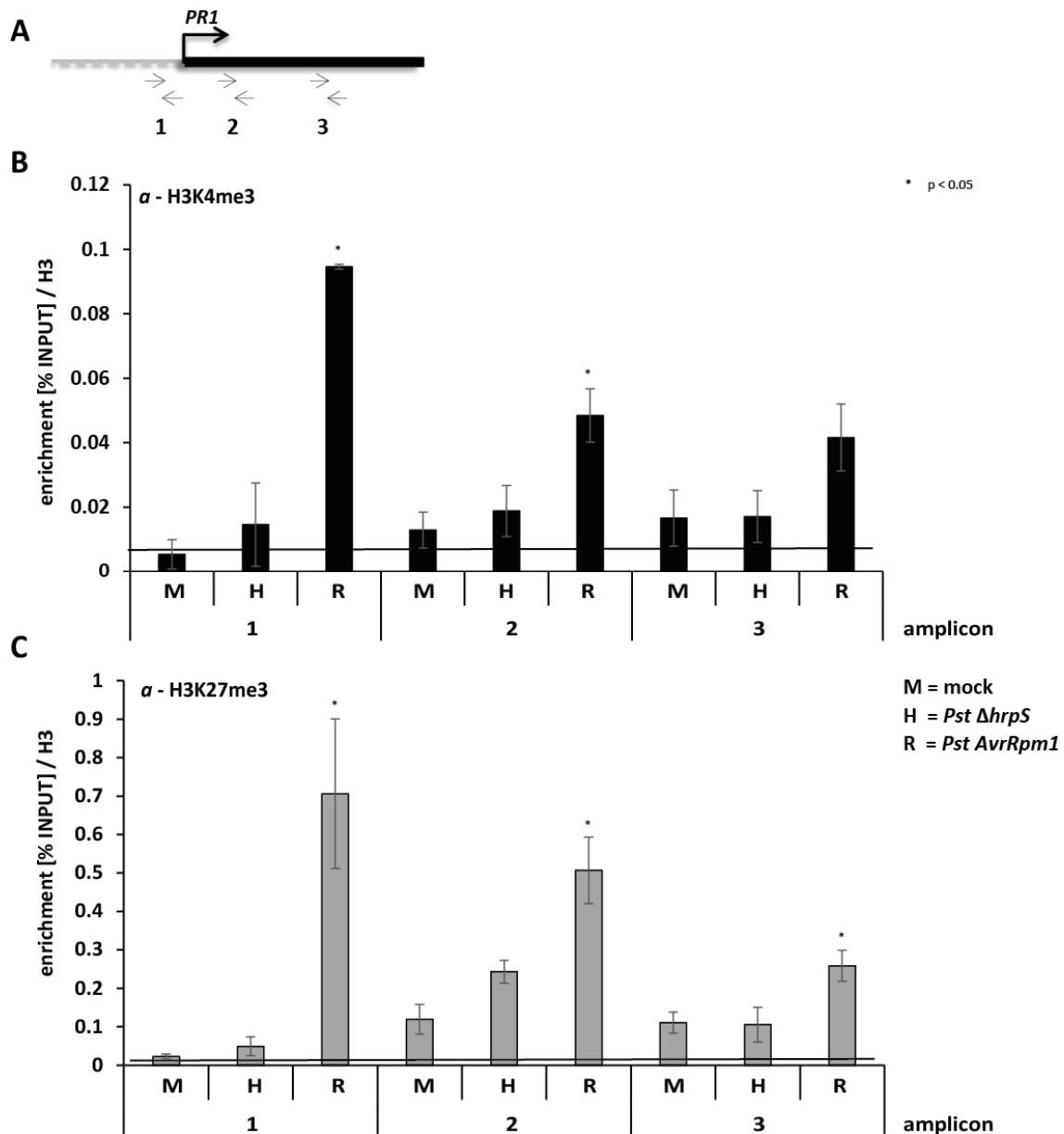


**Figure 17: ChIP of H3K4me3 and H3K27me3 on *PR1* in systemic tissue upon local MTI- and ETI-activation.**

(A) Schematic gene model of *PR1*. Grey dotted line represents the promoter and black box the exonic region. Arrows indicate the amplicon locations numbered from 1 to 3.

(B) and (C) Four-week-old WT plants were syringe-infiltrated in three local leaves with 10 mM MgCl<sub>2</sub> (mock, M), 1x10<sup>8</sup> cfu/ml *Pst*  $\Delta$ hrpS (H) or 1x10<sup>6</sup> cfu/ml *Pst* AvrRpm1 (R). At 48 hpi systemic leaves were harvested and chromatin extracted. ChIP-qPCR results of *PR1* were obtained by amplifying amplicons of DNA immunoprecipitated with H3K4me3 and H3K27me3 specific antibodies. Enrichment of each sample was calculated relative to the respective INPUT (% INPUT) and normalized to the qPCR signal obtained with immunoprecipitated DNA of  $\alpha$ -H3. Error bars represent standard error (SE; n=3) of three biological replicates with three technical replicates each, respectively. P-value, indicated by asterisk, was calculated using Student's t-test comparing the enrichment of H3K4me3 and H3K27me3 upon local treatment with *Pst*  $\Delta$ hrpS (H) or *Pst* AvrRpm1 (R) to the control treatment (M) of the same amplicon.

Solid baseline represents  $\alpha$  background, determined as average of qPCR signals obtained from each sample and replicate with *Ta3* primers.

Interestingly, a significant enrichment of H3K4me3 was found on amplicon 1 and 2 of *PR1* in systemic tissue upon local ETI activation compared to the control treatment. Local MTI activation did not induce a significant H3K4me3 enrichment on *PR1* for all three amplicons tested (Figure 17B).

As shown in Figure 17C, H3K27me3 is enriched above the background, similar to H3K4me3, in nearly all the tested conditions, whereas significant differences in the H3K27me3 levels were detected for all three amplicons upon ETI-induced systemic priming settings. Again, local MTI activation did not induce a significant H3K27me3 enrichment compared to the control treatment.

To further correlate these findings with the mode of action of ATX1 and CLF in the determination of a sustained systemic priming response, the levels of H3K4me3 and H3K27me3 on *PR1* were assessed after local MTI- and ETI-activation in systemic tissue of wild type, *atx1-4* and *clf-28* plants in an initial ChIP experiment. For comparison the same regions of *PR1* were amplified (Figure 18A).

In wild type plants, the H3K4 trimethylation with high enrichment on *PR1* in ETI-primed systemic tissue was detected. Interestingly, also a high level of H3K27me3 was again ascertained for the same three amplicons of *PR1* (Figure 18).

In *atx1-4*, a reduction of H3K4me3 after local ETI-activation compared to wild type was detectable on the *PR1* locus, whereas the ETI-correlated H3K27me3 enrichment was similar to wild type, suggesting that the H3K27me3 level is not correlated with changes in ATX1 activity (Figure 18). Figure 18 also illustrates the reduced level of H3K4me3 and H3K27me3 in *clf-28* plants on *PR1* in this ChIP. Further experiments are required to reveal if the H3K27me3 and H3K4me3 level seen in *atx1-4* and *clf-28* are representative or due to experimental variation such as the histone mark enrichment in *atx1-4* upon local control treatment.

Of note, at this point it cannot be concluded whether the changes of H3K4me3 and H3K27me3 on *PR1* are directly or indirectly influenced by ATX1 and/or CLF. But considering all results, it can be proposed that ATX1 and CLF seem to be required for a proper systemic immune activation and priming, whether directly or indirectly, and further to fine tune the histone methylation orchestration required for the difference in the MTI- and ETI-associated systemic priming response.

## Results

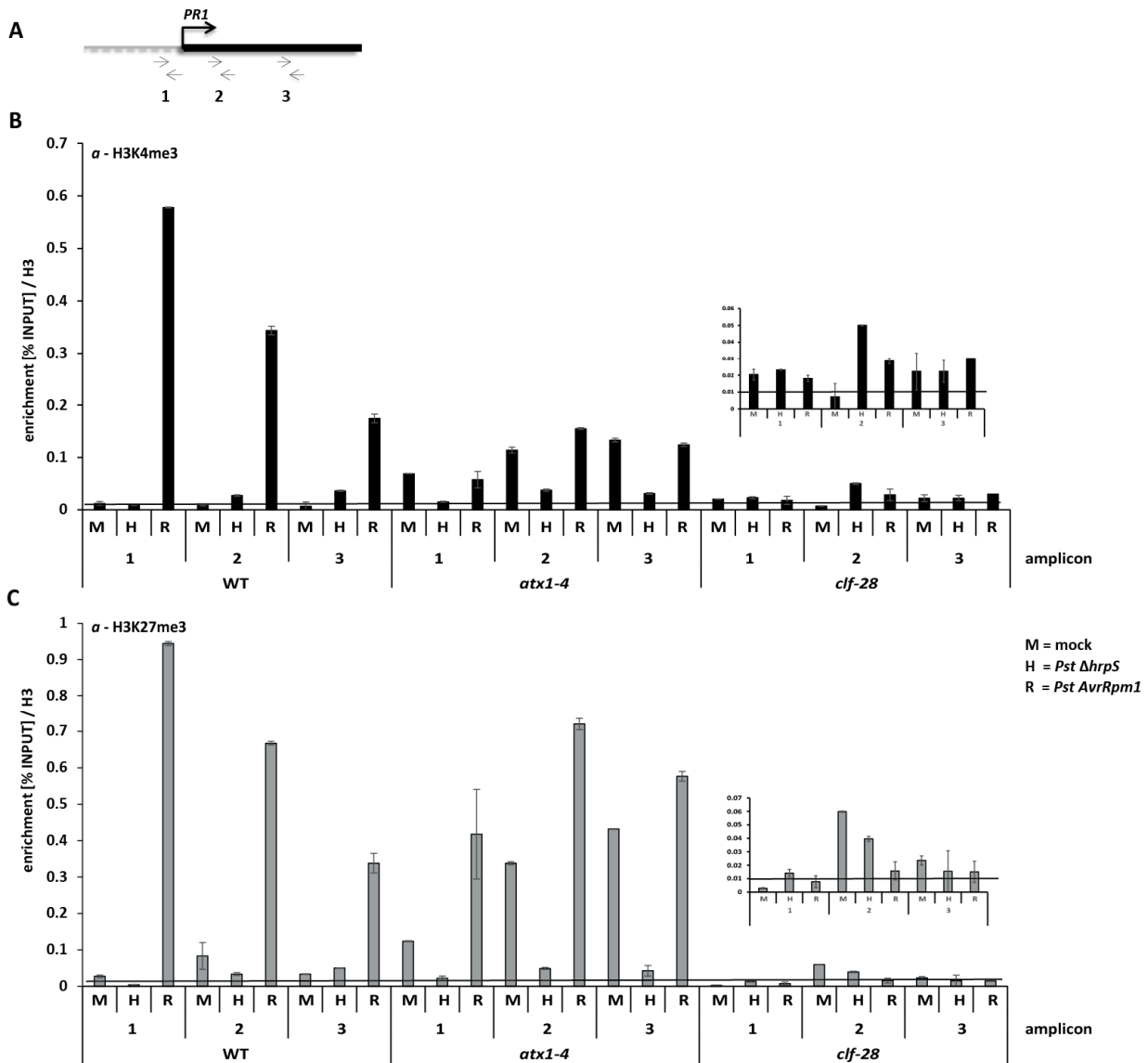


**Figure 18: ChIP of H3K4me3 and H3K27me3 on *PR1* in systemic tissue upon local MTI- and ETI-activation in WT, *atx1-4* and *clf-28* plants.**

(A) Schematic gene model of *PR1*. Grey dotted line represents the promoter and black box the exonic region. Arrows indicate the amplicon locations numbered from 1 to 3.

(B) and (C) 4-week-old WT, *atx1-4* and *clf-28* plants were syringe-infiltrated in three local leaves with 10 mM  $MgCl_2$  (mock, M),  $1 \times 10^8$  cfu/ml *Pst Δhrp5* (H) or  $1 \times 10^6$  cfu/ml *Pst AvrRpm1* (R). At 48 hpi systemic leaves were harvested and chromatin extracted. ChIP-qPCR results of *PR1* were obtained by amplifying amplicons (A) of DNA immunoprecipitated with H3K4me3 and H3K27me3 specific antibodies. Enrichment of each sample was calculated relative to the respective INPUT (% INPUT) and normalized to the qPCR signal obtained with immunoprecipitated DNA of  $\alpha$ -H3. Error bars represent standard deviation (SD; n=3) of one biological replicate of each genotype with three technical replicates each, respectively. The respective values for *clf-28* were enlarged in the small figure above.

Solid baseline represents background, determined as average of qPCR signals obtained from each sample with *Ta3* primers.

### 3 Discussion

#### 3.1 Identification and mechanisms of a local priming response

##### 3.1.1 Several genes associated with defense execution carry H3K27me3 and H3K4me3 at high proportions

The ER glucosidase II  $\alpha$ -subunit mutant allele *rsw3* harbors a point substitution in the catalytic domain of the  $\alpha$ -subunit (GII $\alpha$ ) and is required in the ER during protein quality control (ERQC) (Anelli and Sitia 2008). EFR folding, in contrast to FLS2, seems to rely on the ERQC prior its transport to the plasma membrane (Pattison and Amtmann 2009; Robatzek and Wirthmueller 2013). It was shown that upon elf18 treatment *rsw3* plants induce ROS generation, MAPK activation, ET production, callose deposition and early defense genes such as *WRKY29* and *WRKY22* wild type-like, but exhibit a supersusceptible phenotype against *Pst* DC3000. This indicates that the activation of widely appreciated MTI hallmarks is not sufficient for a robust defense response, but requires a sustained transcriptional reprogramming as demonstrated by the failure of *rsw3* to maintain the gene expression at later time points (8 - 24 hpt) or to induce late defense marker genes such as *PR1* and *PR2* (Lu et al. 2009; Muthamilarasan and Prasad 2013; Tintor et al. 2013; Ross et al. 2014). Of note, it is not fully clarified whether the observed *rsw3* phenotype is dependent on the misfolding of EFR alone as the early signaling events remain wild type-like despite reduced EFR-dependent ligand binding activity (Lu et al. 2009). This might influence the durability and/or stability of the active receptor complexes thus affecting the maintenance of signaling leading to impaired immunity.

The importance of the sustained transcriptional reprogramming suggest that genes, which are specifically involved in this process are most likely be associated with defense execution and therefore are eligible candidates to investigate the involvement of histone marks in the control of transcriptional reprogramming. To this end, 204 genes that were identified to be less expressed in *rsw3* compared to wild type upon elf18 treatment, were used to perform a histone mark survey of H3K4me3 and H3K27me3, associated with active or repressed transcription, respectively, on these genes in non-elicited wild type seedlings (Supplementary Table 1).

Of main interest was the finding that these genes carry H3K27me3, H3K4me3 or even both histone marks with 43 % and 50 %, respectively (Figure 2). The values are higher or similar to the detected occurrence of these marks on all annotated *Arabidopsis* genes of ca. 17 % and ca. 50 % for H3K27me3 and H3K4me3 in non-elicited wild type seedlings, which implies an involvement in the control of the defense-related transcriptome (Zhang et al. 2007; Zhang et al. 2009; Pontvianne et al. 2010). It would be interesting to monitor the level of several histone modifications associated with transcriptional

control (Roudier et al. 2011) also on a genome wide level to get a comprehensive view of the dynamics and stability of histone modifications upon defense activation.

### **3.1.2 Selected local memory target genes are enriched with H3K27me3 prior to a transcriptional priming response**

A priming response is characterized by the ability to react to a subsequent stress encounter with a higher and/or faster secondary response compared to the first mode of activation (Conrath 2011; Fercha et al. 2014; Kissoudis et al. 2014; Li et al. 2014; Minocha et al. 2014). The understanding of the mechanisms underlying successful priming and the corresponding priming response can provide new implementations in modern agricultural crop design.

To access the underlying mechanisms of the priming response in the biotic stress response, *Arabidopsis* seedlings grown under sterile conditions elicited with flg22 were used. As a read-out of the local priming response, the gene expression of four selected marker genes was monitored during the subsequent low-dose stress application revealing *WRKY29* and *PROPEP3* as being priming positive (Figure 3). Interestingly, *PR1* and *PROPEP2* were priming negative and not among the 204 defense-related genes (Figure 3B), whereas *WRKY29* and *PROPEP3* can be found in this list enriched with H3K27me3 (Supplementary Table 1). Of note, *WRKY29* and *PR1* as primed and non-primed genes, both exhibit a wild type-like gene expression pattern during the initial treatment (Supplementary Figure 1). This indicates that the initial transcriptional upregulation is not causative for the differential marker gene selection, but implies the presence of other mechanisms at least for *PR1* under the conditions used in this experimental set up.

H3K27me3 has been described in the long-term somatic memory response required for the vernalization process to maintain a transcriptional inactive state of *FLC* to promote flowering after prolonged exposure to cold (Kim and Sung 2014), but less is known about its role in the stress induced transcriptional response. One recent study suggests that abiotic stress application induces etching of H3K27me3 to an island-like structure correlated with a memory response. This might indicate that H3K27me3 presence on genes is required for the determination of a priming responsive gene (Sani et al. 2013). Whether this is also the case for the presented findings for *WRKY29* and *PROPEP3* needs to be proven experimentally by CHIP.

Beckers et al. propose that dormant MAPKs accumulate during the priming setting as a prerequisite for a faster and enhanced priming response upon secondary pathogen attack (Beckers et al. 2009). In a similar context, the transcript profile analysis of *FLS2* revealed that during the priming response significantly more transcripts accumulate, which might result in elevated steady-state levels of the receptor and thus enhance signaling and/or a faster recycling of the receptor upon ligand binding (Supplementary Figure 3C) (Robatzek and Wirthmueller 2013). These two findings imply the enhanced

capability of the signaling cascade as a priming output to ensure a faster signal transmittance upon secondary stress treatment demonstrated as a combination of enhanced receptor availability and/or downstream signaling components.

### 3.1.3 The local memory response requires functional PcG and trxG complexes

The determination of local memory target genes and the high representation for H3K27me3 and a similar H3K4me3 occurrence to the control group in a large proportion of defense-related target genes prompted me to assess a possible role for the repressive and permissive histone mark, respectively, in defense priming (Figure 2). ATX1 and CLF were both implemented in several developmental processes such as flowering and cell development, and abiotic stress resistance (Ding et al. 2011a; Molitor and Shen 2013; Liu et al. 2014; Shafiq et al. 2014). However, their role in biotic stress management remains less clear, despite the finding that ATX1 functions at the cross-road of JA and SA signaling (Alvarez-Venegas et al. 2007).

The results for the local priming response implemented *WRKY29* as target marker gene of a successful local priming event. *Atx1* and *clf* mutant plants were both reduced in the local priming response upon flg22 (Figure 4). Of note, several well appreciated MTI outputs, such as MAPK activation, anthocyanin suppression and the initial gene activation, remained similar to wild type during an initial MAMP treatment in this mutants (Supplementary Figure 4, Supplementary Figure 5, Supplementary Figure 6) (Asai et al. 2002; Lu et al. 2009; Saijo et al. 2009; Serrano et al. 2012; Tintor et al. 2013). This allows the assumption, that ATX1 and CLF are not required for the initial immune activation, but for the maintenance or establishment of histone marks required for a full priming response. Further time-course experiments as a combination of ChIP-Seq and RNA-Seq need to be conducted to decipher where in a spatial and timely manner the histone mark placement determines a local priming response.

## 3.2 MTI and ETI induce divergent systemic priming responses

MTI and ETI are forms of plant immunity defined by different modes of pathogen recognition in a spatial and temporal manner (Jones and Dangl 2006). MTI recognition occurs extracellular at the plasma membrane by PRR receptor complexes coupled with intensive intracellular signaling events, whereas ETI recognition usually occurs intracellular as pathogens overcome the preformed barriers and the first layer of defense integrating different compartments. Contrary to MTI signaling, less is known of downstream signaling events during ETI (Henry et al. 2013; Jacob et al. 2013; Macho and Zipfel 2014). Of note, MTI and ETI recognition both elicit e.g. defense gene induction with differences in strength, timing and duration of activation (Navarro et al. 2004; Thomma et al. 2011). This might be

correlated with the fact that during the interaction with an incompatible pathogen a combination of MTI, ETS and ETI is induced. This can be circumvented by using plants carrying an inducible *Avr*-gene inducing an artificial pathogen-free ETI response (Tsuda et al. 2013), while in a natural situation ETI is indispensably coupled to MTI and ETS as mentioned above. The robustness of the ETI-induced immune response compared to MTI was further correlated with differences in the usage of immune signaling sectors. MTI, as well as ETI, involves signaling of SA, JA and ET contributing to immunity against necrotrophs and biotrophs. Interestingly, MTI uses these hormone-derived signaling sectors in a synergistic way, probably for fast signal amplification, whereas signaling of distinct sectors can be compensated among each other that counteracts bacterial effector-mediated disruption of ETI signaling and thus providing an explanation of its robustness. Synergistic relationships between the signaling sectors ensure fast and adequate responses in MTI in order to quickly adapt to the sensed bacteria out of the plant surrounding bacteria plethora. Thus, in terms of evolution the lower robustness of the MTI signaling network might be selected as trade-off with other requirements as MAMPs are shared among benign and harmful microbes providing less information of a pathogenic attack as the delivery of effectors does, which avoids unnecessary strong and costly immune activation (Tsuda et al. 2008; Tsuda and Katagiri 2010; Tsuda et al. 2013; Kim et al. 2014). The signatures of MTI and ETI immune responses seem to be extended to distal parts of the plant during SAR as it was demonstrated that the magnitude and extent of systemic defense responses correlates with the level of initiated defense responses such as SA production and *PR* gene expression (Navarro et al. 2004; Mishina and Zeier 2007; Gruner et al. 2013).

Correlating with the published results, differences in the MTI and ETI induced transcriptional reprogramming in local and systemic tissue using *PR1* as marker gene upon local immune activation with *Pst*  $\Delta$ *hrpS* and *Pst* *AvrRpm1* were detected. Contrary, no major differences in the timing rather than a higher gene induction of *PR1* could be observed (Figure 5A and B) (de Torres et al. 2003; Mishina and Zeier 2007). This lowered gene induction upon *Pst*  $\Delta$ *hrpS* treatment might be explained by its representation of several MAMPs that lead to the turnover of several PRRs (Penaloza-Vazquez et al. 2000; Macho and Zipfel 2014). Of note, it cannot be fully excluded that the observed discrepancy in the bacterial growth of *Pst*  $\Delta$ *hrpS* and *Pst* *AvrRpm1* in local tissue contributes to the gene expression pattern, although *Pst*  $\Delta$ *hrpS* was inoculated with a higher density than *Pst* *AvrRpm1* to compensate its reduced ability to multiply *in planta* (Supplementary Figure 7A) (Hamdoun et al. 2013). It would be further interesting to test if these differences in gene expression can also be seen on the proteome level being the direct executor of the defense-related gene expression (Jones et al. 2004).

It was hypothesized that the MTI and ETI induced immune activation causes defense-related genes to remain in a primed state correlated with enhanced and/or faster gene activation upon a secondary

stress encounter designated as priming response and thereby reflecting the first mode of activation not only in the stress-encountered, but also in a transmittance of this information to as yet unchallenged tissue. The plants ability to memorize previous stress induced gene activation was proven by several publications (Beckers et al. 2009; Jaskiewicz et al. 2011; Navarova et al. 2012), but it was not dissected if MTI and ETI are causative for a diverse priming response. To this end, the priming response of *PR1* was monitored before and after secondary stress induction proving a difference in the MTI- and ETI-induced systemic priming response. This holds true for water and pathogen infection of systemic tissue as secondary stress encounter (Figure 6, Supplementary Figure 15).

In addition to *Pst AvrRpm1* and *Pst ΔhrpS*, *Pst AvrRps4*, *Pst AvrRpt2* and *Pst DC3000* were tested regarding their local growth and defense gene induction as well as their priming response signatures. It seems that different ETI trigger and the virulent *Pst* strain induced divergent systemic priming responses (Supplementary Figure 7). In cross-reference to the subcellular localization of ETI-defense induction, it can be speculated that the plasma membrane associated recognition of *AvrRpt2* and *AvrRpm1* requires additional signaling components remitting the signal to the nucleus, whereas *AvrRps4* forms a signaling complex undergoing nuclear shuttling to directly confer a transcriptional regulation at the chromatin level, which might be causative for the observed differences in the systemic priming response output (Heidrich et al. 2012; Heidrich et al. 2013; Buscaill and Rivas 2014).

### 3.2.1 The systemic priming response exhibits a somatic memory

Induced resistance can protect the plant against a wide spectrum of diseases and allows much faster and effective immune response than in a naïve plant (Durrant and Dong 2004; Dempsey and Klessig 2012). Previous studies have shown that systemic immune activation can occur upon a single stimulus such as flg22, SA, pathogen attack, wounding or colonization of commensal root bacteria establishing a broad-spectrum resistance, which is associated with memory formation that is recognized as defense priming (Ross 1961b; Ross 1961a; Green and Ryan 1972; Metraux et al. 1990; Cao et al. 1998; Conrath 2011). Of note, immune activation is often accompanied by enormous fitness costs due to the allocation of resources or toxicity of defense products generated, whereas priming for defense combines the advantages of enhanced disease protection at low fitness costs (van Hulst et al. 2006; Alcazar et al. 2011; Huot et al. 2014). The growth-defense-tradeoff becomes highly emphasized in agricultural settings where crops have been bred for centuries to maximize growth-related traits resulting in the loss of genetic diversity that often compromises defense (Strange and Scott 2005). This becomes obvious in the constitutive priming mutant *enhanced disease resistance 1 (edr1)*, which exhibits an enhanced resistance to fungal and bacterial pathogens without constant expression of defense genes such as *PR1* and thus a significantly higher fitness level in marked contrast to the constitutively activated defense mutant *constitutive expressor of PR genes 1 (cpr1)* (Bowling et al.

1994; Frye and Innes 1998; Frye et al. 2001; van Hulten et al. 2006). In sum, it is detrimental for the plant to have constitutive immune activities, and the defense priming provides a solution for this challenge (Heidel et al. 2004).

The longevity of the priming response was demonstrated by its presence in newly emerged leaves 10 days after priming induction. This holds not only true for *PR1*, but also for *WRKY29*, indicating the presence of a mechanism to globally regulate a large gene set at once (Figure 7).

In cross-reference to the local priming response, now both genes display a systemic priming response (Figure 3, Figure 7). This might be correlated with the difference in the tissue used and the nature of the priming trigger. Of note, both genes are implemented to be SA-dependent reflecting the nature of the hemibiotroph pathogen induced immune activation (Asai et al. 2002; van Loon et al. 2006).

The aforementioned findings can be correlated with several studies over the last years that indicate a role of chromatin modification in determining a transcriptional memory within the lifespan of an individual (somatic memory) or across generations (transgenerational memory) such as loss of methylated DNA, histone methylation changes and/or reactivation of transposable elements in the offspring of environmental challenged plants (Vaillant and Paszkowski 2007; Roudier et al. 2009; Lang-Mladek et al. 2010; Jaskiewicz et al. 2011; Luna et al. 2012; Luna and Ton 2012; Pastor et al. 2012). The heritable stress-induced epigenetic changes might increase survival changes of the species by broadening the phenotypic plasticity and the genetic variation within the population (Boyko and Kovalchuk 2011; Becker and Weigel 2012; Weigel and Colot 2012). It is accepted that a somatic memory as priming induced chromatin marks could outlive changes in transcript, proteins, hormones and metabolites which will underlie more or less rapid turnover as reported for the vernalization process (Angel et al. 2011; Sani et al. 2013).

A subsequent characterization will reveal the underlying mechanisms of the observed somatic priming response in newly emerged leaves and their transmittance to following generations as shown by Luna et al. (Luna et al. 2012; Luna and Ton 2012). The discovery of epigenetically controlled defense priming could also be used for exploitation in sustainable agriculture by selecting for priming-induced epialleles in progenies from induced crop plants (Pastor et al. 2013a).

### **3.3 The systemic priming response represents a distinct phase of plant immunity**

The presence of a general priming mechanism detectable in sterile grown seedlings using MAMP treatment and the identification of a yet unknown distinction of MTI and ETI during the systemic priming response were further quantified using a genome wide analysis in order to identify an inventory of genes that are associated with the differences in MTI- and ETI-induced systemic transcriptional reprogramming (SAR) and the subsequent priming response. Of note, it is difficult to

distinguish those genes, which are only responsive to the pathogen-associated immune activation and those that may have other roles during infections as the modulation of metabolic and cellular needs. Both groups are important in the global change of gene expression upon pathogen encounter and cannot be seen separately (Katagiri 2004). Although resistance-specific responses exist, large sections of the global expression profiles are qualitatively similar in resistant and susceptible responses to *Pst* strains, which justified the use of the binary *Arabidopsis-Pst* system for the performed transcriptome profiling (Tao et al. 2003).

The raw data analysis revealed a satisfactorily high number of sequenced reads that could be aligned to the *Arabidopsis* genome yielding in a coverage around 90 % (Table 1, Supplementary Figure 8A). For systemic acquired resistance it is accepted that local MTI- and ETI-induction elicit largely overlapping signaling components (Jones et al. 2004; Mishina and Zeier 2007; Navarova et al. 2012; Gruner et al. 2013). It was shown that both required core regulatory factors such as SID2, SA, NPR1, PAD4, EDS1, ALD1, Pip and FMO1. For instance, Pip production by ALD1 and FMO1-dependent transduction of Pip signaling of defense amplifications are indispensable for SAR and occurs in both tissues, whereas in local resistance the extent of its impact relies on the nature of pathogen encountered (Navarova et al. 2012; Shah and Zeier 2013). This general principle could be confirmed for the SAR correlated samples as demonstrated in the MDS-plot. The pathogen-associated samples assemble in a close group for both dimensions (time; treatment) compared to the control group. Interestingly, the MTI and ETI pathogen-primed samples loosened its assembly and were differently clustered during the systemic priming response (Supplementary Figure 8B).

The current knowledge appreciates that ETI is a stronger and amplified MTI response indicating a quantitative difference of the immune response in local and systemic tissue (Tao et al. 2003; Navarro et al. 2004; Jones and Dangl 2006; Boller and He 2009; Katagiri and Tsuda 2010; Tsuda and Katagiri 2010). This quantitative difference was also seen in the presented analysis for the SAR correlated time point by more genes getting directly upregulated in systemic tissue upon local ETI activation than MTI (Figure 8A). Interestingly, the amount of the primed genes is greater in the ETI-specific class than the MTI-specific class in the different range of the cut-off ratio (Figure 8B and C).

Another layer of qualitative difference was indicated by using Venn diagram analysis. While the number of common genes remains similar, the number of genes specific for MTI and ETI differ significantly during SAR and the systemic priming response (Figure 8A and B).

This unexpected high number of differently assigned genes between MTI and ETI was strengthened by a subsequent analysis regarding the number of genes that are differentially expressed at 0 h and 1 h upon MTI and ETI elicitation. To ensure this notion, these differentially expressed genes during SAR and the systemic priming response were again compared to each other, demonstrating that a higher

number of genes are differentially expressed between MTI and ETI during the systemic priming response (after second water stimulation) than during SAR (without the second stimulation) (Figure 9). This can be cross-referenced with the results of the MDS-plot visualization (Supplementary Figure 8B).

In sum, a) more genes are directly upregulated during ETI-induced SAR, b) during systemic priming this effect becomes equalized still displaying a higher gene expression upon ETI-priming, and c) MTI and ETI use partially different gene sets during systemic immunity, which becomes more prominent in the systemic priming response.

Thus, it seems that systemic priming represents a distinct phase of plant immunity beyond local and systemic resistance. In further experiments it is therefore inalienable to explore the underlying molecular mechanisms of the systemic priming response.

### **3.3.1 The Top100 significant differentially expressed genes are grouped into 12 clusters based on their expression patterns, providing MTI- and ETI-specific SAR and priming target genes**

One aim of this study was to provide insight into the underlying mechanisms and patterns of the systemic priming response upon local MTI and ETI elicitation. This could also allow the identification of MTI- and ETI-specific marker genes of SAR and the systemic priming response, which might provide certain starting point in the discovery of a general underlying mechanism or the disproval of such.

To this end, the Top100 differentially expressed genes of each comparison, mock and MTI as well as mock and ETI, for both time points (0 h, 1 h) were extracted and the union of these gene sets was visualized in a heatmap. Genes were sorted according to their expression patterns yielding in 12 defined clusters (Figure 10), which are further visualized by a trace plot (Supplementary Figure 9). A preliminary search for conserved *cis*-elements in the defined clusters using the MEME suite, revealed no specific enrichment of any known or predicted motif (Bailey et al. 2009; Priest et al. 2009). This suggests that the present clustering, which is defined on expression patterns, may not be powerful to correlate the identified clusters to the control of a certain transcription factor(s), which can be proven by genome-wide transcription factor binding studies such as DNaseI-Seq or a mechanism that involves epigenetic modifications (Madrigal and Krajewski 2012).

The gene ontology analysis, with a focus on biological process for all genes included in the heatmap, revealed the allocation to several stimuli including the response to abiotic stimulus such as the water infiltration, as well as defense specific responses (Supplementary Figure 11).

In order to reveal SAR and priming response specific genes, those clusters were first excluded that showed an upregulation of gene expression upon control treatment for the 0 h time point and in the non-primed plants at 1 h a higher gene expression than the pathogen-primed plants. For these clusters it can be assumed that a wound induced gene expression pattern would mimic the presence of clear

candidate genes so that the clusters I, II, III, IV, VII, VIII, IX and X were dislodged. Indeed, the large cluster I is correlated with response to water, lipid metabolic process, JA biosynthetic process and genes such as *DELAYED DEHISCENCE 1 (DDE1)*, *LIPOXYGENASE 2/3 (LOX2/3)*, which are assigned to JA biosynthesis and wound-induced JA accumulation, which is detectable 1-4 h after wounding stimulus (Supplementary Figure 12A, Supplementary Table 2) (Park et al. 2002; Glauser et al. 2009; Gfeller et al. 2010; Chauvin et al. 2013). Cluster II, III and IV showed a similar expression pattern for the SAR-responsive genes being less expressed or downregulated upon immune activation correlating with the fact that JA signaling is significantly reduced in the SAR-induced state. SAR is characterized by activated SA signaling and the well-established negative crosstalk between SA- and JA-pathways might be responsible for the attenuation of JA responses (Spoel et al. 2003; Robert-Seilaniantz et al. 2011; Pieterse et al. 2012; Gruner et al. 2013). For cluster II, III and X no GO term could be assigned, but cluster IV, VII and VIII showed a highly specific correlation with response to abiotic stimulus and water (Supplementary Figure 12). Cluster IX exhibited a GO term allocation with response to several biosynthetic and metabolic processes mainly less expressed in the systemic priming response (Supplementary Figure 12F, Figure 8). Metabolites are end products of gene expression and protein activity and therefore penultimate regulatory components for the phenotypic expression under stress conditions (Kissoudis et al. 2014). This cluster contains genes associated with flavonoid biosynthesis such as *FLAVANONE 3-HYDROXYLASE (F3'H)* and the key-enzyme *CHS* (Supplementary Table 2). These compounds have a diverse array of physiological functions, such as antioxidants or protecting pigments, and they are reported to be downregulated in several plant-pathogen interactions (Logemann and Hahlbrock 2002; Saijo et al. 2009; Schenke et al. 2011; Serrano et al. 2012). In agreement with previous findings, the RNA-Seq data revealed a similar expression trend for *CHS* during SAR and the systemic priming response, interestingly showing a mirrored expression pattern as observed for *PR1* (Supplementary Figure 10A and B). For both *PR1* and *CHS*, an opposite epigenetic regulation of gene expression by writing and removal of transcription positive histone modifications such as H3K4me3 and H3K9ac upon defense activation has been reported (Jaskiewicz et al. 2011; Schenke and Cai 2014; Schenke et al. 2014).

A priming positive gene was therefore defined as a) not being upregulated during SAR, either upon local MTI- or ETI-elicitation and exhibiting enhanced gene expression during the defense-induced priming response and b) being upregulated during SAR and illustrating a further enhanced gene transcription profile during the priming response. This holds true for both a) and b) regardless if MTI- or ETI-specifically and by being higher expressed in an ETI-specific manner than MTI-specific. According to the heatmap and trace plot visualization this definitions are valid for cluster V and VI for a) and for cluster XI and XII for b) (Figure 10, Supplementary Figure 9). This correlates with the GO term

assignment of cluster VI and XI indicating a strong coherence with response to defense, immune system process, biotic stimulus and defense response to bacterium (Supplementary Figure 12C and G). For these four clusters, one gene was chosen as a representative marker gene and the transcript profile was monitored in systemic tissue with and without second water stimulation at an extended number of time points. Generally, it can be said that the gene expression profile obtained by qRT-PCR analysis and RNA-Seq largely overlap for the selected genes (Figure 11, Supplementary Table 2), validating that the observed patterns are not due to MTI- and ETI-associated differences in the timing of gene expression.

The chosen marker gene for Cluster V was *CRK39*, of which the qRT-PCR results resembled the ETI-specific priming response with an upregulation as observed in the RNA-Seq (Figure 11A, Figure 10, Supplementary Table 2). The cystein-rich repeat RLK residues at the plasma membrane within an extracellular domain, which might implement the binding capacity of yet unknown ligand(s) (Chen et al. 2004). Further investigation will reveal their direct or indirect role in the ETI-specific priming response. MPK4 was also present in this cluster correlating with published results as being induced upon MAMP or avirulent pathogen treatment (Qiu et al. 2008). MPK4 phosphorylation leads to the release of WRKY33 that can bind to its cognate target genes such as *PHYTOALEXIN DEFICIENT 3 (PAD3)* responsible for camalexin biosynthesis (Zhou et al. 1999; Andreasson et al. 2005; Qiu et al. 2008). Interestingly, the upstream kinase of MPK4 (MEK1) and WRKY33 were both present in cluster XI (Supplementary Table 2). Although both represent different clades of the MAPK signaling network, WRKY33 can also be regulated by MPK3 and MPK6, suggesting a model where WRKY33 is released from MPK4 and MKS1 upon MPK4 activation and phosphorylated by MPK3/MPK6 to induce expression of *PAD3* (Mao et al. 2011; Rasmussen et al. 2012). This pathway is required for the resistance against necrotrophic fungi as WRKY33 negatively and positively regulates SA and JA pathway, respectively (Birkenbihl et al. 2012). Contrary, WRKY70, a transcription factor favoring SA and repressing JA signaling, was also represented in cluster XI as an important node of convergence between JA and SA pathway (Li et al. 2004; Li et al. 2006; Ren et al. 2008). Not surprisingly, *PR1* as one downstream target of WRKY70 was also assigned cluster XI with both resembling the expression profile of the RNA-Seq (Figure 11C, Supplementary Figure 10A, Supplementary Table 2). Additionally, the *PR1* negative regulator NIMIN-2 was also identified in this cluster suggesting the control of expression by a negative feedback loop in SAR and the systemic priming response (Weigel et al. 2001; Weigel et al. 2005). At a first glance it seems illogic to activate components of the two mutually antagonistic pathways (SA vs. JA) upon secondary immune stimulus, although this might simply reflect the broad spectrum of resistance that is correlated with the immunization of the systemic tissue (Fu and Dong 2013) and the strength of the response is designated by the mode of the local immunization.

Cluster VI was associated with a MTI-priming specific gene expression pattern that is reflected by the qRT-PCR analysis of *RPP5* (Figure 11B). This is going along with the proposed idea of the broad spectrum systemic immunization, as *RPP5* was shown to mediate resistance specificity to the downy mildew *Hpa*. Of note, in *Arabidopsis* Col-0 *RPP5* is defined as multigene locus harboring several clustered NB-LRR genes such as *SNC1* or *RPP4* (Parker et al. 1997; van der Biezen et al. 2002).

The last selected cluster XII displayed a comparable level of gene induction in systemic tissue upon MTI and ETI, whereas the systemic priming response was strengthened in an ETI-specific manner for the selected marker gene *EVR*. *EVR* or *SUPPRESSOR OF BIR 1 (SOBIR1)* has been implicated to work in a receptor complex at the plasma membrane during MAMP-triggered immunity against necrotrophic fungi (Zhang et al. 2013b; Liebrand et al. 2014).

In sum, it can be said that the systemic immunity and priming response, whether MTI- and/or ETI-specific, extends the inventory for the influenced genes, compared to the solely systemic gene induction upon local immune activation. In future studies, the underlying network needs to be determined that could provide valuable tools for breeders to design pathogen resistant crop plants while avoiding detrimental fitness impairment.

### **3.3.2 The SA-dependent systemic immune activation and priming response can be circumvented by ETI in a NPR1-dependent manner**

SA as central signaling component of SAR is inalienable for the establishment of SAR in both local and systemic leaves and mutants exhibiting a SAR-deficient phenotype are often defective in SA signaling (Bowling et al. 1994; Delaney et al. 1995; Glazebrook et al. 1996; Shah et al. 1997). The presence of SA-independent pathways or the bypass of the SA-signaling sector upon specific immune activation in local and systemic tissue suggest the emergence of other paradigms that in terms of evolutionary fitness provide the plant with alternative ways of immune activation and immunization.

The meta-expression analysis by Genevestigator of the four selected cluster V, VI, XI and XII revealed that genes within these clusters are upregulated by SA. Interestingly, this SA-dependency was hi-jacked upon avirulent pathogen infection as demonstrated in the *sid2* mutant (Figure 12). In correlation to the meta-expression analysis it is known that local MTI- and ETI-activation can lead to significantly different levels of SA accumulation (Mishina and Zeier 2007). Therefore it can be assumed that the SA level difference can (in part) contribute to the observed difference in systemic priming between MTI and ETI. The qRT-PCR data of *PR1* further support the Genevestigator analysis indicating that genes involved in SAR and the priming response require NPR1 for the proper systemic activation and priming of defenses, whereas SA is indispensable for systemic immune activation and priming response after MTI, but dispensable after ETI (Supplementary Figure 13). In addition, recent findings indicate that SAR also occurs upon local ETI- and prolonged MAPK activation in a SID2-independent manner (Y. Wang,

personal communication). Further experiments will therefore clarify the spatial and temporal requirement of SA during MTI- and ETI-induced systemic immunity and priming response.

A large-scale bioinformatics approach by Gruner et al. could define three specific clusters of genes that are important for the transcriptional reprogramming of SAR (Gruner et al. 2013). Several critical SAR regulators such as *ALD1*, *FMO1* and *SID2* can be expressed independently of SA. Those components are part of the amplification loop in the distal unchallenged leaves that involves Pip, SA and *NPR1* by promoting Pip and SA accumulation. Pip and FMO1 are required for the amplification of *SID2* expression and accumulation of SA in the systemic unchallenged part of the plant upon local immune activation, indicating the importance of *FMO1* in SAR. Additionally, AzA and Pip signaling converge on *ALD1*, whereas Pip acts in an amplification loop including *FMO1* to promote *ALD1* expression and thus its own biosynthesis (Navarova et al. 2012; Gruner et al. 2013; Shah and Zeier 2013; Shah et al. 2014). *ALD1*, *FMO1* and *SID2* were also identified in the presented RNA-Seq data set, but not included in the heatmap since they were not among the Top100 differentially regulated genes. *ALD1* and *FMO1* mainly resemble the gene expression of *PR1* during SAR and the systemic priming response (Supplementary Figure 10C and D), indicating their involvement in the priming process. *SID2* showed a similar transcriptional upregulation during SAR and systemic priming (Supplementary Figure 10E), suggesting that the level of SA production is tightly controlled via feedback mechanisms (Durrant and Dong 2004; Chen et al. 2009; Lu 2009; Fu and Dong 2013). The requirement and interconnection of partially SA-dependent genes such as *NPR3*, *EDS1*, *PAD4*, *PR2* and *PR5* and fully SA-dependent genes such as *PR1*, *WRKY70* and *NPR1*, as well as the aforementioned SA-independent ones, are required for the full development of SAR already indicating that those signaling processes cannot be regarded as separately acting units, which does not exclude additional regulatory processes (Mauch et al. 1988a; Mauch et al. 1988b; Li et al. 2004; Li et al. 2006; Rietz et al. 2011; Fu et al. 2012; Gruner et al. 2013). In order to reveal the genetic requirements and network of the systemic priming response, which seems to use gene sets in a different way than during SAR upon local MTI- and ETI-activation (see 3.3), a large-scale mutant screen will be required.

In correlation with the presented results, Tsuda et al. proposed an SA-independent alternative mechanism, which can regulate a majority of SA-responsive genes during ETI but not MTI, contributing to ETI signaling network robustness. This provides one explanation for the observed *SID2*-independent ETI-systemic immunity and priming response. The authors identified a prolonged MAPK activation of MPK6 and MPK3 resulting in an SA-independent *PR1* expression at late time points during ETI activation by *Pst AvrRpt2* in *sid2*. *SID2*- and *NPR1*-independent *PR1* activation could also be detected upon *Pst AvrRps4* treatment although its induction was lower than upon elicitation with other ETI-inducing strains indicating the requirement of *NPR1* for its full expression. By using a transgenic line

that induces a constitutive activation of MPK6 and MPK3 after dexamethasone treatment, it was further demonstrated that wild type-like *PR1* induction could be observed upon prolonged MAPK activation in *sid2* and *npr1*, which holds true for numerous SA-dependent genes. Interestingly, it seems that prolonged activation of MPK3 is required for SA-independent *PR1* induction, while MPK6 seems to contribute to the *PR1* expression in *sid2*, but to a lesser extent than MPK3. Of note, the authors did not see such dependency during ETI activation by *Pst AvrRpm1* in local tissue (Tsuda et al. 2008; Tsuda et al. 2009; Tsuda and Katagiri 2010; Tsuda et al. 2013).

In the RNA-Seq analysis of this study *MPK3* transcript accumulation was detectable during SAR, whereas in MTI-induced SAR *MPK3* is less expressed than during ETI (Supplementary Figure 10). Thus, it is possible that in systemic tissue upon local ETI-induction, MPK3 provides a direct and quick SA-independent link to transcriptional reprogramming in correlation with its ability to accumulate highly in an inactive form in the cell as priming mechanism, which could explain the stronger BTH and ETI-induced systemic priming response (Beckers et al. 2009). In yeast it was shown that prolonged MAPK activation could lead to nuclear translocation (Traverse et al. 1992), as well as in *Arabidopsis* where stress-induced nuclear MAPK accumulation was detectable (Ahlfors et al. 2004; Lee et al. 2004). To verify this hypothesis, the gene expression pattern needs to be retested using the same conditions applied for the RNA-Seq by qRT-PCR. Furthermore, western blot analysis of active and inactive MPK3 accumulation in systemic tissue would provide evidence to support this hypothesis. The identification of downstream MPK3 targets upon ETI-induction (compared to MTI-induction) such as transcription factors or co-regulators, whether nuclear or cytoplasmic, will provide further insight into the regulatory mechanism (Conaway and Conaway 2011b; Conaway and Conaway 2011a; Mao et al. 2011; Rasmussen et al. 2012; Meng et al. 2013; Pecher et al. 2014). One missing link to the chromatin might be supplied by the identification of certain chromatin remodelers such as the histone methyltransferase ATX1 and/or CLF. This can be achieved by *in silico* co-expression analysis combined with an unbiased co-immunoprecipitation assays *in vivo*. In a subsequent characterization it would be of high interest to determine the biological significance by classical genetic approaches such as mutant analysis.

Of note, the highly complex network of local immune activation leading to SAR establishment, to a systemic priming response and also to a transgenerational memory, seem to fully rely on the presence of NPR1 during SA-associated immune activation (Beckers et al. 2009; Jaskiewicz et al. 2011; Luna et al. 2012; Luna and Ton 2012; Pastor et al. 2012; Fu and Dong 2013). Transcriptional co-regulators such as the Mediator complexes are known to provide the bridge between NPR1 and the transcriptional machinery or are required to positively regulate the NPR1 abundance during SAR (Canet et al. 2012; Zhang et al. 2012). The Mediator complex is highly conserved in eukaryotes with *Arabidopsis* having

21 conserved and six putative ones. Mediator exists in the cell in multiple combinations and serves as either transcriptional activator or repressor, depending on its associated components. Its core complex can associate with the RNA Pol II to form the holoenzyme stimulating basal transcription or with a kinase module excluding its binding to RNA Pol II in order to repress transcription (Bourbon 2008; Conaway and Conaway 2011b; Conaway and Conaway 2011a; Zhang et al. 2012). To this end individual Mediator subunits interact with the approximately 1.500 transcription factors encoded in the *Arabidopsis* genome such as WRKYs, TGAs or NIMINs that are closely working together with NPR1 to modulate the expression of target genes (Riechmann et al. 2000; Weigel et al. 2001; Jakoby et al. 2002; Weigel et al. 2005; Shearer et al. 2012). Accumulating evidence further demonstrated that Mediator could serve as a docking site for chromatin modifiers (Black et al. 2006; Kagey et al. 2010). Thus the NPR1-signalosome could provide one explanation of how the target genes are modulated in a general way during MTI and ETI in correlation with epigenetic modifiers.

### **3.4 The establishment and differentiation of an MTI- and ETI-induced systemic priming response is dependent on the presence of ATX1 and CLF in systemic tissue**

Epigenetic modifications, such as DNA methylation and histone methylation/acetylation, contribute to the transcriptional control of adaptive responses to environmental stimuli, whereas a portion of these modifications was shown to persist across generations and significantly contribute to phenotypic variation (Johannes et al. 2009; Mirouze and Paszkowski 2011; Meagher and Mussar 2012). Of note, the involvement of histone modifications, histone replacement, DNA methylation, somatic recombination and ATP-dependent chromatin remodeling in the control of rapid, reversible and heritable gene expression is known to be associated with numerous developmental processes such as flowering time control, root, organ and seed development (Berr et al. 2011; Molitor and Shen 2013). To date a comprehensive understanding of epigenetic modifications in the control of the defense-related transcriptome is fairly lacking behind, although several publications in the last years started to elucidate its roles.

In this study I focused on two histone marks, namely H3K4me3 and H2K27me3, that are known to be correlated with active and repressed transcriptional activity of genes, despite several other possibilities in the control of the systemic priming response, which are not under the scope of this thesis (Roudier et al. 2009; Berr et al. 2011; Roudier et al. 2011). Of note, these marks cannot be seen alone, but it is suggested that rather the combinations/patterns of different histone modifications and their spatial relationship to each other define the chromatin structure and transcriptional competence of the locus

and it would be of high interest to explore this assumption in follow up studies (Zhang and Reinberg 2001; Roudier et al. 2009; Roudier et al. 2011; Schwammle et al. 2014).

These marks further require writer and eraser protein (-complexes) to exhibit its dynamic and flexible way of transcriptional regulation of a larger gene set at once (Henikoff and Shilatifard 2011; Badeaux and Shi 2013). A high percentage of defense-related genes enriched with H3K4me3 and H3K27me3 identified on non-elicited wild type seedlings in combination with the failure of ATX1 and CLF to conduct a local priming response in seedlings (Figure 2, Figure 4) justified the assumption that they might be further required for the systemic priming response.

ATX1 serves to recruit the pre-initiation complex, including the TATA-box binding protein and RNA Pol II, to its target gene promoters. Upon transcription initiation, the RNA Pol II Ser5P clears the promoter and shifts to the transcriptional starting site to recruit ATX1 in a second event for H3K4 trimethylation. This implies that the posttranscriptional H3K4 trimethylation by ATX1 could serve as a memory platform for a subsequent priming response (Ding et al. 2011a; Ding et al. 2011b; Ding et al. 2012b; Fromm and Avramova 2014). ATX1 was linked in further studies with abiotic stress responses and developmental processes such as the flowering time control (Pien et al. 2008; Tamada et al. 2009; Deal and Henikoff 2011a) and only one study describes the requirement of ATX1 for resistance and defense-associated gene regulation (Alvarez-Venegas et al. 2007). On the other hand, H3K27me3 is considered as a repressive mark counterbalancing the activating functions of H3K4me3 correlated with the activity of the PcG protein complex, such as harboring CLF. In animals and plants, the involvement of H3K27me3/CLF has been well documented in developmental processes, as well as in the control of environmental responses (Schwartz and Pirrotta 2007; Molitor and Shen 2013; Liu et al. 2014; Shafiq et al. 2014).

In a first experiment exploring the involvement of these histone modifiers in the systemic immune response upon local immune activation, the failure of ATX1 and CLF to develop a wild type-like NPR1-dependent SAR response was revealed (Supplementary Figure 14). In a subsequent experiment it was tested whether ATX1 and CLF are required for the distinction of a local MTI- and ETI-induced systemic immunity. In wild-type plants, local ETI-elicitation caused a higher level of immunity than MTI and mock correlating to published results, which indicate that the level of local immune activation is reflected by the level of the systemic one (Mishina and Zeier 2007; Navarova et al. 2012). In *atx1* and *clf-28* mutants a level of systemic immune activation could be detected similar to the MTI-induced extent of immunity in wild type plants (Figure 13A, Supplementary Figure 14). Of note, *atx1* and *clf-28* plants were impaired to build up the distinction between MTI- and ETI-induced systemic immunity compared to wild type plants (Figure 13A). In sum, it can be concluded, that ETI causes a greater systemic immunity than MTI in a manner dependent on a functional ATX1 and CLF complex, and NPR1.

This NPR1-dependency was further detected in the systemic priming response assay using *PR1* as marker gene. This correlates with the aforementioned findings, claiming the difference and dependency on ATX1, CLF and NPR1 of the systemic immune response (Figure 14, Supplementary Figure 15). Interestingly, the ETI-induced systemic priming response, regarding the *PR1* expression, reached a level similar to the wild-type MTI response in *atx1* and *clf-28* plants, whereas the MTI-response in these mutants was strongly reduced or not detectable (Figure 14). Thus, it is speculated that both MTI and ETI rely on the presence of functional histone modifier complexes but some compensatory mechanism or redundant HMT are recruited to provide a certain level of systemic immunization. To this end, it would be of great interest to test the SA-dependency of the systemic priming response in *atx1* and *clf-28* plants, assuming that the proposed ETI-induced prolonged MAPK activation could provide one direct link to chromatin modulation by recruitment of histone modifier or direct nucleosome phosphorylation to compensate to a certain extent or in addition the loss of ATX1 and/or CLF (Feilner et al. 2005; Badeaux and Shi 2013). Of course this does not exclude additional or independent underlying mechanisms and needs to be integrated in the transcriptional network control of SAR and the systemic priming response (Moore et al. 2011).

A subsequent characterization of the local immune response in *atx1* and *clf-28* plants underpinned that the mutants were defective solely in the generation of a systemic immune response, despite their wild type-like local immune activation. The bacterial growth of *Pst ΔhrpS* and *Pst AvrRpm1* clearly demonstrated no significant differences at 48 hpi, correlating with the ion leakage results (Figure 15, Supplementary Figure 16). The cell death evaluation, as well as the bacterial growth data, suggests that the local response is already reduced in *npr1* mutants. Together with the impaired SAR and systemic priming response, this could explain the lack for ETI > MTI differences in *npr1* mutants. It can be concluded that ATX1 and CLF are required in systemic but not in local tissue for the differentiation of locally induced MTI and ETI in a NPR1-dependent manner under the conditions used in this study. This is in accordance with the demonstration of a tissue- and developmental specificity of trxG and PcG protein complexes (Alvarez-Venegas and Avramova 2005; Saleh et al. 2008a; Saleh et al. 2008b; Farrona et al. 2011).

Differences in the tissue-specific usage of immune system components during local and systemic immunity are e.g. supported by genetic studies, claiming that defects for basal defense in ALD1 and FMO1 are more severe in systemic than in local immunity (Song et al. 2004; Bartsch et al. 2006; Mishina and Zeier 2007; Navarova et al. 2012; Gruner et al. 2013). The use of tissue-specific inducible transgenic ATX1 and CLF lines could verify the systemic need upon local pathogen challenge in subsequent experiments.

Of note, to date the significance of defense marker gene activation for host immunity has been elusive

(Fu and Dong 2013) as knocking-out of a single *PR* gene would not lead to a dramatic change in the phenotype at the whole level, the expression of a subset of genes need to be manipulated at a time to test this hypothesis. Therefore, the chosen marker gene *PR1* might serve as paradigm to understand the epigenetic mechanisms underlying the systemic priming response dependent on NPR1, ATX1 and/or CLF. This assumption can be strengthened by the identification of clusters of SAR and systemic priming specific genes of which it would be interesting to determine the molecular- and chromatin-associated traits based on their expression pattern (Figure 10).

Whether target(s) of the systemic priming response identify direct and/or indirect target gene(s) of ATX1 and/or CLF, such as *PR1*, remains open at this stage. Thus, it cannot be excluded that the pleiotropic defects in those mutants indirectly, directly and/or collectively cause the observed phenomena, although the phenotypic appearance at the stage of usage, grown under short day conditions, does not differ significantly compared to wild type (Figure 13B) (Alvarez-Venegas et al. 2003; Schubert et al. 2006).

#### **3.4.1 H3K4me3 and H3K27me3 enrichment on *PR1* is specific for ETI-induced systemic priming**

The aforementioned genetic evidence implementing CLF and ATX1 in the systemic tissue specific control of SAR and the systemic priming response requested further characterization at the molecular level. The PcG and trxG protein complex with their catalytic subunits, CLF and ATX1, are associated with the deposition of H3K27me3 and H3K4me3 at their target chromatin loci, respectively (Rea et al. 2000; Alvarez-Venegas et al. 2003; Alvarez-Venegas and Avramova 2005; Alvarez-Venegas et al. 2007; Alvarez et al. 2010; Lafos et al. 2011; He et al. 2012). H3K27me3 mediated by CLF has been extensively described as prerequisite for a successful vernalization process to promote flowering after prolonged exposure to cold in a dosage dependent manner (Kim and Sung 2014), but less is known about its role in the stress induced priming response. One study suggests that abiotic stress application induces fragmentation of H3K27me3 to an island-like structure correlated with a memory response. This might indicate that H3K27me3 presence on genes is required for the determination of a priming responsive gene as discussed above (see 3.1.2). This is going along with recent findings, which imply that the chromatin environment, determined by H3K27me3/CLF, plays different and gene specific roles in the transcriptional control of developmentally regulated and environmentally responsive genes by restricting the cellular specificity of developmentally regulated genes and setting the dynamic range of environmentally responsive genes (Liu et al. 2014).

ATX1, together with ATX2, ATXR7 and other regulators are on the other hand correlated with expression of *FLC* and in abiotic stress pathways as aforementioned. One study also implements ATX1 as a modulator of defense responsive genes by directly regulating the SA-JA convergence node

*WRKY70* (Alvarez-Venegas et al. 2007). But to date it is less understood how H3K27me3 and H3K4me3 determine SAR and systemic priming responsive genes in a spatial and temporal manner.

The detected total protein level of H3K4me3 by western blot was not significantly different in wild type, *atx1-4* and *clf-28* plants upon pathogen treatments (Figure 16, Supplementary Figure 17). The similar level of H3K4me3 in *atx1-4* might be correlated with redundant function of other members of the ATX1 family or other methyltransferases. This is going along with published results, indicating that *atx1* plants exhibit only 15 % lowered H3K4me3 levels in correlation to wild type plants (Baumbusch et al. 2001; Alvarez-Venegas and Avramova 2005; Pontvianne et al. 2010). In addition, no significant differences of H3K27me3 levels could be detected in wild type and *atx1* mutants, irrespective of a local immune activation, whereas in *clf-28* H3K27me3 was significantly lowered in all samples despite the detection of H3K4me3 and H3 (Figure 16). This is in contrast to published results, demonstrating that H3K27me3 is only partially reduced in *clf* mutants on developmental genes, which is correlated by the overlapping function of CLF and SWN but might be explained by the general lowered total protein level (Chanvivattana et al. 2004; Farrona et al. 2011; Lopez-Vernaza et al. 2012).

Thus, it can be concluded that the total level of H3K4me3 and H3K27me3 does not significantly differ in wild type plants upon different pathogen treatments indicating that local changes of histone modifications at defined target genes might be responsible for the observed SAR and systemic priming phenotype.

Indeed, ChIP qPCR analysis revealed an ETI-specific enrichment of H3K4me3 on the target gene loci *PR1* in systemic tissue compared to mock, whereas no significant differences could be detected between mock and MTI-activated systemic tissue (Figure 17B). Furthermore, H3K27me3 was also enriched in systemic tissue in an ETI-specific manner on *PR1* (Figure 17C).

The presence of mutually antagonistic bivalent histone marks, H3K4me3 and H3K27me3, on one gene amplicon has been documented in animals and plants and correlated with a poised, not yet determined, epigenetic state. This “bivalent” chromatin, which is established at lineage-specific genes within pluripotent cells, is thought to poise genes for rapid activation upon induction of differentiation (Bernstein et al. 2006; Fisher and Fisher 2011; Grafi et al. 2011; Roudier et al. 2011; Sachs et al. 2013). In line with this, a dual methylation of H3K4me3 and H3K27me3 mediated by ATX1 and CLF was also found on chromatin of the flower homeotic gene *AGAMOUS* (*AG*) (Goodrich et al. 1997; Saleh et al. 2007; Alvarez et al. 2010). Following this line, the bivalent chromatin state on *PR1* might be correlated with the prerequisite for functional PcG- and trxG protein complexes in systemic tissue for a systemic priming response (Figure 14, Figure 17). It can be speculated that the enrichment of H3K4me3 and H3K27me3 needs to be tightly balanced and is required for a poised transcriptional state of the systemic priming target gene for enhanced gene expression upon secondary stress application. This

model is supported by the systemic defense phenotype and the failure in an ETI-induced systemic priming response of *atx1* and *clf-28* (Figure 13, Figure 14). The preliminary ChIP results for *atx1-4* indicate that this might go along with the fact that the loss of ATX1 results in a lowered H3K4me3 level on *PR1* after local ETI-activation, which needs to be confirmed in further experiments (Figure 18). Thus, it seems that the levels of H3K4me3 reflect the transcriptional state of the preceding enhanced systemic gene expression upon local ETI-activation compared to MTI and mock, and H3K27me3 might be required for the correct modulation of the memory storage and systemic priming response (Figure 5B, Figure 14, Figure 17).

As already hypothesized, the pathogen-induced H3K27me3 enrichment might be required for the dynamic range of expression of the memory target gene *PR1* and loss of CLF leads to an unbalanced reduced systemic memory response (Figure 14, Figure 17, Figure 18). Whether CLF is directly or indirectly responsible for the H3K27 trimethylation detected on *PR1* in wild type needs to be determined in further experiments. Irrespective of this fact, there is a major difference from the simplified “on/off” repressive role of CLF and H3K27me3 at developmental genes compared to the hypothesis that H3K27me3 is required for the dynamic range of expression at stress responsive genes (Carles and Fletcher 2009; Bouyer et al. 2011; Molitor and Shen 2013). Liu et al. recently reported a similar mechanism by analyzing the role of H3K4me3 and H3K27me3 in the dehydration stress memory response. In correlation to the presented results, the authors detected high-level presence of H3K27me3 at the stress-response genes, which did not preclude accumulation of H3K4me3 when genes were actively transcribed (Liu et al. 2014) (Figure 5, Figure 17). So it can be speculated that developmental and environmental genes might be regulated by a common epigenetic machinery but in a different way. This hypothesis needs to be validated in further experiments, determining the spatial and temporal distribution of H3K4me3 and H3K27me3 during systemic immunity and priming response correlated with the gene expression state.

A drawback of this model is the lack of a clear distinction between truly bivalent nucleosomes and interpretations made based on results with mixed populations of cells or nucleosomes. A conserved mechanism in human, mouse and fly indicates that the H3K4me3 and H3K36me2/3 marks allosterically inhibit the PRC2 activity avoiding to overwrite active chromatin marks (Schmitges et al. 2011). Although this assumption might also be simplified as each nucleosome contains two H3 tails that could be modified independently. Of note, the high-level of H3K4me3 present at *PR1* upon active transcription did not preclude accumulation of H3K27me3 and vice versa (Figure 14, Figure 18), although at this point it cannot be stated which histone mark antedated the other assuming that both, H3K4me3 and H3K27me3, are deposited at the same locus. The application of a tandem ChIP approach, probing H3K4me3 followed by H3K27me3 ChIP and vice versa of the *PR1* locus as marker gene, would clarify if

both marks are present at the same amplicon and which mark precedes the other or if the quantity of cells marks by H3K4me3 or H3K27me3 determines the defense output (Finnegan et al. 2011). Definitely, the levels of H3K4me3 and H3K27me3 need to be determined in a genome wide approach before and after a secondary systemic retreatment upon local MTI- and ETI-activation in wild type, *atx1* and *clf* plants to test if the H3K4me3 and H3K27me3 level shift upon secondary treatment towards an higher enrichment of the active histone modification as indicated by Jaskiewicz et al. and to a reduced repressive histone mark (Jaskiewicz et al. 2011). This would also verify the histone mark pattern in *atx1-4* and *clf-28* seen here in a preliminary ChIP experiment. These results can then be cross-referenced with the obtained RNA-Seq data (at least for wild type) to determine the prerequisites for the definition of SAR and systemic priming response specific genes. The reduced but not lost H3K4me3 enrichment after local ETI-elicitation on *PR1* in *atx1-4* is correlated with a reduced systemic memory response (Figure 14, Figure 18). This could be explained by the redundancy between five ATX and seven ATXR proteins in Arabidopsis, of which some were shown to exhibit H3K4 methyltransferase activity, which might then compensate for the loss of ATX1 to a certain extent, but presumably with less specificity (Baumbusch et al. 2001; Pontvianne et al. 2010).

The pathogen-induced H3K4me3 enrichment on *PR1* is contrary to the observations by Alvarez-Venegas et al. who did not detect significant changes of H3K4me3 on *PR1*, which can be explained by the use of a different time point and pathogen (24 hpi) (Alvarez-Venegas et al. 2007). Going along with this line, *WRKY70* was found in the same cluster than *PR1* (Figure 10, Figure 11, Supplementary Table 2) that could allow the assumption that *WRKY70* transcription is controlled in a similar way than *PR1* both depending on ATX1. Another explanation could be, that the actively transcribed *WRKY70* protein is known to regulate the transcription of *PR1* (Li et al. 2004; Li et al. 2006; Wang et al. 2006; Shim and Choi 2013; Shim et al. 2013) that in turn requires ATX1 or a redundant HMT for its H3K4 trimethylation. e-FP browser analysis further revealed that ATX1 and CLF were not differentially expressed upon pathogen treatment compared to mock (data not shown), suggesting that an upstream mechanism, or its recruitment and release to a chromatin binding complex, determines the control of transcription and definition of “memory marks” (Winter et al. 2007). To ensure this notion, the INTACT method using transgenic lines expressing ATX1 and/or CLF in a tissue specific manner tagged to different fluorophores could allow cell sorting coupled with ChIP to determine their tissue specific target genes and to rule out if the effects seen in this study are direct or indirect (Deal and Henikoff 2011b). ChIP using ATX1 and/or CLF coupled to HA or GFP could also demonstrate if *PR1* represents a direct target gene or not. This technique could also allow the identification of interacting partners or complex components that work closely together with ATX1 and CLF to mediate the transcriptional control yielding in a transcriptional memory of gene expression.

In later experiments it would be also interesting to determine the role of histone replacement and other modifications in the transcriptional memory of SAR and the following systemic priming response (van den Burg and Takken 2009; Bourbousse et al. 2012; To and Kim 2014; Zou et al. 2014). Of note, other chromatin modifications such as acetylation of H3 and H4 were coordinated with gene expression levels and priming but they were rapidly increased upon gene activation and decreased after gene repression at comparable levels before induction, which strengthens the role of H3K4me3 as memory mark (Jaskiewicz et al. 2011; Ding et al. 2012a; Kim et al. 2012). In this context it would be interesting to explore the requirements for a MTI-priming response, which according to the presented data seems to be partially dependent on ATX1 and CLF as a MTI-priming response is reduced in *atx1* and *clf-28* plants, but not directly correlated with H3K4me3 and H3K27me3 enrichment (Figure 14, Figure 17). To date it also remains elusive, how the systemic signal is perceived and imparted in the systemic tissue.

Histone methylation has been implemented not directly affecting transcription but instead to recruit in a context dependent manner transcription-activating or -repressing complexes (“reader”) that themselves can serve as a platform for other complexes (Strahl and Allis 2000; Jenuwein and Allis 2001). CLF and ATX1 can be regarded as “writer”, but the defined spatial and temporal role of “eraser” proteins during SAR and the systemic priming response as well as the defined “reader” proteins need to be determined in further studies.

### 3.5 Conclusions and working model

The results presented here strengthen the existence of epigenetic regulatory mechanisms, which implement a transcriptional control of defense related genes during SAR and the systemic priming response. Priming of defense-related genes is associated with changes of histone modifications by specific histone modifier at their promoters and gene bodies to facilitate the access of the transcriptional machinery upon subsequent stresses for an enhanced immune activation.

During this study I could demonstrate that the magnitude of SAR and the systemic priming response is correlated with the extent of the local immune activation, whereas local ETI activation induces a stronger systemic immunity and priming response. The systemic priming response provides a novel layer of systemic immunity in terms of gene usage upon local MTI- or ETI-activation. The gene collection that is activated during SAR and the systemic priming response seems to be SA- and NPR1-dependent, although ETI activation can potentially circumvent the SA-dependency. The RNA-Seq experiment implies that the ETI-correlated *MPK3* transcript accumulation during SAR could provide a mechanism to sidestep this SA dependency. This hypothesis is strengthened by a study that demonstrates the accumulation of dormant MPK3 proteins in systemic tissue upon locally induced

systemic immunity by BTH or ETI (Beckers et al. 2009). The enhanced ETI systemic priming response is correlated with an enrichment of H3K4me3 on *PR1*, whereas the accumulation of H3K27me3 in immunized systemic tissue correlates with the presence of this mark on genes in non-elicited seedlings that are capable to exhibit a local priming response. Thus, it is suggested that H3K27me3 is required for the fine-tuning and extent of the priming response. Going along with this, the histone modifiers ATX1 and CLF are required for a priming response in seedlings as well as for a systemic priming response specifically in systemic tissue.

For those genes identified in the RNA-seq experiment where no gene expression in systemic tissue but a priming response was detectable, it is assumed that non-coding and/or short RNA stretches are transcribed that serve to recruit the histone modifier(s), beside the possibility of other recruiting and transcriptional control mechanisms. The presence of a MTI-specific priming response also requires further molecular characterization as it seems that H3K4me3 and H3K27me3 plays a minor role in this regulation.

In sum, the following working hypothesis based on the marker gene *PR1* and the conditions used in this study is proposed:

Infection of local tissue leads to the activation of MTI and ETI that in turn triggers the release of a diverse set of systemic signals. The translocation of the signal(s) increases the immunization of distal yet unchallenged parts of the plant. The perception of the signal(s) induces signaling mechanisms leading to enhanced ETI-induced systemic gene expression compared to MTI. Local ETI activation can induce an SA-independent signaling mechanism in systemic tissue, possibly through enhanced and/or prolonged MPK3 activation that in turn might phosphorylate the CTD domain of the RNA Pol II to induce gene expression as a potentiation of transcription. Such stress-responsive CTD phosphorylation by MAPKs is not yet reported in plants, but well understood in yeast (Sukegawa et al. 2011). The use of the MAPK signaling pathway would provide a direct link to transcriptional regulation, although the exact composition and specificity needs to be determined. The serine 5 phosphorylation (Ser5P) of the CTD domain is primarily found at promoters and 5'-ends of genes and considered as biochemical marker for transcription initiation and early elongation (Hajheidari et al. 2013; Heidemann et al. 2013). ATX1 first is required to "guide" the unphosphorylated RNA Pol II (and the remaining parts of the preinitiation complex) to its target genes and the secondary recruitment of ATX1 is dependent on the RNA Pol II CTD Ser5 phosphorylation to promote H3K4me3 after the transcriptional induction, whereas upon Ser2 phosphorylation ATX1 is released from the complex (Ding et al. 2011b; Fromm and Avramova 2014). The level of H3K4me3 enrichment might thereby be correlated with the level of ETI-induced systemic transcription of the gene and the subsequent secondary priming response. On the other hand, MTI-induced systemic priming seems to be SA-dependent and is not correlated with

significant H3K4me3 and H3K27me3 enrichment on *PR1*, which matches with the lower gene expression and immunity level of MTI signaling compared to ETI.

NPR1 seems to be required for target gene determination and as transcriptional co-activator. Despite the hypothesized MPK3-correlated phosphorylation of the RNA-Pol II, another possibility includes the classical recruitment of the transcriptional machinery by the preinitiation complex including Mediator, which was also correlated with the recruitment of chromatin modifying proteins. Again, the deposition of H3K4me3 and H3K27me3 could serve as prerequisite for the subsequent enhanced memory response. H3K27me3 is supposed to modulate and fine-tune the systemic priming response, indicating that a balanced H3K4me3 and H3K27me3 level and pattern is required for a successful systemic priming response.

Of note, both MTI- and ETI-induced systemic priming are fully dependent on NPR1 and most likely with its associated transcriptional machinery, such as TGAs, WRKYs and the Mediator complex, NPR1 is needed for target gene determination under the conditions used in this study. Interestingly, ETI-priming requires NPR1 despite its SA-independency, which provides another layer of complexity to the system of how and where NPR1 promotes transcription and the priming response.

Future studies are therefore required to unravel the exact spatial and temporal composition of the transcription and memory machinery in a NPR1-dependent and partially SA-independent manner including ATX1 and CLF.

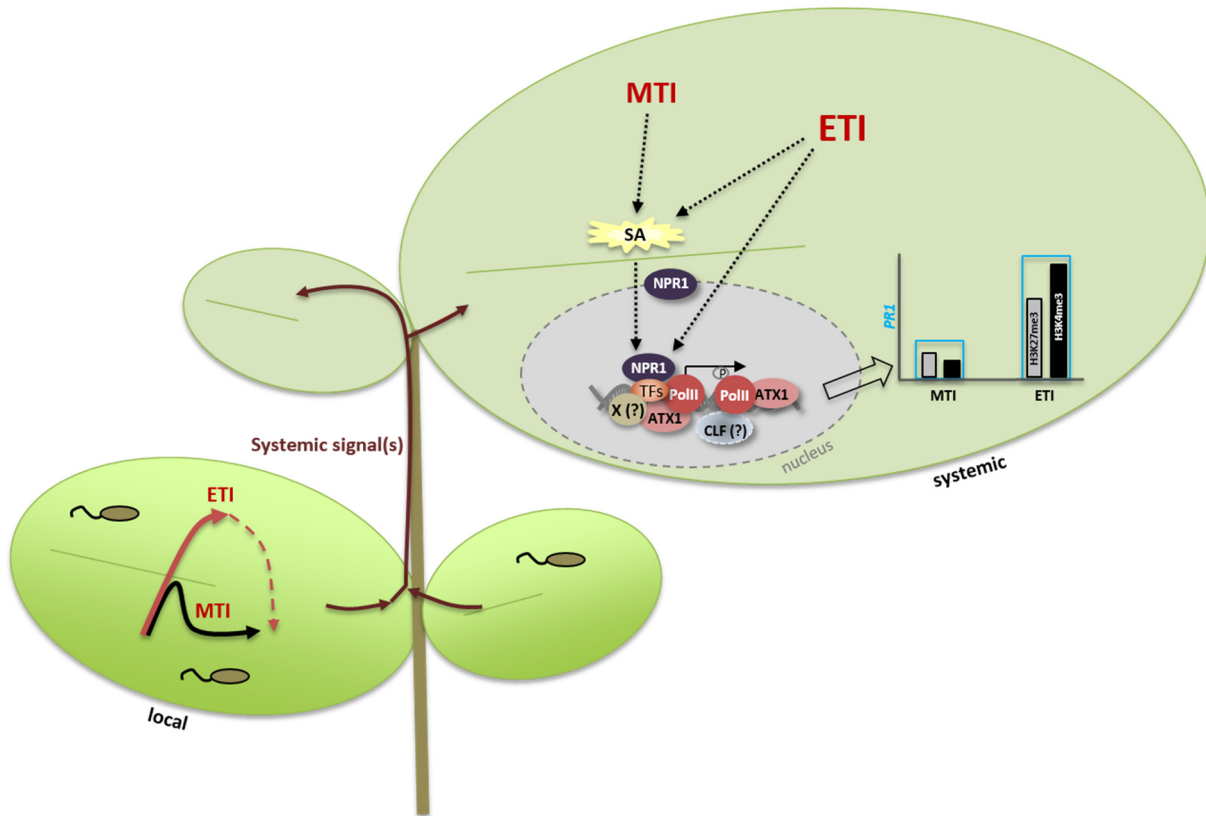


**Figure 19: Working model of MTI- and ETI-induced systemic priming for PR1.**

MTI- and ETI-induced local immune activation triggers the release of a collection of systemic signals that in turn leads to the immunization of systemic tissue, whereas systemic immune activation mirrors the level of MTI or ETI activation in local tissue. MTI- and ETI-transcriptional priming are both NPR1-dependent, whereas for the ETI-induced immunity and priming response SA is potential indispensable. NPR1 and its associated transcriptional machinery, as well as ATX1, are associated with RNA Pol II recruitment to target genes providing the link to gene transcription. The Ser5 phosphorylation of the RNA Pol II CTD domain leads to a possible secondary recruitment of ATX1 for its H3K4 trimethylation activity that serves as memory mark for the subsequent priming response. The level of H3K4me3 is thereby correlated with the strength of the gene activation. H3K27me3 seems to be required for a successful priming response.

## 4 Materials and Methods

### 4.1 Materials

#### 4.1.1 Plant Material

*Arabidopsis thaliana* (*Arabidopsis*) accession Columbia-0 (Col-0) was used as wild type (WT) in this study and all mutants used are in Col-0 background.

**Table 2: Plant material used in this study**

Mutant allele	Gene locus	Accession	Source/Reference
<i>fls2</i>	At5g46330	Col-0	C. Zipfel (2009), GB
<i>sid2-2</i>	At1g74710	Col-0	F. Ausubel (2001), USA
<i>npr1-1</i>	At1g64280	Col-0	N3726
<i>rpm1-3</i>	At3g07040	Col-0	Kenichi Tsuda (2013), DE
<i>atx1-4</i>	At2g31650	Col-0	SALK_140755
<i>atx1-2</i>	At2g31650	Col-0	SALK_149002
<i>clf-28</i>	At2g23380	Col-0	SALK_139371
<i>swn-7</i>	At4g02020	Col-0	SALK_109121

#### 4.1.2 Plant Pathogens

##### 4.1.2.1 *Pseudomonas syringae* (*Pst*)

**Table 3: *Pseudomonas syringae* (*Pst*) strains used in this study**

Strain	Resistance
<i>Pseudomonas syringae</i> pv. <i>tomato</i> ( <i>Pst</i> ) DC3000 ( <i>Pst</i> DC3000)	Rif
<i>Pst</i> DC3000 $\Delta$ <i>hrpS</i> ( <i>Pst</i> $\Delta$ <i>hrpS</i> )	Rif
<i>Pst</i> DC3000 <i>AvrRpm1</i> ( <i>Pst</i> <i>AvrRpm1</i> )	Rif/Kan
<i>Pst</i> DC3000 <i>AvrRpt2</i> ( <i>Pst</i> <i>AvrRpt2</i> )	Rif/Kan
<i>Pst</i> DC3000 <i>AvrRps4</i> ( <i>Pst</i> <i>AvrRps4</i> )	Rif/Kan
<i>Pseudomonas syringae</i> pv. <i>maculicola</i> ( <i>Psm</i> )	Strep

*Pst* was grown on NYGA medium containing the respective antibiotic(s) at 28 °C for 48 h.

##### 4.1.2.2 *Hyaloperonospora arabidopsidis* (*Hpa*)

*Hyaloperonospora arabidopsidis* Noco2 (Coates and Beynon 2010) was used in this study.

#### 4.1.3 Oligonucleotides

Oligonucleotides used were purchased from Sigma (Deisenhofen, Germany), metabion international AG (Martinsried, Germany) or Eurofins (Ebersberg Germany). They were designed using Primer3 software (Rozen and Skaletsky 2000) and used in a working concentration of 10 pmol/μl.

**Table 4: Oligonucleotides used for qRT-PCR**

Locus	AGI	forward	reverse
<b>PR1</b>	At2g14610	GGTAGCGGTGACTTGCTGCTGG	CAAACCTCATTGCACGTGTT
<b>WRKY29</b>	At4g23550	TCCTATGATCCCATCCGCTG	CGCTTGGTGCGTACTCGTT
<b>PROPEP2</b>	At5g64890	AGAAAAGCCTAGTTCAGGTCGTC	CTCCTTATAAACTTGATTGCCGC
<b>PROPEP3</b>	At5g64905	GTTCCGGTCTCGAAGTTCATC	ATCTTCCTCGCTGTGTGATGAC
<b>FLS2</b>	At5g46330	GCGAAACAGAGCTTTGAACC	GTGTCGTAACGAACCGATGA
<b>CRK39</b>	At4g04540	AGTGAGACAAATATCATTCT	AACTTAACTCCGTGAAGACAT
<b>RPP5</b>	At4g16950	GCTTTGAACATTTTGTCTGCC	ACGCAAAGTCTGATTTCTCTA
<b>WRKY70</b>	At3g56400	CTCATCGTCATCATGGTTTCG	CATTGACGTAACCTGGCCTGA
<b>EVR</b>	At2g31880	AGTGTTCATATGTATTGTT	CCATTTAAATTTTACAGTCGC
<b>ExPro</b>	At4g26410	GAGCTGAAGTGGCTTCCATGAC	GGTCCGACATACCCATGATCC

Table 5: Oligonucleotides used for ChIP-qPCR

Locus		forward	reverse
<b>PR1</b> (At2g14610)	amplicon 1	TCTTAATAAACTTCATTTAGGG	TTAGTAATATTCATTGCAATTGT
	amplicon 2	G TTCACAACCAGGCACGAGG	GTTTTCCCCGTAAGGCC
	amplicon 3	GTTTGTGGTCACTACACTCAAGT	TTAGTATGGCTTCTCGTTCACA
<b>Ta3</b>		GATTCTTACTGTAAAGAACATGGCATTGAGAGA	TCCAAATTTCTGAGGTGCTTGTAACC

#### 4.1.4 Chemicals

Laboratory grade chemicals and reagents were purchased from Serva (Heidelberg, Germany), Sigma-Aldrich (Deisenhofen, Germany), Invitrogen (Karlsruhe, Germany), Becton (Franklin Lakes, USA), Duchefa (Haarlem, Netherlands), Roche (Mannheim, Germany), Roth (Karlsruhe, Germany), Bio-Rad (München, Germany), Merck (Darmstadt, Germany) and Invitrogen (Karlsruhe, Germany), if not stated otherwise.

##### 4.1.4.1 Antibiotics

Table 6: Antibiotics used in this study

Antibiotic	Concentration used
Rifampicin (Rif)	100 mg/ml in DMSO
Kanamycin (Kan)	50 mg/ml in dH <sub>2</sub> O
Streptomycin (Strep)	50 mg/ml in dH <sub>2</sub> O

Stock solutions were prepared 1000x and stored at –20 °C until use.

##### 4.1.4.2 Elicitor

Flg22 and elf18 were used as elicitor originally identified to be the bioactive epitope from bacterial flagellin or elongation factor Tu, respectively. Flg22 and elf18 peptides were synthesized at EZBiolab Inc. (Carmel, USA) or JPT Peptide Technology (Berlin, Germany) with the following sequence:  
 flg22 – QRLSTGSRINSAKDDAAGLQIA (Felix et al. 1999),  
 elf18 – AcSKEKFERTKPHVNVGTIG (Kunze et al. 2004).

4.1.4.3 Antibodies

**Table 7: Antibodies used in this study**

Antibody	Concentration used	Source
α - p44/p42 MPK	1:1000	#9101S, Cell Signaling Technology (Boston, USA)
α – rabbit HRP	1:5000	sc-2004, Santa Cruz Biotechnologie (Heidelberg, Germany)
α - H3	1:1000 (for western blot)	Ab1791, Abcam (Cambridge, UK)
	1: 500 (for ChIP)	
α - rat IgG	1:1000 (for western blot)	Ab6703, Abcam (Cambridge, UK)
	1:500 (for ChIP)	
α - H3K4me3	1:1000 (for western blot)	pAb-003-050, Diagenode (Denville, USA)
	1:200 (for ChIP)	
α - H3K27me3	1:1000 (for western blot)	07-449, Millipore (Darmstadt, Germany)
	1:100 (for ChIP)	

**4.1.5 Media, Buffers and Solutions**

4.1.5.1 Media

Media were sterilized by autoclaving at 121 °C for 20 minutes (min). Heat instable ingredients were filter sterilized before addition to the autoclaved chilled media.

**Table 8: NYG media for *Pst***

0.5 % (w/v)	Bactopeptone
0.3 % (w/v)	Yeast extract
2 % (v/v)	Glycerol
	pH 7.0

For solid NYG plates (NYGA) 1 % (w/v) bacto agar was added prior autoclaving.

**Table 9: ½ MS medium for *Arabidopsis***

½ MS (Murashige & Skoog medium incl. Vitamins and MES buffer)
+ 0.8 % (w/v) sucrose
pH 5.8

For solid MS plates 0.8 % (w/v) plant agar was added prior autoclaving.

#### 4.1.5.2 Buffers and solutions

Buffers and solutions used in this study were prepared in dH<sub>2</sub>O and aqueous solutions were sterilized by autoclaving at 121 °C for 20 min. For ChIP buffers only autoclaved dH<sub>2</sub>O was used.

## 4.2 Methods

### 4.2.1 Cultivation of *Arabidopsis* plants

*Arabidopsis* seeds were sowed directly onto moist compost (Stender, Schermbeck, Germany), stratified for 3-4 days at 4 °C and grown in a controlled environment growth chamber under short day conditions (10 h light/14 h darkness, 23 °C/20 °C, 60 % humidity). For pathogen treatments, plants were grown for 4-5 weeks and then used for infections.

Seeds were surface sterilized by washing with 70 % (v/v) ethanol for 5 min, followed by 10 min washing with 1 % (v/v) bleach, 0.01 % (v/v) Triton X-100 and three rounds of washing with sterilized water. After 2-4 days of stratification at 4 °C, seedlings were grown on ½ MS agar plates for 5 days and subsequently transferred to ½ MS liquid medium and grown under controlled conditions (10 h light/14 h darkness, 21 °C, 70 % humidity) if not stated otherwise.

### 4.2.2 Maintenance of *Hyaloperonospora arabidopsidis* (*Hpa*) Noco2

The obligate biotrophic oomycete was maintained by re-inoculating 2-3-week-old soil-grown *Arabidopsis* Col-0 plants with 4x10<sup>4</sup> spores per ml water in a regular interval of 7 days. Infected plants were kept under controlled growth conditions of (10 h light/14 h darkness, 18 °C, 60 % humidity).

### 4.2.3 Elicitor-induced gene expression

Ten-day-old seedlings grown in liquid ½ MS liquid media were treated with 1 µM flg22 for the indicated time points. Subsequently, the seedlings were directly frozen in liquid nitrogen.

#### **4.2.4 MAMP-induced anthocyanin accumulation**

Surface sterilized and stratified seeds (see 4.2.1) were grown in ½ MS liquid-medium in 48-well plates for 3 days under continuous light and 23 °C. The medium was replaced by ½ MS liquid-medium without sucrose or supplied with 30 mM sucrose, 100 mM sucrose or 100 mM sucrose plus 1 µM flg22. Seedlings were further grown for additional 3 days.

Anthocyanin isolation was done in triplicates for each condition with ca. 10 seedlings per batch. Each batch of seedlings was weighed and frozen in liquid nitrogen. After homogenization 1 % (v/v) HCl (in 100 % MeOH) was added, mixed by vortexing and incubated at 4 °C overnight. The samples were centrifuged at 13,000 rpm for 5 min and the absorbance of the supernatant was measured at 530 nm and 657 nm. Anthocyanin concentration was calculated with the formula  $(A_{530}-A_{657}/4)/\text{gFW}$  (Teng et al. 2005).

#### **4.2.5 Local memory response assay**

Surface sterilized and stratified seeds were grown for 3 days on solid ½ MS media. Then, the seedlings were transferred to 48-well plates filled with ½ liquid media, each well containing 3-4 seedlings. Five-day-old seedlings were treated with 0.5 µM flg22, 0.5 µM elf18 or kept in liquid media (mock) for 48 h, which was terminated by replacing the MAMP-containing media with fresh liquid media. Another washing step was added 24 h later to remove flg22/elf18 as much as possible. Subsequently, the seedlings were cultivated for additional 48 h without MAMPs. To both, the treated (primed) and untreated (non-primed) samples, 10 nM flg22 or 10 nM elf18 was added in ½ MS liquid-medium. Seedlings were harvested at the indicated time points and frozen in liquid nitrogen. The zero hour time point corresponds to the samples immediately before second elicitation.

#### **4.2.6 Pathogen infection assays**

Pathogen infections were usually conducted directly after onset of light in the growth chamber at ca. 9 am.

##### **4.2.6.1 Bacterial growth assay - *Pst***

Single colonies were used for the inoculation of a liquid culture, which was cultivated overnight at 28 °C at 180 rounds per minute (rpm). Cultures were collected by centrifugation at 4,000 rpm for 5 min at room temperature (RT), washed once and resuspended in sterile 10 mM MgCl<sub>2</sub>. Then 3 well-expanded leaves of 8 plants per genotype were syringe-infiltrated with the bacteria solution at the indicated concentrations. Two days after inoculation, a leaf disc (5 mm diameter) was excised from 12 representative leaves. The 12 leaf discs were separated into three pools and then ground in 10 mM MgCl<sub>2</sub>. After grinding, the samples were vortex-mixed and diluted 1:10 serially. Samples (10 µL out of 1 ml) were plated on NYGA plates with the respective antibiotic(s). After two days incubation at

28 °C, colony-forming units were counted. Bacterial infections were performed at least in three independent experiments for each condition.

#### 4.2.6.2 Systemic assays

##### 4.2.6.2.1 *Hpa*

To monitor the development of SAR in WT and mutant plants, the procedure described by Zhang et al. was followed (Zhang et al. 2010). Briefly, 4-week-old plants were syringe-infiltrated in 3 well-expanded local leaves (expanded rosette leaves in the lower layer of the plant) with  $1 \times 10^6$  cfu/ml *Pst AvrRpm1*,  $1 \times 10^8$  cfu/ml *Pst ΔhrpS* or 10 mM MgCl<sub>2</sub> (mock). At 48 hpi the local leaves were removed and the remaining systemic leaves (young expanded rosette leaves in the upper layer of the plant) were inoculated with *Hpa* Noco2 at a concentration of  $4 \times 10^4$  spores/ml of water (Coates and Beynon 2010). At seven days pi (dpi) the disease symptoms were scored by counting the number of conidiophores on systemic leaves. Up to 18 plants were counted for each genotype and treatment, and were grouped into five categories (Table 10).

**Table 10: Disease categories**

Category	Symptoms
0	no conidiophores on the plant
1	one leaf infected with no more than five conidiophores
2	one leaf infected with more than five conidiophores
3	two leaves infected, but with no more than five conidiophores on each infected leaf
4	two leaves infected with more than five conidiophores on each infected leaf
5	more than two leaves infected with more than five conidiophores

##### 4.2.6.2.2 *Psm*

For bacterial growth measurement in systemic tissue, 3 well-expanded local leaves of 4-week-old *Arabidopsis* plants were syringe-infiltrated with  $1 \times 10^6$  cfu/ml *Pst AvrRpm1*,  $1 \times 10^8$  cfu/ml *Pst ΔhrpS* or 10 mM MgCl<sub>2</sub> (mock). Two days later  $1 \times 10^4$  cfu/ml *Pseudomonas syringae* pv. *maculicola* (*Psm*) were syringe-infiltrated in systemic leaves and the bacterial titer of *Psm* was assessed three days later as described in 4.2.6.1.

##### 4.2.6.3 Memory response assay in systemic leaves (Systemic priming)

Four-week-old plants were syringe-infiltrated (3 local leaves per plant and 8 plants per genotype) with 10 mM MgCl<sub>2</sub> (mock),  $1 \times 10^8$  cfu/ml *Pst ΔhrpS*,  $1 \times 10^6$  cfu/ml *Pst AvrRpm1*,  $1 \times 10^6$  cfu/ml *Pst AvrRps4*,  $1 \times 10^6$  cfu/ml *Pst AvrRpt2* or  $1 \times 10^4$  cfu/ml *Pst* DC3000. At 48 hpi local leaves were removed and systemic leaves were syringe-infiltrated with water. At the indicated time points the systemic infiltrated leaves

were harvested (one systemic leaf of each plant and pooled for each genotype) and frozen in liquid nitrogen.

In further experiments, systemic leaves were syringe-infiltrated with  $1 \times 10^4$  cfu/ml *Psm* and samples were harvested before (0 h, -) and 10 h (+) after infection (adapted from (Navarova et al. 2012)).

#### 4.2.6.4 Memory response assay in newly emerged leaves

Four-week-old wild type plants were syringe-infiltrated (3 local leaves per plant and 8 plants per genotype) with  $1 \times 10^6$  cfu/ml *Pst* DC3000 or 10 mM  $MgCl_2$ . At 48 hpi the local leaves were removed and young leaves present at this growth stage were marked to distinguish those from newly emerged leaves. Seven days later three newly emerged leaves per plant were syringe-infiltrated with water, harvested at the indicated time points and frozen in liquid nitrogen.

#### 4.2.7 **Ion leakage measurement**

Leaves of 4-week-old plants were syringe-infiltrated with  $1 \times 10^6$  cfu/ml *Pst AvrRpm1* and 10 mM  $MgCl_2$  (mock). Leaf discs (5 mm diameter) were excised post infiltration from 4 leaves per plant and at least 6 plants per genotype. The leaf discs were pooled, washed in sterile water for 30 min and then 4 leaf discs per sample and replicate were transferred to 2 ml  $H_2O$ . From each sample 60  $\mu$ L were removed and the electrolyte concentration was measured with a conductometer (Twin Compact Conductivity Meter B-173, Horiba) at the indicated time points and recovered after measurement.

#### 4.2.8 **Molecular biological methods**

##### 4.2.8.1 RNA extraction using TRI reagent

Frozen tissue samples were homogenized in liquid nitrogen and RNA was isolated using TRI Reagent (Ambion, Darmstadt, Germany) following the manufacturer's protocol. Concentration and quality was determined using a NanoDrop photometer (PeqLab, Erlangen, Germany). RNA with a 260/280 nm and 160/230 nm ratio of  $\sim 2.0$  was used for cDNA synthesis.

##### 4.2.8.2 cDNA synthesis

2.5  $\mu$ g RNA were used for cDNA synthesis following the manufacturer's protocol (Transcriptor Reverse Transcriptase, Roche) using oligo(dT)-primer.

##### 4.2.8.3 Quantitative real-time PCR (qRT-PCR)

RNA extraction and cDNA synthesis were performed as described above (4.2.8.1; 4.2.8.2.). qRT-PCR was performed for 96er plates on the IQ5 real-time PCR Thermocycler and for 384er plates on the CFX 384 Touch™ Real-Time Detection System (both Bio-Rad) using the primers listed in Table 4. The PCR reaction mix and thermal profile is shown in Table 11. Expression of the genes of interest were

normalized to the reference gene At4g26410, that exhibits a constant expression profile throughout various biotic and abiotic stresses (Czechowski et al. 2005). The results were analyzed using the comparative cycle threshold ( $\Delta\Delta C_t$ ) method (Livak and Schmittgen 2001). If not stated otherwise, fold-changes were calculated relative to wild type samples at 0 hours post treatment set to 1.

**Table 11: qRT-PCR reaction mix and thermal profile**

cDNA (1:10)	1 $\mu$ l	95 °C	2 min	
PCR buffer (10x)	2.5 $\mu$ l	95 °C	20 s	} 40x
dNTPs (10 mM)	0.5 $\mu$ l	55 °C	30 s	
Forward Primer	1 $\mu$ l	72 °C	25 s	
Reverse Primer	1 $\mu$ l	95 °C	1 min	
EVA Green	1.25 $\mu$ l	55 °C	1 min	
Fluorescin*	1.2 $\mu$ l			
Glycerol (50 % (v/v))	4 $\mu$ l			
DMSO (100% (v/v))	0.75 $\mu$ l			
Taq (Ambion)	0.5 $\mu$ l			
dH <sub>2</sub> O	up to 25 $\mu$ l			
		Melting curve (81 x)	55-95 °C	10 s; à 0.5 °C

\* 1:1000 diluted with 0.1 x TE buffer

#### 4.2.8.4 RNA-Seq

Local leaves of 4-week-old WT plants were infiltrated with  $1 \times 10^6$  cfu/ml *Pst AvrRpm1*,  $1 \times 10^8$  cfu/ml *Pst  $\Delta hrpS$*  or 10 mM MgCl<sub>2</sub> (mock). Systemic leaves were harvested in liquid nitrogen before (0 h) and 1 h after water infiltration in systemic leaves 48 h after the local infection. The experiment was performed in biological triplicates. Total RNA was isolated with RNeasy Mini kit supplied with RNase-Free DNase set (Qiagen) according to the manufacturer's instructions. RNA quality was assessed with RNA Nano-chips on a Bioanalyzer (Agilent). RNA-seq libraries were prepared from an input of 4  $\mu$ g total RNA according to recommendations of the supplier (TruSeq RNA sample preparation v2 guide, Illumina). Libraries were quantified by fluorometry, immobilized and processed onto a flow cell with a cBot (Illumina) followed by sequencing-by-synthesis with TruSeq v3 chemistry on a HiSeq2000. Library preparation, sequencing and raw data analysis were performed by the Genome Center at the Max Planck Institute for Plant Breeding Research, Cologne. Sequencing resulted in 5 to 40 Mio (average: 12 Mio, total: 220 Mio) 100bp single-end reads per sample

After an initial quality control with FastQC, the sequencing reads were mapped to the *Arabidopsis* genome (tair10) using TopHat2 with a minimum anchor length of 10 (-a 10) and allowing 10 alignments to the reference for a given read (-g 10) including information on known splice sites based on the tair10 gene models with option -G.

To analyze differential gene expression, a 3 × 2 factorial design was used with treatment (mock, *Pst ΔhrpS*, *Pst AvrRpm1*) and time (0, 1 h) as factors. Each condition contained three biological replicates totaling 18 samples. The mapped RNA-seq reads were transformed into a count per gene per sample using the function `coverageBed` of the `bedTools` suite (<http://bedtools.readthedocs.org>). Genes with less than 100 reads in all samples together were regarded as “not expressed” and thus discarded for the further analysis. Subsequently the count data of the remaining genes were log-transformed and normalized by the function `voom` from the R package `limma` to yield log<sub>2</sub> counts per million. To analyze differential gene expression, first a linear model with the coefficient “`treatment_time`” was fitted to each gene using function `lmFit` (R package `limma`). To find genes that are differentially expressed in response to *Pst ΔhrpS* or *Pst AvrRpm1* treatment, the gene expression at both time points between *Pst ΔhrpS/Pst AvrRpm1* and mock treatment were compared; i.e. moderated t-tests were applied to the following contrasts “*Pst ΔhrpS*\_0 h vs. mock\_0 h”, “*Pst ΔhrpS*\_1 h vs. mock\_1 h”, “*Pst AvrRpm1*\_0 h vs. mock\_0 h”, and “*Pst AvrRpm1*\_1 h vs. mock\_1 h”. The resulting P-values were adjusted for false discoveries due to multiple hypothesis testing via the Benjamini–Hochberg procedure.

The MDS-plot was generated using the default settings of the function `plotMDS` from the R package `limma`. The log<sub>2</sub>-transformed and normalized read counts per million (log<sub>2</sub>cpm) were used as input. For visualization of gene expression patterns, the Top100 most significant genes for each comparison were extracted and the union of these gene sets was visualized using the `annHeatmap` function (R package `Heatplus`). Genes were clustered according to their expression pattern, using complete linkage hierarchical clustering with the Pearson correlation as distance measure. Cutting the obtained dendrogram at height 1 yielded 12 clusters of expression patterns.

Trace plots were created to visualize average expression for each of the twelve clusters. To this end, for each cluster the mean and standard deviation of the genewise standardized log<sub>2</sub>-transformed counts per million were calculated and plotted per condition (i.e. time point & treatment) over all genes in this cluster

A similar procedure was followed for the comparison of differently expressed genes between “*Pst ΔhrpS* vs. mock” and “*Pst AvrRpm1* vs. mock” for each time point (0, 1 h) yielding 8 different clusters, whereas here the fold changes of the heatmap represent the differences between MTI and

ETI of the differences between 0 h and 1 h. The number of differentially expressed genes was shown in a Venn diagram.

Bioinformatics analysis was performed and supported by Dr. Barbara Kracher, MPIPZ Cologne.

Venn diagrams were created using the web tool GeneVenn (<http://genevenn.sourceforge.net/>).

Analysis of overrepresented gene ontologies was carried out by using the online tool VirtualPlant 1.3 (Katari et al. 2010) and cross-referenced with AgriGO (<http://bioinfo.cau.edu.cn/agriGO/>) (Du et al. 2010). Meta-analysis of gene expression was assessed by Genevestigator V3 (<https://www.genevestigator.com/gv/index.jsp>) (Hruz et al. 2008).

#### 4.2.9 Biochemical methods

##### 4.2.9.1 MAPK – protein lysis

To analyze the abundance of activated MAPKs upon MAMP treatment, 10-day-old seedlings were treated with 1  $\mu$ M flg22 and harvested at the indicated time points in liquid nitrogen and homogenized. Proteins were extracted in 150  $\mu$ L MAPK lysis buffer, mixed and centrifuged for 15 min at 15.000 rpm at 4 °C. The supernatant was transferred to a fresh tube, 6x SDS samples buffer was added and the sample either stored at -20 °C or directly used for SDS-PAGE and western blot analysis.

**Table 12: MAPK lysis buffer**

50 mM	Tris-HCl pH 7.5
200 mM	NaCl
1 mM	EDTA
10 mM	NaF
25 mM	beta-glycerophosphate
2 mM	sodium orthovanadate
10 % (v/v)	glycerol
0.1 mM	Tween-20
0.5 mM	DTT
1 mM	PMSF
1x	Plant Proteinase Inhibitor (Sigma)

**Table 13: 6x SDS loading buffer**

7 ml	4x Upper buffer
1 g	SDS
93 mg	DTT
3 ml	Glycerol
+	bromphenol blue

4.2.9.2 SDS-PAGE for MAPK detection and total level of histone modifications

The samples were incubated at 95 °C for 5 min (for MAPK detection) or for 30 min (for total level of histone modifications) and subsequently loaded on a SDS page (10 % SDS-PAGE resolving gel for MAPK, 15 % SDS-PAGE resolving gel for total histone modification level).

**Table 14: Resolving gel (10 % & 15 %, 1.5 mm)**

10 % SDS-PAGE		15 % SDS-PAGE	
4 x lower buffer	2 ml	4 x lower buffer	2 ml
30 % (v/v) acryl amid	2.7 ml	30 % (v/v) acryl amid	5 ml
dH <sub>2</sub> O	5.3 ml	dH <sub>2</sub> O	3 ml
10 % (w/v) APS	40 µl	10 % (w/v) APS	40 µl
TEMED	2.5 µl	TEMED	2.5 µl

**Table 15: Stacking gel (3 %)**

4 x upper buffer	0.75 ml
30 % (v/v) acryl amid	300 µl
dH <sub>2</sub> O	1.89 ml
10 % (w/v) APS	60 µl
TEMED	1.5 µl

**Table 16: 4 x Upper and Lower buffer**

0.5 M Tris-HCl	1.5 M Tris-HCl
0.4 % (v/v) SDS	0.4 % (v/v) SDS
pH 6.8	pH 8.8

15 µl of the sample and 8 µl the prestained molecular-weight marker (Precision plus protein standard dual color; Bio-Rad) were loaded stacking gel. Gels were run in electrophoresis tanks (Mini-Protean 3 Cell; Bio-Rad) in 1x SDS-running buffer at 30 mA/gel (constant) until the marker suggested a sufficient separation of the proteins in the resolving gel.

**Table 17: 1x SDS-running buffer**

25 mM	Tris-Base
192 mM	Glycin
0.1 % (w/v)	SDS

#### 4.2.9.3 Western Blot

Proteins were transferred from SDS-gels to PVDF-membranes (Millipore) using a semidry-blotting system (Trans-Blot SD Semi-Dry Transfer Cell, Bio-Rad) filled with 1 x semi-dry buffer. The membrane was activated in 100 % (v/v) MeOH for 30 s and incubated in 1 x semi-dry blotting buffer together with Whatman paper and the gel(s) before blotting. Blotting was performed at 100 mA/gel (constant) for 90 min at RT. Afterwards the membrane was incubated in PBS-T plus 5 % (w/v) milk powder (or plus 5 % (w/v) BSA for  $\alpha$  - H3K27me3 antibody) for 1 h at RT to block free binding sites. The blot was then transferred to PBS-T plus 3 % (w/v) milk powder (or plus 3 % (w/v) BSA for  $\alpha$  - H3K27me3 antibody) containing the first antibody and incubated at 4 °C over night gently shaking. Afterwards, the membranes were at least washed three times for 5 min in PBS-T and incubated with the secondary antibody in PBS-T for 1 h at RT. After washing twice in PBS-T, an enhanced chemi-luminescence (ECL) detection was performed according to the manufacturer's instructions (SuperSignal® West Pico Chemiluminescent kit (Pierce, Rockford, USA). Luminescence was detected and recorded by the ChemiDoc™ system (Bio-Rad).

Ponceau staining was used to visualize equal loading after MAPK detection. Therefore the membrane was incubated for 5 min in Ponceau S staining solution (ATX Ponceau S, 1:5 in dH<sub>2</sub>O (Sigma-Aldrich) and rinsed with tap water to get rid of an excess of the staining solution.

Protein abundance of H3K27me3 and H3K4me3 was calculated comparing the signal intensities relative to those from H3 using the Image Lab™ software provided with the ChemiDoc™ system (Bio-Rad).

**Table 18: 1x PBS buffer**

8 % (w/v)	NaCl
0.2 % (w/v)	KCl
1.44 % (w/v)	Na <sub>2</sub> HPO <sub>4</sub>
0.24 % (w/v)	KH <sub>2</sub> PO <sub>4</sub>
pH 7.4	
PBS-T buffer:	1x PBS buffer + 0.1% Tween20

**Table 19: 1x Semi-dry blotting buffer**

5.8 % (w/v)	Tris-Base
2.9 % (w/v)	Glycin
0.37 % (w/v)	SDS
dissolved in 800 ml dH <sub>2</sub> O	
plus 200 ml MeOH for 1 l	

### 4.2.9.4 Chromatin Immunoprecipitation (ChIP)

Two grams plant material was harvested per sample and immersed in PBS supplemented with 1 % formaldehyde. The plant tissue was then vacuum infiltrated for 20 min. Glycine was added to a final concentration of 0.1 M and incubated for additional 5 min. The plant tissue was removed from the solution and frozen in liquid nitrogen. The ground tissue was then resuspended in 30 ml NIB, filtered through a 20  $\mu$ m and 70  $\mu$ m nylon mesh into a new 50 ml Falcon tube and the volume was readjusted to 30 ml with fresh NIB. After centrifugation at 2.500 *g* for 20 min at 4 °C, the nuclear pellet was resuspended and washed in NWB. After centrifugation, the pellet was resuspended in 1 ml 1x TE buffer supplemented with 0.5 % SDS and mixed on a rotator for 20 min at 4 °C. The chromatin was diluted with 1x TE buffer to a final SDS concentration of 0.25 % and the DNA was sheared by sonication (Bioruptor<sup>TM</sup>Next Gen, Diagenode, Germany) to approximately 500–1.000 bp fragments. After centrifugation to clear the chromatin extract (15 min, 13.000 rpm, 4 °C), 100  $\mu$ l chromatin extract was mixed with 300  $\mu$ l IP dilution buffer and 100  $\mu$ l 1x TE buffer. Additionally, 1 mM DTT, 0.5  $\mu$ g/ml RNase A and 0.2 % proteinase inhibitor cocktail (Sigma) were added. Depending on the IP, the following antibody was added: 5  $\mu$ l  $\alpha$ -H3, 1  $\mu$ l  $\alpha$ -rat IgG, 5  $\mu$ l  $\alpha$ -H3K27me3 or 3  $\mu$ l  $\alpha$ -H3K4me3 (Table 7). After incubation overnight with rotation at 4 °C, the samples were cleared by centrifugation (14.000 rpm, 15 min, 4 °C). A 30  $\mu$ l aliquot of RIPA-washed ProteinA-coupled sepharose beads (rProteinA-sepharose<sup>TM</sup> Fast Flow, GE Healthcare, Solingen, Germany) was added to the supernatant and the incubation continued on the rotating wheel for 1 h at 4°C. The sepharose beads were then washed five times with 1 ml of RIPA buffer. The immunocomplexes were eluted from the beads with two times 200  $\mu$ l of glycine elution buffer and the combined elutes neutralized with 100  $\mu$ l 1 M Tris-HCl (pH 9.7). Crosslinks were reversed by incubation at 37 °C for at least 6 h in the presence of 60  $\mu$ g/ml Proteinase K followed by at least 8 h incubation at 65 °C. The DNA was purified by two successive phenol/chloroform/isoamyl alcohol extractions and ethanol precipitation. Pellets were washed with 70 % (v/v) ethanol and resuspended in 50 – 100  $\mu$ l H<sub>2</sub>O (Searle et al. 2006; Farrona et al. 2011). For protein detection, 100  $\mu$ l chromatin extract was mixed with 20  $\mu$ l 6x SDS-loading buffer (see 4.2.9.1) and subsequently used for SDS-PAGE and western blot (see 4.2.9.2 and 4.2.9.3).

**Table 20: Buffers and solutions used for Chromatin-Immunoprecipitation (ChIP)**

<b>NIB</b>	
50 mM	HEPES pH 7.4
5 mM	MgCl <sub>2</sub>
25 mM	NaCl
5 % (w/v)	Sucrose
30 % (w/v)	Glycerol
0.25 % (v/v)	Triton X-100
0.1 % (v/v)	β-mercaptoethanol
+ 1x Plant Protease Inhibitor Cocktail (Sigma)	

<b>3x NWB</b>	
50 mM	HEPES pH 7.4
20 mM	MgCl <sub>2</sub>
100 mM	NaCl
40 % (w/v)	Sucrose
40 % (v/v)	Glycerol

1x NWB: 60 ml 3x wash buffer, 120 ml dH<sub>2</sub>O, 0.45 ml TritonX-100, 180 μl β-mercaptoethanol + 1x Plant Protease Inhibitor Cocktail (Sigma).

<b>IP dilution</b>	
80 mM	Tris-HCl pH 7.4
230 mM	NaCl
1.7 % (v/v)	NP40
0.17 (w/v)	DOC

RIPA buffer: 60 ml IP dilution buffer, 1 ml 10 % (v/v) SDS + 39 ml dH<sub>2</sub>O.

<b>Glycin elution buffer</b>	
0.1 M	Glycin pH 2.5
0.5 M	NaCl
0.05 % (v/v)	Tween-20

<b>1x TE</b>	
1mM	EDTA pH 8.0
10mM	Tris-HCl pH 7.4

#### 4.2.9.4.1 qPCR of ChIP DNA samples

4 μl DNA was added to 1 μl primer mix (10 pmol/μl each) and 5 μl 2x SYBR Green Ready Mix (Bio-Rad) per sample. Each sample was quantified in triplicates in a 384 well plate using the LightCycler480 machine (Roche) with the program depicted in Table 21 and the oligonucleotides in Table 5. The enrichment of each IP was calculated relative to an appropriate dilution of the INPUT, which was obtained by processing 10 % of the supernatant of each control antibody precipitation with α-rat IgG in parallel during the de-crosslinking and DNA purification procedure. This value of each sample was further normalized to the qPCR signal obtained from the respective immunoprecipitated DNA with

$\alpha$ -H3. The background of each ChIP experiment was determined by amplifying a region of the *Ta3 Arabidopsis* retrotransposon calculated as average of qPCR signal from each sample (Farrona et al. 2011).

**Table 21: ChIP qPCR program**

95 °C	3 min	
95 °C	15 s	
58 °C	30 s	50x
72 °C	30 s	
95 °C	5 min	+ melting curve (55 – 95 °C, 10 s á 0.5 °C)

#### 4.2.10 Statistics

To assess differences in bacterial growth, a linear mixed-effects model was fitted to the log-transformed bacterial count data (function lme, R package nlme). Significant effects were identified by analysis of variance (ANOVA) and post hoc testing using Tukey contrasts (function glht, R package multcomp). Statistical significance was defined as  $p < 0.05$  or higher and indicated with different letters (a, b, c, d).

Otherwise, the t-test function in Excel (Microsoft Office 2013) was used for two-tailed homoscedastic comparisons and significant difference(s) indicated by asterik(s).

## 5 Supplementary information

**Supplementary Table 1: Gene list of 209 differentially regulated genes in *rsw3* compared to WT 10 h after *elf18* application (< 2-fold,  $p < 0.05$ ) that were analyzed regarding their histone mark status of H3K27me3, H3K4me3 or both.**

H3K27me3 only 55 genes		H3K4me3 only 70 genes		both 32 genes	total >2 209 genes					
AT1G02940	AT4G20000	AT1G05300	AT4G01750	AT1G24140	AT5G39580	AT5G44568	AT3G47480	AT2G47140	AT1G69900	AT4G36670
AT1G14540	AT4G23550	AT1G11310	AT4G04330	AT1G24147	AT5G05340	AT2G39530	AT4G23170	AT1G70520	AT3G04070	AT2G35930
AT1G26410	AT4G26200	AT1G12940	AT4G11280	AT1G25400	AT2G19190	AT2G39380	AT5G43285	AT4G33050	AT1G19380	AT3G13790
AT1G26420	AT4G28420	AT1G13110	AT4G13510	AT1G27730	AT3G18250	AT5G26340	AT2G39210	AT4G39670	AT1G05300	AT1G18300
AT1G29860	AT4G35180	AT1G18300	AT4G14365	AT1G30720	AT1G53625	AT3G07390	AT4G11280	AT2G41380	AT2G20142	AT5G24530
AT1G30700	AT5G05340	AT1G19380	AT4G20860	AT2G27660	AT4G12500	AT2G22880	AT4G15417	AT4G21680	AT1G65510	AT5G04340
AT1G30900	AT5G13080	AT1G25390	AT4G21120	AT2G28630	AT1G69930	AT4G12490	AT5G55050	AT2G39400	AT5G64810	AT4G17500
AT1G33840	AT5G22570	AT1G49000	AT4G23270	AT2G35930	AT5G13320	AT1G51800	AT4G11170	AT3G10930	AT5G50200	AT1G66090
AT1G33960	AT5G25250	AT1G56300	AT4G23300	AT2G39200	AT5G25260	AT2G43620	AT2G27660	AT2G40080	AT4G16146	AT1G65845
AT1G35230	AT5G39580	AT1G66090	AT4G23610	AT2G43570	AT5G36925	AT3G25882	AT5G61890	AT3G57260	AT1G25400	AT4G03460
AT1G51800	AT5G44390	AT1G66920	AT4G23810	AT2G44370	AT1G51913	AT4G23550	AT1G56300	AT5G06320	AT1G61560	AT4G01250
AT1G51820	AT5G44568	AT1G69720	AT4G31550	AT3G13790	AT3G23250	AT5G35735	AT4G02330	AT3G50260	AT1G11310	AT3G59700
AT1G51850	AT5G46050	AT1G69900	AT4G33050	AT3G45260	AT4G01700	AT5G46050	AT2G18660	AT5G01540	AT1G80820	AT1G70530
AT1G51890	AT5G48430	AT1G70520	AT4G36430	AT3G50260	AT5G23240	AT5G42830	AT5G25250	AT4G20860	AT3G21781	
AT1G51913	AT5G61890	AT1G70530	AT4G36670	AT3G52450	AT1G14540	AT3G02240	AT4G18250	AT4G23215	AT1G35230	
AT1G56240	AT5G64905	AT1G73680	AT4G39830	AT4G02330	AT4G35180	AT5G26920	AT1G02430	AT4G08555	AT1G51890	
AT1G65500		AT1G73805	AT5G01540	AT4G11170	AT1G26410	AT5G43290	AT5G16170	AT2G28400	AT3G46690	
AT1G69930		AT1G74710	AT5G03350	AT4G14450	AT5G64905	AT5G03350	AT4G31550	AT1G12940	AT1G33840	
AT2G18660		AT1G78000	AT5G03700	AT4G17500	AT2G17740	AT2G43570	AT4G18940	AT3G51660	AT4G01750	
AT2G36690		AT1G80820	AT5G04340	AT4G18250	AT5G48430	AT5G40780	AT1G51850	AT2G25000	AT2G42060	
AT2G39518		AT1G80840	AT5G06320	AT4G21380	AT2G39200	AT5G52750	AT4G08040	AT1G30900	AT5G38900	
AT2G39530		AT2G25000	AT5G16170	AT4G22470	AT2G39518	AT1G51820	AT5G03700	AT2G44290	AT4G21380	
AT2G43620		AT2G39210	AT5G23240	AT4G23170	AT2G36690	AT5G67450	AT1G27730	AT1G78000	AT1G80840	
AT2G47140		AT2G39400	AT5G24530	AT4G23210	AT1G30720	AT5G22570	AT2G28630	AT5G44390	AT4G23150	
AT3G02240		AT2G41380	AT5G25440	AT5G10760	AT1G13480	AT1G65500	AT1G13110	AT2G42360	AT4G19810	
AT3G13950		AT2G44290	AT5G35735	AT5G20230	AT2G44370	AT1G65481	AT1G64400	AT1G33960	AT5G25440	
AT3G23250		AT3G04070	AT5G52750	AT5G26340	AT4G26200	AT1G74710	AT2G44380	AT1G57630	AT1G56240	
AT3G46280		AT3G07390	AT5G53110	AT5G26920	AT1G30700	AT3G15518	AT3G47380	AT4G23810	AT1G66920	
AT3G47380		AT3G10930	AT5G54490	AT5G43290	AT5G44575	AT3G46280	AT1G64170	AT1G29860	AT1G69720	
AT3G47480		AT3G18830	AT5G57220	AT5G50200	AT3G15536	AT1G49000	AT3G52450	AT1G73805	AT3G26210	
AT3G57260		AT3G20340	AT5G67450	AT5G55050	AT1G36622	AT1G26420	AT4G14450	AT4G14365	AT2G18680	
AT4G03460		AT3G25882		AT5G64810	AT4G20000	AT3G54420	AT5G54490	AT4G13510	AT1G25390	
AT4G08040		AT3G26210			AT5G22270	AT3G13950	AT4G19970	AT4G21120	AT4G23270	
AT4G12490		AT3G51660			AT4G36430	AT4G22470	AT5G44910	AT4G23610	AT4G04330	
AT4G12500		AT3G52400			AT5G10760	AT5G57220	AT4G28420	AT1G24140	AT1G73680	
AT4G15417		AT3G54420			AT5G60630	AT4G23210	AT4G39830	AT4G23300	AT1G24147	
AT4G18940		AT3G56710			AT1G02450	AT2G43510	AT2G31335	AT1G02940	AT3G18830	
AT4G19810		AT3G59700			AT5G53110	AT1G31885	AT5G39670	AT3G45260	AT3G20340	
AT4G19970		AT4G01250			AT1G65690	AT5G20230	AT5G13080	AT1G13540	AT3G52400	

**Supplementary Table 2: List of genes used for the heatmap extracted from the original data file with indicated fold changes and p-values. Chosen marker genes were marked in dark red. AGI: *Arabidopsis* genome initiative; FC: fold change.**

Cluster	AGI	Name	0 h				1 h			
			Pst ΔhrpS vs. mock log <sub>2</sub> FC	Pst ΔhrpS vs. mock p-value	Pst AvrRpm1 vs. mock log <sub>2</sub> FC	Pst AvrRpm1 vs. mock p-value	Pst ΔhrpS vs. mock log <sub>2</sub> FC	Pst ΔhrpS vs. mock p-value	Pst AvrRpm1 vs. mock log <sub>2</sub> FC	Pst AvrRpm1 vs. mock p-value
	AT5G52410	NA	-0.01	9.55E-01	-0.15	2.78E-01	0.15	3.53E-01	0.03	8.78E-01
	AT5G56160	NA	-2.91	4.39E-06	-3.11	1.77E-07	1.66	5.28E-06	-1.37	2.83E-03
	AT5G52020	NA	-4.45	1.65E-06	-4.03	6.42E-08	1.91	2.91E-05	-1.07	6.18E-02
	AT5G07920	ATDGK1	-2.60	1.19E-06	-2.38	3.68E-07	1.39	6.00E-05	-0.36	2.64E-01
	AT1G11960	NA	-2.84	8.97E-07	-2.60	3.73E-07	1.44	9.01E-05	-0.81	1.86E-02
	AT2G32150	NA	-2.35	1.32E-06	-1.77	4.75E-06	0.69	1.77E-02	-0.02	9.46E-01
	AT2G22010	RKP	-1.05	1.40E-06	-0.74	1.42E-05	0.37	8.44E-03	0.11	4.27E-01
	AT1G17420	ATLOX3	-3.33	2.25E-07	-2.59	5.35E-07	0.27	4.76E-01	-0.82	2.29E-02
	AT2G06050	DDE1	-3.35	1.02E-06	-2.59	3.37E-06	0.66	1.13E-01	-0.24	5.75E-01
	AT1G42470	NA	-1.36	1.69E-06	-1.14	2.38E-06	0.80	8.67E-05	-0.96	4.61E-05
	AT3G62010	NA	-1.42	1.78E-07	-1.19	3.24E-07	0.77	4.65E-05	-0.43	8.40E-03
	AT1G66760	NA	-2.31	7.65E-07	-2.80	4.31E-08	0.50	7.41E-02	-1.12	7.11E-04
	AT1G12610	DDF1	-3.54	1.78E-07	-4.93	3.61E-08	2.83	1.41E-06	-1.26	7.31E-02
	AT3G19240	NA	-1.97	9.80E-07	-2.14	9.38E-08	1.56	3.17E-06	-0.66	2.81E-02
	AT5G62520	SRO5	-2.27	2.38E-06	-3.23	4.63E-08	2.32	5.37E-07	0.08	8.45E-01
	AT4G19960	ATKUP9	-1.36	2.80E-06	-1.24	1.91E-06	1.56	1.11E-07	0.09	6.66E-01
	AT3G14590	NTMC2T6.2	-2.37	1.84E-06	-1.94	1.17E-06	2.36	3.94E-08	-0.54	7.94E-02
	AT2G24330	NA	-1.30	8.42E-06	-1.08	9.77E-06	1.78	1.98E-08	-0.15	4.56E-01
	AT1G78280	NA	-2.50	8.46E-09	-1.93	4.57E-08	1.79	3.94E-08	-0.16	4.33E-01
	AT5G63370	NA	-1.27	1.84E-06	-1.00	6.51E-06	0.71	1.96E-04	-0.22	1.76E-01
	AT4G36900	DEAR4	-3.68	6.58E-07	-2.47	6.75E-08	0.04	9.01E-01	-1.16	4.43E-04
	AT2G33380	AtCLO3	-3.48	3.04E-09	-2.80	5.05E-09	-1.22	1.11E-05	-2.06	7.85E-08
	AT1G73480	NA	-2.60	2.25E-06	-2.10	4.28E-06	-0.41	2.32E-01	-0.63	5.42E-02
	AT4G15450	NA	-2.03	1.96E-06	-2.37	6.42E-08	-0.92	1.72E-04	-1.36	5.11E-06
	AT1G01030	NGA3	-3.45	4.87E-06	-3.45	2.10E-07	-1.18	8.55E-04	-1.28	3.57E-04
	AT2G23340	DEAR3	-2.39	4.96E-07	-2.39	3.84E-08	-0.59	6.74E-03	-0.95	1.53E-04
	AT3G12920	BRG3	-1.55	2.50E-06	-1.76	1.28E-07	-0.41	2.94E-02	-0.21	2.33E-01
	AT2G29450	AT103-1A	-2.68	1.02E-07	-2.73	3.84E-08	-0.74	4.52E-03	-0.43	6.47E-02
	AT3G59940	NA	-1.87	2.12E-06	-1.10	4.88E-05	-0.37	9.23E-02	-0.10	6.59E-01
	AT4G01026	PYL7	-1.83	4.54E-07	-1.31	1.21E-06	-0.06	7.94E-01	0.07	7.11E-01
	AT2G43018	NA	-2.20	1.22E-06	-1.55	3.82E-06	-0.50	3.51E-02	-0.31	1.59E-01
	AT2G43020	ATPAO2	-2.20	1.22E-06	-1.55	3.82E-06	-0.50	3.51E-02	-0.31	1.59E-01
	AT5G53048	NA	-2.40	5.06E-07	-1.83	8.51E-07	-0.63	1.32E-02	-0.20	3.98E-01
	AT5G53050	NA	-2.30	2.25E-07	-1.96	3.31E-07	-0.66	8.55E-03	-0.21	3.82E-01
	AT3G25760	AOC1	-4.96	1.84E-06	-3.54	3.45E-07	-0.88	1.87E-02	-0.83	2.04E-02
	AT5G54170	NA	-2.45	4.97E-08	-1.94	1.24E-07	-0.43	3.95E-02	-0.28	1.48E-01
	AT3G45140	ATLOX2	-2.44	3.62E-07	-1.82	1.87E-06	0.11	7.13E-01	0.14	5.89E-01
	AT3G25770	AOC2	-3.77	1.02E-06	-2.90	6.79E-07	-0.03	9.41E-01	-0.69	3.06E-02
	AT1G58200	MSL3	-1.85	7.82E-08	-1.33	5.30E-07	-0.01	9.53E-01	-0.34	3.49E-02
	AT3G05640	NA	-2.15	6.93E-06	-1.64	4.69E-06	-0.93	1.28E-04	-2.40	5.53E-08
	AT4G23600	COR13	-3.03	1.32E-06	-1.60	3.70E-05	-1.07	4.80E-04	-2.26	4.96E-07
	AT1G51090	NA	-2.98	1.23E-05	-3.73	2.05E-07	-0.61	7.45E-03	-1.84	7.63E-07
	AT4G27520	AtENODL2	-1.46	4.39E-06	-2.01	6.42E-08	0.01	9.70E-01	-0.85	1.77E-04
	AT3G17800	NA	-1.14	6.58E-07	-1.01	7.26E-07	0.04	7.87E-01	-0.72	1.07E-05
	AT1G76180	ERD14	-1.35	8.09E-07	-1.07	2.83E-06	0.62	2.90E-04	-0.46	3.82E-03
	AT1G10090	NA	-2.07	2.38E-06	-1.95	5.49E-07	0.18	4.02E-01	-0.78	5.54E-04
	AT1G01470	LEA14	-2.20	1.61E-06	-1.76	2.85E-06	0.59	1.18E-02	-0.39	8.61E-02
	AT2G17840	ERD7	-3.01	1.78E-07	-2.60	1.93E-07	0.35	1.94E-01	-0.58	2.85E-02
	AT5G08500	NA	-1.68	6.42E-07	-1.60	1.77E-07	0.98	3.88E-06	-0.17	3.12E-01
	AT3G20500	ATPAP18	-1.42	2.38E-06	-1.29	1.21E-06	0.42	1.14E-02	-0.36	2.74E-02
	AT4G37790	HAT22	-1.47	4.54E-07	-1.37	1.88E-07	0.22	1.52E-01	0.05	7.49E-01
	AT5G63770	ATDGK2	-3.14	4.97E-08	-2.85	3.84E-08	1.08	3.37E-04	-0.09	7.60E-01
	AT4G21570	NA	-2.46	2.32E-07	-2.10	3.02E-07	0.81	2.34E-03	-0.54	3.25E-02
	AT5G44050	NA	-3.11	1.98E-06	-3.03	1.24E-07	0.34	2.23E-01	-1.54	8.31E-05
	AT4G04840	ATMSRB6	-1.47	1.01E-05	-1.81	3.30E-07	-0.03	9.18E-01	-1.25	9.89E-06
	AT5G61810	NA	-1.92	2.51E-06	-2.10	2.10E-07	0.09	7.26E-01	-1.09	6.20E-05
	AT2G45820	NA	-1.66	1.78E-07	-1.80	3.84E-08	0.44	8.26E-03	-0.88	2.13E-05
	AT1G20450	ERD10	-2.20	6.35E-07	-2.34	9.64E-08	0.30	2.14E-01	-1.26	3.56E-05
	AT3G48520	CYP94B3	-4.28	1.07E-06	-4.92	6.42E-08	0.66	5.58E-02	-0.94	1.48E-02
	AT3G02570	MEE31	-1.21	2.53E-06	-1.54	6.42E-08	-0.04	8.33E-01	-0.65	2.75E-04
	AT1G77680	NA	-1.72	6.42E-07	-1.87	6.42E-08	-0.33	6.30E-02	-0.78	1.62E-04
	AT5G41600	BT13	-2.22	2.06E-07	-2.08	5.53E-08	-0.24	2.52E-01	-0.74	8.66E-04
	AT1G19570	ATDHAR1	-2.97	8.46E-09	-2.81	1.21E-08	-0.51	2.33E-02	-1.06	5.85E-05
	AT2G46370	FIN219	-2.24	8.46E-09	-1.84	3.84E-08	-0.28	1.15E-01	-0.83	6.39E-05

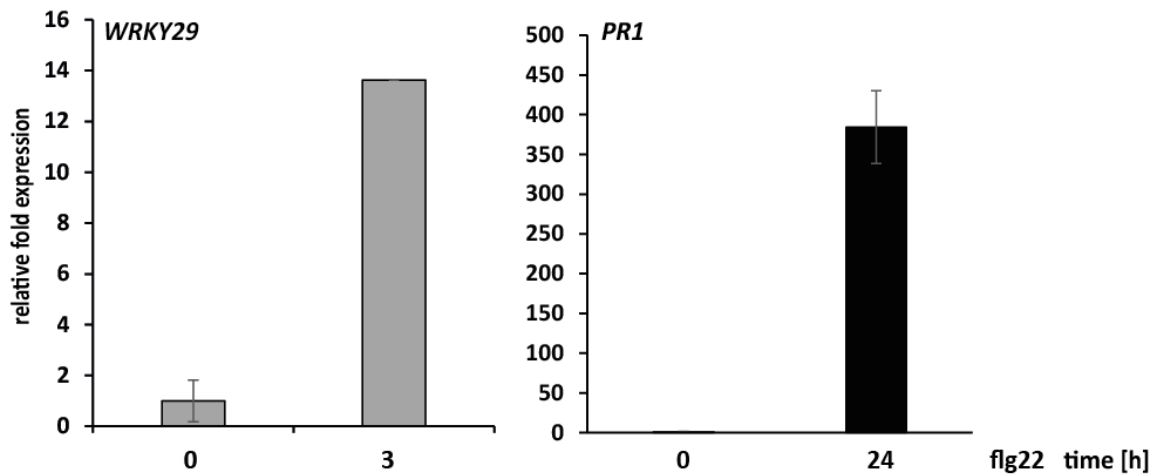
Cluster	AGI	Name	0 h				1 h			
			<i>Pst</i> $\Delta$ hrpS vs. mock log <sub>2</sub> FC	<i>Pst</i> $\Delta$ hrpS vs. mock p-value	<i>Pst</i> AvrRpm1 vs. mock log <sub>2</sub> FC	<i>Pst</i> AvrRpm1 vs. mock p-value	<i>Pst</i> $\Delta$ hrpS vs. mock log <sub>2</sub> FC	<i>Pst</i> $\Delta$ hrpS vs. mock p-value	<i>Pst</i> AvrRpm1 vs. mock log <sub>2</sub> FC	<i>Pst</i> AvrRpm1 vs. mock p-value
			II	AT3G55840	NA	-0.44	1.20E-01	-0.41	6.20E-02	1.65
	AT1G02270	NA	-1.25	4.53E-05	-0.89	2.39E-04	2.18	4.30E-09	0.46	1.89E-02
	AT5G65630	GTE7	0.29	1.56E-01	-0.21	2.15E-01	2.03	1.57E-09	0.04	8.45E-01
	AT4G09030	AGP10	0.22	6.26E-01	-0.34	2.55E-01	1.95	4.40E-08	-1.24	2.93E-04
	AT1G68410	NA	-0.16	5.48E-01	-0.14	4.82E-01	1.48	4.34E-08	-1.06	5.56E-06
	AT1G02660	NA	-1.06	2.83E-05	-1.11	5.16E-06	1.50	4.61E-08	-0.84	7.36E-05
	AT4G38420	skt9	-0.54	1.29E-01	-1.16	4.50E-04	2.42	6.93E-09	-1.11	3.35E-04
	AT5G24030	SLAH3	-0.35	2.44E-01	-1.35	2.38E-05	1.89	5.98E-08	-0.36	1.04E-01
	AT1G72790	NA	-0.29	4.23E-01	-0.99	9.94E-04	2.69	2.35E-08	0.39	2.42E-01
	AT1G75310	AUL1	-0.53	2.85E-02	-0.84	3.30E-04	1.84	4.87E-08	-0.21	3.75E-01
	AT5G64310	AGP1	0.01	9.82E-01	-0.40	1.65E-01	2.75	2.25E-08	-1.41	6.88E-04
	AT1G17620	NA	-0.59	7.29E-03	-0.98	2.64E-05	1.87	1.61E-08	-0.69	2.62E-03
	AT4G26690	GDDL2	-0.32	1.12E-01	-0.64	5.96E-04	1.49	6.29E-08	-0.42	1.74E-02
	AT2G21500	NA	-0.95	5.47E-04	-0.37	6.74E-02	1.91	4.61E-08	0.51	1.94E-02
	AT4G19520	NA	-0.48	1.93E-02	0.09	6.12E-01	2.03	3.72E-09	-0.30	8.04E-02
	AT2G21120	NA	-0.31	1.55E-01	0.17	3.25E-01	1.72	1.63E-08	-0.28	1.20E-01
	AT1G56510	ADR2	-0.30	1.08E-01	0.14	3.79E-01	1.89	3.57E-09	-0.40	1.47E-02
III	AT3G60290	NA	-0.22	3.82E-01	-0.37	4.73E-02	-0.31	5.95E-02	-2.16	3.37E-08
	AT5G17050	UGT78D2	-0.09	7.16E-01	-0.50	3.35E-03	-0.61	1.69E-04	-1.54	3.93E-08
	AT3G49220	NA	-0.27	2.33E-01	-0.77	2.55E-04	-0.55	2.45E-03	-1.69	5.64E-08
	AT4G38400	ATEXLA2	-1.71	7.91E-05	-2.75	2.73E-07	0.51	2.47E-02	-2.18	1.99E-06
	AT5G02940	NA	-2.05	1.40E-06	-2.24	1.77E-07	0.13	6.39E-01	-1.94	1.04E-06
	AT4G12000	NA	-2.09	2.62E-06	-2.19	2.32E-07	0.53	2.23E-02	-1.52	1.29E-05
	AT4G32190	NA	-1.21	1.37E-06	-1.32	1.70E-07	0.02	9.27E-01	-1.09	1.06E-06
	AT1G50040	NA	-1.06	5.26E-05	-3.51	3.48E-09	1.15	1.01E-05	-1.09	4.81E-04
	AT3G19680	NA	-0.54	5.28E-02	-2.41	8.97E-08	0.82	1.32E-03	-0.69	7.61E-03
	AT2G35290	NA	-1.48	4.65E-05	-2.91	4.90E-08	2.08	2.68E-08	-1.24	7.58E-04
	AT5G67300	ATMYB44	-0.58	6.29E-03	-1.73	6.42E-08	0.81	1.00E-04	-0.96	3.19E-05
	AT2G40400	NA	-0.45	4.34E-03	-1.23	8.32E-08	-0.53	4.00E-04	-1.22	9.29E-08
	AT3G14810	MSL5	-0.16	4.26E-01	-0.79	3.51E-05	-0.05	7.96E-01	-1.82	3.37E-08
	AT2G39010	PIP2;6	-0.80	8.23E-07	-0.93	6.42E-08	0.21	4.13E-02	-1.40	3.44E-09
IV	AT2G36590	ATPROT3	-2.56	2.89E-06	-3.02	6.88E-08	-2.93	4.30E-09	-1.96	6.44E-08
	AT1G48100	NA	-1.54	3.31E-04	-2.45	1.19E-06	-3.46	5.27E-09	-3.31	2.33E-08
	AT2G37180	PIP2;3	-1.04	7.22E-05	-1.17	5.14E-06	-1.45	1.95E-07	-1.50	2.13E-07
	AT4G38810	NA	-1.15	4.15E-06	-0.86	2.10E-05	-1.30	1.15E-07	-1.56	3.63E-08
	AT1G02820	NA	-0.61	2.05E-01	-0.35	3.15E-01	-2.20	2.85E-07	-2.85	9.46E-08
	AT4G37760	SQE3	-0.52	2.56E-04	-0.35	2.16E-03	-0.52	4.15E-05	-1.14	2.87E-08
	AT1G72130	NA	-0.71	7.52E-03	-1.00	1.16E-04	-1.18	7.63E-06	-1.77	2.36E-07
	AT3G27170	ATCLC-B	-0.95	1.76E-05	-1.05	1.74E-06	-0.71	3.44E-05	-1.33	7.85E-08
	AT2G36830	GAMMA-TIP	-1.12	4.15E-06	-1.61	4.31E-08	-1.31	6.29E-08	-1.77	1.74E-08
	AT5G54130	NA	0.59	1.16E-03	0.20	1.81E-01	-1.29	3.94E-08	-1.50	2.87E-08
	AT5G67360	ARA12	-0.01	9.75E-01	0.07	7.09E-01	-2.16	4.30E-09	-1.86	2.87E-08
	AT4G26850	VTC2	-0.09	6.24E-01	-0.12	3.59E-01	-0.96	3.31E-07	-1.04	2.01E-07
	AT3G22121	NA	-0.06	8.91E-01	0.06	8.35E-01	-2.21	4.14E-08	-1.27	8.28E-06
	AT3G22120	CWLP	0.02	9.59E-01	0.10	6.97E-01	-2.23	1.33E-08	-1.10	1.31E-05
	AT5G59050	NA	-0.26	4.01E-01	-0.37	8.53E-02	-1.85	1.16E-08	-1.35	2.22E-07
	AT4G36360	BGAL3	-0.68	1.31E-03	-0.94	1.94E-05	-1.76	7.14E-09	-1.63	3.37E-08
	AT3G54400	NA	-0.47	2.59E-01	-1.91	2.32E-05	-3.07	4.30E-09	-2.38	4.78E-08
	AT1G55690	NA	-0.25	3.29E-01	-0.71	1.08E-03	-1.55	6.69E-08	-1.25	8.18E-07
	AT3G13470	NA	-0.82	1.56E-03	-1.92	1.88E-07	-0.98	2.16E-04	0.97	3.07E-05
	AT1G23170	NA	1.11	1.72E-02	1.00	9.71E-03	-2.25	4.46E-08	-0.24	1.66E-01
	AT4G30190	AHA2	0.21	2.44E-01	-0.09	5.32E-01	-1.32	1.94E-08	0.22	6.32E-02
	AT4G36220	CYP84A1	0.11	7.68E-01	0.33	1.32E-01	-2.01	1.86E-08	-0.36	3.85E-02
	AT1G04120	ABCC5	-0.17	3.71E-01	-0.07	6.68E-01	-1.22	4.61E-08	-0.40	2.67E-03
	AT3G03780	ATMS2	-0.17	6.53E-01	-0.40	1.20E-01	-2.20	2.66E-08	-0.81	4.73E-04
	AT3G55450	PBL1	0.34	1.80E-01	1.17	3.05E-06	-1.47	1.56E-08	0.30	1.22E-02
	AT1G51850	NA	0.41	7.14E-01	1.19	5.59E-02	-2.15	1.89E-08	0.09	6.47E-01
	AT5G55930	ATOPT1	-0.25	4.75E-01	0.36	1.07E-01	-1.40	9.76E-09	-0.05	6.78E-01
	AT1G74790	NA	-0.44	4.90E-02	0.02	9.10E-01	-1.73	4.30E-09	-0.17	1.62E-01
	AT4G36670	NA	-0.97	5.86E-02	0.34	3.28E-01	-2.21	2.27E-08	-0.36	6.42E-02
	AT5G48430	NA	0.50	8.62E-01	0.75	6.69E-01	-5.07	3.94E-08	-0.20	3.04E-01
	AT4G24240	ATWRKY7	0.23	6.90E-01	0.09	8.17E-01	-1.91	2.35E-08	-0.20	1.95E-01
	AT2G16430	ATPAP10	0.27	9.41E-02	0.36	8.72E-03	-1.20	1.82E-08	-0.40	1.03E-03
	AT5G55920	OLI2	0.00	9.91E-01	0.03	9.15E-01	-1.82	1.52E-08	-0.69	1.40E-04
	AT3G61150	HD-GL2-1	0.21	5.22E-01	0.35	1.12E-01	-1.67	1.27E-08	-0.70	5.11E-05
	AT5G24140	SQP2	0.09	9.75E-01	-1.84	2.45E-01	-2.73	2.79E-07	-2.98	3.04E-07
	AT5G47330	NA	-0.50	7.79E-01	-1.55	1.84E-01	-2.47	1.43E-07	-2.61	1.40E-07
	AT1G69870	NRT1.7	-0.99	6.86E-04	-0.85	4.19E-04	-1.22	1.76E-06	-1.75	7.48E-08

			0 h				1 h			
Cluster	AGI	Name	Pst ΔhrpS vs. mock log <sub>2</sub> FC	Pst ΔhrpS vs. mock p-value	Pst AvrRpm1 vs. mock log <sub>2</sub> FC	Pst AvrRpm1 vs. mock p-value	Pst ΔhrpS vs. mock log <sub>2</sub> FC	Pst ΔhrpS vs. mock p-value	Pst AvrRpm1 vs. mock log <sub>2</sub> FC	Pst AvrRpm1 vs. mock p-value
IV	AT2G28900	<i>ATOEP16-1</i>	-0.75	3.49E-02	-1.44	7.41E-05	-1.27	4.35E-06	-2.14	4.78E-08
	AT1G29395	<i>COR413-TM1</i>	-2.10	7.51E-06	-1.25	7.37E-05	-1.18	3.15E-06	-2.00	3.37E-08
	AT2G42530	<i>COR15B</i>	-2.61	5.81E-06	-2.42	5.35E-07	-1.14	4.59E-06	-2.28	3.37E-08
	AT2G42540	<i>COR15</i>	-4.30	4.02E-09	-4.20	7.95E-10	-1.75	9.09E-08	-3.03	2.22E-09
	AT5G62350	NA	-2.34	4.47E-07	-2.32	6.42E-08	-0.48	1.48E-02	-0.91	7.14E-05
	AT4G24960	<i>ATHVA22D</i>	-3.43	4.97E-08	-3.19	3.61E-08	-0.90	5.04E-04	-1.38	6.15E-06
	AT5G15970	<i>AtCor6.6</i>	-2.28	8.46E-09	-1.79	4.31E-08	-0.56	8.95E-04	-1.33	1.70E-07
	AT1G20440	<i>AtCOR47</i>	-2.66	3.77E-08	-2.52	3.61E-08	-0.27	1.71E-01	-1.50	7.33E-07
	AT1G02400	<i>ATGA2OX4</i>	-3.05	1.65E-06	-1.90	3.79E-06	0.14	5.85E-01	-0.81	1.06E-03
	AT1G01650	<i>ATSPPL4</i>	-1.67	1.98E-07	-0.92	1.79E-05	0.27	7.84E-02	-0.24	1.11E-01
	AT4G35110	NA	-1.09	3.47E-06	-0.79	2.74E-05	0.19	1.58E-01	0.09	5.09E-01
	AT5G15650	<i>ATRG2</i>	-1.83	3.97E-07	-1.28	3.77E-06	0.27	1.24E-01	0.27	1.04E-01
	AT5G61780	<i>AtTudor2</i>	-1.75	2.38E-06	-1.77	5.49E-07	-0.65	2.85E-03	-0.09	6.46E-01
	AT5G20190	NA	-1.21	2.81E-06	-1.28	4.91E-07	-0.86	9.86E-06	-0.47	2.17E-03
	AT3G47380	NA	-1.04	5.00E-02	-0.47	1.80E-01	-1.69	4.87E-08	-0.62	5.76E-04
	AT2G43620	NA	-2.13	3.07E-02	-1.35	2.31E-02	-2.96	2.17E-09	-0.92	9.19E-05
	AT2G39200	<i>ATMLO12</i>	-2.74	7.70E-04	-1.32	2.45E-03	-1.83	1.63E-08	-0.22	1.68E-01
AT2G38870	NA	-1.82	1.04E-04	-1.48	4.29E-05	-1.59	5.57E-08	-0.44	9.13E-03	
V	AT5G66620	<i>DAR6</i>	-0.25	4.85E-01	0.32	1.89E-01	1.99	5.38E-08	1.55	1.30E-06
	AT4G04540	<i>CRK39</i>	0.64	9.80E-02	1.79	4.81E-06	1.86	4.46E-07	2.04	2.11E-07
	AT1G72280	<i>AERO1</i>	-0.23	5.24E-01	0.76	2.00E-03	1.43	3.07E-06	1.92	1.06E-07
	AT5G42140	NA	0.04	9.35E-01	0.62	6.72E-03	0.94	8.12E-05	1.71	7.97E-08
	AT5G12890	NA	-0.04	9.20E-01	0.93	1.00E-04	0.70	6.23E-04	1.43	2.15E-07
	AT5G21090	NA	0.29	9.89E-02	0.89	5.05E-06	0.96	1.08E-06	1.37	3.37E-08
	AT5G60930	NA	-0.03	9.79E-01	0.31	5.52E-01	1.29	5.00E-03	3.14	2.00E-07
	AT2G35020	<i>GlcNAc1pUT2</i>	0.43	1.35E-01	0.64	6.18E-03	0.97	7.89E-05	1.88	5.03E-08
	AT1G65540	NA	0.17	3.72E-01	0.49	1.08E-03	0.69	3.66E-05	1.29	4.55E-08
	AT1G72330	<i>ALAA2</i>	0.52	2.42E-01	1.30	3.69E-04	1.69	9.48E-06	2.75	4.52E-08
	AT4G16660	NA	0.52	2.42E-01	1.30	3.69E-04	1.69	9.48E-06	2.75	4.52E-08
	AT1G59860	NA	0.67	5.64E-01	1.57	2.47E-02	-0.33	3.74E-01	2.51	3.37E-08
	AT2G20560	NA	-0.25	8.51E-01	0.72	2.78E-01	-0.34	4.13E-01	2.53	1.47E-07
	AT5G47730	NA	0.27	3.68E-01	0.51	2.51E-02	0.12	6.29E-01	1.78	8.43E-08
	AT5G53400	<i>BOB1</i>	0.30	3.52E-01	0.32	1.73E-01	-0.11	6.77E-01	1.94	3.63E-08
	AT3G57470	NA	-0.37	6.48E-02	-0.08	6.69E-01	0.52	2.84E-03	1.38	1.16E-07
	AT5G53550	<i>ATYSL3</i>	0.99	4.88E-05	1.77	3.84E-08	-0.56	1.72E-03	1.22	3.87E-07
	AT1G26380	NA	1.73	3.96E-02	3.42	3.26E-05	1.43	1.95E-04	3.13	3.37E-08
	AT4G25900	NA	0.56	4.48E-02	1.25	1.64E-05	0.41	6.06E-02	1.73	1.31E-07
	AT4G01370	<i>ATMPK4</i>	0.47	1.18E-02	0.71	1.06E-04	0.42	5.94E-03	1.15	2.59E-07
AT2G05520	<i>ATGRP-3</i>	0.73	5.43E-05	1.05	3.24E-07	0.10	4.82E-01	0.38	3.07E-03	
AT2G29720	<i>CTF2B</i>	0.47	1.28E-01	1.42	4.36E-06	0.33	5.78E-02	1.60	3.37E-08	
AT1G13110	<i>CYP71B7</i>	1.12	2.33E-04	1.90	1.90E-07	0.44	1.99E-02	1.25	1.12E-06	
AT4G13505	NA	1.20	1.13E-04	1.96	1.46E-07	0.19	3.21E-01	0.52	5.07E-03	
AT4G13510	<i>AMT1;1</i>	1.12	2.38E-04	1.88	2.29E-07	0.18	3.56E-01	0.50	7.05E-03	
VI	AT4G16950	<i>RPP5</i>	0.49	3.58E-03	1.15	2.10E-07	0.78	4.86E-06	0.06	6.78E-01
	AT4G11850	<i>MEE54</i>	0.92	1.84E-03	1.90	2.54E-07	0.73	9.54E-04	0.75	5.90E-04
	AT4G33300	<i>ADR1-L1</i>	1.02	3.81E-05	1.66	6.42E-08	0.73	1.58E-04	0.40	1.46E-02
	AT4G33050	<i>EDA39</i>	1.13	4.98E-04	2.09	1.83E-07	0.90	5.07E-04	0.50	2.82E-02
	AT2G17220	NA	0.15	4.24E-01	0.55	3.53E-04	1.30	2.35E-08	0.68	3.68E-05
	AT2G42950	NA	0.48	8.88E-02	1.21	1.12E-05	2.14	4.30E-09	1.27	1.89E-06
	AT5G66640	<i>DAR3</i>	0.73	2.45E-02	1.68	3.68E-06	2.27	3.94E-08	1.44	8.37E-06
	AT2G32140	NA	-0.37	3.52E-01	0.44	9.71E-02	2.02	4.61E-08	0.00	9.93E-01
	AT1G17600	NA	0.06	8.45E-01	0.82	3.86E-05	1.49	1.33E-08	0.58	4.65E-04
	AT5G61910	NA	0.26	2.90E-01	0.96	3.03E-05	1.98	4.54E-09	0.37	3.46E-02
	AT4G34390	<i>XLG2</i>	0.15	6.76E-01	0.84	1.13E-03	2.64	4.54E-09	0.77	2.18E-03
	AT5G61900	<i>BON</i>	0.41	1.87E-01	1.26	3.40E-05	2.72	4.30E-09	0.55	2.38E-02
	VII	AT4G25470	<i>ATCBF2</i>	3.64	4.97E-08	1.39	1.05E-03	0.93	1.41E-01	0.36
AT4G27657		NA	2.73	6.62E-07	1.32	6.67E-04	-0.88	6.22E-02	-0.15	7.29E-01
AT1G70940		<i>ATPIN3</i>	1.38	3.97E-07	0.77	7.54E-05	-0.98	3.17E-05	-0.39	2.56E-02
AT2G30020		NA	2.00	3.55E-06	1.46	4.03E-05	0.78	2.95E-02	-0.28	4.94E-01
AT3G44260		<i>AtCAF1a</i>	1.54	3.55E-06	1.00	1.28E-04	0.37	1.83E-01	-0.73	1.75E-02
AT1G74930		<i>ORA47</i>	3.52	8.46E-09	2.77	6.42E-08	-0.30	8.29E-01	0.36	7.48E-01
AT1G72910		NA	2.21	4.37E-09	2.56	5.62E-10	0.88	2.37E-04	0.68	2.02E-03
AT3G46600		NA	1.39	4.25E-06	1.79	8.80E-08	0.39	8.70E-02	0.07	7.82E-01
AT5G61600		<i>ERF104</i>	3.85	1.40E-06	3.26	3.65E-06	0.46	4.53E-01	-1.08	1.40E-01
AT1G72940		NA	2.17	4.71E-07	2.36	6.42E-08	0.41	1.28E-01	-0.75	1.68E-02
AT1G27730		<i>STZ</i>	2.00	2.19E-06	1.92	1.21E-06	0.51	7.01E-02	-0.40	1.60E-01
AT3G50800		NA	2.33	4.14E-06	1.92	1.24E-05	2.39	5.30E-06	-0.52	3.71E-01
AT1G73540	<i>NUDT21</i>	2.28	2.25E-06	1.84	9.19E-06	2.68	9.80E-07	0.15	7.57E-01	

			0 h				1 h			
Cluster	AGI	Name	Pst ΔhrpS vs. mock log <sub>2</sub> FC	Pst ΔhrpS vs. mock p-value	Pst AvrRpm1 vs. mock log <sub>2</sub> FC	Pst AvrRpm1 vs. mock p-value	Pst ΔhrpS vs. mock log <sub>2</sub> FC	Pst ΔhrpS vs. mock p-value	Pst AvrRpm1 vs. mock log <sub>2</sub> FC	Pst AvrRpm1 vs. mock p-value
VII	AT5G45340	<i>CYP707A3</i>	2.15	4.07E-06	1.58	4.29E-05	2.41	4.40E-06	-0.85	9.87E-02
	AT4G29780	NA	1.88	3.70E-06	1.49	1.72E-05	1.26	2.19E-04	-0.95	6.34E-03
	AT3G27690	<i>LHCB2</i>	-0.62	4.36E-03	-0.88	6.48E-05	-0.14	4.88E-01	-1.66	2.31E-07
	AT1G32200	<i>ACT1</i>	-0.41	2.90E-02	-0.73	1.17E-04	0.23	1.57E-01	-1.48	2.68E-07
	AT1G80030	NA	-0.18	2.40E-01	-0.59	8.31E-05	0.03	8.64E-01	-1.27	6.44E-08
	AT2G20890	<i>PSB29</i>	-0.18	2.29E-01	-0.52	2.60E-04	0.00	9.99E-01	-1.09	1.87E-07
	AT1G06360	NA	-0.37	2.47E-01	-2.79	1.77E-07	0.97	4.87E-02	-1.63	3.11E-02
	AT3G06880	NA	-1.15	3.04E-04	-2.09	3.06E-07	0.03	9.66E-01	-1.46	1.92E-02
	AT2G38170	<i>ATCAX1</i>	0.49	5.91E-02	0.29	1.72E-01	0.13	6.24E-01	-2.31	1.16E-07
	AT1G60950	<i>ATFD2</i>	-0.16	2.34E-01	-0.44	3.46E-04	0.11	3.80E-01	-1.09	7.85E-08
	AT2G10940	NA	-0.23	4.75E-01	-0.77	2.65E-03	-0.09	7.59E-01	-2.45	1.70E-07
	AT4G00430	<i>PIP1;4</i>	-0.15	3.87E-01	-0.56	2.07E-04	-1.03	7.29E-07	-1.48	3.63E-08
	AT3G26520	<i>GAMMA-TIP2</i>	-0.24	1.89E-01	-0.55	9.42E-04	-0.35	3.66E-02	-1.67	5.07E-08
	AT3G53420	<i>PIP2</i>	-0.44	1.18E-02	-0.63	2.28E-04	-0.74	9.72E-05	-1.59	5.21E-08
	AT2G34660	<i>ABCC2</i>	-0.07	6.82E-01	-0.04	7.71E-01	-0.55	2.54E-04	-1.15	2.09E-07
	AT2G15620	<i>ATHNIR</i>	-0.14	4.95E-01	-0.54	1.19E-03	-0.88	5.33E-05	-1.73	1.06E-07
AT3G61430	<i>ATPIP1</i>	-0.15	4.33E-01	-0.37	1.12E-02	-0.79	4.65E-05	-1.48	8.43E-08	
AT2G45960	<i>ATHH2</i>	-0.07	6.72E-01	-0.12	2.79E-01	-0.86	7.93E-07	-1.31	2.87E-08	
VIII	AT4G27100	NA	1.04	2.24E-05	0.85	5.46E-05	1.46	2.66E-08	-0.28	1.03E-01
	AT3G25600	NA	1.02	5.63E-04	1.41	4.13E-06	2.03	1.94E-08	0.37	1.09E-01
	AT1G33720	<i>CYP76C6</i>	1.43	2.51E-04	2.00	1.75E-06	3.27	4.30E-09	0.79	1.45E-02
	AT5G56340	<i>ATCRT1</i>	0.79	1.61E-03	1.23	4.35E-06	1.95	7.99E-09	0.23	2.46E-01
	AT1G30810	NA	0.40	8.30E-02	0.90	6.23E-05	1.68	2.66E-08	0.23	2.03E-01
	AT3G46620	NA	1.94	3.79E-06	1.64	8.58E-06	1.51	9.57E-06	-0.23	4.33E-01
	AT4G27280	NA	2.50	3.12E-06	2.16	5.72E-06	2.32	6.56E-07	-0.72	5.18E-02
	AT5G64870	NA	0.78	2.83E-02	0.70	1.60E-02	3.15	4.61E-08	0.42	3.45E-01
	AT1G13260	<i>EDF4</i>	0.43	1.43E-01	0.57	1.66E-02	2.20	4.84E-08	0.56	2.90E-02
	AT5G58120	NA	0.22	2.60E-01	0.68	1.45E-04	1.47	3.20E-08	-0.11	5.32E-01
	AT1G56520	NA	0.70	9.53E-04	1.12	2.38E-06	2.48	7.26E-10	0.19	2.74E-01
	AT3G45640	<i>ATMAPK3</i>	0.97	5.62E-04	1.63	6.65E-07	2.05	3.49E-08	0.10	6.89E-01
	AT3G50060	<i>MYB77</i>	1.58	1.03E-05	0.26	3.39E-01	2.37	1.53E-08	-1.05	1.81E-03
	AT3G54810	<i>BME3</i>	1.42	3.58E-07	0.28	9.23E-02	1.34	1.27E-07	-0.45	9.32E-03
	AT4G08950	<i>EXO</i>	0.91	4.00E-03	-1.13	3.93E-04	3.16	4.91E-09	-1.49	2.10E-04
	AT4G37260	<i>ATMYB73</i>	0.89	1.28E-03	0.02	9.39E-01	2.40	4.97E-08	-1.02	1.06E-02
	AT2G27080	NA	0.17	5.74E-01	-0.72	2.00E-03	2.06	4.61E-08	-1.18	1.88E-04
	AT1G66150	<i>TMK1</i>	0.23	2.36E-01	-0.24	1.34E-01	1.80	4.30E-08	-0.18	4.35E-01
	AT5G11070	NA	0.04	9.01E-01	-1.04	3.71E-05	2.78	1.62E-08	-0.27	4.79E-01
	AT4G01950	<i>ATGPAT3</i>	0.12	7.38E-01	-0.86	7.85E-04	2.58	2.35E-08	-0.27	4.10E-01
	AT3G06070	NA	-0.35	4.95E-02	-0.55	9.44E-04	1.49	3.27E-08	0.00	9.92E-01
	AT5G62090	<i>SLK2</i>	-0.11	5.94E-01	-0.76	3.77E-05	1.63	1.27E-08	-0.43	1.74E-02
	AT5G65470	NA	-0.53	2.67E-02	-1.62	5.35E-07	2.36	2.34E-08	-0.64	3.06E-02
	AT5G66210	<i>CPK28</i>	-0.63	9.79E-03	-0.14	5.08E-01	2.30	8.83E-09	-0.01	9.66E-01
	AT3G24550	<i>ATPERK1</i>	-0.23	2.81E-01	-0.41	1.73E-02	1.80	1.62E-08	-0.24	2.08E-01
	AT1G76650	<i>CML38</i>	-0.43	1.66E-01	-0.67	8.81E-03	2.46	4.00E-08	-0.91	5.53E-03
AT5G54380	<i>THE1</i>	0.46	2.39E-02	-0.19	2.90E-01	2.14	4.30E-09	-0.39	5.56E-02	
AT3G28180	<i>ATCSLCO4</i>	0.52	9.53E-03	0.19	2.80E-01	1.96	5.27E-09	-0.29	1.10E-01	
AT2G44500	NA	0.36	1.59E-01	0.09	6.90E-01	2.18	2.35E-08	-0.29	2.46E-01	
AT4G33920	NA	0.08	8.01E-01	0.12	5.43E-01	1.89	2.80E-08	0.09	6.99E-01	
AT5G24590	<i>ANAC091</i>	0.21	4.19E-01	0.23	2.27E-01	2.11	1.34E-08	-0.12	6.19E-01	
IX	AT2G36910	<i>ABCB1</i>	0.25	1.10E-01	0.17	1.72E-01	-1.24	6.29E-08	-0.49	4.65E-04
	AT3G19450	<i>ATCAD4</i>	0.03	9.28E-01	-0.20	2.01E-01	-1.73	1.02E-08	-1.03	1.65E-06
	AT3G56290	NA	0.10	7.19E-01	-0.14	4.31E-01	-0.96	1.14E-05	-1.42	2.81E-07
	AT1G06430	<i>FTSH8</i>	-0.04	8.57E-01	0.02	9.14E-01	-0.52	1.47E-04	-1.11	6.82E-08
	AT1G68530	<i>CER6</i>	-0.02	9.26E-01	0.32	6.30E-03	-1.12	3.53E-08	-0.78	1.88E-06
	AT3G51240	<i>F3'H</i>	-0.13	7.06E-01	-0.69	4.40E-03	-2.10	1.64E-07	-2.42	9.27E-08
	AT2G37170	<i>PIP2;2</i>	-0.62	1.06E-03	-0.75	5.11E-05	-1.31	1.80E-07	-1.54	6.29E-08
	AT4G25700	<i>B1</i>	-0.15	4.68E-01	-0.50	2.04E-03	-0.62	4.23E-04	-1.51	8.26E-08
	AT3G24190	NA	-0.20	2.00E-01	-0.36	5.85E-03	-0.77	4.56E-06	-1.27	4.55E-08
	AT5G24150	<i>SQE5</i>	-0.27	4.12E-01	-0.44	6.86E-02	-1.71	1.89E-06	-2.28	1.81E-07
	AT4G39800	<i>ATIPS1</i>	0.04	8.59E-01	-0.04	8.34E-01	-1.27	1.15E-07	-1.66	2.87E-08
	AT1G73390	NA	-0.21	2.03E-01	-0.26	5.52E-02	-1.24	1.18E-07	-1.24	1.70E-07
	AT4G00050	<i>UNE10</i>	0.11	6.16E-01	0.00	9.97E-01	-1.45	2.85E-07	-1.75	8.43E-08
	AT3G21670	NA	-0.07	8.10E-01	-0.46	1.36E-02	-1.20	5.30E-06	-1.89	1.00E-07
AT5G13930	<i>ATCH5</i>	0.03	9.60E-01	-0.97	7.46E-03	-2.18	9.89E-05	-2.51	3.65E-05	

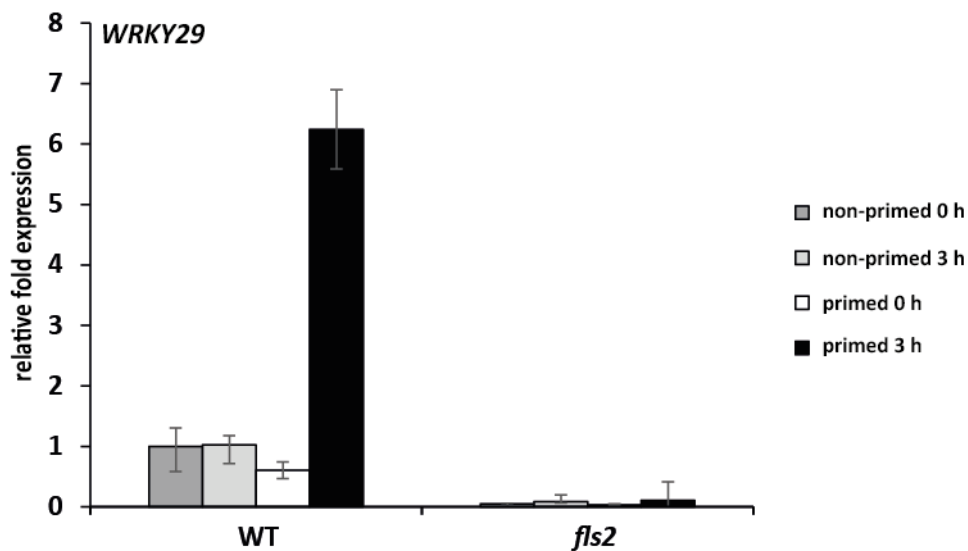
Supplementary information

			0 h				1 h			
Cluster	AGI	Name	Pst ΔhrpS vs. mock log <sub>2</sub> FC	Pst ΔhrpS vs. mock p-value	Pst AvrRpm1 vs. mock log <sub>2</sub> FC	Pst AvrRpm1 vs. mock p-value	Pst ΔhrpS vs. mock log <sub>2</sub> FC	Pst ΔhrpS vs. mock p-value	Pst AvrRpm1 vs. mock log <sub>2</sub> FC	Pst AvrRpm1 vs. mock p-value
X	AT5G60890	ATMYB34	-3.10	2.19E-06	-3.64	6.42E-08	-1.82	1.89E-03	-0.77	6.06E-02
	AT5G53060	NA	-1.79	8.97E-07	-1.73	1.31E-07	-0.43	5.14E-02	-0.33	1.06E-01
	AT5G62920	ARR6	-1.35	5.30E-05	-2.53	5.53E-08	-0.63	5.44E-02	-0.70	2.71E-02
	AT3G24518	NA	-1.71	4.24E-06	-2.13	9.64E-08	-0.81	3.03E-02	-1.27	2.34E-03
	AT2G37570	SLT1	-1.22	9.14E-07	-0.97	1.91E-06	-0.33	4.39E-02	-0.31	4.87E-02
	AT5G06870	ATPGIP2	-2.32	1.84E-06	-1.82	3.74E-06	0.37	2.81E-01	-0.02	9.56E-01
	AT3G19830	NTMC2T5.2	-1.49	1.84E-06	-1.57	3.18E-07	0.05	8.47E-01	-0.58	6.47E-03
	AT3G17860	JAI3	-1.75	2.25E-06	-1.54	2.33E-06	0.36	1.46E-01	-0.50	4.38E-02
XI	AT3G15760	NA	1.94	4.26E-06	2.44	8.80E-08	-0.46	6.62E-02	0.32	1.33E-01
	AT5G49760	NA	0.68	3.58E-04	1.20	2.68E-07	0.64	1.42E-04	0.97	1.35E-06
	AT5G24210	NA	1.13	2.57E-05	1.87	4.31E-08	0.25	1.84E-01	1.09	4.49E-06
	AT1G66880	NA	0.99	7.39E-03	2.38	2.96E-07	0.76	1.47E-02	1.60	1.08E-05
	AT4G18880	AT-HSFA4A	1.91	1.12E-04	2.91	2.96E-07	0.99	2.80E-03	1.01	1.74E-03
	AT5G44568	NA	1.15	2.25E-05	1.76	6.42E-08	0.68	8.56E-04	1.01	1.00E-05
	AT3G16720	ATL2	2.30	4.14E-06	2.54	4.39E-07	0.91	2.05E-03	-0.07	8.46E-01
	AT2G40140	ATSZF2	2.11	6.42E-07	2.86	1.31E-08	1.61	9.98E-07	-0.07	7.77E-01
	AT2G38470	ATWRKY33	1.64	2.97E-05	2.49	8.80E-08	1.22	8.07E-05	0.28	2.85E-01
	AT5G60800	NA	2.02	5.94E-06	2.88	4.77E-08	3.12	1.98E-08	3.24	3.37E-08
	AT3G56400	ATWRKY70	2.25	8.97E-07	2.55	7.04E-08	3.19	1.02E-08	3.13	3.37E-08
	AT5G39670	NA	2.25	1.79E-05	3.33	6.75E-08	2.47	1.80E-07	1.11	1.25E-03
	AT5G52760	NA	2.44	7.51E-06	3.34	7.04E-08	3.37	2.91E-08	1.95	2.13E-05
	AT2G44290	NA	1.02	5.33E-04	1.83	2.76E-07	1.81	1.45E-07	1.62	8.00E-07
	AT5G10380	ATRNG1	1.46	1.77E-04	2.44	1.85E-07	1.44	3.48E-05	1.54	1.35E-05
	AT3G60190	ADL1E	0.70	3.18E-02	1.50	1.27E-05	1.56	5.33E-05	2.55	1.66E-07
	AT3G29240	NA	0.74	4.89E-04	1.05	3.68E-06	0.76	2.20E-04	2.19	3.50E-09
	AT1G11310	ATMLO2	0.57	1.23E-02	1.29	1.54E-06	0.62	2.79E-03	1.72	7.10E-08
	AT3G14620	CYP72A8	0.91	5.66E-02	1.98	3.17E-05	0.70	1.37E-01	3.73	5.35E-08
	AT2G29400	PP1-AT	0.96	2.00E-04	1.26	3.00E-06	0.85	2.38E-04	1.83	5.07E-08
	AT4G22670	AtHip1	0.75	6.31E-04	0.94	1.94E-05	0.74	3.79E-04	1.76	3.37E-08
	AT1G79690	NUDT3	0.18	3.67E-01	0.28	5.27E-02	0.47	2.63E-03	1.29	6.44E-08
	AT3G25882	NIMIN-2	0.84	1.03E-01	1.57	4.29E-04	2.14	1.59E-05	3.35	7.61E-08
	AT4G24190	AtHsp90-7	1.13	5.66E-03	1.44	2.30E-04	1.50	1.71E-04	3.00	7.23E-08
	AT5G10760	NA	1.39	6.43E-03	2.47	6.50E-06	1.61	2.61E-04	2.95	2.83E-07
	AT5G27830	NA	0.60	1.95E-02	1.22	1.01E-05	1.09	2.87E-05	1.95	4.78E-08
	AT5G49570	ATPNG1	0.83	6.98E-04	1.38	8.40E-07	1.13	4.37E-06	1.52	1.70E-07
	AT4G26070	ATMEK1	0.75	3.87E-03	1.31	5.04E-06	0.85	3.19E-04	1.63	2.78E-07
AT1G70160	NA	0.51	1.44E-02	1.00	9.30E-06	0.78	1.42E-04	1.54	7.48E-08	
AT5G24530	DMR6	0.55	8.75E-02	1.15	1.58E-04	1.45	1.93E-05	2.46	5.35E-08	
AT3G61280	NA	1.18	4.06E-03	2.08	3.68E-06	1.88	1.54E-05	2.92	8.26E-08	
AT1G08450	AtCRT3	1.47	1.06E-04	2.17	4.79E-07	1.92	1.88E-06	2.68	5.35E-08	
AT2G14610	PR1	-2.21	4.63E-01	2.06	1.35E-01	0.76	8.62E-01	5.51	4.04E-02	
XII	AT2G42890	AML2	0.10	7.53E-01	0.94	6.94E-05	2.92	1.57E-09	1.53	1.56E-06
	AT5G45110	ATNPR3	0.58	6.27E-03	0.90	3.26E-05	2.02	4.90E-09	1.10	5.18E-06
	AT2G38790	NA	1.18	1.46E-04	1.93	1.31E-07	3.16	2.17E-07	2.15	2.82E-05
	AT4G25940	NA	1.04	1.71E-05	1.27	5.49E-07	1.96	9.80E-09	1.00	2.62E-05
	AT1G27100	NA	0.55	2.77E-03	0.58	6.12E-04	1.80	6.93E-09	0.53	3.06E-03
	AT2G23810	TET8	0.86	1.62E-03	1.22	1.65E-05	2.18	5.57E-08	0.59	1.96E-02
	AT5G03350	NA	1.43	9.71E-05	1.65	6.48E-06	1.96	5.44E-04	4.38	4.78E-08
	AT1G72930	TIR	0.93	4.14E-06	1.23	6.42E-08	1.12	4.71E-07	0.62	2.53E-04
	AT2G17040	NAC036	2.04	5.55E-06	3.04	3.84E-08	1.19	1.97E-02	1.73	6.52E-04
	AT5G53370	ATPMEPCRF	0.81	8.61E-06	1.15	6.42E-08	0.92	2.00E-06	1.07	4.66E-07
	AT3G13080	ABCC3	0.82	1.94E-03	1.71	2.76E-07	0.39	8.87E-02	0.95	1.69E-04
	AT5G52750	NA	1.99	5.07E-05	2.81	3.30E-07	1.15	2.99E-03	0.75	3.74E-02
	AT1G23710	NA	1.91	6.93E-06	2.30	2.87E-07	1.45	1.70E-04	0.51	1.46E-01
	AT2G26190	NA	1.51	4.00E-05	2.37	8.32E-08	1.72	1.09E-05	0.98	2.41E-03
	AT3G04210	NA	1.05	2.57E-05	1.51	1.61E-07	1.17	4.16E-06	0.75	3.65E-04
	AT4G13810	AtRLP47	0.92	1.47E-03	1.31	1.02E-05	1.57	1.14E-05	2.15	3.04E-07
	AT2G41090	NA	0.93	3.79E-06	1.09	2.21E-07	0.66	7.17E-05	0.81	6.30E-06
	AT3G56710	SIB1	2.44	1.44E-06	3.30	3.61E-08	2.04	2.98E-05	2.82	6.26E-07
	AT2G14560	LURP1	2.99	3.67E-06	3.68	1.24E-07	2.82	4.21E-05	4.87	7.55E-08
	AT2G31890	ATRAP	1.09	7.53E-05	1.79	8.97E-08	1.42	2.00E-06	1.93	7.23E-08
	AT2G31880	EVR	1.23	1.90E-05	2.02	3.84E-08	1.53	7.29E-07	2.01	4.78E-08
	AT1G79380	NA	-0.14	3.86E-01	0.35	5.00E-03	1.14	4.87E-08	0.59	7.12E-05



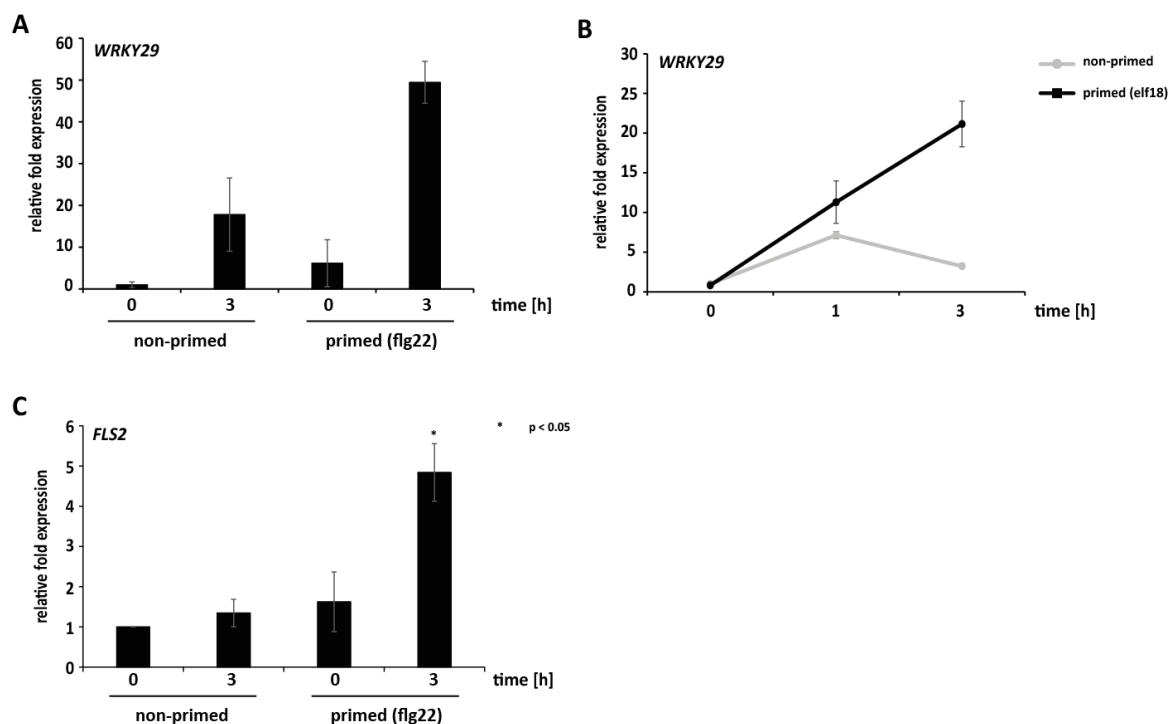
**Supplementary Figure 1: Gene expression of *WRKY29* and *PR1* during the initial MAMP-treatment in local priming.**

Five-day-old WT seedlings were treated with 0.5  $\mu$ M flg22 and harvested at the indicated time points. Gene expression of *WRKY29* and *PR1* was assessed by qRT-PCR. Fold changes were calculated relative to the untreated sample (0 h) and normalized against the endogenous reference gene *At4g26410*. Error bars represent standard deviation of one biological with four technical replicates (SD; n=4) each, respectively. Experiment was repeated twice with similar results.



**Supplementary Figure 2: Local priming in WT and *fls2*.**

Five-day-old seedlings were treated for 48 h with 0.5  $\mu$ M flg22 (primed) or kept in MAMP-free media (non-primed) followed by incubation for 72 h in MAMP-free media before retreatment. The gene expression of *WRKY29* was analysed by qRT-PCR before (0 h) and 3 h after the retreatment with 10 nM flg22 in WT and *fls2* primed and non-primed seedlings. Fold changes were calculated relative to non-primed WT samples at 0 h and normalized against the endogenous reference gene *At4g26410*. Error bars represent standard deviation (SD; n=4) of one biological replicate with four technical replicates each, respectively.

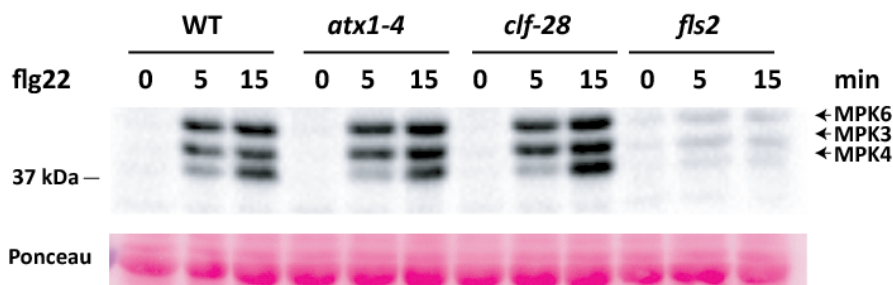


#### Supplementary Figure 3: Local memory response assays.

(A) Five-day-old WT seedlings were treated for 48 h with 0.5  $\mu$ M flg22 (primed) or kept in MAMP-free media (non-primed). The seedlings were then incubated for 144 h in MAMP-free media before retreatment. The expression of *WRKY29* was assessed by qRT-PCR before and after the retreatment with 10 nM flg22. Fold changes are relative to non-primed samples at 0 h and normalized against the endogenous reference gene *At4g26410*. Error bars represent standard deviation (SD; n=3) of one biological replicate with three technical replicates, respectively.

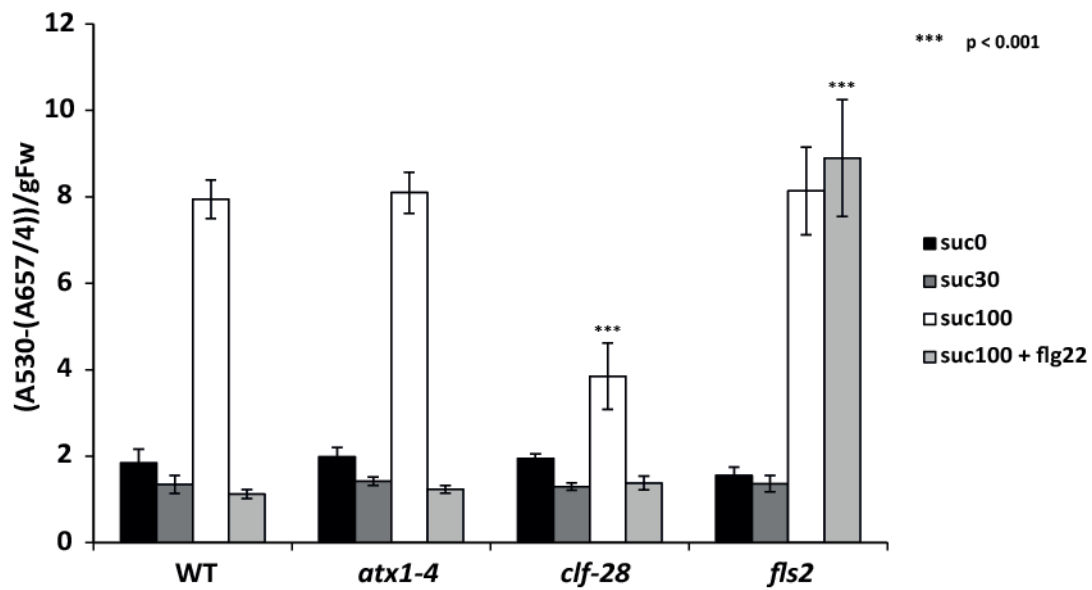
(B) Five-day-old WT seedlings were treated for 48 h with 0.5  $\mu$ M elf18 (primed) or kept in MAMP-free media (non-primed). The seedlings were then incubated for 72 h in MAMP-free media before retreatment. The expression of *WRKY29* was assessed by qRT-PCR before and after the retreatment with 10 nM elf18. Fold changes are relative to non-primed samples at 0 h and normalized against the endogenous reference gene *At4g26410*. Error bars represent standard deviation (SD; n=3) of one biological replicate with three technical replicates, respectively.

(C) Five-day-old WT seedlings were treated as described in (B) using flg22 instead of elf18. The expression of *FLS2* was assessed by qRT-PCR before and after the retreatment with 10 nM flg22. Fold changes are relative to non-primed samples at 0 h and normalized against the endogenous reference gene *At4g26410*. Error bars represent standard error (SE; n=3) of three biological replicates with four technical replicates each, respectively. P-values of  $p < 0.05$ , indicated by asterisk, were calculated using Student's t-test comparing the gene expression at 3 h of primed vs. unprimed seedlings.



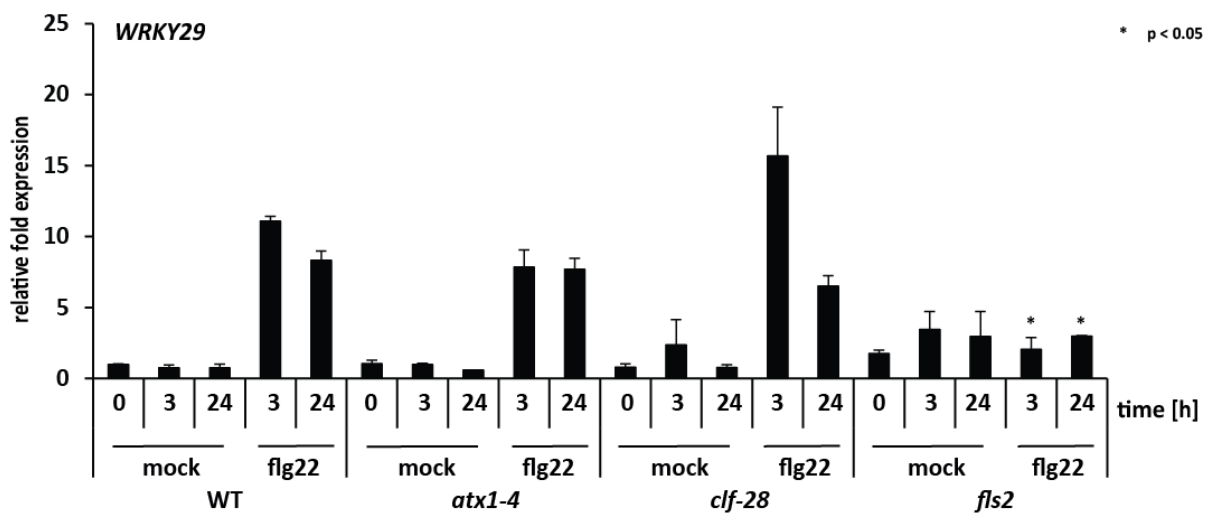
#### Supplementary Figure 4: MAPK activation upon flg22 treatment.

Ten-day old seedlings of WT, *atx1-4*, *clf-28* and *fls2* plants were treated with 1  $\mu$ M flg22 and subsequently harvested for protein detection before and after 5 and 15 minutes of flg22 treatment. Positions of active MPK3, MPK6 and MPK4 and molecular weight markers are indicated. Representative result is shown. Experiment was repeated twice with similar results.



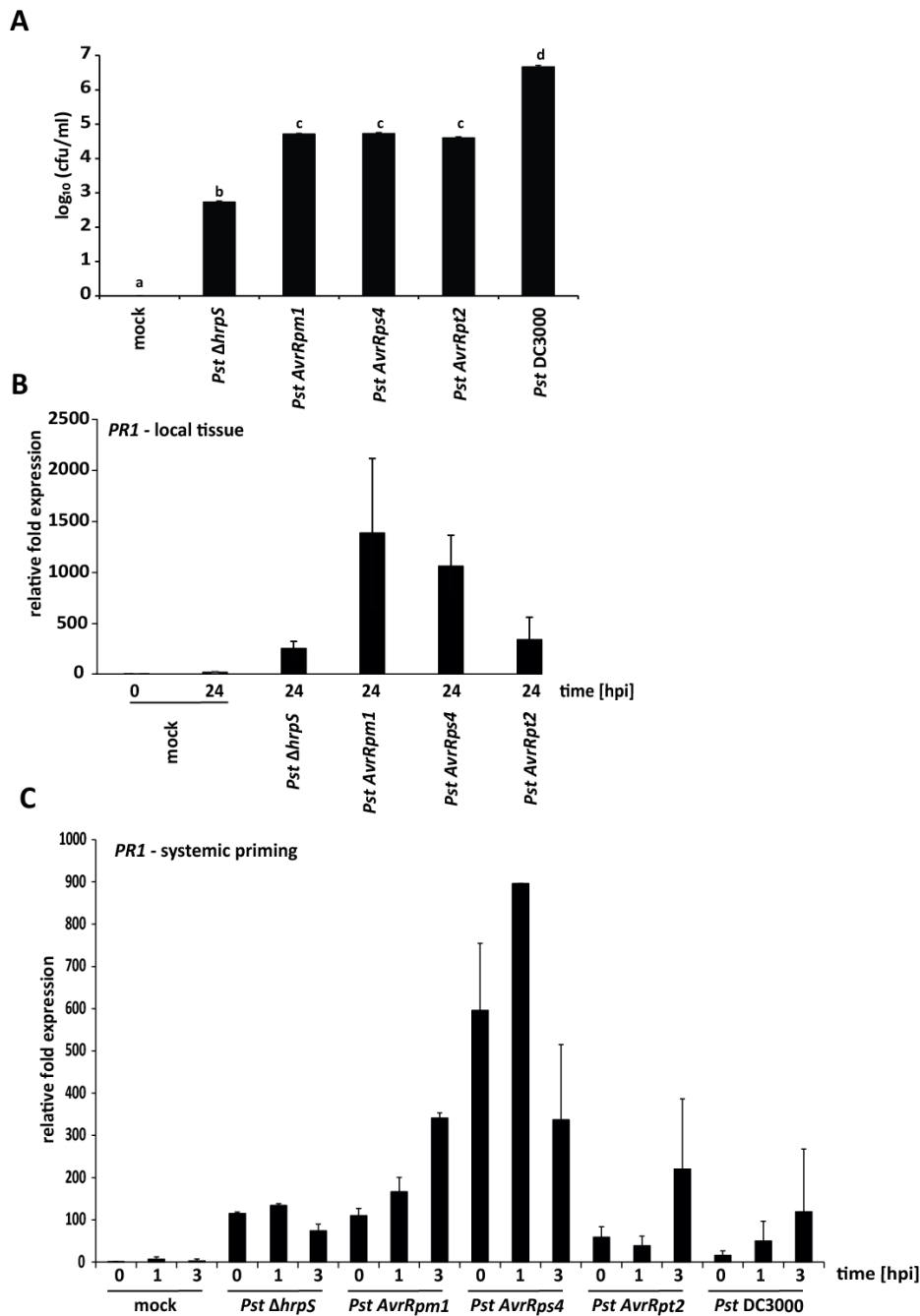
**Supplementary Figure 5: Anthocyanin suppression upon flg22 treatment.**

Anthocyanin content of 10-day-old WT, *atx1-4*, *clf-28* and *fls2* seedlings measured after incubation in sucrose free liquid MS-media (suc0), media containing 30 mM (suc30), and 100 mM sucrose (suc100) as well as liquid media containing 10 mM sucrose and 1  $\mu$ M flg22. P-value of  $p < 0.001$ , indicated by asterisks, was calculated using Student's t-test comparing the respective expression values with WT. Error bars represent standard error (SE,  $n=6$ ) of six biological replicates with three technical replicates each, respectively. More than eight seedlings were used per set.



**Supplementary Figure 6: Gene expression of WRKY29 upon flg22 treatment in WT, *atx1-4*, *clf-28* and *fls2*.**

Ten-day-old seedlings were treated with 0.5  $\mu$ M flg22 and harvested at the indicated time points. Gene expression was analyzed by qRT-PCR. Fold changes are relative to the non-treated WT sample at 0 h and normalized against the endogenous reference gene *At4g26410*. Error bars indicate standard error of two biological replicates with three technical replicates each, respectively (SE;  $n=2$ ). P-value of  $p < 0.05$ , indicated by asterisk, was calculated using Student's t-test comparing the respective expression values after flg22 treatment with WT.



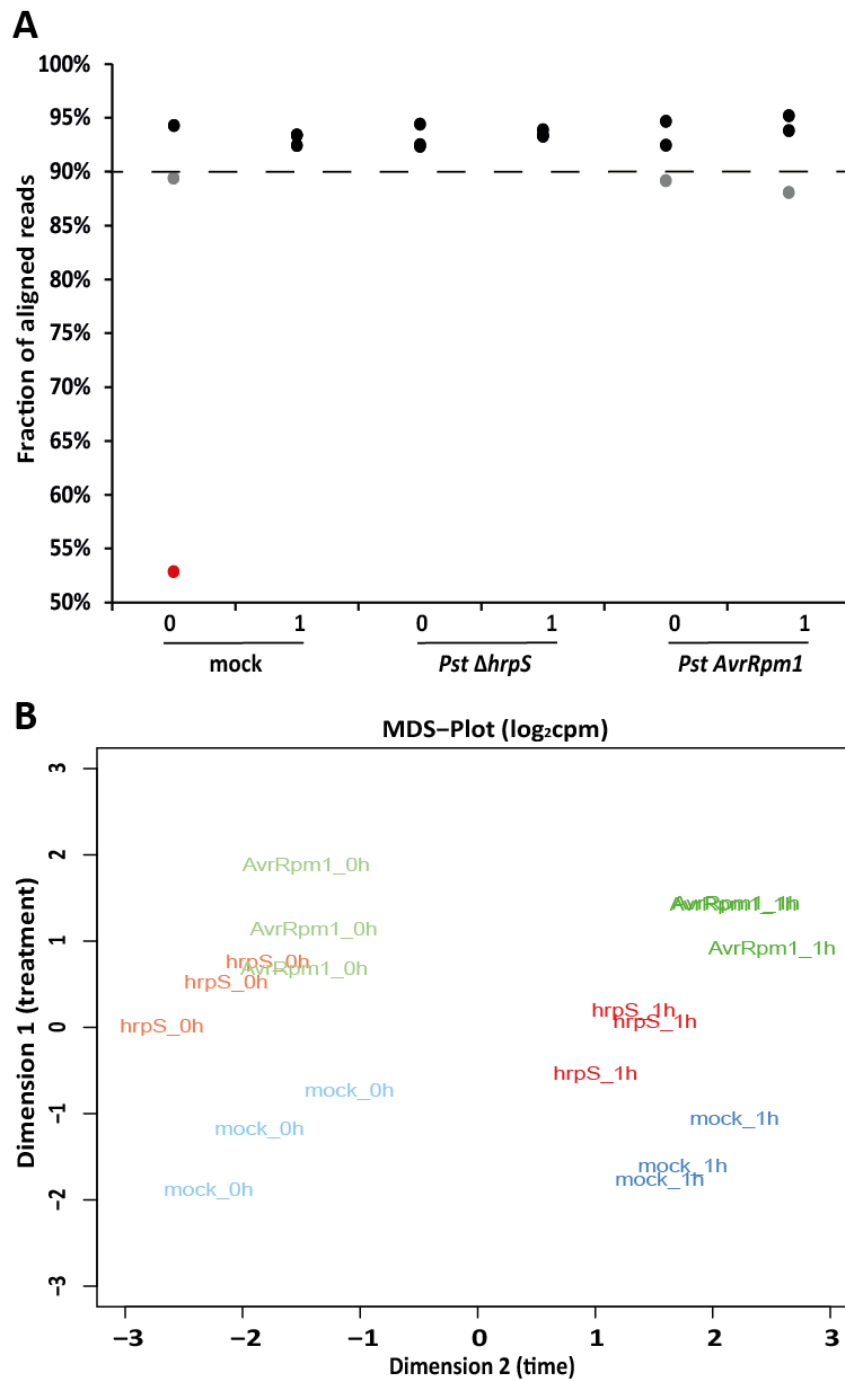
**Supplementary Figure 7: Different ETI-trigger cause divergent systemic priming responses.**

(A) Four-week-old plants were syringe-infiltrated in local leaves with 10 mM MgCl<sub>2</sub> (mock), 1x10<sup>8</sup> cfu/ml *Pst ΔhrpS*, 1x10<sup>6</sup> cfu/ml *Pst AvrRpm1*, 1x10<sup>6</sup> cfu/ml *Pst AvrRps4*, 1x10<sup>6</sup> cfu/ml *Pst AvrRpt2* or 1x10<sup>4</sup> cfu/ml *Pst DC3000*. At 48 hpi the bacteria were re-isolated and the bacterial growth evaluated. Significant effects were identified by analysis of variance (ANOVA) and post hoc testing using Tukey contrasts. Statistical significance was defined as  $p < 0.05$  and indicated by different letters (a, b, c, d). Error bars represent standard error (SE; n=2) of two biological with six technical replicates each, respectively.

(B) At 24 hpi (see (A)) local leaves were harvested and gene expression of *PR1* was monitored by qRT-PCR.

(C) At 48 hpi (see (A)) local infiltrated leaves were removed and systemic leaves infiltrated with water. At the indicated time points, *PR1* transcript abundance was measured by qRT-PCR.

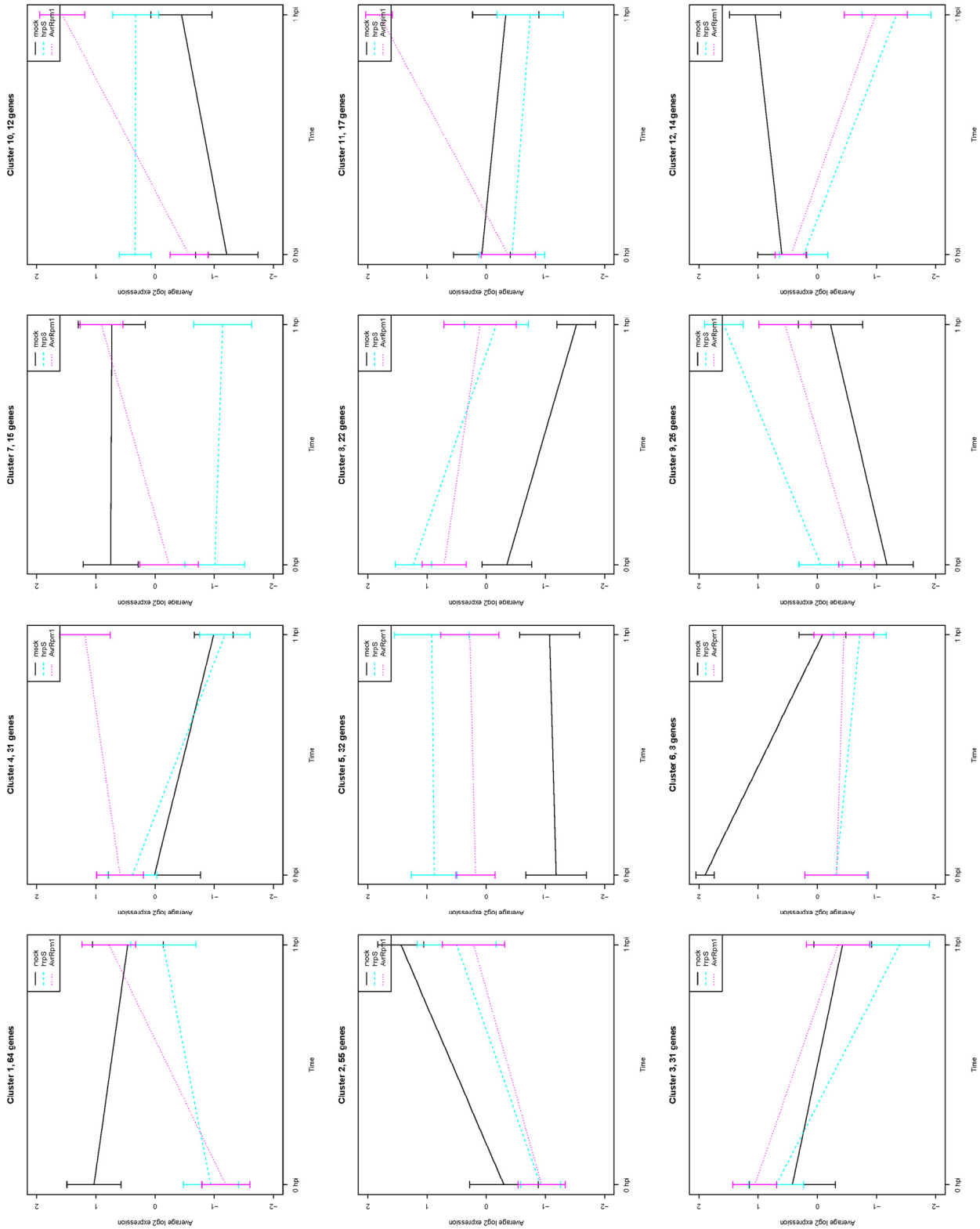
Fold changes were calculated relative to mock WT samples at 0 h and normalized against the endogenous reference gene *At4g26410*. Error bars represent standard error (SE; n=2) of two biological and three technical replicates each, respectively.



**Supplementary Figure 8: Alignment statistics and MDS-plot of the RNA-Seq experiment.**

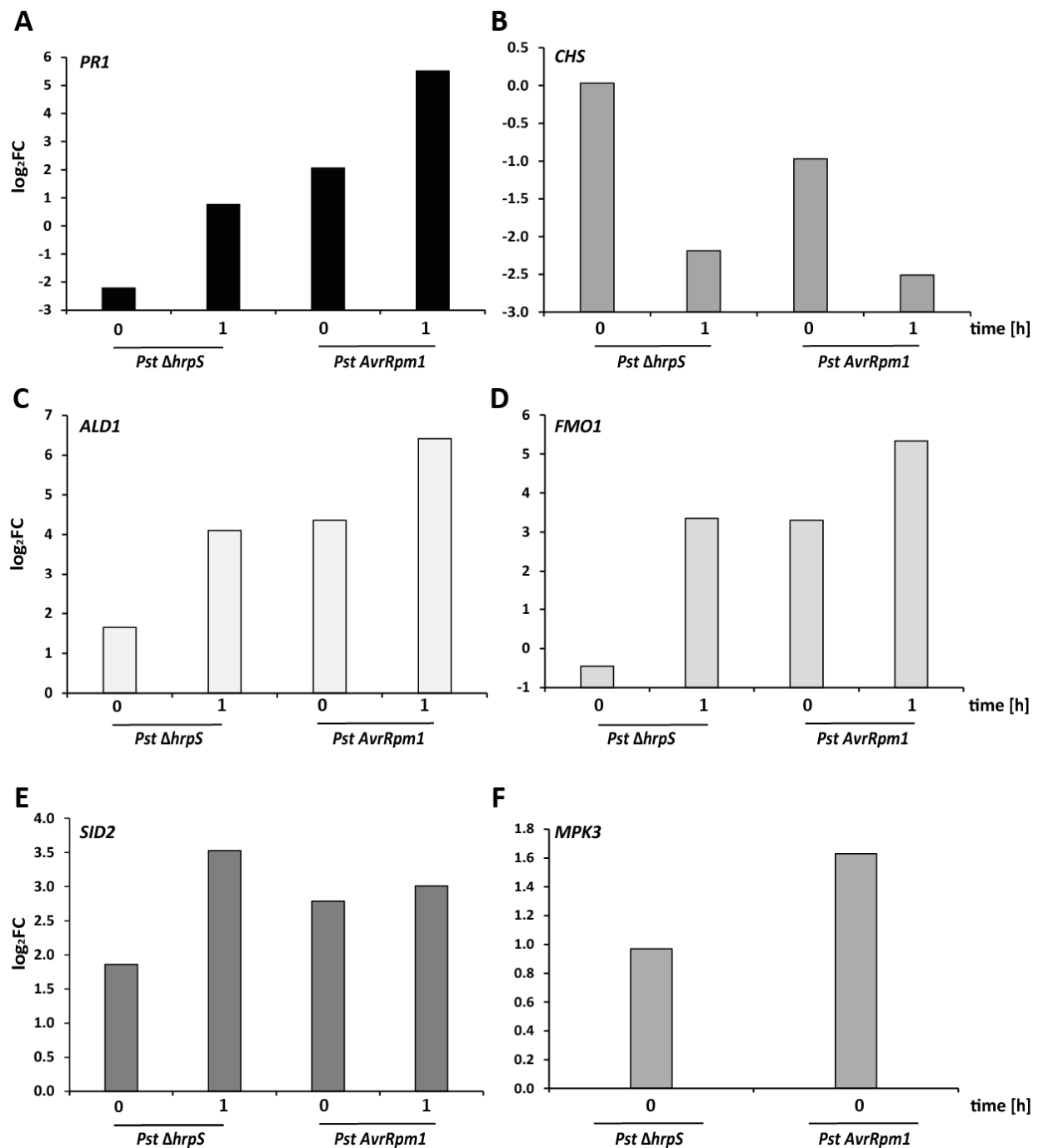
(A) Fraction of aligned reads was calculated as the percentage of aligned reads of sequenced reads of three biological replicates per time point and treatment. Grey dots represent a percentage of aligned reads below the average of 90 %. Red dot represent outlier with a low coverage due to sequence contaminations.

(B) MDS-plot analysis. Dimension 1: treatment (*hrpS* = *Pst*  $\Delta$ *hrpS*; *AvrRpm1* = *Pst* *AvrRpm1*), Dimension 2: time (0 h; 1 h).

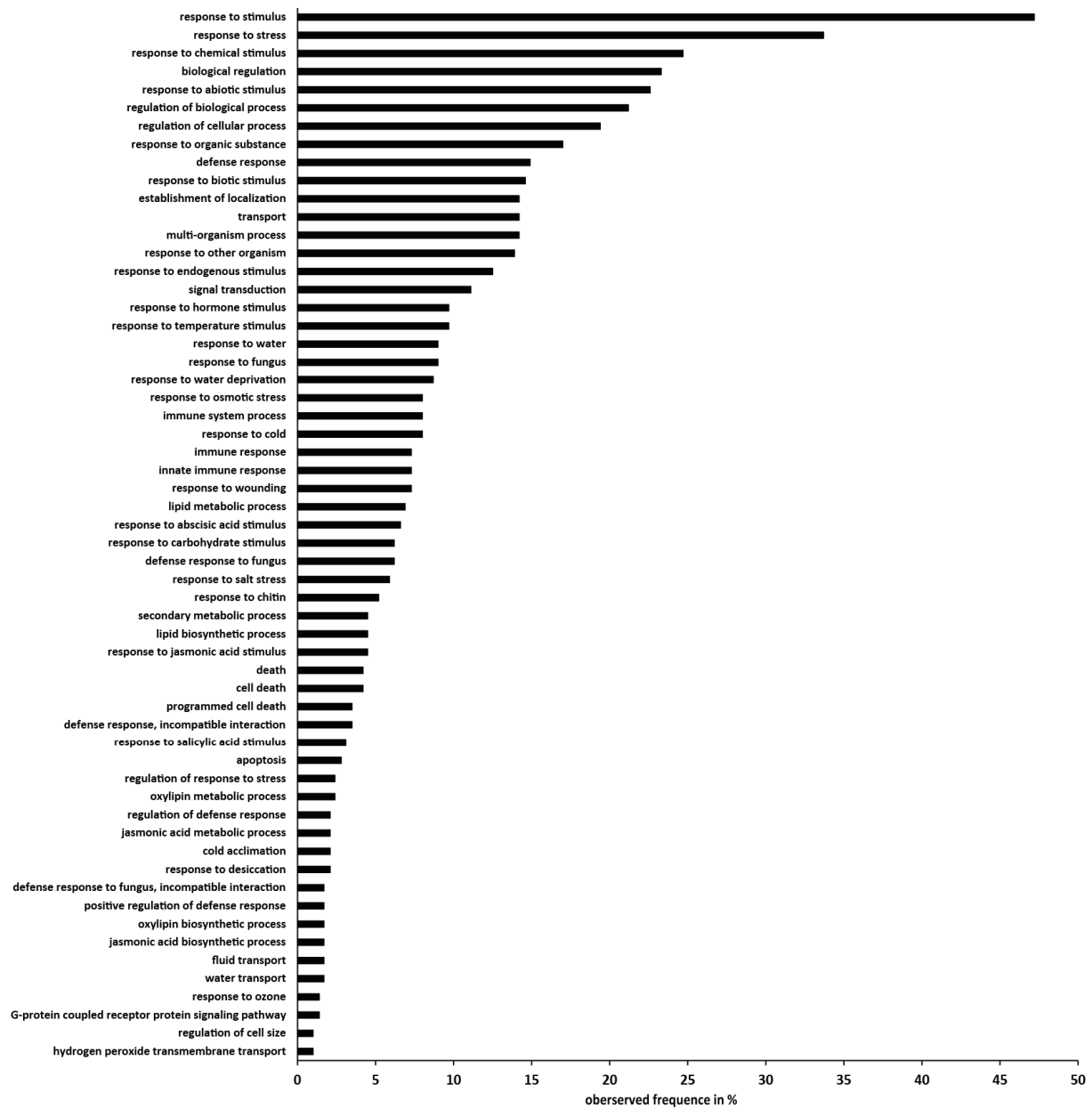


**Supplementary Figure 9: Trace Plot for the 12 clusters of the heatmap.**

Trace plots were visualized for each of the twelve clusters. To this end the genewise standardized log<sub>2</sub>-transformed counts per million (mean expression) were calculated for each time point and treatment for all genes in one cluster. From this the standard deviation was calculated and additionally plotted. hrpS = *Pst*  $\Delta$ hrpS, AvrRpm1 = *Pst* AvrRpm1.



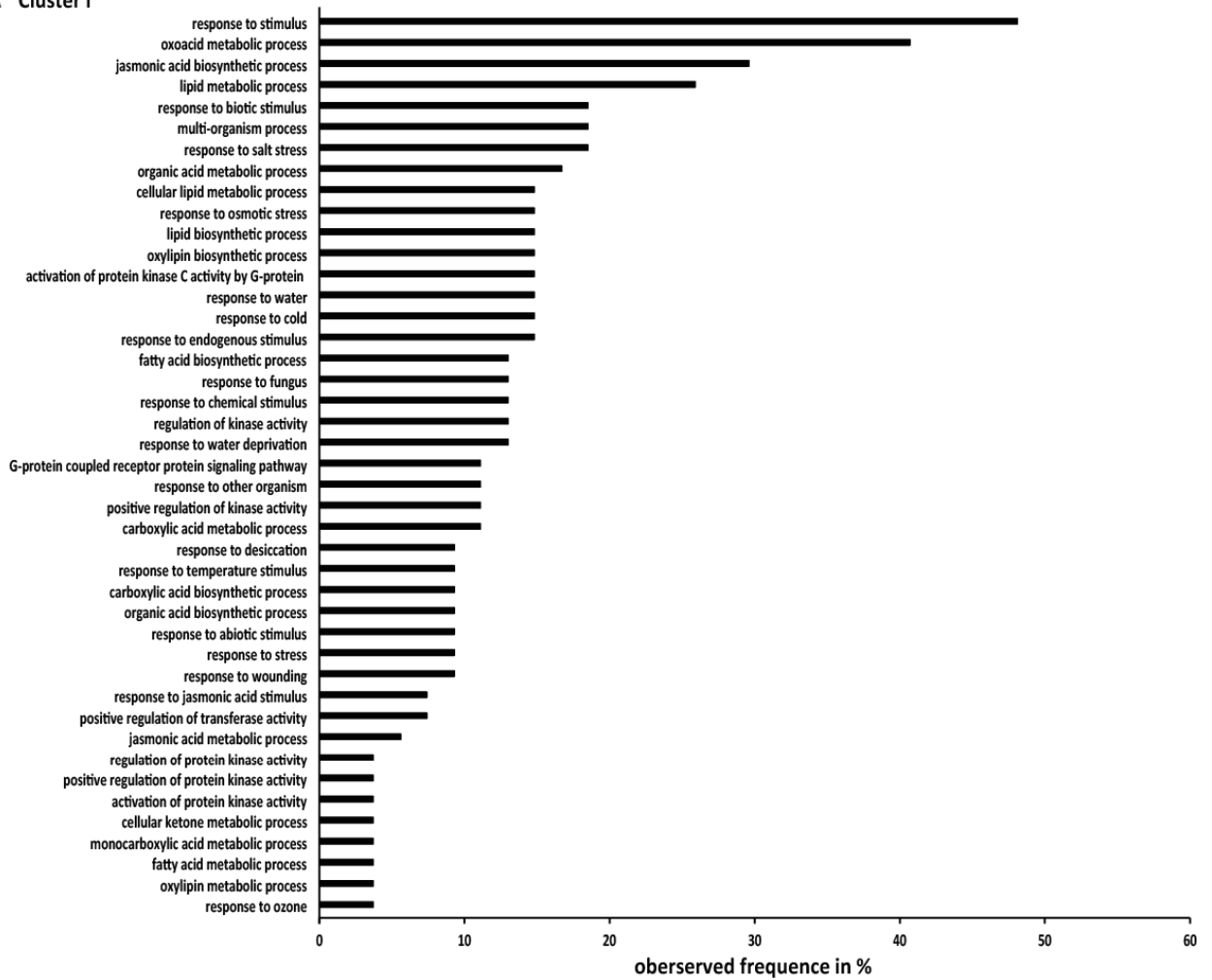
**Supplementary Figure 10: Gene expression pattern of *PR1*, *CHS*, *ALD1*, *FMO1*, *SID2* and *MPK3* withdrawn from the RNA-Seq.** Expression pattern of *PR1* (A), *CHS* (B), *ALD1* (C), *FMO1* (D), *SID2* (E) and *MPK3* (F) were withdrawn from the RNA-Seq results and illustrated by plotting the  $\log_2FC$  expression values of each time point and treatment.



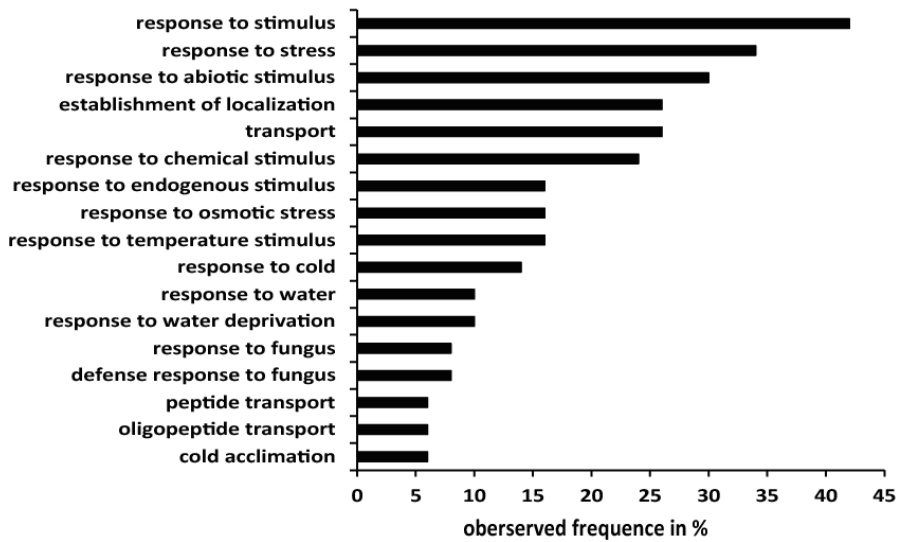
**Supplementary Figure 11: GO term analysis.**

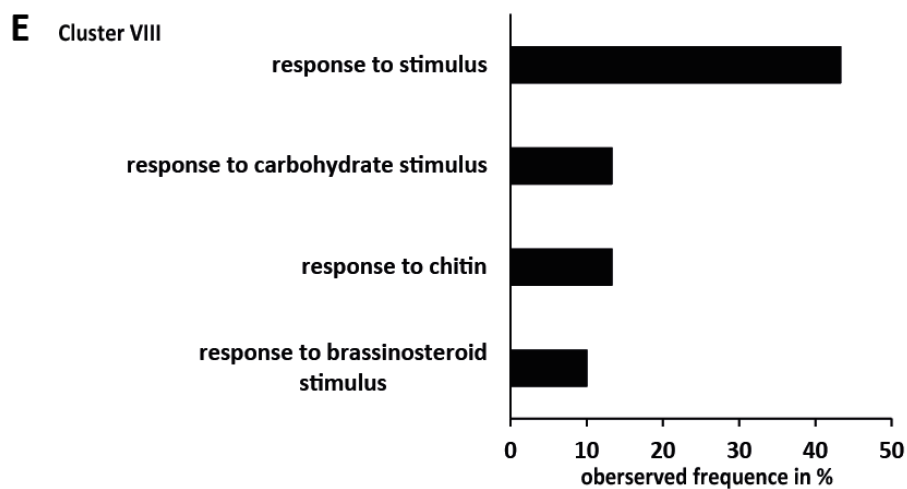
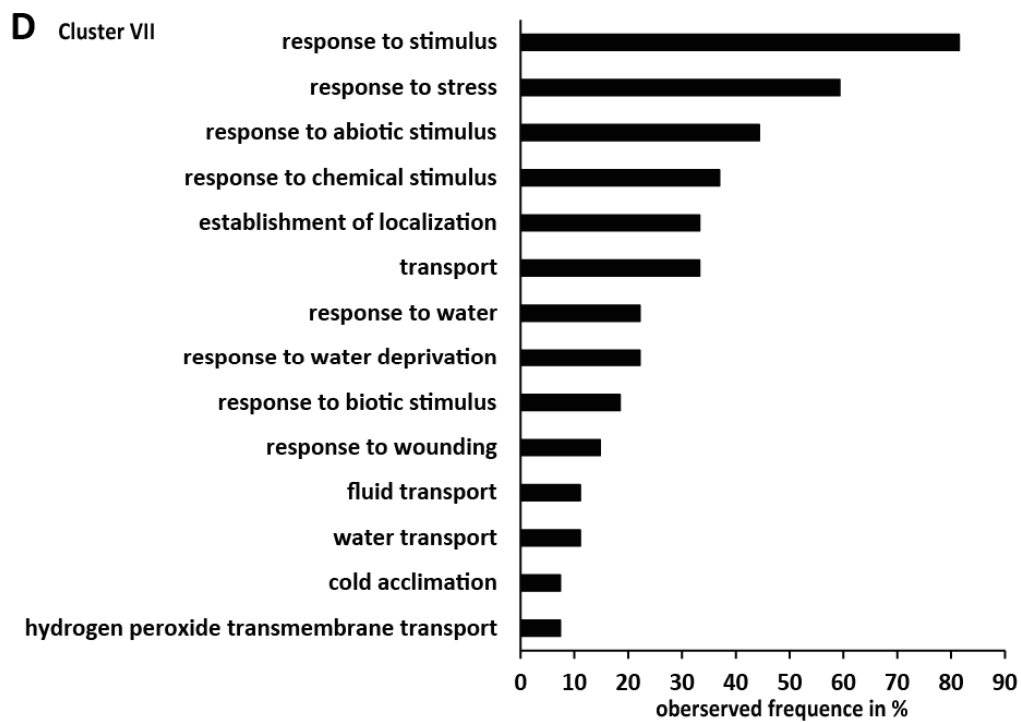
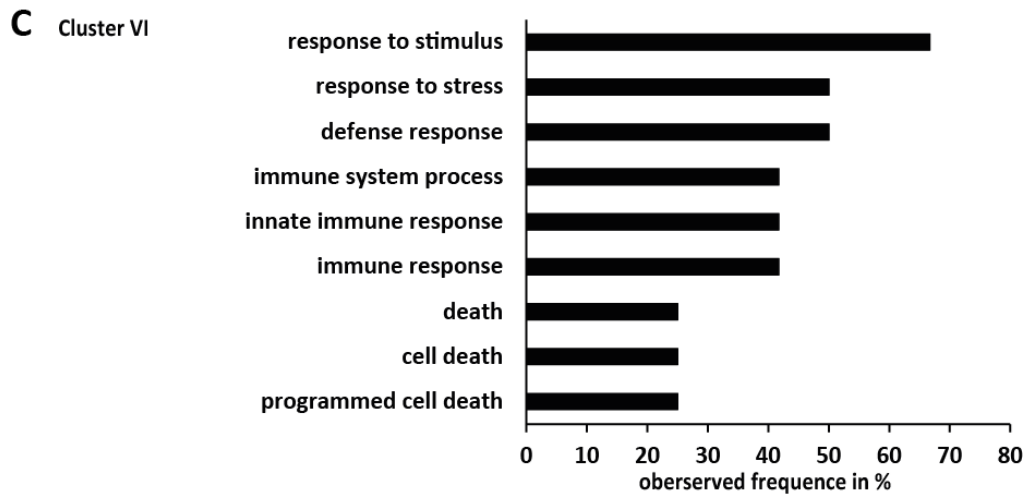
Gene ontology (GO) term enrichment analysis of all differentially expressed genes extracted from the heatmap analysis (Supplementary Table 2, Figure 10) for all cluster with 326 genes. GO terms were clustered into functional groups. The GO term (GO biological process) was performed using the platform VirtualPlant1.3 (Katari et al. 2010). P-values were calculated via Fisher Exact Test (with FDR correction) set as 0.01. As background *Arabidopsis thaliana* Col-0 tair10 genome was used.

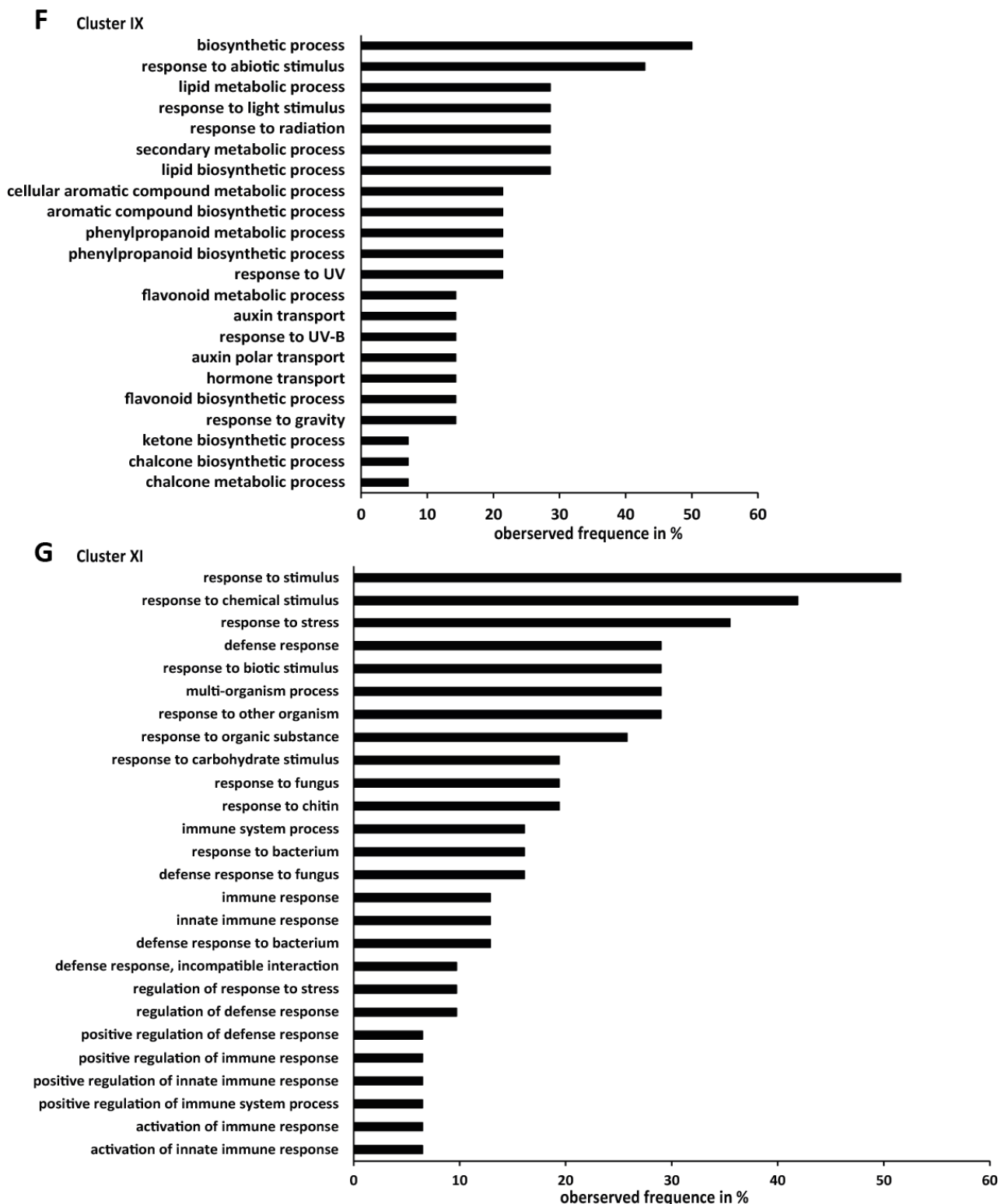
**A Cluster I**



**B Cluster IV**

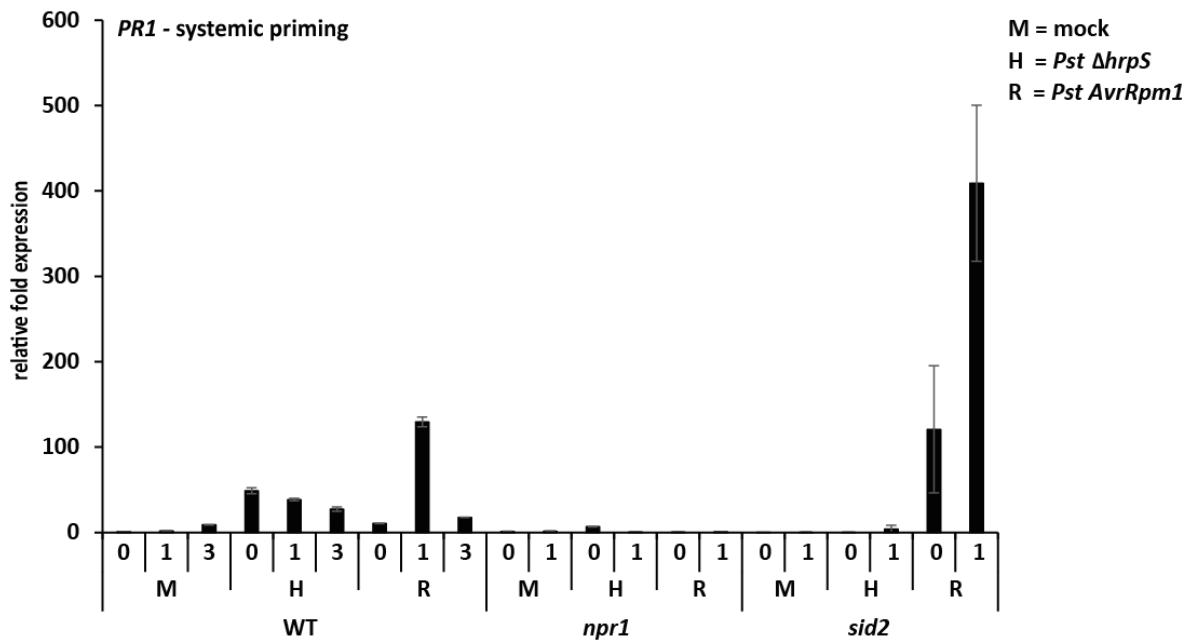






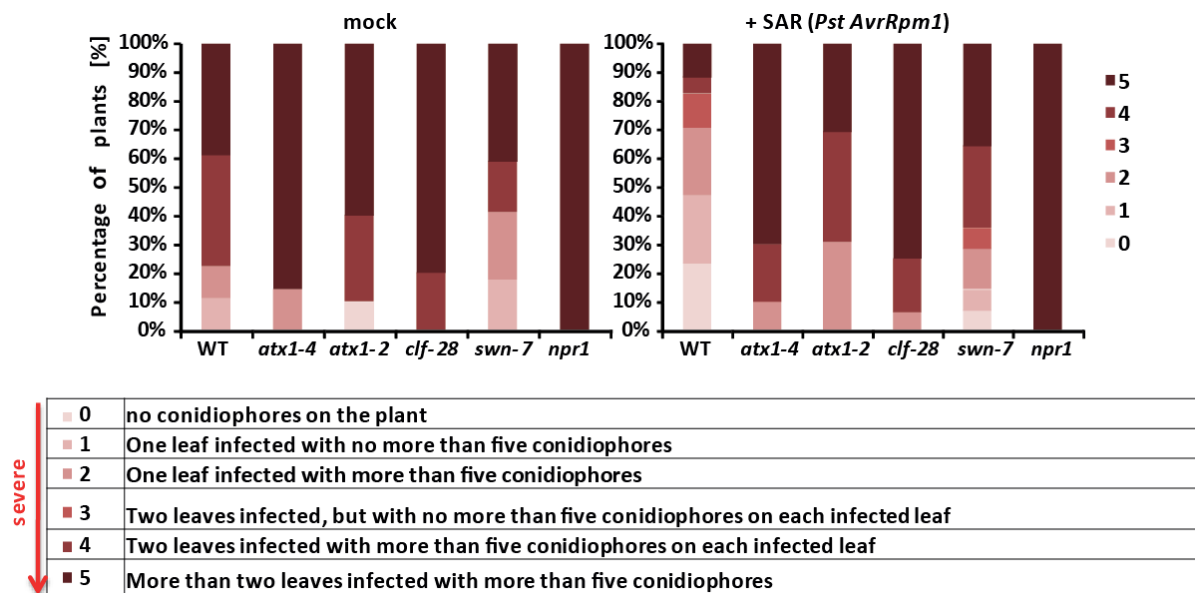
**Supplementary Figure 12: GO term analysis.**

Gene ontology (GO) term enrichment analysis of all differentially expressed genes extracted from the heatmap analysis (Supplementary Table 2, Figure 10) for cluster I 64 genes (A), cluster IV 55 genes (B), cluster VI 12 genes (C), cluster VII 31 genes (D), cluster VIII 32 genes (E), cluster IX 15 genes (F) and cluster XI 33 genes (G). GO terms were clustered into functional groups. The GO term (GO biological process) was performed using the platform VirtualPlant1.3 (Katari et al. 2010). p-values were calculated via Fisher Exact Test (with FDR correction) set as 0.01. As background *Arabidopsis thaliana* Col-0 tair10 genome was used.



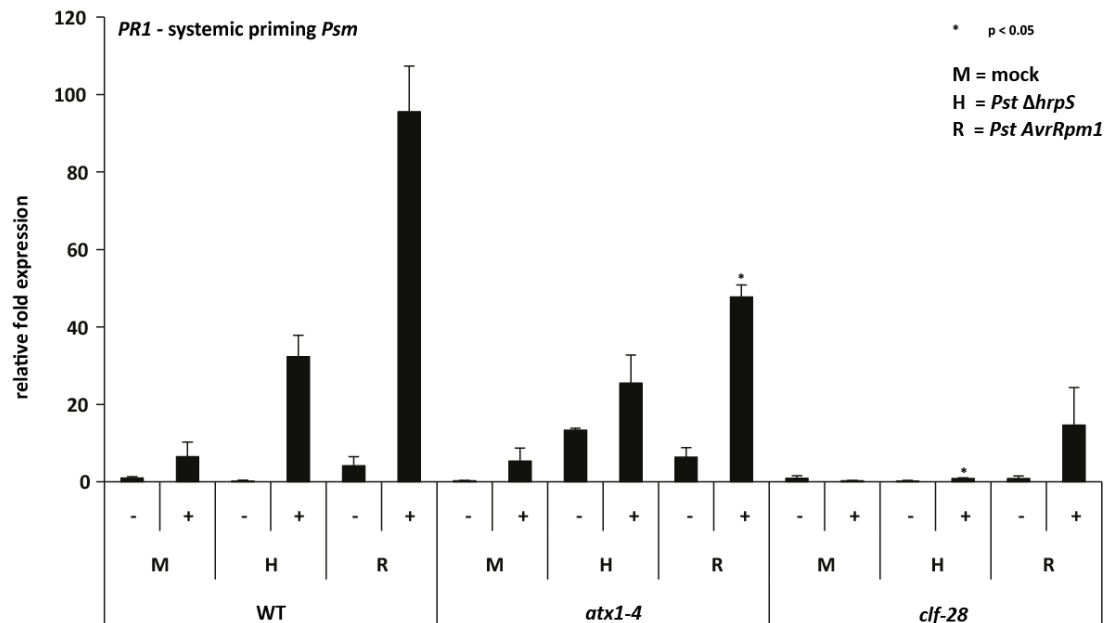
**Supplementary Figure 13: Systemic priming assay in WT, *npr1* and *sid2*.**

Four-week-old plants were syringe-infiltrated in three well-expanded local leaves with 10 mM MgCl<sub>2</sub> (mock, M), 1x10<sup>8</sup> cfu/ml *Pst ΔhrpS* (H) or 1x10<sup>6</sup> cfu/ml *Pst AvrRpm1* (R). At 48 hpi local infiltrated leaves were removed and systemic leaves infiltrated with water. At the indicated time points, *PR1* transcript abundance was measured by qRT-PCR in WT, *npr1* and *sid2*. Fold changes are calculated relative to mock WT samples at 0 h and normalized against the endogenous reference gene At4g26410. Error bars represent standard deviation (SD; n=3) of one biological replicate with three technical replicates, respectively.



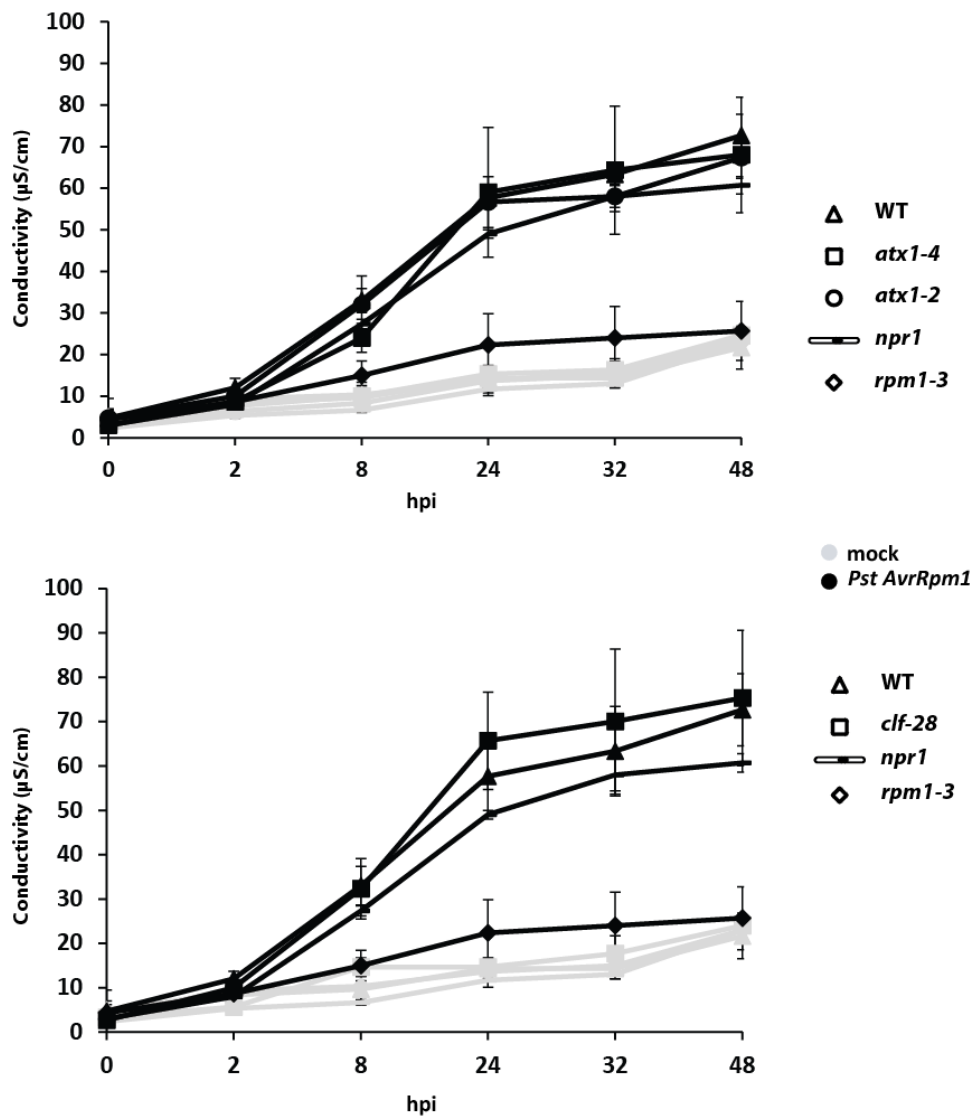
**Supplementary Figure 14: SAR assay in *trxG* and *PcG* mutant plants.**

Four-week-old plants were syringe-infiltrated in three local leaves with  $1 \times 10^6$  cfu/ml, *Pst AvrRpm1* or 10 mM  $MgCl_2$  (mock). At 48 hpi the local leaves were removed and the remaining systemic leaves inoculated with *Hpa Noco2* at a concentration of  $4 \times 10^4$  spores/ml of water. At seven dpi the disease symptoms were scored by counting the number of conidiophores on systemic leaves. Up to 18 plants were counted for each genotype and treatment, and grouped into five categories. Representative result is shown. Experiment was repeated four times with similar results.



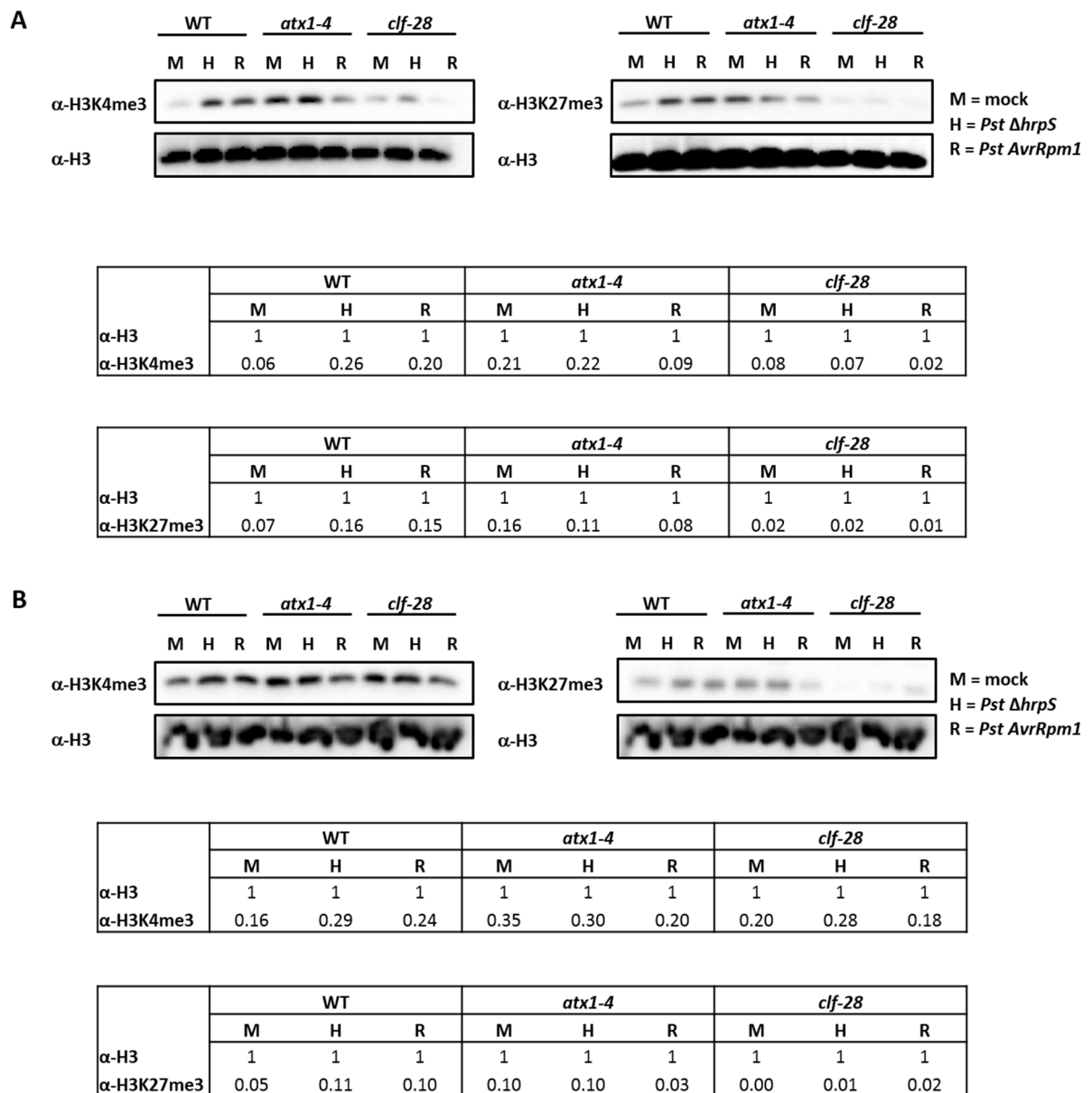
**Supplementary Figure 15: ETI- and MTI-induced systemic priming response after *Psm* infection of systemic leaves in WT, *atx1-4* and *clf-28*.**

Four-week-old plants were syringe-infiltrated in three local leaves with 10 mM  $MgCl_2$  (mock, M),  $1 \times 10^8$  cfu/ml *Pst ΔhrpS* (H) or  $1 \times 10^5$  cfu/ml *Pst AvrRpm1* (R). At 48 hpi the local leaves were removed and the remaining systemic leaves infiltrated with  $1 \times 10^4$  cfu/ml *Psm*. Systemic samples were harvested before (-) or 10 hpi (+) and *PR1* expression was evaluated by qRT-PCR. Fold changes are calculated relative to mock WT samples at 0 h and normalized against the endogenous reference gene At4g26410. Error bars represent standard error (SE; n=2) of two biological with three technical replicates each, respectively. P-value of  $p < 0.05$ , indicated by asterisk, was calculated using Student's t-test comparing the gene expression after secondary treatment of *atx1-4* and *clf-28* to the respective WT expression.



**Supplementary Figure 16: RPM1-induced cell death evaluated by ion leakage measurement.**

Four-week-old plant leaves were infiltrated with *Pst AvrRpm1* with  $1 \times 10^6$  cfu/ml or 10 mM  $MgCl_2$  (mock). At 0, 2, 8, 24, 32 and 48 hpi samples were subjected to ion leakage measurements. Error bars represent standard deviation (SD; n=6) of one biological replicate. Experiment was repeated twice with similar results.



**Supplementary Figure 17: Histone mark survey of H3K4me3 and H3K27me3 in systemic leaves of WT, *atx1-4* and *clf-28* upon local MTI- and ETI-activation.**

(A) and (B) Four-week-old plants were syringe-infiltrated in three well-expanded local leaves with 10 mM MgCl<sub>2</sub> (mock, M), 1x10<sup>8</sup> cfu/ml *Pst ΔhrpS* (H) or 1x10<sup>6</sup> cfu/ml *Pst AvrRpm1* (R). At 48 hpi systemic leaves were harvested and chromatin extracted. Chromatin extract was subjected to SDS-PAGE and western blot analysis probing the membrane with α-H3K4me3, α-H3K27me3 and α-H3, detecting the unmodified C-terminal part of H3. Relative protein abundance of H3K4me3 and H3K27me3 to H3, (set as 1), is depicted in the table below, respectively.

Two independent biological replicates are shown.



## 6 Literature

- Aarts N, Metz M, Holub E, Staskawicz BJ, Daniels MJ, Parker JE. 1998. Different requirements for EDS1 and NDR1 by disease resistance genes define at least two R gene-mediated signaling pathways in Arabidopsis. *Proc Natl Acad Sci U S A* **95**: 10306-10311.
- Ahlfors R, Macioszek V, Rudd J, Brosche M, Schlichting R, Scheel D, Kangasjarvi J. 2004. Stress hormone-independent activation and nuclear translocation of mitogen-activated protein kinases in Arabidopsis thaliana during ozone exposure. *Plant J* **40**: 512-522.
- Ahn IP, Kim S, Lee YH, Suh SC. 2007. Vitamin B1-induced priming is dependent on hydrogen peroxide and the NPR1 gene in Arabidopsis. *Plant Physiol* **143**: 838-848.
- Alcazar R, Reymond M, Schmitz G, de Meaux J. 2011. Genetic and evolutionary perspectives on the interplay between plant immunity and development. *Curr Opin Plant Biol* **14**: 378-384.
- Alvarez-Venegas R. 2010. Regulation by polycomb and trithorax group proteins in Arabidopsis. *Arabidopsis Book* **8**: e0128.
- Alvarez-Venegas R, Abdallat AA, Guo M, Alfano JR, Avramova Z. 2007. Epigenetic control of a transcription factor at the cross section of two antagonistic pathways. *Epigenetics* **2**: 106-113.
- Alvarez-Venegas R, Avramova Z. 2005. Methylation patterns of histone H3 Lys 4, Lys 9 and Lys 27 in transcriptionally active and inactive Arabidopsis genes and in atx1 mutants. *Nucleic Acids Res* **33**: 5199-5207.
- Alvarez-Venegas R, Pien S, Sadler M, Witmer X, Grossniklaus U, Avramova Z. 2003. ATX-1, an Arabidopsis homolog of trithorax, activates flower homeotic genes. *Curr Biol* **13**: 627-637.
- Alvarez-Venegas R, Sadler M, Hlavacka A, Baluska F, Xia Y, Lu G, Firsov A, Sarath G, Moriyama H, Dubrovsky JG et al. 2006. The Arabidopsis homolog of trithorax, ATX1, binds phosphatidylinositol 5-phosphate, and the two regulate a common set of target genes. *Proc Natl Acad Sci U S A* **103**: 6049-6054.
- Alvarez ME, Nota F, Cambiagno DA. 2010. Epigenetic control of plant immunity. *Mol Plant Pathol* **11**: 563-576.
- An C, Mou Z. 2013. The function of the Mediator complex in plant immunity. *Plant Signal Behav* **8**: e23182.
- Andreasson E, Jenkins T, Brodersen P, Thorgrimsen S, Petersen NH, Zhu S, Qiu JL, Micheelsen P, Rocher A, Petersen M et al. 2005. The MAP kinase substrate MKS1 is a regulator of plant defense responses. *EMBO J* **24**: 2579-2589.
- Anelli T, Sitia R. 2008. Protein quality control in the early secretory pathway. *EMBO J* **27**: 315-327.
- Angel A, Song J, Dean C, Howard M. 2011. A Polycomb-based switch underlying quantitative epigenetic memory. *Nature* **476**: 105-108.
- Asai T, Tena G, Plotnikova J, Willmann MR, Chiu WL, Gomez-Gomez L, Boller T, Ausubel FM, Sheen J. 2002. MAP kinase signalling cascade in Arabidopsis innate immunity. *Nature* **415**: 977-983.
- Attaran E, Zeier TE, Griebel T, Zeier J. 2009. Methyl salicylate production and jasmonate signaling are not essential for systemic acquired resistance in Arabidopsis. *Plant Cell* **21**: 954-971.
- Badeaux AI, Shi Y. 2013. Emerging roles for chromatin as a signal integration and storage platform. *Nat Rev Mol Cell Biol* **14**: 211-224.
- Bailey K, Cevik V, Holton N, Byrne-Richardson J, Sohn KH, Coates M, Woods-Tor A, Aksoy HM, Hughes L, Baxter L et al. 2011. Molecular cloning of ATR5(Emoy2) from Hyaloperonospora arabidopsidis, an avirulence determinant that triggers RPP5-mediated defense in Arabidopsis. *Mol Plant Microbe Interact* **24**: 827-838.
- Bailey TL, Boden M, Buske FA, Frith M, Grant CE, Clementi L, Ren J, Li WW, Noble WS. 2009. MEME SUITE: tools for motif discovery and searching. *Nucleic Acids Res* **37**: W202-208.

- Baldwin IT, Schmelz EA, Zhang ZP. 1996. Effects of octadecanoid metabolites and inhibitors on induced nicotine accumulation in *Nicotiana sylvestris*. *J Chem Ecol* **22**: 61-74.
- Bartsch M, Gobbato E, Bednarek P, Debey S, Schultze JL, Bautor J, Parker JE. 2006. Salicylic acid-independent ENHANCED DISEASE SUSCEPTIBILITY1 signaling in Arabidopsis immunity and cell death is regulated by the monooxygenase FMO1 and the Nudix hydrolase NUDT7. *Plant Cell* **18**: 1038-1051.
- Baumbusch LO, Thorstensen T, Krauss V, Fischer A, Naumann K, Assalkhou R, Schulz I, Reuter G, Aalen RB. 2001. The Arabidopsis thaliana genome contains at least 29 active genes encoding SET domain proteins that can be assigned to four evolutionarily conserved classes. *Nucleic Acids Res* **29**: 4319-4333.
- Baumgarten A, Cannon S, Spangler R, May G. 2003. Genome-level evolution of resistance genes in Arabidopsis thaliana. *Genetics* **165**: 309-319.
- Becker C, Weigel D. 2012. Epigenetic variation: origin and transgenerational inheritance. *Curr Opin Plant Biol* **15**: 562-567.
- Beckers GJ, Conrath U. 2007. Priming for stress resistance: from the lab to the field. *Curr Opin Plant Biol* **10**: 425-431.
- Beckers GJ, Jaskiewicz M, Liu Y, Underwood WR, He SY, Zhang S, Conrath U. 2009. Mitogen-activated protein kinases 3 and 6 are required for full priming of stress responses in Arabidopsis thaliana. *Plant Cell* **21**: 944-953.
- Bernoux M, Ellis JG, Dodds PN. 2011. New insights in plant immunity signaling activation. *Curr Opin Plant Biol* **14**: 512-518.
- Bernstein BE, Mikkelsen TS, Xie X, Kamal M, Huebert DJ, Cuff J, Fry B, Meissner A, Wernig M, Plath K et al. 2006. A bivalent chromatin structure marks key developmental genes in embryonic stem cells. *Cell* **125**: 315-326.
- Berr A, McCallum EJ, Alioua A, Heintz D, Heitz T, Shen WH. 2010. Arabidopsis histone methyltransferase SET DOMAIN GROUP8 mediates induction of the jasmonate/ethylene pathway genes in plant defense response to necrotrophic fungi. *Plant Physiol* **154**: 1403-1414.
- Berr A, Menard R, Heitz T, Shen WH. 2012. Chromatin modification and remodelling: a regulatory landscape for the control of Arabidopsis defence responses upon pathogen attack. *Cell Microbiol* **14**: 829-839.
- Berr A, Shafiq S, Shen WH. 2011. Histone modifications in transcriptional activation during plant development. *Biochim Biophys Acta* **1809**: 567-576.
- Bezhani S, Winter C, Hershman S, Wagner JD, Kennedy JF, Kwon CS, Pfluger J, Su Y, Wagner D. 2007. Unique, shared, and redundant roles for the Arabidopsis SWI/SNF chromatin remodeling ATPases BRAHMA and SPLAYED. *Plant Cell* **19**: 403-416.
- Bhattacharjee S, Halane MK, Kim SH, Gassmann W. 2011. Pathogen effectors target Arabidopsis EDS1 and alter its interactions with immune regulators. *Science* **334**: 1405-1408.
- Birkenbihl RP, Diezel C, Somssich IE. 2012. Arabidopsis WRKY33 is a key transcriptional regulator of hormonal and metabolic responses toward Botrytis cinerea infection. *Plant Physiol* **159**: 266-285.
- Bisgrove SR, Simonich MT, Smith NM, Sattler A, Innes RW. 1994. A disease resistance gene in Arabidopsis with specificity for two different pathogen avirulence genes. *Plant Cell* **6**: 927-933.
- Black JC, Choi JE, Lombardo SR, Carey M. 2006. A mechanism for coordinating chromatin modification and preinitiation complex assembly. *Mol Cell* **23**: 809-818.
- Boller T, He SY. 2009. Innate immunity in plants: an arms race between pattern recognition receptors in plants and effectors in microbial pathogens. *Science* **324**: 742-744.
- Bourbon HM. 2008. Comparative genomics supports a deep evolutionary origin for the large, four-module transcriptional mediator complex. *Nucleic Acids Res* **36**: 3993-4008.

- Bourbousse C, Ahmed I, Roudier F, Zabulon G, Blondet E, Balzergue S, Colot V, Bowler C, Barneche F. 2012. Histone H2B Monoubiquitination Facilitates the Rapid Modulation of Gene Expression during Arabidopsis Photomorphogenesis. *PLoS Genet* **8**: e1002825.
- Bouyer D, Roudier F, Heese M, Andersen ED, Gey D, Nowack MK, Goodrich J, Renou JP, Grini PE, Colot V et al. 2011. Polycomb repressive complex 2 controls the embryo-to-seedling phase transition. *PLoS Genet* **7**: e1002014.
- Bowling SA, Guo A, Cao H, Gordon AS, Klessig DF, Dong X. 1994. A mutation in Arabidopsis that leads to constitutive expression of systemic acquired resistance. *Plant Cell* **6**: 1845-1857.
- Boyko A, Kovalchuk I. 2011. Genome instability and epigenetic modification--heritable responses to environmental stress? *Curr Opin Plant Biol* **14**: 260-266.
- Bradford MM. 1976. A rapid and sensitive method for the quantitation of microgram quantities of protein utilizing the principle of protein-dye binding. *Anal Biochem* **72**: 248-254.
- Bratzel F, Lopez-Torrejon G, Koch M, Del Pozo JC, Calonje M. 2010. Keeping cell identity in Arabidopsis requires PRC1 RING-finger homologs that catalyze H2A monoubiquitination. *Curr Biol* **20**: 1853-1859.
- Broekaert WF, Delaure SL, De Bolle MF, Cammue BP. 2006. The role of ethylene in host-pathogen interactions. *Annu Rev Phytopathol* **44**: 393-416.
- Bruce TJA, Matthes MC, Napier JA, Pickett JA. 2007. Stressful "memories" of plants: Evidence and possible mechanisms. *Plant Science* **173**: 603-608.
- Buscaill P, Rivas S. 2014. Transcriptional control of plant defence responses. *Curr Opin Plant Biol* **20C**: 35-46.
- Butenko Y, Ohad N. 2011. Polycomb-group mediated epigenetic mechanisms through plant evolution. *Biochim Biophys Acta* **1809**: 395-406.
- Caldo RA, Nettleton D, Wise RP. 2004. Interaction-dependent gene expression in Mla-specified response to barley powdery mildew. *Plant Cell* **16**: 2514-2528.
- Calonje M. 2014. PRC1 Marks the Difference in Plant PcG Repression. *Mol Plant* **7**: 459-471.
- Canet JV, Dobon A, Tornero P. 2012. Non-recognition-of-BTH4, an Arabidopsis mediator subunit homolog, is necessary for development and response to salicylic acid. *Plant Cell* **24**: 4220-4235.
- Cao H, Li X, Dong X. 1998. Generation of broad-spectrum disease resistance by overexpression of an essential regulatory gene in systemic acquired resistance. *Proc Natl Acad Sci U S A* **95**: 6531-6536.
- Cao X, Aufsatz W, Zilberman D, Mette MF, Huang MS, Matzke M, Jacobsen SE. 2003. Role of the DRM and CMT3 methyltransferases in RNA-directed DNA methylation. *Curr Biol* **13**: 2212-2217.
- Cao X, Jacobsen SE. 2002a. Locus-specific control of asymmetric and CpNpG methylation by the DRM and CMT3 methyltransferase genes. *Proc Natl Acad Sci U S A* **99 Suppl 4**: 16491-16498.
- . 2002b. Role of the arabidopsis DRM methyltransferases in de novo DNA methylation and gene silencing. *Curr Biol* **12**: 1138-1144.
- Carles CC, Fletcher JC. 2009. The SAND domain protein ULTRAPETALA1 acts as a trithorax group factor to regulate cell fate in plants. *Genes Dev* **23**: 2723-2728.
- Cazzonelli CI, Millar T, Finnegan EJ, Pogson BJ. 2009. Promoting gene expression in plants by permissive histone lysine methylation. *Plant Signal Behav* **4**: 484-488.
- Chanda B, Xia Y, Mandal MK, Yu K, Sekine KT, Gao QM, Selote D, Hu Y, Stromberg A, Navarre D et al. 2011. Glycerol-3-phosphate is a critical mobile inducer of systemic immunity in plants. *Nat Genet* **43**: 421-427.
- Chanvivattana Y, Bishopp A, Schubert D, Stock C, Moon YH, Sung ZR, Goodrich J. 2004. Interaction of Polycomb-group proteins controlling flowering in Arabidopsis. *Development* **131**: 5263-5276.
- Chaturvedi R, Krothapalli K, Makandar R, Nandi A, Sparks AA, Roth MR, Welti R, Shah J. 2008. Plastid omega3-fatty acid desaturase-dependent accumulation of a systemic acquired resistance inducing activity in petiole exudates of Arabidopsis thaliana is independent of jasmonic acid. *Plant J* **54**: 106-117.

- Chaturvedi R, Venables B, Petros RA, Nalam V, Li M, Wang X, Takemoto LJ, Shah J. 2012. An abietane diterpenoid is a potent activator of systemic acquired resistance. *Plant J* **71**: 161-172.
- Chauvin A, Caldelari D, Wolfender JL, Farmer EE. 2013. Four 13-lipoxygenases contribute to rapid jasmonate synthesis in wounded *Arabidopsis thaliana* leaves: a role for lipoxygenase 6 in responses to long-distance wound signals. *New Phytol* **197**: 566-575.
- Chen K, Du L, Chen Z. 2003. Sensitization of defense responses and activation of programmed cell death by a pathogen-induced receptor-like protein kinase in *Arabidopsis*. *Plant Mol Biol* **53**: 61-74.
- Chen K, Fan B, Du L, Chen Z. 2004. Activation of hypersensitive cell death by pathogen-induced receptor-like protein kinases from *Arabidopsis*. *Plant Mol Biol* **56**: 271-283.
- Chen Z, Zheng Z, Huang J, Lai Z, Fan B. 2009. Biosynthesis of salicylic acid in plants. *Plant Signal Behav* **4**: 493-496.
- Cheng C, Gao X, Feng B, Sheen J, Shan L, He P. 2013. Plant immune response to pathogens differs with changing temperatures. *Nat Commun* **4**: 2530.
- Cheng YT, Germain H, Wiermer M, Bi D, Xu F, Garcia AV, Wirthmueller L, Despres C, Parker JE, Zhang Y et al. 2009. Nuclear pore complex component MOS7/Nup88 is required for innate immunity and nuclear accumulation of defense regulators in *Arabidopsis*. *Plant Cell* **21**: 2503-2516.
- Chester KS. 1933a. The problem of acquired physiological immunity in plants. *Quarterly Review of Biology* **8**: 129-154.
- . 1933b. The problem of acquired physiological immunity in plants (continued). *Quarterly Review of Biology* **8**: 275-324.
- Chinchilla D, Bauer Z, Regenass M, Boller T, Felix G. 2006. The *Arabidopsis* receptor kinase FLS2 binds flg22 and determines the specificity of flagellin perception. *Plant Cell* **18**: 465-476.
- Chinnusamy V, Zhu JK. 2009. RNA-directed DNA methylation and demethylation in plants. *Sci China C Life Sci* **52**: 331-343.
- Choi SM, Song HR, Han SK, Han M, Kim CY, Park J, Lee YH, Jeon JS, Noh YS, Noh B. 2012. HDA19 is required for the repression of salicylic acid biosynthesis and salicylic acid-mediated defense responses in *Arabidopsis*. *Plant J* **71**: 135-146.
- Chung EH, da Cunha L, Wu AJ, Gao Z, Cherkis K, Afzal AJ, Mackey D, Dangl JL. 2011. Specific threonine phosphorylation of a host target by two unrelated type III effectors activates a host innate immune receptor in plants. *Cell Host Microbe* **9**: 125-136.
- Clapier CR, Cairns BR. 2009. The biology of chromatin remodeling complexes. *Annu Rev Biochem* **78**: 273-304.
- Clarke JD, Volko SM, Ledford H, Ausubel FM, Dong X. 2000. Roles of salicylic acid, jasmonic acid, and ethylene in cpr-induced resistance in *Arabidopsis*. *Plant Cell* **12**: 2175-2190.
- Clayton AL, Mahadevan LC. 2003. MAP kinase-mediated phosphoacetylation of histone H3 and inducible gene regulation. *FEBS Lett* **546**: 51-58.
- Coates ME, Beynon JL. 2010. *Hyaloperonospora Arabidopsisidis* as a pathogen model. *Annu Rev Phytopathol* **48**: 329-345.
- Coll NS, Epple P, Dangl JL. 2011. Programmed cell death in the plant immune system. *Cell Death Differ* **18**: 1247-1256.
- Conaway RC, Conaway JW. 2011a. Function and regulation of the Mediator complex. *Curr Opin Genet Dev* **21**: 225-230.
- . 2011b. Origins and activity of the Mediator complex. *Semin Cell Dev Biol* **22**: 729-734.
- Conrath U. 2011. Molecular aspects of defence priming. *Trends Plant Sci* **16**: 524-531.
- Cunnac S, Lindeberg M, Collmer A. 2009. *Pseudomonas syringae* type III secretion system effectors: repertoires in search of functions. *Curr Opin Microbiol* **12**: 53-60.
- Czechowski T, Stitt M, Altmann T, Udvardi MK, Scheible WR. 2005. Genome-wide identification and testing of superior reference genes for transcript normalization in *Arabidopsis*. *Plant physiology* **139**: 5-17.

- da Cunha L, Sreerekha MV, Mackey D. 2007. Defense suppression by virulence effectors of bacterial phytopathogens. *Curr Opin Plant Biol* **10**: 349-357.
- Dangl JL, Horvath DM, Staskawicz BJ. 2013. Pivoting the plant immune system from dissection to deployment. *Science* **341**: 746-751.
- De-La-Pena C, Rangel-Cano A, Alvarez-Venegas R. 2012. Regulation of disease-responsive genes mediated by epigenetic factors: interaction of Arabidopsis-Pseudomonas. *Mol Plant Pathol* **13**: 388-398.
- de Torres M, Sanchez P, Fernandez-Delmond I, Grant M. 2003. Expression profiling of the host response to bacterial infection: the transition from basal to induced defence responses in RPM1-mediated resistance. *Plant J* **33**: 665-676.
- De Vos M, Van Zaanen W, Koornneef A, Korzelius JP, Dicke M, Van Loon LC, Pieterse CM. 2006. Herbivore-induced resistance against microbial pathogens in Arabidopsis. *Plant Physiol* **142**: 352-363.
- Deal RB, Henikoff S. 2011a. Histone variants and modifications in plant gene regulation. *Curr Opin Plant Biol* **14**: 116-122.
- . 2011b. The INTACT method for cell type-specific gene expression and chromatin profiling in Arabidopsis thaliana. *Nat Protoc* **6**: 56-68.
- Deal RB, Topp CN, McKinney EC, Meagher RB. 2007. Repression of flowering in Arabidopsis requires activation of FLOWERING LOCUS C expression by the histone variant H2A.Z. *Plant Cell* **19**: 74-83.
- Delaney TP, Friedrich L, Ryals JA. 1995. Arabidopsis signal transduction mutant defective in chemically and biologically induced disease resistance. *Proc Natl Acad Sci U S A* **92**: 6602-6606.
- Dempsey DA, Klessig DF. 2012. SOS - too many signals for systemic acquired resistance? *Trends Plant Sci* **17**: 538-545.
- Denance N, Sanchez-Vallet A, Goffner D, Molina A. 2013. Disease resistance or growth: the role of plant hormones in balancing immune responses and fitness costs. *Front Plant Sci* **4**: 155.
- Deslandes L, Rivas S. 2012. Catch me if you can: bacterial effectors and plant targets. *Trends Plant Sci*.
- Dhawan R, Luo H, Foerster AM, Abuqamar S, Du HN, Briggs SD, Mittelsten Scheid O, Mengiste T. 2009. HISTONE MONOUBIQUITINATION1 interacts with a subunit of the mediator complex and regulates defense against necrotrophic fungal pathogens in Arabidopsis. *Plant Cell* **21**: 1000-1019.
- Ding B, Bellizzi Mdel R, Ning Y, Meyers BC, Wang GL. 2012a. HDT701, a histone H4 deacetylase, negatively regulates plant innate immunity by modulating histone H4 acetylation of defense-related genes in rice. *Plant Cell* **24**: 3783-3794.
- Ding Y, Avramova Z, Fromm M. 2011a. The Arabidopsis trithorax-like factor ATX1 functions in dehydration stress responses via ABA-dependent and ABA-independent pathways. *Plant J* **66**: 735-744.
- . 2011b. Two distinct roles of ARABIDOPSIS HOMOLOG OF TRITHORAX1 (ATX1) at promoters and within transcribed regions of ATX1-regulated genes. *Plant Cell* **23**: 350-363.
- Ding Y, Ndamukong I, Xu Z, Lapko H, Fromm M, Avramova Z. 2012b. ATX1-generated H3K4me3 is required for efficient elongation of transcription, not initiation, at ATX1-regulated genes. *PLoS Genet* **8**: e1003111.
- Dodds PN, Rathjen JP. 2010. Plant immunity: towards an integrated view of plant-pathogen interactions. *Nat Rev Genet* **11**: 539-548.
- Downen RH, Pelizzola M, Schmitz RJ, Lister R, Downen JM, Nery JR, Dixon JE, Ecker JR. 2012. Widespread dynamic DNA methylation in response to biotic stress. *Proc Natl Acad Sci U S A* **109**: E2183-2191.
- Du L, Chen Z. 2000. Identification of genes encoding receptor-like protein kinases as possible targets of pathogen- and salicylic acid-induced WRKY DNA-binding proteins in Arabidopsis. *Plant J* **24**: 837-847.

- Du Z, Zhou X, Ling Y, Zhang ZH, Su Z. 2010. agriGO: a GO analysis toolkit for the agricultural community. *Nucleic acids research* **38**: W64-W70.
- Durrant WE, Dong X. 2004. Systemic acquired resistance. *Annu Rev Phytopathol* **42**: 185-209.
- Durrant WE, Wang S, Dong X. 2007. Arabidopsis SNI1 and RAD51D regulate both gene transcription and DNA recombination during the defense response. *Proc Natl Acad Sci U S A* **104**: 4223-4227.
- Enyedí AJ, Yalpani N, Silverman P, Raskin I. 1992a. Localization, conjugation, and function of salicylic acid in tobacco during the hypersensitive reaction to tobacco mosaic virus. *Proc Natl Acad Sci U S A* **89**: 2480-2484.
- . 1992b. Signal molecules in systemic plant resistance to pathogens and pests. *Cell* **70**: 879-886.
- Eskeland R, Freyer E, Leeb M, Wutz A, Bickmore WA. 2010. Histone acetylation and the maintenance of chromatin compaction by Polycomb repressive complexes. *Cold Spring Harb Symp Quant Biol* **75**: 71-78.
- Falk A, Feys BJ, Frost LN, Jones JD, Daniels MJ, Parker JE. 1999. EDS1, an essential component of R gene-mediated disease resistance in Arabidopsis has homology to eukaryotic lipases. *Proc Natl Acad Sci U S A* **96**: 3292-3297.
- Farrona S, Coupland G, Turck F. 2008. The impact of chromatin regulation on the floral transition. *Semin Cell Dev Biol* **19**: 560-573.
- Farrona S, Thorpe FL, Engelhorn J, Adrian J, Dong X, Sarid-Krebs L, Goodrich J, Turck F. 2011. Tissue-specific expression of FLOWERING LOCUS T in Arabidopsis is maintained independently of polycomb group protein repression. *Plant Cell* **23**: 3204-3214.
- Feilner T, Hultschig C, Lee J, Meyer S, Immink RG, Koenig A, Possling A, Seitz H, Beveridge A, Scheel D et al. 2005. High throughput identification of potential Arabidopsis mitogen-activated protein kinases substrates. *Mol Cell Proteomics* **4**: 1558-1568.
- Felix G, Duran JD, Volko S, Boller T. 1999. Plants have a sensitive perception system for the most conserved domain of bacterial flagellin. *Plant Journal* **18**: 265-276.
- Fercha A, Capriotti AL, Caruso G, Cavaliere C, Samperi R, Stampachiachiere S, Lagana A. 2014. Comparative analysis of metabolic proteome variation in ascorbate-primed and unprimed wheat seeds during germination under salt stress. *J Proteomics* **108C**: 238-257.
- Fiil BK, Petersen K, Petersen M, Mundy J. 2009. Gene regulation by MAP kinase cascades. *Curr Opin Plant Biol* **12**: 615-621.
- Finnegan EJ, Bond DM, Buzas DM, Goodrich J, Helliwell CA, Tamada Y, Yun JY, Amasino RM, Dennis ES. 2011. Polycomb proteins regulate the quantitative induction of VERNALIZATION INSENSITIVE 3 in response to low temperatures. *Plant Journal* **65**: 382-391.
- Fisher CL, Fisher AG. 2011. Chromatin states in pluripotent, differentiated, and reprogrammed cells. *Curr Opin Genet Dev* **21**: 140-146.
- Flor HH. 1971. Current Status of Gene-for-Gene Concept. *Annual Review of Phytopathology* **9**: 275-+.
- Fonseca S, Chini A, Hamberg M, Adie B, Porzel A, Kramell R, Miersch O, Wasternack C, Solano R. 2009. (+)-7-iso-Jasmonoyl-L-isoleucine is the endogenous bioactive jasmonate. *Nat Chem Biol* **5**: 344-350.
- Fontana MF, Vance RE. 2011. Two signal models in innate immunity. *Immunol Rev* **243**: 26-39.
- Francis NJ, Kingston RE, Woodcock CL. 2004. Chromatin compaction by a polycomb group protein complex. *Science* **306**: 1574-1577.
- Fromm M, Avramova Z. 2014. ATX1/AtCOMPASS and the H3K4me3 marks: how do they activate Arabidopsis genes? *Curr Opin Plant Biol* **21C**: 75-82.
- Frye CA, Innes RW. 1998. An Arabidopsis mutant with enhanced resistance to powdery mildew. *Plant Cell* **10**: 947-956.
- Frye CA, Tang D, Innes RW. 2001. Negative regulation of defense responses in plants by a conserved MAPKK kinase. *Proc Natl Acad Sci U S A* **98**: 373-378.
- Fu ZQ, Dong X. 2013. Systemic acquired resistance: turning local infection into global defense. *Annu Rev Plant Biol* **64**: 839-863.

- Fu ZQ, Yan S, Saleh A, Wang W, Ruble J, Oka N, Mohan R, Spoel SH, Tada Y, Zheng N et al. 2012. NPR3 and NPR4 are receptors for the immune signal salicylic acid in plants. *Nature* **486**: 228-232.
- Fuchs J, Demidov D, Houben A, Schubert I. 2006. Chromosomal histone modification patterns--from conservation to diversity. *Trends Plant Sci* **11**: 199-208.
- Gao QM, Kachroo A, Kachroo P. 2014. Chemical inducers of systemic immunity in plants. *J Exp Bot* **65**: 1849-1855.
- Garcia AV, Blanvillain-Baufume S, Huibers RP, Wiermer M, Li G, Gobbato E, Rietz S, Parker JE. 2010. Balanced nuclear and cytoplasmic activities of EDS1 are required for a complete plant innate immune response. *PLoS Pathog* **6**: e1000970.
- Garcia AV, Parker JE. 2009. Heaven's Gate: nuclear accessibility and activities of plant immune regulators. *Trends Plant Sci* **14**: 479-487.
- Gentry M, Hennig L. 2014. Remodelling chromatin to shape development of plants. *Exp Cell Res* **321**: 40-46.
- Gfeller A, Dubugnon L, Liechti R, Farmer EE. 2010. Jasmonate biochemical pathway. *Sci Signal* **3**: cm3.
- Glauser G, Dubugnon L, Mousavi SA, Rudaz S, Wolfender JL, Farmer EE. 2009. Velocity estimates for signal propagation leading to systemic jasmonic acid accumulation in wounded *Arabidopsis*. *J Biol Chem* **284**: 34506-34513.
- Glazebrook J. 2005. Contrasting mechanisms of defense against biotrophic and necrotrophic pathogens. *Annu Rev Phytopathol* **43**: 205-227.
- Glazebrook J, Rogers EE, Ausubel FM. 1996. Isolation of *Arabidopsis* mutants with enhanced disease susceptibility by direct screening. *Genetics* **143**: 973-982.
- Goh CH, Nam HG, Park YS. 2003. Stress memory in plants: a negative regulation of stomatal response and transient induction of rd22 gene to light in abscisic acid-entrained *Arabidopsis* plants. *Plant J* **36**: 240-255.
- Gohre V, Spallek T, Haweker H, Mersmann S, Mentzel T, Boller T, de Torres M, Mansfield JW, Robatzek S. 2008. Plant pattern-recognition receptor FLS2 is directed for degradation by the bacterial ubiquitin ligase AvrPtoB. *Curr Biol* **18**: 1824-1832.
- Gomez-Gomez L, Boller T. 2000. FLS2: an LRR receptor-like kinase involved in the perception of the bacterial elicitor flagellin in *Arabidopsis*. *Mol Cell* **5**: 1003-1011.
- Goodrich J, Puangsomlee P, Martin M, Long D, Meyerowitz EM, Coupland G. 1997. A Polycomb-group gene regulates homeotic gene expression in *Arabidopsis*. *Nature* **386**: 44-51.
- Grafi G, Florentin A, Ransbotyn V, Morgenstern Y. 2011. The stem cell state in plant development and in response to stress. *Front Plant Sci* **2**: 53.
- Green TR, Ryan CA. 1972. Wound-Induced Proteinase Inhibitor in Plant Leaves: A Possible Defense Mechanism against Insects. *Science* **175**: 776-777.
- Greenberg JT, Yao N. 2004. The role and regulation of programmed cell death in plant-pathogen interactions. *Cell Microbiol* **6**: 201-211.
- Griebel T, Zeier J. 2008. Light regulation and daytime dependency of inducible plant defenses in *Arabidopsis*: phytochrome signaling controls systemic acquired resistance rather than local defense. *Plant Physiol* **147**: 790-801.
- Ghini PE, Thorstensen T, Alm V, Vizcay-Barrena G, Windju SS, Jorstad TS, Wilson ZA, Aalen RB. 2009. The ASH1 HOMOLOG 2 (ASHH2) histone H3 methyltransferase is required for ovule and anther development in *Arabidopsis*. *PLoS One* **4**: e7817.
- Gruner K, Griebel T, Navarova H, Attaran E, Zeier J. 2013. Reprogramming of plants during systemic acquired resistance. *Front Plant Sci* **4**: 252.
- Guedes MEM, Richmond S, Kuc J. 1980. Induced Systemic Resistance to Anthracnose in Cucumber as Influenced by the Location of the Inducer Inoculation with *Colletotrichum-Lagenarium* and the Onset of Flowering and Fruiting. *Physiological Plant Pathology* **17**: 229-233.
- Hajheidari M, Koncz C, Eick D. 2013. Emerging roles for RNA polymerase II CTD in *Arabidopsis*. *Trends in Plant Science* **18**: 633-643.

- Hamdoun S, Liu Z, Gill M, Yao N, Lu H. 2013. Dynamics of defense responses and cell fate change during Arabidopsis-Pseudomonas syringae interactions. *PLoS One* **8**: e83219.
- Haring M, Offermann S, Danker T, Horst I, Peterhansel C, Stam M. 2007. Chromatin immunoprecipitation: optimization, quantitative analysis and data normalization. *Plant Methods* **3**: 11.
- He C, Chen X, Huang H, Xu L. 2012. Reprogramming of H3K27me3 is critical for acquisition of pluripotency from cultured Arabidopsis tissues. *PLoS Genet* **8**: e1002911.
- He G, Elling AA, Deng XW. 2011. The epigenome and plant development. *Annu Rev Plant Biol* **62**: 411-435.
- He Y, Michaels SD, Amasino RM. 2003. Regulation of flowering time by histone acetylation in Arabidopsis. *Science* **302**: 1751-1754.
- Heidel AJ, Clarke JD, Antonovics J, Dong X. 2004. Fitness costs of mutations affecting the systemic acquired resistance pathway in Arabidopsis thaliana. *Genetics* **168**: 2197-2206.
- Heidemann M, Hintermair C, Voss K, Eick D. 2013. Dynamic phosphorylation patterns of RNA polymerase II CTD during transcription. *Biochim Biophys Acta* **1829**: 55-62.
- Heidrich K, Blanvillain-Baufume S, Parker JE. 2012. Molecular and spatial constraints on NB-LRR receptor signaling. *Curr Opin Plant Biol* **15**: 385-391.
- Heidrich K, Tsuda K, Blanvillain-Baufume S, Wirthmueller L, Bautor J, Parker JE. 2013. Arabidopsis TNL-WRKY domain receptor RRS1 contributes to temperature-conditioned RPS4 auto-immunity. *Front Plant Sci* **4**: 403.
- Heidrich K, Wirthmueller L, Tasset C, Pouzet C, Deslandes L, Parker JE. 2011. Arabidopsis EDS1 connects pathogen effector recognition to cell compartment-specific immune responses. *Science* **334**: 1401-1404.
- Henikoff S, Shilatifard A. 2011. Histone modification: cause or cog? *Trends Genet* **27**: 389-396.
- Hennig L, Derkacheva M. 2009. Diversity of Polycomb group complexes in plants: same rules, different players? *Trends Genet* **25**: 414-423.
- Henry E, Yadeta KA, Coaker G. 2013. Recognition of bacterial plant pathogens: local, systemic and transgenerational immunity. *New Phytol* **199**: 908-915.
- Heo JB, Sung S. 2011. Vernalization-mediated epigenetic silencing by a long intronic noncoding RNA. *Science* **331**: 76-79.
- Holec S, Berger F. 2012. Polycomb group complexes mediate developmental transitions in plants. *Plant Physiol* **158**: 35-43.
- Holeski LM, Jander G, Agrawal AA. 2012. Transgenerational defense induction and epigenetic inheritance in plants. *Trends Ecol Evol* **27**: 618-626.
- Hruz T, Laule O, Szabo G, Wessendorp F, Bleuler S, Oertle L, Widmayer P, Gruissem W, Zimmermann P. 2008. Genevestigator v3: a reference expression database for the meta-analysis of transcriptomes. *Adv Bioinformatics* **2008**: 420747.
- Hua J. 2013. Modulation of plant immunity by light, circadian rhythm, and temperature. *Curr Opin Plant Biol* **16**: 406-413.
- Huckelhoven R, Panstruga R. 2011. Cell biology of the plant-powdery mildew interaction. *Curr Opin Plant Biol* **14**: 738-746.
- Huffaker A, Ryan CA. 2007. Endogenous peptide defense signals in Arabidopsis differentially amplify signaling for the innate immune response. *Proc Natl Acad Sci U S A* **104**: 10732-10736.
- Huot B, Yao J, Montgomery BL, He SY. 2014. Growth-Defense Tradeoffs in Plants: A Balancing Act to Optimize Fitness. *Mol Plant*.
- Jacob F, Vernaldi S, Maekawa T. 2013. Evolution and Conservation of Plant NLR Functions. *Front Immunol* **4**: 297.
- Jakoby M, Weisshaar B, Droge-Laser W, Vicente-Carbajosa J, Tiedemann J, Kroj T, Parcy F, b ZIPRG. 2002. bZIP transcription factors in Arabidopsis. *Trends Plant Sci* **7**: 106-111.

- Jaskiewicz M, Conrath U, Peterhansel C. 2011. Chromatin modification acts as a memory for systemic acquired resistance in the plant stress response. *EMBO Rep* **12**: 50-55.
- Jeddeloh JA, Stokes TL, Richards EJ. 1999. Maintenance of genomic methylation requires a SWI2/SNF2-like protein. *Nat Genet* **22**: 94-97.
- Jenns AE, Kuc J. 1979. Graft Transmission of Systemic Resistance of Cucumber to Anthracnose Induced by Colletotrichum-Lagenarium and Tobacco Necrosis Virus. *Phytopathology* **69**: 753-756.
- Jenuwein T, Allis CD. 2001. Translating the histone code. *Science* **293**: 1074-1080.
- Jeong CW, Roh H, Dang TV, Choi YD, Fischer RL, Lee JS, Choi Y. 2011. An E3 ligase complex regulates SET-domain polycomb group protein activity in Arabidopsis thaliana. *Proc Natl Acad Sci U S A* **108**: 8036-8041.
- Jing B, Xu S, Xu M, Li Y, Li S, Ding J, Zhang Y. 2011. Brush and spray: a high-throughput systemic acquired resistance assay suitable for large-scale genetic screening. *Plant Physiol* **157**: 973-980.
- Johannes F, Porcher E, Teixeira FK, Saliba-Colombani V, Simon M, Agier N, Bulski A, Albuissou J, Heredia F, Audigier P et al. 2009. Assessing the impact of transgenerational epigenetic variation on complex traits. *PLoS Genet* **5**: e1000530.
- Jones AM, Thomas V, Truman B, Lilley K, Mansfield J, Grant M. 2004. Specific changes in the Arabidopsis proteome in response to bacterial challenge: differentiating basal and R-gene mediated resistance. *Phytochemistry* **65**: 1805-1816.
- Jones JD, Dangl JL. 2006. The plant immune system. *Nature* **444**: 323-329.
- Jung HW, Tschaplinski TJ, Wang L, Glazebrook J, Greenberg JT. 2009. Priming in systemic plant immunity. *Science* **324**: 89-91.
- Jung SC, Martinez-Medina A, Lopez-Raez JA, Pozo MJ. 2012. Mycorrhiza-induced resistance and priming of plant defenses. *J Chem Ecol* **38**: 651-664.
- Kagey MH, Newman JJ, Bilodeau S, Zhan Y, Orlando DA, van Berkum NL, Ebmeier CC, Goossens J, Rahl PB, Levine SS et al. 2010. Mediator and cohesin connect gene expression and chromatin architecture. *Nature* **467**: 430-435.
- Kanhere A, Viiri K, Araujo CC, Rasaiyaah J, Bouwman RD, Whyte WA, Pereira CF, Brookes E, Walker K, Bell GW et al. 2010. Short RNAs are transcribed from repressed polycomb target genes and interact with polycomb repressive complex-2. *Mol Cell* **38**: 675-688.
- Katagiri F. 2004. A global view of defense gene expression regulation--a highly interconnected signaling network. *Curr Opin Plant Biol* **7**: 506-511.
- Katagiri F, Tsuda K. 2010. Understanding the plant immune system. *Mol Plant Microbe Interact* **23**: 1531-1536.
- Katari MS, Nowicki SD, Aceituno FF, Nero D, Kelfer J, Thompson LP, Cabello JM, Davidson RS, Goldberg AP, Shasha DE et al. 2010. VirtualPlant: a software platform to support systems biology research. *Plant Physiol* **152**: 500-515.
- Katz VA, Thulke OU, Conrath U. 1998. A benzothiadiazole primes parsley cells for augmented elicitation of defense responses. *Plant Physiol* **117**: 1333-1339.
- Kesarwani M, Yoo J, Dong X. 2007. Genetic interactions of TGA transcription factors in the regulation of pathogenesis-related genes and disease resistance in Arabidopsis. *Plant Physiol* **144**: 336-346.
- Kidd BN, Cahill DM, Manners JM, Schenk PM, Kazan K. 2011. Diverse roles of the Mediator complex in plants. *Semin Cell Dev Biol* **22**: 741-748.
- Kiefer IW, Slusarenko AJ. 2003. The pattern of systemic acquired resistance induction within the Arabidopsis rosette in relation to the pattern of translocation. *Plant Physiology* **132**: 840-847.
- Kim DH, Sung S. 2014. Genetic and epigenetic mechanisms underlying vernalization. *Arabidopsis Book* **12**: e0171.
- Kim MY, Zilberman D. 2014. DNA methylation as a system of plant genomic immunity. *Trends Plant Sci.*
- Kim Y, Tsuda K, Igarashi D, Hillmer RA, Sakakibara H, Myers CL, Katagiri F. 2014. Mechanisms underlying robustness and tunability in a plant immune signaling network. *Cell Host Microbe* **15**: 84-94.

- Kinkema M, Fan W, Dong X. 2000. Nuclear localization of NPR1 is required for activation of PR gene expression. *Plant Cell* **12**: 2339-2350.
- Kissoudis C, van de Wiel C, Visser RG, van der Linden G. 2014. Enhancing crop resilience to combined abiotic and biotic stress through the dissection of physiological and molecular crosstalk. *Front Plant Sci* **5**: 207.
- Klose RJ, Cooper S, Farcas AM, Blackledge NP, Brockdorff N. 2013. Chromatin sampling--an emerging perspective on targeting polycomb repressor proteins. *PLoS Genet* **9**: e1003717.
- Kohler A, Schwindling S, Conrath U. 2002. Benzothiadiazole-induced priming for potentiated responses to pathogen infection, wounding, and infiltration of water into leaves requires the NPR1/NIM1 gene in Arabidopsis. *Plant Physiol* **128**: 1046-1056.
- Kohler C, Aichinger E. 2010. Antagonizing Polycomb group-mediated gene repression by chromatin remodelers. *Epigenetics* **5**: 20-23.
- Koornneef A, Leon-Reyes A, Ritsema T, Verhage A, Den Otter FC, Van Loon LC, Pieterse CM. 2008. Kinetics of salicylate-mediated suppression of jasmonate signaling reveal a role for redox modulation. *Plant Physiol* **147**: 1358-1368.
- Korneli C, Danisman S, Staiger D. 2014. Differential Control Of Pre-Invasive And Post-Invasive Antibacterial Defense By The Arabidopsis Circadian Clock. *Plant Cell Physiol*.
- Kouzarides T. 2007a. Chromatin modifications and their function. *Cell* **128**: 693-705.
- . 2007b. SnapShot: Histone-modifying enzymes. *Cell* **128**: 802.
- Kunze G, Zipfel C, Robatzek S, Niehaus K, Boller T, Felix G. 2004. The N terminus of bacterial elongation factor Tu elicits innate immunity in Arabidopsis plants. *Plant Cell* **16**: 3496-3507.
- Lafos M, Kroll P, Hohenstatt ML, Thorpe FL, Clarenz O, Schubert D. 2011. Dynamic regulation of H3K27 trimethylation during Arabidopsis differentiation. *PLoS Genet* **7**: e1002040.
- Lang-Mladek C, Popova O, Kiok K, Berlinger M, Rakic B, Aufsatz W, Jonak C, Hauser MT, Luschnig C. 2010. Transgenerational inheritance and resetting of stress-induced loss of epigenetic gene silencing in Arabidopsis. *Mol Plant* **3**: 594-602.
- Lawton KA, Potter SL, Uknes S, Ryals J. 1994. Acquired Resistance Signal Transduction in Arabidopsis Is Ethylene Independent. *Plant Cell* **6**: 581-588.
- Lazaro A, Gomez-Zambrano A, Lopez-Gonzalez L, Pineiro M, Jarillo JA. 2008. Mutations in the Arabidopsis SWC6 gene, encoding a component of the SWR1 chromatin remodelling complex, accelerate flowering time and alter leaf and flower development. *J Exp Bot* **59**: 653-666.
- Lee J, Rudd JJ, Macioszek VK, Scheel D. 2004. Dynamic changes in the localization of MAPK cascade components controlling pathogenesis-related (PR) gene expression during innate immunity in parsley. *J Biol Chem* **279**: 22440-22448.
- Leon-Reyes A, Spoel SH, De Lange ES, Abe H, Kobayashi M, Tsuda S, Millenaar FF, Welschen RA, Ritsema T, Pieterse CM. 2009. Ethylene modulates the role of NONEXPRESSOR OF PATHOGENESIS-RELATED GENES1 in cross talk between salicylate and jasmonate signaling. *Plant Physiol* **149**: 1797-1809.
- Levine A, Tenhaken R, Dixon R, Lamb C. 1994. H<sub>2</sub>O<sub>2</sub> from the oxidative burst orchestrates the plant hypersensitive disease resistance response. *Cell* **79**: 583-593.
- Li J, Brader G, Kariola T, Palva ET. 2006. WRKY70 modulates the selection of signaling pathways in plant defense. *Plant J* **46**: 477-491.
- Li J, Brader G, Palva ET. 2004. The WRKY70 transcription factor: a node of convergence for jasmonate-mediated and salicylate-mediated signals in plant defense. *Plant Cell* **16**: 319-331.
- Li T, Chen X, Zhong X, Zhao Y, Liu X, Zhou S, Cheng S, Zhou DX. 2013. Jumonji C domain protein JMJ705-mediated removal of histone H3 lysine 27 trimethylation is involved in defense-related gene activation in rice. *Plant Cell* **25**: 4725-4736.
- Li X, Cai J, Liu F, Dai T, Cao W, Jiang D. 2014. Cold priming drives the sub-cellular antioxidant systems to protect photosynthetic electron transport against subsequent low temperature stress in winter wheat. *Plant Physiol Biochem* **82C**: 34-43.

- Li X, Zhang Y, Clarke JD, Li Y, Dong X. 1999. Identification and cloning of a negative regulator of systemic acquired resistance, SNI1, through a screen for suppressors of npr1-1. *Cell* **98**: 329-339.
- Liebrand TW, van den Berg GC, Zhang Z, Smit P, Cordewener JH, America AH, Sklenar J, Jones AM, Tameling WI, Robatzek S et al. 2013. Receptor-like kinase SOBIR1/EVR interacts with receptor-like proteins in plant immunity against fungal infection. *Proc Natl Acad Sci U S A* **110**: 10010-10015.
- Liebrand TW, van den Burg HA, Joosten MH. 2014. Two for all: receptor-associated kinases SOBIR1 and BAK1. *Trends Plant Sci* **19**: 123-132.
- Liu C, Lu F, Cui X, Cao X. 2010. Histone methylation in higher plants. *Annu Rev Plant Biol* **61**: 395-420.
- Liu N, Fromm M, Avramova Z. 2014. H3K27me3 and H3K4me3 chromatin environment at super-induced dehydration stress memory genes of *Arabidopsis thaliana*. *Mol Plant* **7**: 502-513.
- Liu PP, von Dahl CC, Park SW, Klessig DF. 2011. Interconnection between methyl salicylate and lipid-based long-distance signaling during the development of systemic acquired resistance in *Arabidopsis* and tobacco. *Plant Physiol* **155**: 1762-1768.
- Livak KJ, Schmittgen TD. 2001. Analysis of relative gene expression data using real-time quantitative PCR and the 2(-Delta Delta C(T)) Method. *Methods* **25**: 402-408.
- Logemann E, Birkenbihl RP, Rawat V, Schneeberger K, Schmelzer E, Somssich IE. 2013. Functional dissection of the PROPEP2 and PROPEP3 promoters reveals the importance of WRKY factors in mediating microbe-associated molecular pattern-induced expression. *New Phytol* **198**: 1165-1177.
- Logemann E, Hahlbrock K. 2002. Crosstalk among stress responses in plants: pathogen defense overrides UV protection through an inversely regulated ACE/ACE type of light-responsive gene promoter unit. *Proc Natl Acad Sci U S A* **99**: 2428-2432.
- Lopez-Vernaza M, Yang S, Muller R, Thorpe F, de Leau E, Goodrich J. 2012. Antagonistic roles of SEPALLATA3, FT and FLC genes as targets of the polycomb group gene CURLY LEAF. *PLoS One* **7**: e30715.
- Lu F, Cui X, Zhang S, Jenuwein T, Cao X. 2011. *Arabidopsis* REF6 is a histone H3 lysine 27 demethylase. *Nat Genet* **43**: 715-719.
- Lu F, Cui X, Zhang S, Liu C, Cao X. 2010. JMJ14 is an H3K4 demethylase regulating flowering time in *Arabidopsis*. *Cell Res* **20**: 387-390.
- Lu H. 2009. Dissection of salicylic acid-mediated defense signaling networks. *Plant Signal Behav* **4**: 713-717.
- Lu X, Tintor N, Mentzel T, Kombrink E, Boller T, Robatzek S, Schulze-Lefert P, Saijo Y. 2009. Uncoupling of sustained MAMP receptor signaling from early outputs in an *Arabidopsis* endoplasmic reticulum glucosidase II allele. *Proc Natl Acad Sci U S A* **106**: 22522-22527.
- Luna E, Bruce TJ, Roberts MR, Flors V, Ton J. 2012. Next-generation systemic acquired resistance. *Plant Physiol* **158**: 844-853.
- Luna E, Ton J. 2012. The epigenetic machinery controlling transgenerational systemic acquired resistance. *Plant Signal Behav* **7**: 615-618.
- Ma KW, Flores C, Ma W. 2011. Chromatin configuration as a battlefield in plant-bacteria interactions. *Plant Physiol* **157**: 535-543.
- Macho AP, Schwessinger B, Ntoukakis V, Brutus A, Segonzac C, Roy S, Kadota Y, Oh MH, Sklenar J, Derbyshire P et al. 2014. A bacterial tyrosine phosphatase inhibits plant pattern recognition receptor activation. *Science* **343**: 1509-1512.
- Macho AP, Zipfel C. 2014. Plant PRRs and the activation of innate immune signaling. *Mol Cell* **54**: 263-272.
- Madrigal P, Krajewski P. 2012. Current bioinformatic approaches to identify DNase I hypersensitive sites and genomic footprints from DNase-seq data. *Front Genet* **3**: 230.
- Maekawa T, Kracher B, Vernaldi S, Ver Loren van Themaat E, Schulze-Lefert P. 2012. Conservation of NLR-triggered immunity across plant lineages. *Proc Natl Acad Sci U S A* **109**: 20119-20123.

- Maldonado AM, Doerner P, Dixon RA, Lamb CJ, Cameron RK. 2002. A putative lipid transfer protein involved in systemic resistance signalling in Arabidopsis. *Nature* **419**: 399-403.
- Maleck K, Levine A, Eulgem T, Morgan A, Schmid J, Lawton KA, Dangl JL, Dietrich RA. 2000. The transcriptome of Arabidopsis thaliana during systemic acquired resistance. *Nat Genet* **26**: 403-410.
- Malinovsky FG, Fangel JU, Willats WG. 2014. The role of the cell wall in plant immunity. *Front Plant Sci* **5**: 178.
- Mao G, Meng X, Liu Y, Zheng Z, Chen Z, Zhang S. 2011. Phosphorylation of a WRKY transcription factor by two pathogen-responsive MAPKs drives phytoalexin biosynthesis in Arabidopsis. *Plant Cell* **23**: 1639-1653.
- March-Diaz R, Garcia-Dominguez M, Lozano-Juste J, Leon J, Florencio FJ, Reyes JC. 2008. Histone H2A.Z and homologues of components of the SWR1 complex are required to control immunity in Arabidopsis. *Plant J* **53**: 475-487.
- Margueron R, Reinberg D. 2011. The Polycomb complex PRC2 and its mark in life. *Nature* **469**: 343-349.
- Mauch F, Hadwiger LA, Boller T. 1988a. Antifungal Hydrolases in Pea Tissue : I. Purification and Characterization of Two Chitinases and Two beta-1,3-Glucanases Differentially Regulated during Development and in Response to Fungal Infection. *Plant Physiol* **87**: 325-333.
- Mauch F, Mauch-Mani B, Boller T. 1988b. Antifungal Hydrolases in Pea Tissue : II. Inhibition of Fungal Growth by Combinations of Chitinase and beta-1,3-Glucanase. *Plant Physiol* **88**: 936-942.
- Meagher RB, Mussar KJ. 2012. The Influence of DNA Sequence on Epigenome-Induced Pathologies. *Epigenetics Chromatin* **5**: 11.
- Meier I, Somers DE. 2011. Regulation of nucleocytoplasmic trafficking in plants. *Curr Opin Plant Biol* **14**: 538-546.
- Meng X, Xu J, He Y, Yang KY, Mordorski B, Liu Y, Zhang S. 2013. Phosphorylation of an ERF transcription factor by Arabidopsis MPK3/MPK6 regulates plant defense gene induction and fungal resistance. *Plant Cell* **25**: 1126-1142.
- Meng X, Zhang S. 2013. MAPK cascades in plant disease resistance signaling. *Annu Rev Phytopathol* **51**: 245-266.
- Merchante C, Alonso JM, Stepanova AN. 2013. Ethylene signaling: simple ligand, complex regulation. *Curr Opin Plant Biol* **16**: 554-560.
- Mettraux JP, Signer H, Ryals J, Ward E, Wyss-Benz M, Gaudin J, Raschdorf K, Schmid E, Blum W, Inverardi B. 1990. Increase in salicylic Acid at the onset of systemic acquired resistance in cucumber. *Science* **250**: 1004-1006.
- Meyers BC, Kozik A, Griego A, Kuang H, Michelmore RW. 2003. Genome-wide analysis of NBS-LRR-encoding genes in Arabidopsis. *Plant Cell* **15**: 809-834.
- Milutinovic S, Zhuang Q, Niveleau A, Szyf M. 2003. Epigenomic stress response. Knockdown of DNA methyltransferase 1 triggers an intra-S-phase arrest of DNA replication and induction of stress response genes. *J Biol Chem* **278**: 14985-14995.
- Minocha R, Majumdar R, Minocha SC. 2014. Polyamines and abiotic stress in plants: a complex relationship. *Front Plant Sci* **5**: 175.
- Mirouze M, Paszkowski J. 2011. Epigenetic contribution to stress adaptation in plants. *Curr Opin Plant Biol* **14**: 267-274.
- Mishina TE, Zeier J. 2006. The Arabidopsis flavin-dependent monooxygenase FMO1 is an essential component of biologically induced systemic acquired resistance. *Plant Physiol* **141**: 1666-1675.
- . 2007. Pathogen-associated molecular pattern recognition rather than development of tissue necrosis contributes to bacterial induction of systemic acquired resistance in Arabidopsis. *Plant J* **50**: 500-513.
- Molitor A, Shen WH. 2013. The polycomb complex PRC1: composition and function in plants. *J Genet Genomics* **40**: 231-238.

- Moore JW, Loake GJ, Spoel SH. 2011. Transcription dynamics in plant immunity. *Plant Cell* **23**: 2809-2820.
- Mosher RA, Durrant WE, Wang D, Song J, Dong X. 2006. A comprehensive structure-function analysis of Arabidopsis SNI1 defines essential regions and transcriptional repressor activity. *Plant Cell* **18**: 1750-1765.
- Mou Z, Fan W, Dong X. 2003. Inducers of plant systemic acquired resistance regulate NPR1 function through redox changes. *Cell* **113**: 935-944.
- Mukhtar MS, Nishimura MT, Dangl J. 2009. NPR1 in Plant Defense: It's Not over 'til It's Turned over. *Cell* **137**: 804-806.
- Muthamilarasan M, Prasad M. 2013. Plant innate immunity: an updated insight into defense mechanism. *J Biosci* **38**: 433-449.
- Navarova H, Bernsdorff F, Doring AC, Zeier J. 2012. Pipecolic acid, an endogenous mediator of defense amplification and priming, is a critical regulator of inducible plant immunity. *Plant Cell* **24**: 5123-5141.
- Navarro L, Zipfel C, Rowland O, Keller I, Robatzek S, Boller T, Jones JD. 2004. The transcriptional innate immune response to flg22. Interplay and overlap with Avr gene-dependent defense responses and bacterial pathogenesis. *Plant Physiol* **135**: 1113-1128.
- Ndamukong I, Jones DR, Lapko H, Divecha N, Avramova Z. 2010. Phosphatidylinositol 5-phosphate links dehydration stress to the activity of ARABIDOPSIS TRITHORAX-LIKE factor ATX1. *PLoS One* **5**: e13396.
- Netea MG, Quintin J, van der Meer JW. 2011. Trained immunity: a memory for innate host defense. *Cell Host Microbe* **9**: 355-361.
- Noutoshi Y, Okazaki M, Kida T, Nishina Y, Morishita Y, Ogawa T, Suzuki H, Shibata D, Jikumaru Y, Hanada A et al. 2012. Novel plant immune-priming compounds identified via high-throughput chemical screening target salicylic acid glucosyltransferases in Arabidopsis. *Plant Cell* **24**: 3795-3804.
- Pajerowska-Mukhtar KM, Emerine DK, Mukhtar MS. 2013. Tell me more: roles of NPRs in plant immunity. *Trends Plant Sci* **18**: 402-411.
- Palma K, Thorgrimsen S, Malinovsky FG, Fiil BK, Nielsen HB, Brodersen P, Hofius D, Petersen M, Mundy J. 2010. Autoimmunity in Arabidopsis *acd11* is mediated by epigenetic regulation of an immune receptor. *PLoS Pathog* **6**: e1001137.
- Pandey SP, Somssich IE. 2009. The role of WRKY transcription factors in plant immunity. *Plant Physiol* **150**: 1648-1655.
- Panstruga R, Dodds PN. 2009. Terrific protein traffic: the mystery of effector protein delivery by filamentous plant pathogens. *Science* **324**: 748-750.
- Park JH, Halitschke R, Kim HB, Baldwin IT, Feldmann KA, Feyereisen R. 2002. A knock-out mutation in allene oxide synthase results in male sterility and defective wound signal transduction in Arabidopsis due to a block in jasmonic acid biosynthesis. *Plant J* **31**: 1-12.
- Parker JE, Coleman MJ, Szabo V, Frost LN, Schmidt R, van der Biezen EA, Moores T, Dean C, Daniels MJ, Jones JD. 1997. The Arabidopsis downy mildew resistance gene RPP5 shares similarity to the toll and interleukin-1 receptors with N and L6. *Plant Cell* **9**: 879-894.
- Pastor V, Luna E, Mauch-Mani B, Ton J, Flors V. 2012. Primed Plants do not forget. *Environmental and Experimental Botany*.
- . 2013a. Primed plants do not forget. *Environmental and Experimental Botany* **94**: 46-56.
- Pastor V, Luna E, Ton J, Cerezo M, Garcia-Agustin P, Flors V. 2013b. Fine tuning of reactive oxygen species homeostasis regulates primed immune responses in Arabidopsis. *Mol Plant Microbe Interact* **26**: 1334-1344.
- Pattison RJ, Amtmann A. 2009. N-glycan production in the endoplasmic reticulum of plants. *Trends Plant Sci* **14**: 92-99.
- Pecher P, Eschen-Lippold L, Herklotz S, Kuhle K, Naumann K, Bethke G, Uhrig J, Weyhe M, Scheel D, Lee J. 2014. The Arabidopsis thaliana mitogen-activated protein kinases MPK3 and MPK6 target a

- subclass of 'VQ-motif'-containing proteins to regulate immune responses. *New Phytol* **203**: 592-606.
- Pecinka A, Mittelsten Scheid O. 2012. Stress-induced chromatin changes: a critical view on their heritability. *Plant Cell Physiol* **53**: 801-808.
- Penaloza-Vazquez A, Preston GM, Collmer A, Bender CL. 2000. Regulatory interactions between the Hrp type III protein secretion system and coronatine biosynthesis in *Pseudomonas syringae* pv. tomato DC3000. *Microbiology* **146 ( Pt 10)**: 2447-2456.
- Pien S, Fleury D, Mylne JS, Crevillen P, Inze D, Avramova Z, Dean C, Grossniklaus U. 2008. ARABIDOPSIS TRITHORAX1 dynamically regulates FLOWERING LOCUS C activation via histone 3 lysine 4 trimethylation. *Plant Cell* **20**: 580-588.
- Pien S, Grossniklaus U. 2007. Polycomb group and trithorax group proteins in Arabidopsis. *Biochim Biophys Acta* **1769**: 375-382.
- Pieterse CM, van der Does D, Zamioudis C, Leon-Reyes A, van Wees SC. 2012. Hormonal Modulation of Plant Immunity. *Annu Rev Cell Dev Biol*.
- Pitzschke A, Schikora A, Hirt H. 2009. MAPK cascade signalling networks in plant defence. *Curr Opin Plant Biol* **12**: 421-426.
- Pontvianne F, Blevins T, Pikaard CS. 2010. Arabidopsis Histone Lysine Methyltransferases. *Adv Bot Res* **53**: 1-22.
- Pozo MJ, Azcon-Aguilar C. 2007. Unraveling mycorrhiza-induced resistance. *Curr Opin Plant Biol* **10**: 393-398.
- Pray-Grant MG, Daniel JA, Schieltz D, Yates JR, 3rd, Grant PA. 2005. Chd1 chromodomain links histone H3 methylation with SAGA- and SLIK-dependent acetylation. *Nature* **433**: 434-438.
- Priest HD, Filichkin SA, Mockler TC. 2009. Cis-regulatory elements in plant cell signaling. *Curr Opin Plant Biol* **12**: 643-649.
- Qiu JL, Fiil BK, Petersen K, Nielsen HB, Botanga CJ, Thorgrimsen S, Palma K, Suarez-Rodriguez MC, Sandbech-Clausen S, Lichota J et al. 2008. Arabidopsis MAP kinase 4 regulates gene expression through transcription factor release in the nucleus. *Embo Journal* **27**: 2214-2221.
- Quintin J, Cheng SC, van der Meer JW, Netea MG. 2014. Innate immune memory: towards a better understanding of host defense mechanisms. *Curr Opin Immunol* **29C**: 1-7.
- Rasmann S, De Vos M, Casteel CL, Tian D, Halitschke R, Sun JY, Agrawal AA, Felton GW, Jander G. 2012. Herbivory in the previous generation primes plants for enhanced insect resistance. *Plant Physiol* **158**: 854-863.
- Rasmussen MW, Roux M, Petersen M, Mundy J. 2012. MAP Kinase Cascades in Arabidopsis Innate Immunity. *Front Plant Sci* **3**: 169.
- Rate DN, Greenberg JT. 2001. The Arabidopsis aberrant growth and death2 mutant shows resistance to *Pseudomonas syringae* and reveals a role for NPR1 in suppressing hypersensitive cell death. *Plant J* **27**: 203-211.
- Rea S, Eisenhaber F, O'Carroll D, Strahl BD, Sun ZW, Schmid M, Opravil S, Mechtler K, Ponting CP, Allis CD et al. 2000. Regulation of chromatin structure by site-specific histone H3 methyltransferases. *Nature* **406**: 593-599.
- Ren CM, Zhu Q, Gao BD, Ke SY, Yu WC, Xie DX, Peng W. 2008. Transcription factor WRKY70 displays important but no indispensable roles in jasmonate and salicylic acid signaling. *J Integr Plant Biol* **50**: 630-637.
- Riechmann JL, Heard J, Martin G, Reuber L, Jiang C, Keddie J, Adam L, Pineda O, Ratcliffe OJ, Samaha RR et al. 2000. Arabidopsis transcription factors: genome-wide comparative analysis among eukaryotes. *Science* **290**: 2105-2110.
- Rietz S, Stamm A, Malonek S, Wagner S, Becker D, Medina-Escobar N, Vlot AC, Feys BJ, Niefind K, Parker JE. 2011. Different roles of Enhanced Disease Susceptibility1 (EDS1) bound to and dissociated from Phytoalexin Deficient4 (PAD4) in Arabidopsis immunity. *New Phytol* **191**: 107-119.

- Robatzek S, Wirthmueller L. 2013. Mapping FLS2 function to structure: LRRs, kinase and its working bits. *Protoplasma* **250**: 671-681.
- Robert-Seilaniantz A, Grant M, Jones JD. 2011. Hormone crosstalk in plant disease and defense: more than just jasmonate-salicylate antagonism. *Annu Rev Phytopathol* **49**: 317-343.
- Roine E, Wei W, Yuan J, Nurmiaho-Lassila EL, Kalkkinen N, Romantschuk M, He SY. 1997. Hrp pilus: an hrp-dependent bacterial surface appendage produced by *Pseudomonas syringae* pv. tomato DC3000. *Proc Natl Acad Sci U S A* **94**: 3459-3464.
- Romeis T, Herde M. 2014. From local to global: CDPKs in systemic defense signaling upon microbial and herbivore attack. *Curr Opin Plant Biol* **20C**: 1-10.
- Ross A, Yamada K, Hiruma K, Yamashita-Yamada M, Lu X, Takano Y, Tsuda K, Saijo Y. 2014. The Arabidopsis PEPR pathway couples local and systemic plant immunity. *EMBO J* **33**: 62-75.
- Ross AF. 1961a. Localized acquired resistance to plant virus infection in hypersensitive hosts. *Virology* **14**: 329-339.
- 1961b. Systemic acquired resistance induced by localized virus infections in plants. *Virology* **14**: 340-358.
- Roudier F, Ahmed I, Berard C, Sarazin A, Mary-Huard T, Cortijo S, Bouyer D, Caillieux E, Duvernois-Berthet E, Al-Shikhley L et al. 2011. Integrative epigenomic mapping defines four main chromatin states in Arabidopsis. *EMBO J* **30**: 1928-1938.
- Roudier F, Teixeira FK, Colot V. 2009. Chromatin indexing in Arabidopsis: an epigenomic tale of tails and more. *Trends Genet* **25**: 511-517.
- Rozen S, Skaletsky H. 2000. Primer3 on the WWW for general users and for biologist programmers. *Methods Mol Biol* **132**: 365-386.
- Sachs M, Onodera C, Blaschke K, Ebata KT, Song JS, Ramalho-Santos M. 2013. Bivalent chromatin marks developmental regulatory genes in the mouse embryonic germline in vivo. *Cell Rep* **3**: 1777-1784.
- Saijo Y, Tintor N, Lu X, Rauf P, Pajeroska-Mukhtar K, Haweker H, Dong X, Robatzek S, Schulze-Lefert P. 2009. Receptor quality control in the endoplasmic reticulum for plant innate immunity. *EMBO J* **28**: 3439-3449.
- Saleh A, Al-Abdallat A, Ndamukong I, Alvarez-Venegas R, Avramova Z. 2007. The Arabidopsis homologs of trithorax (ATX1) and enhancer of zeste (CLF) establish 'bivalent chromatin marks' at the silent AGAMOUS locus. *Nucleic Acids Res* **35**: 6290-6296.
- Saleh A, Alvarez-Venegas R, Avramova Z. 2008a. Dynamic and stable histone H3 methylation patterns at the Arabidopsis FLC and AP1 loci. *Gene* **423**: 43-47.
- Saleh A, Alvarez-Venegas R, Yilmaz M, Le O, Hou G, Sadler M, Al-Abdallat A, Xia Y, Lu G, Ladunga I et al. 2008b. The highly similar Arabidopsis homologs of trithorax ATX1 and ATX2 encode proteins with divergent biochemical functions. *Plant Cell* **20**: 568-579.
- Sang Y, Wu MF, Wagner D. 2009. The stem cell--chromatin connection. *Semin Cell Dev Biol* **20**: 1143-1148.
- Sani E, Herzyk P, Perrella G, Colot V, Amtmann A. 2013. Hyperosmotic priming of Arabidopsis seedlings establishes a long-term somatic memory accompanied by specific changes of the epigenome. *Genome Biol* **14**: R59.
- Schenke D, Bottcher C, Scheel D. 2011. Crosstalk between abiotic ultraviolet-B stress and biotic (flg22) stress signalling in Arabidopsis prevents flavonol accumulation in favor of pathogen defence compound production. *Plant Cell Environ* **34**: 1849-1864.
- Schenke D, Cai D. 2014. The interplay of transcription factors in suppression of UV-B induced flavonol accumulation by flg22. *Plant Signal Behav* **9**.
- Schenke D, Cai D, Scheel D. 2014. Suppression of UV-B stress responses by flg22 is regulated at the chromatin level via histone modification. *Plant Cell Environ*.
- Schmitges FW, Prusty AB, Faty M, Stutzer A, Lingaraju GM, Aiwezian J, Sack R, Hess D, Li L, Zhou S et al. 2011. Histone methylation by PRC2 is inhibited by active chromatin marks. *Mol Cell* **42**: 330-341.

- Schubert D, Clarenz O, Goodrich J. 2005. Epigenetic control of plant development by Polycomb-group proteins. *Curr Opin Plant Biol* **8**: 553-561.
- Schubert D, Primavesi L, Bishopp A, Roberts G, Doonan J, Jenuwein T, Goodrich J. 2006. Silencing by plant Polycomb-group genes requires dispersed trimethylation of histone H3 at lysine 27. *EMBO J* **25**: 4638-4649.
- Schuettengruber B, Chourrout D, Vervoort M, Leblanc B, Cavalli G. 2007. Genome regulation by polycomb and trithorax proteins. *Cell* **128**: 735-745.
- Schuettengruber B, Martinez AM, Iovino N, Cavalli G. 2011. Trithorax group proteins: switching genes on and keeping them active. *Nat Rev Mol Cell Biol* **12**: 799-814.
- Schwammle V, Aspalter CM, Sidoli S, Jensen ON. 2014. Large Scale Analysis of Co-existing Post-translational Modifications in Histone Tails Reveals Global Fine Structure of Cross-talk. *Mol Cell Proteomics* **13**: 1855-1865.
- Schwartz YB, Pirrotta V. 2007. Polycomb silencing mechanisms and the management of genomic programmes. *Nat Rev Genet* **8**: 9-22.
- Searle I, He Y, Turck F, Vincent C, Fornara F, Krober S, Amasino RA, Coupland G. 2006. The transcription factor FLC confers a flowering response to vernalization by repressing meristem competence and systemic signaling in Arabidopsis. *Genes Dev* **20**: 898-912.
- Segonzac C, Zipfel C. 2011. Activation of plant pattern-recognition receptors by bacteria. *Curr Opin Microbiol* **14**: 54-61.
- Serrano M, Kanehara K, Torres M, Yamada K, Tintor N, Kombrink E, Schulze-Lefert P, Saijo Y. 2012. Repression of sucrose/ultraviolet B light-induced flavonoid accumulation in microbe-associated molecular pattern-triggered immunity in Arabidopsis. *Plant Physiol* **158**: 408-422.
- Shafiq S, Berr A, Shen WH. 2014. Combinatorial functions of diverse histone methylations in Arabidopsis thaliana flowering time regulation. *New Phytol* **201**: 312-322.
- Shah J, Chaturvedi R, Chowdhury Z, Venables B, Petros RA. 2014. Signaling by small metabolites in systemic acquired resistance. *Plant J*.
- Shah J, Tsui F, Klessig DF. 1997. Characterization of a salicylic acid-insensitive mutant (sai1) of Arabidopsis thaliana, identified in a selective screen utilizing the SA-inducible expression of the tms2 gene. *Mol Plant Microbe Interact* **10**: 69-78.
- Shah J, Zeier J. 2013. Long-distance communication and signal amplification in systemic acquired resistance. *Front Plant Sci* **4**: 30.
- Shearer HL, Cheng YT, Wang L, Liu J, Boyle P, Despres C, Zhang Y, Li X, Fobert PR. 2012. Arabidopsis clade I TGA transcription factors regulate plant defenses in an NPR1-independent fashion. *Mol Plant Microbe Interact* **25**: 1459-1468.
- Shi Y, Lan F, Matson C, Mulligan P, Whetstone JR, Cole PA, Casero RA, Shi Y. 2004. Histone demethylation mediated by the nuclear amine oxidase homolog LSD1. *Cell* **119**: 941-953.
- Shim JS, Choi YD. 2013. Direct regulation of WRKY70 by AtMYB44 in plant defense responses. *Plant Signal Behav* **8**: e20783.
- Shim JS, Jung C, Lee S, Min K, Lee YW, Choi Y, Lee JS, Song JT, Kim JK, Choi YD. 2013. AtMYB44 regulates WRKY70 expression and modulates antagonistic interaction between salicylic acid and jasmonic acid signaling. *Plant J* **73**: 483-495.
- Shoresh M, Harman GE, Mastouri F. 2010. Induced systemic resistance and plant responses to fungal biocontrol agents. *Annu Rev Phytopathol* **48**: 21-43.
- Simon JA, Tamkun JW. 2002. Programming off and on states in chromatin: mechanisms of Polycomb and trithorax group complexes. *Curr Opin Genet Dev* **12**: 210-218.
- Sims RJ, 3rd, Millhouse S, Chen CF, Lewis BA, Erdjument-Bromage H, Tempst P, Manley JL, Reinberg D. 2007. Recognition of trimethylated histone H3 lysine 4 facilitates the recruitment of transcription postinitiation factors and pre-mRNA splicing. *Mol Cell* **28**: 665-676.
- Sims RJ, 3rd, Reinberg D. 2006. Histone H3 Lys 4 methylation: caught in a bind? *Genes Dev* **20**: 2779-2786.

- Sims RJ, 3rd, Trojer P, Li G, Reinberg D. 2006. Methods to identify and functionally analyze factors that specifically recognize histone lysine methylation. *Methods* **40**: 331-338.
- Singh P, Yekondi S, Chen PW, Tsai CH, Yu CW, Wu K, Zimmerli L. 2014a. Environmental History Modulates Arabidopsis Pattern-Triggered Immunity in a HISTONE ACETYLTRANSFERASE1-Dependent Manner. *Plant Cell*.
- Singh V, Roy S, Giri MK, Chaturvedi R, Chowdhury Z, Shah J, Nandi AK. 2013. Arabidopsis thaliana FLOWERING LOCUS D is required for systemic acquired resistance. *Mol Plant Microbe Interact* **26**: 1079-1088.
- Singh V, Roy S, Singh D, Nandi AK. 2014b. Arabidopsis FLOWERING LOCUS D influences systemic-acquired-resistance-induced expression and histone modifications of WRKY genes. *Journal of Biosciences* **39**: 119-126.
- Slaughter A, Daniel X, Flors V, Luna E, Hohn B, Mauch-Mani B. 2012. Descendants of primed Arabidopsis plants exhibit resistance to biotic stress. *Plant Physiol* **158**: 835-843.
- Slootweg E, Roosien J, Spiridon LN, Petrescu AJ, Tameling W, Joosten M, Pomp R, van Schaik C, Dees R, Borst JW et al. 2010. Nucleocytoplasmic distribution is required for activation of resistance by the potato NB-LRR receptor Rx1 and is balanced by its functional domains. *Plant Cell* **22**: 4195-4215.
- Song JT, Lu H, McDowell JM, Greenberg JT. 2004. A key role for ALD1 in activation of local and systemic defenses in Arabidopsis. *Plant J* **40**: 200-212.
- Spoel SH, Dong X. 2008. Making sense of hormone crosstalk during plant immune responses. *Cell Host Microbe* **3**: 348-351.
- . 2012. How do plants achieve immunity? Defence without specialized immune cells. *Nat Rev Immunol* **12**: 89-100.
- Spoel SH, Koornneef A, Claessens SM, Korzelius JP, Van Pelt JA, Mueller MJ, Buchala AJ, Mettraux JP, Brown R, Kazan K et al. 2003. NPR1 modulates cross-talk between salicylate- and jasmonate-dependent defense pathways through a novel function in the cytosol. *Plant Cell* **15**: 760-770.
- Spoel SH, Mou Z, Tada Y, Spivey NW, Genschik P, Dong X. 2009. Proteasome-mediated turnover of the transcription coactivator NPR1 plays dual roles in regulating plant immunity. *Cell* **137**: 860-872.
- Sticher L, MauchMani B, Mettraux JP. 1997. Systemic acquired resistance. *Annual Review of Phytopathology* **35**: 235-270.
- Strahl BD, Allis CD. 2000. The language of covalent histone modifications. *Nature* **403**: 41-45.
- Strange RN, Scott PR. 2005. Plant disease: a threat to global food security. *Annu Rev Phytopathol* **43**: 83-116.
- Sukegawa Y, Yamashita A, Yamamoto M. 2011. The fission yeast stress-responsive MAPK pathway promotes meiosis via the phosphorylation of Pol II CTD in response to environmental and feedback cues. *PLoS Genet* **7**: e1002387.
- Sun JQ, Jiang HL, Li CY. 2011. Systemin/Jasmonate-mediated systemic defense signaling in tomato. *Mol Plant* **4**: 607-615.
- Swiezewski S, Crevillen P, Liu F, Ecker JR, Jerzmanowski A, Dean C. 2007. Small RNA-mediated chromatin silencing directed to the 3' region of the Arabidopsis gene encoding the developmental regulator, FLC. *Proc Natl Acad Sci U S A* **104**: 3633-3638.
- Tamada Y, Yun JY, Woo SC, Amasino RM. 2009. ARABIDOPSIS TRITHORAX-RELATED7 is required for methylation of lysine 4 of histone H3 and for transcriptional activation of FLOWERING LOCUS C. *Plant Cell* **21**: 3257-3269.
- Tao Y, Xie Z, Chen W, Glazebrook J, Chang HS, Han B, Zhu T, Zou G, Katagiri F. 2003. Quantitative nature of Arabidopsis responses during compatible and incompatible interactions with the bacterial pathogen *Pseudomonas syringae*. *Plant Cell* **15**: 317-330.
- Tena G, Boudsocq M, Sheen J. 2011. Protein kinase signaling networks in plant innate immunity. *Curr Opin Plant Biol* **14**: 519-529.

- Teng S, Keurentjes J, Bentsink L, Koornneef M, Smeekens S. 2005. Sucrose-specific induction of anthocyanin biosynthesis in *Arabidopsis* requires the MYB75/PAP1 gene. *Plant physiology* **139**: 1840-1852.
- Thellier M, Luttge U. 2013. Plant memory: a tentative model. *Plant Biol (Stuttg)* **15**: 1-12.
- Thilmony R, Underwood W, He SY. 2006. Genome-wide transcriptional analysis of the *Arabidopsis thaliana* interaction with the plant pathogen *Pseudomonas syringae* pv. tomato DC3000 and the human pathogen *Escherichia coli* O157:H7. *Plant J* **46**: 34-53.
- Thomma BP, Nurnberger T, Joosten MH. 2011. Of PAMPs and effectors: the blurred PTI-ETI dichotomy. *Plant Cell* **23**: 4-15.
- Thordal-Christensen H. 2003. Fresh insights into processes of nonhost resistance. *Curr Opin Plant Biol* **6**: 351-357.
- Thorstensen T, Grini PE, Aalen RB. 2011. SET domain proteins in plant development. *Biochim Biophys Acta* **1809**: 407-420.
- Thulke O, Conrath U. 1998. Salicylic acid has a dual role in the activation of defence-related genes in parsley. *Plant J* **14**: 35-42.
- Tian D, Traw MB, Chen JQ, Kreitman M, Bergelson J. 2003. Fitness costs of R-gene-mediated resistance in *Arabidopsis thaliana*. *Nature* **423**: 74-77.
- Tintor N, Ross A, Kanehara K, Yamada K, Fan L, Kemmerling B, Nurnberger T, Tsuda K, Saijo Y. 2013. Layered pattern receptor signaling via ethylene and endogenous elicitor peptides during *Arabidopsis* immunity to bacterial infection. *Proc Natl Acad Sci U S A* **110**: 6211-6216.
- To TK, Kim JM. 2014. Epigenetic regulation of gene responsiveness in. *Front Plant Sci* **4**: 548.
- Ton J, Jakab G, Toquin V, Flors V, Iavicoli A, Maeder MN, Mettraux JP, Mauch-Mani B. 2005. Dissecting the beta-aminobutyric acid-induced priming phenomenon in *Arabidopsis*. *Plant Cell* **17**: 987-999.
- Traverse S, Gomez N, Paterson H, Marshall C, Cohen P. 1992. Sustained activation of the mitogen-activated protein (MAP) kinase cascade may be required for differentiation of PC12 cells. Comparison of the effects of nerve growth factor and epidermal growth factor. *Biochem J* **288 (Pt 2)**: 351-355.
- Truman W, Bennett MH, Kubigsteltig I, Turnbull C, Grant M. 2007. *Arabidopsis* systemic immunity uses conserved defense signaling pathways and is mediated by jasmonates. *Proc Natl Acad Sci U S A* **104**: 1075-1080.
- Tsuda K, Katagiri F. 2010. Comparing signaling mechanisms engaged in pattern-triggered and effector-triggered immunity. *Curr Opin Plant Biol* **13**: 459-465.
- Tsuda K, Mine A, Bethke G, Igarashi D, Botanga CJ, Tsuda Y, Glazebrook J, Sato M, Katagiri F. 2013. Dual regulation of gene expression mediated by extended MAPK activation and salicylic acid contributes to robust innate immunity in *Arabidopsis thaliana*. *PLoS Genet* **9**: e1004015.
- Tsuda K, Sato M, Glazebrook J, Cohen JD, Katagiri F. 2008. Interplay between MAMP-triggered and SA-mediated defense responses. *Plant J* **53**: 763-775.
- Tsuda K, Sato M, Stoddard T, Glazebrook J, Katagiri F. 2009. Network properties of robust immunity in plants. *PLoS Genet* **5**: e1000772.
- Turck F, Roudier F, Farrona S, Martin-Magniette ML, Guillaume E, Buisine N, Gagnot S, Martienssen RA, Coupland G, Colot V. 2007. *Arabidopsis* TFL2/LHP1 specifically associates with genes marked by trimethylation of histone H3 lysine 27. *PLoS Genet* **3**: e86.
- Tuzun S, Kuc J. 1985. Movement of a Factor in Tobacco Infected with *Peronospora-Tabacina* Adam Which Systemically Protects against Blue Mold. *Physiological Plant Pathology* **26**: 321-330.
- Uknes S, Mauch-Mani B, Moyer M, Potter S, Williams S, Dincher S, Chandler D, Slusarenko A, Ward E, Ryals J. 1992. Acquired resistance in *Arabidopsis*. *Plant Cell* **4**: 645-656.
- Vaillant I, Paszkowski J. 2007. Role of histone and DNA methylation in gene regulation. *Curr Opin Plant Biol* **10**: 528-533.

- van den Burg HA, Takken FL. 2009. Does chromatin remodeling mark systemic acquired resistance? *Trends Plant Sci* **14**: 286-294.
- van der Biezen EA, Freddie CT, Kahn K, Parker JE, Jones JD. 2002. Arabidopsis RPP4 is a member of the RPP5 multigene family of TIR-NB-LRR genes and confers downy mildew resistance through multiple signalling components. *Plant J* **29**: 439-451.
- Van der Ent S, Van Hulten M, Pozo MJ, Czechowski T, Udvardi MK, Pieterse CM, Ton J. 2009. Priming of plant innate immunity by rhizobacteria and beta-aminobutyric acid: differences and similarities in regulation. *New Phytol* **183**: 419-431.
- van Hulten M, Pelsler M, van Loon LC, Pieterse CM, Ton J. 2006. Costs and benefits of priming for defense in Arabidopsis. *Proc Natl Acad Sci U S A* **103**: 5602-5607.
- van Loon LC, Rep M, Pieterse CM. 2006. Significance of inducible defense-related proteins in infected plants. *Annu Rev Phytopathol* **44**: 135-162.
- Vernooij B, Friedrich L, Morse A, Reist R, Kolditz-Jawhar R, Ward E, Uknes S, Kessmann H, Ryals J. 1994a. Salicylic Acid Is Not the Translocated Signal Responsible for Inducing Systemic Acquired Resistance but Is Required in Signal Transduction. *Plant Cell* **6**: 959-965.
- Vernooij B, Uknes S, Ward E, Ryals J. 1994b. Salicylic acid as a signal molecule in plant-pathogen interactions. *Curr Opin Cell Biol* **6**: 275-279.
- Verrier L, Vandromme M, Trouche D. 2011. Histone demethylases in chromatin cross-talks. *Biol Cell* **103**: 381-401.
- Walley JW, Rowe HC, Xiao Y, Chehab EW, Kliebenstein DJ, Wagner D, Dehesh K. 2008. The chromatin remodeler SPLAYED regulates specific stress signaling pathways. *PLoS Pathog* **4**: e1000237.
- Wang C, Gao F, Wu J, Dai J, Wei C, Li Y. 2010. Arabidopsis putative deacetylase AtSRT2 regulates basal defense by suppressing PAD4, EDS5 and SID2 expression. *Plant Cell Physiol* **51**: 1291-1299.
- Wang D, Amornsiripanitch N, Dong X. 2006. A genomic approach to identify regulatory nodes in the transcriptional network of systemic acquired resistance in plants. *PLoS Pathog* **2**: e123.
- Wang D, Weaver ND, Kesarwani M, Dong X. 2005. Induction of protein secretory pathway is required for systemic acquired resistance. *Science* **308**: 1036-1040.
- Wang W, Barnaby JY, Tada Y, Li H, Tor M, Caldelari D, Lee DU, Fu XD, Dong X. 2011. Timing of plant immune responses by a central circadian regulator. *Nature* **470**: 110-114.
- Wang Y, An C, Zhang X, Yao J, Zhang Y, Sun Y, Yu F, Amador DM, Mou Z. 2013. The Arabidopsis elongator complex subunit2 epigenetically regulates plant immune responses. *Plant Cell* **25**: 762-776.
- Wasternack C, Forner S, Strnad M, Hause B. 2013. Jasmonates in flower and seed development. *Biochimie* **95**: 79-85.
- Wasternack C, Hause B. 2013. Jasmonates: biosynthesis, perception, signal transduction and action in plant stress response, growth and development. An update to the 2007 review in Annals of Botany. *Ann Bot* **111**: 1021-1058.
- Wei W, Plovianich-Jones A, Deng WL, Jin QL, Collmer A, Huang HC, He SY. 2000. The gene coding for the Hrp pilus structural protein is required for type III secretion of Hrp and Avr proteins in *Pseudomonas syringae* pv. tomato. *Proc Natl Acad Sci U S A* **97**: 2247-2252.
- Weigel D, Colot V. 2012. Epialleles in plant evolution. *Genome Biol* **13**: 249.
- Weigel RR, Bauscher C, Pfitzner AJ, Pfitzner UM. 2001. NIMIN-1, NIMIN-2 and NIMIN-3, members of a novel family of proteins from Arabidopsis that interact with NPR1/NIM1, a key regulator of systemic acquired resistance in plants. *Plant Mol Biol* **46**: 143-160.
- Weigel RR, Pfitzner UM, Gatz C. 2005. Interaction of NIMIN1 with NPR1 modulates PR gene expression in Arabidopsis. *Plant Cell* **17**: 1279-1291.
- Wiermer M, Feys BJ, Parker JE. 2005. Plant immunity: the EDS1 regulatory node. *Curr Opin Plant Biol* **8**: 383-389.
- Wildermuth MC, Dewdney J, Wu G, Ausubel FM. 2001. Isochorismate synthase is required to synthesize salicylic acid for plant defence. *Nature* **414**: 562-565.

- Winter D, Vinegar B, Nahal H, Ammar R, Wilson GV, Provart NJ. 2007. An "Electronic Fluorescent Pictograph" browser for exploring and analyzing large-scale biological data sets. *PLoS One* **2**: e718.
- Wright CA, Beattie GA. 2004. Pseudomonas syringae pv. tomato cells encounter inhibitory levels of water stress during the hypersensitive response of Arabidopsis thaliana. *Proc Natl Acad Sci U S A* **101**: 3269-3274.
- Wu Y, Zhang D, Chu JY, Boyle P, Wang Y, Brindle ID, De Luca V, Despres C. 2012. The Arabidopsis NPR1 protein is a receptor for the plant defense hormone salicylic acid. *Cell Rep* **1**: 639-647.
- Xia S, Cheng YT, Huang S, Win J, Soards A, Jinn TL, Jones JD, Kamoun S, Chen S, Zhang Y et al. 2013. Regulation of transcription of nucleotide-binding leucine-rich repeat-encoding genes SNC1 and RPP4 via H3K4 trimethylation. *Plant Physiol* **162**: 1694-1705.
- Yamaguchi Y, Huffaker A. 2011. Endogenous peptide elicitors in higher plants. *Curr Opin Plant Biol* **14**: 351-357.
- Yan S, Wang W, Marques J, Mohan R, Saleh A, Durrant WE, Song J, Dong X. 2013. Salicylic acid activates DNA damage responses to potentiate plant immunity. *Mol Cell* **52**: 602-610.
- Yang H, Howard M, Dean C. 2014. Antagonistic Roles for H3K36me3 and H3K27me3 in the Cold-Induced Epigenetic Switch at Arabidopsis FLC. *Curr Biol*.
- Yi H, Richards EJ. 2007. A cluster of disease resistance genes in Arabidopsis is coordinately regulated by transcriptional activation and RNA silencing. *Plant Cell* **19**: 2929-2939.
- . 2009. Gene duplication and hypermutation of the pathogen Resistance gene SNC1 in the Arabidopsis bal variant. *Genetics* **183**: 1227-1234.
- Yu CW, Liu X, Luo M, Chen C, Lin X, Tian G, Lu Q, Cui Y, Wu K. 2011. HISTONE DEACETYLASE6 interacts with FLOWERING LOCUS D and regulates flowering in Arabidopsis. *Plant Physiol* **156**: 173-184.
- Zeng L, Velasquez AC, Munkvold KR, Zhang J, Martin GB. 2012. A tomato LysM receptor-like kinase promotes immunity and its kinase activity is inhibited by AvrPtoB. *Plant J* **69**: 92-103.
- Zhang C, Xie Q, Anderson RG, Ng G, Seitz NC, Peterson T, McClung CR, McDowell JM, Kong D, Kwak JM et al. 2013a. Crosstalk between the circadian clock and innate immunity in Arabidopsis. *PLoS Pathog* **9**: e1003370.
- Zhang W, Fraiture M, Kolb D, Loffelhardt B, Desaki Y, Boutrot FF, Tor M, Zipfel C, Gust AA, Brunner F. 2013b. Arabidopsis receptor-like protein30 and receptor-like kinase suppressor of BIR1-1/EVERSHED mediate innate immunity to necrotrophic fungi. *Plant Cell* **25**: 4227-4241.
- Zhang X. 2008. The epigenetic landscape of plants. *Science* **320**: 489-492.
- Zhang X, Bernatavichute YV, Cokus S, Pellegrini M, Jacobsen SE. 2009. Genome-wide analysis of mono-, di- and trimethylation of histone H3 lysine 4 in Arabidopsis thaliana. *Genome Biol* **10**: R62.
- Zhang X, Clarenz O, Cokus S, Bernatavichute YV, Pellegrini M, Goodrich J, Jacobsen SE. 2007. Whole-genome analysis of histone H3 lysine 27 trimethylation in Arabidopsis. *PLoS Biol* **5**: e129.
- Zhang X, Wang C, Zhang Y, Sun Y, Mou Z. 2012. The Arabidopsis mediator complex subunit16 positively regulates salicylate-mediated systemic acquired resistance and jasmonate/ethylene-induced defense pathways. *Plant Cell* **24**: 4294-4309.
- Zhang Y, Goritschnig S, Dong X, Li X. 2003a. A gain-of-function mutation in a plant disease resistance gene leads to constitutive activation of downstream signal transduction pathways in suppressor of npr1-1, constitutive 1. *Plant Cell* **15**: 2636-2646.
- Zhang Y, Reinberg D. 2001. Transcription regulation by histone methylation: interplay between different covalent modifications of the core histone tails. *Genes Dev* **15**: 2343-2360.
- Zhang Y, Tessaro MJ, Lassner M, Li X. 2003b. Knockout analysis of Arabidopsis transcription factors TGA2, TGA5, and TGA6 reveals their redundant and essential roles in systemic acquired resistance. *Plant Cell* **15**: 2647-2653.
- Zhang Y, Xu S, Ding P, Wang D, Cheng YT, He J, Gao M, Xu F, Li Y, Zhu Z et al. 2010. Control of salicylic acid synthesis and systemic acquired resistance by two members of a plant-specific family of transcription factors. *Proc Natl Acad Sci U S A* **107**: 18220-18225.

- Zheng XY, Spivey NW, Zeng W, Liu PP, Fu ZQ, Klessig DF, He SY, Dong X. 2012. Coronatine promotes *Pseudomonas syringae* virulence in plants by activating a signaling cascade that inhibits salicylic acid accumulation. *Cell Host Microbe* **11**: 587-596.
- Zhou N, Tootle TL, Glazebrook J. 1999. Arabidopsis PAD3, a gene required for camalexin biosynthesis, encodes a putative cytochrome P450 monooxygenase. *Plant Cell* **11**: 2419-2428.
- Zhu Z, An F, Feng Y, Li P, Xue L, A M, Jiang Z, Kim JM, To TK, Li W et al. 2011. Derepression of ethylene-stabilized transcription factors (EIN3/EIL1) mediates jasmonate and ethylene signaling synergy in Arabidopsis. *Proc Natl Acad Sci U S A* **108**: 12539-12544.
- Zimmerli L, Jakab G, Mettraux JP, Mauch-Mani B. 2000. Potentiation of pathogen-specific defense mechanisms in Arabidopsis by beta -aminobutyric acid. *Proc Natl Acad Sci U S A* **97**: 12920-12925.
- Zipfel C, Kunze G, Chinchilla D, Caniard A, Jones JD, Boller T, Felix G. 2006. Perception of the bacterial PAMP EF-Tu by the receptor EFR restricts Agrobacterium-mediated transformation. *Cell* **125**: 749-760.
- Zipfel C, Robatzek S, Navarro L, Oakeley EJ, Jones JD, Felix G, Boller T. 2004. Bacterial disease resistance in Arabidopsis through flagellin perception. *Nature* **428**: 764-767.
- Zou B, Yang DL, Shi Z, Dong H, Hua J. 2014. Monoubiquitination of Histone 2B at the disease resistance gene locus regulates its expression and impacts immune responses in Arabidopsis. *Plant Physiol.*
- Zougrafou, T. 2013 Distinct impact of CURLY LEAF and SWINGER on the Arabidopsis Histone H3 Lysine 27 trimethylation pattern is linked to the underlying genetic code. Inaugural Dissertation, Universität zu Köln.
- [https://www.mcdb.ucla.edu/Research/Jacobsen/LabWebSite/P\\_EpigenomicsData.php](https://www.mcdb.ucla.edu/Research/Jacobsen/LabWebSite/P_EpigenomicsData.php)



## Abbreviations

%	percent
(v/v)	volume per volume
(w/v)	weight per volume
°C	Celsius temperature
μ	micro
A	Ampere
ABA	abscisic acid
ac	acetylation
<i>acd11</i>	<i>accelerated cell death 11</i>
AG	AGAMOUS
AGI	<i>Arabidopsis</i> genome initiative
ALD1	AGD2-LIKE DEFENSE RESPONSE PROTEIN 1
ANOVA	analysis of variance
APS	ammonium persulfate
Ash2L	absent, small, or homeotic-like
ATP	adenosine triphosphate
ATX1	HOMOLOG OF TRITHORAX 1
ATXR	ATX-related
Avr	avirulence
AzA	azelaic acid
BABA	b-amino butyric acid
BON1	BONZAI 1
bp	base pair(s)
BRM	BRAHMA
BSA	bovine serum albumin
BTH	acibenzolar-S-methyl
CC	coiled-coil
cDNA	copied DNA
CDPK	calcium-dependent protein kinase
CFP1	CXXC finger protein 1
cfu	colony forming unit
ChIP	chromatin immunoprecipitation
CHS	CHALCONE SYNTHASE
CLF	CURLY LEAF
CMT1	CHROMOMETHYLASE 1
Col-0	Columbia-0
<i>cpr1</i>	<i>constitutive expressor of PR genes 1</i>
CRK39	CYSTEINE-RICH RLK 39
CS	chromatin state
CUL3	cullin-based
DA	abietane diterpenoid dehydroabietinal
DAMP	danger-associated molecular pattern
dCBP	Drosophila CREB-binding protein
DDE1	DELAYED DEHISCENCE 1

## Abbreviations

---

DDM1	DECREASED DNA METHYLATION 1
DIR1	DEFECTIVE IN INDUCED RESISTANCE 1
DMSO	dimethyl sulfoxide
DNA	deoxyribonucleic acid
dNTP	deoxynucleosidetriphosphate
DOC	sodium deoxycholate
dpi	day(s) post inoculation
Dpy30	dosage compensation-related protein 30
DRM1	DOMAINS REARRANGED METHYLASE 1
<i>Drosophila</i>	<i>Drosophila melanogaster</i>
DTT	dithiothreitol
E(z)	Enhancer of Zeste
ECL	enhanced chemi-luminescence
<i>edr1</i>	<i>enhanced disease resistance 1</i>
EDS1	ENHANCED DISEASE SUSCEPTIBILITY 1
EDTA	ethylenediaminetetraacetic acid
EFR	EFR-TU RECEPTOR
EF-Tu	elongation factor Tu
ELP2	Elongator complex subunit 2
EMF	EMBRYONIC FLOWER
ER	endoplasmatic-reticulum
ERQC	ER quality control
Esc	Extra Sex Combs
ET	ethylene
ETI	effector-triggered immunity
ETS	effector-triggered susceptibility
EVR	EVERSHED
f. sp.	forma specialis
F3'H	FLAVANONE 3-HYDROXYLASE
FC	fold change
FDR	false discovery rate
FIE	FERTILIZATION INDEPENDENT ENDOSPERM
FIS2	FERTILIZATION INDEPENDENT SEEDS 2
FLC	FLOWERING LOCUS C
FLD	FLOWERING LOCUS D
flg	flagellin
FLS2	FLAGELLIN SENSING 2
FMO1	FLAVIN-DEPENDENT MONOOXYGENASE 1
g	gram
<i>g</i>	gravity constant (9.81 ms <sup>-1</sup> )
G3P	glycerol-3-phosphate
GFP	green fluorescent protein
gFW	gram fresh weight
GO	gene ontology
H	histone
h	hour

---

H2Aub1	H2A monoubiquitination
HA	hemagglutinin
<i>hac1-1</i>	<i>histone acetyltransferase 1-1</i>
HCl	hydrochloric acid
HDA19	HISTONE DEACYTELASE 19
HMT	histone methyltransferase
<i>Hpa</i>	<i>Hyaloperonospora arabidopsidis</i>
hpi	hour(s) post inoculation
hpt	hour(s) post transcription
HR	hypersensitive response
ICS1	ISOCHORISMATE SYNTHASE 1
ISR	induced-systemic resistance
JA	jasmonate
K	lysine
KCl	potassium chloride
kDa	kilo Dalton
LOX2/3	LIPOXYGENASE 2/3
LPS	lipopolysaccharides
LRR-RLK	Leu-rich repeat receptor-like protein kinase
M	molar (mol/l)
m	milli
MAMP	microbe-associated molecular-pattern
MAPK	mitogen-activated protein kinase
MDS	multi-dimensional scaling
me	methylation
MEA	MEDEA
MED	Mediator
MeJA	methyl jasmonate
MeOH	methanol
MeSA	methyl salicylate
MET1	DNA METHYLTRANSFERASE 1
MgCl <sub>2</sub>	magnesium chloride
min	minute(s)
ml	milliliter
MLL	mixed-lineage leukemia
MOS9	MODIFIER OF SNC1.9
mRNA	messenger RNA
MS	Murashige & Skoog
MSI1-5	MULTICOPY SUPPRESSOR OF IRA 1-5
MSK1	MAP KINASE 4 SUBSTRATE 1
MTI	MAMP-triggered immunity
n	nano
N55	Nucleosome remodelling factor 55
NaCl	sodium chloride
NaF	sodium fluoride
NB-LRR	nucleotide-binding leucine-rich repeat

## Abbreviations

---

nc	non-coding
NDR1	NON-RACE-SPECIFIC DISEASE RESISTANCE 1
NIM1	NON-INDUCIBLE IMMUNITY 1
NIMIN	NIM1-INTERACTING
nm	nanometer
NPR1	NON-EXPRESSER OF PR GENES 1
NPR3	NONEXPRESSER OF PATHOGENESIS-RELATED 3
N-terminal	amino-terminal
OPDA	12-oxophytodienoic acid
p	pico
PAD3	PHYTOALEXIN DEFICIENT 3
PAD4	PHYTOALEXIN DEFICIENT 4
PAGE	polyacrylamide gel-electrophoresis
PAL	PHENYLALANINE AMMONIA LYASE
PBS-T	phosphat buffered saline tween
PCD	programmed cell death
PcG	Polycomb group
PCR	polymerase chain reaction
PEPR	Pep-receptor
Pex	petiole exudates
PGN	peptidoglycans
pH	negative decimal logarithm of H <sup>+</sup> concentration
PIE1	PHOTOPERIOD-INDEPENDENT EARLY FLOWERING 1
Pip	pipecolic acid
PR1	PATHOGENESIS-RELATED 1
PRC	Polycomb Repressive Complex
PRE	Polycomb responsive element
PROPEP	precursor of Pep
PRR	pattern recognition receptor
<i>Psm</i>	<i>Pseudomonas syringae</i> pv. <i>maculicola</i>
<i>Pst</i>	<i>Pseudomonas syringae</i> pv. <i>tomato</i>
pv.	pathovar
p-value	probability value
PVDF	polyvinylidene fluoride
qRT	quantitative real-time
R	resistance
RbBP5	retinoblastoma binding protein 5
RdDM	RNA-directed DNA methylation
REF6	RELATIVE OF EARLY FLOWERING 6
RIN4	RPM1-interacting protein 4
RIPK	RIN4-interacting receptor like kinase
RLK	receptor-like protein kinase
RNA	ribonucleic acid
RNA PolII	RNA Polymerase II
RNA-Seq	RNA sequencing
ROS	reactive oxygen species

---

rpm	rounds per minute
RPM1	RESISTANCE TO P. MACULICULA 1
RPP5	RECOGNITION OF PERONOSPORA PARASITICA 5
RPS2	RESISTANT TO P. SYRINGAE 2
RPS4	RESISTANCE TO P. SYRINGAE 4
RRS1	RESISTANT TO RALSTONIA SOLANACEARUM 1
RSW3	RADIAL SWOLLEN ROOT 3
RT	room temperature
s	second(s)
SA	salicylic acid
SAG101	SENESCENCE ASSOCIATED GENE 101
SAR	systemic acquired resistance
Sbf1	SET binding factor 1
SD	standard deviation
SDG8	SET DOMAIN GROUP 8
SDS	sodium dodecyl sulphate
SE	standard error
Ser/Thr	serine/threonine
Ser5P	serine 5 phosphorylation
SET	Su[ <sup>var</sup> 3-9, Enhancer of Zeste, Trithorax
SID2	SALICYLIC ACID INDUCTION DEFICIENT 2
SNC1	SUPPRESSOR OF npr1-1 CONSITUTIVE 1
SNI1	SUPPRESSOR OF NPR1, INDUCIBLE 1
SOBIR1	SUPRESSOR OF BIR 1
Su(z)	Supressor of Zeste
SWN	SWINGER
SYD	SPLAYED
<i>Taq</i>	<i>Thermophilus aquaticus</i>
T-DNA	transfer DNA
TE	Tris EDTA
TEMED	N,N,N',N'-Tetramethylethylenediamine
TIR	Toll/Interleukin-1 Receptor
TPR1	TOPLESS-RELATED 1
TRE	trithorax responsive element
TRIS	tris-(hydroxymethyl)-aminomethan
Trx	Trithorax
trxG	trithorax group
TTSS	type III secretion system
VRN2	VERNALIZATION 2
vs.	versus
WDR5	WD40 repeat domain 5
WIR	wound-induced resistance
WT	wild type



## Danksagung

An erster Stelle möchte ich Dir Paul danken, dass Du mich in deinem Department beheimatetest und mir die Möglichkeit gegeben hast meine Doktorarbeit hier anfertigen zu können.

Yusuke, thank you very much for all your efforts, time, emails, skype calls and Mochis from Japan. I learned to get stress-tolerant, independent and flexible, which strengthens me a lot during the last three years and during the writing period.

Vielen Dank auch an Herrn Prof. Dr. Flügge für die Übernahme der Zweitkorrektur und an Frau Prof. Dr. Höcker für den Prüfungsvorsitz.

Danke möchte ich auch Dr. Daniel Schubert für die Übernahme des externen Referats.

Danke Dir Franziska für die Übernahme des Schriftführers. Vor allem auch für Deine immer offene Bürotür und Deine tolle Gruppe, die mir bei jeder ChiPingen Frage weitergeholfen hat.

Tausend Dank gilt auch Dir Barbara für die wahnsinnig gute bioinformatische Unterstützung und Analysen! Ohne Dich wären manche Sachen dieser Arbeit nicht möglich gewesen.

A big Thank you also to Misuzu and Kohji in Japan, Nico in Amsterdam and Annegret for all the cheerful hours in- and outside the lab. I enjoyed a lot coming to work every day and I really miss you here!

Thanks also to the Tsuda group, who adopted me as the last Saijo group member for some time. Thank you, Kenichi for your great help with any upcoming question! Your way of loving science is incredibly motivating.

Thanks also to the whole PSL department, my present and former office and neighbor-office people and especially Nina, Florence, Matze, Annegret, Anne, Caro, Misuzu and Nico..... I'm glad to have such nice colleagues and friends!

Ein ganz spezielles Danke geht dabei an Caro und Nina für das Korrekturlesen der Arbeit und Imre für ein immer offenes Ohr und weise Ratschläge! Du hast mir enorm geholfen, Danke!

Danke auch an alle die Menschen, die mich und mein Leben seit Jahren begleiten und tragen. Ein ganz besonderes Danke schön gilt Melle, Sylvi und Franzi für eure Freundschaft, die es auch schafft weite Entfernungen ganz klein werden zu lassen. Ich bin glücklich solch wunderbare Freunde haben zu dürfen!

Ein unermesslich großes DANKE geht auch an meine Familie, die seit 2009 rasant angewachsen ist. Auf einen Schlag bekommt man eine ganze "Sippe" dazu. Ich danke besonders euch beiden, Mutti und Vatti, dass ihr immer an mich geglaubt und mir die Möglichkeit gegeben habt genau den Weg gehen zu können, den ich gehen wollte.. Danke, dass ihr alle immer für mich da seid!

Ein allerletzter Gruß gilt dir, Heiko, meinem besten Freund und seit nunmehr 3 Jahren auch Ehemann: "You raise me up, so I can stand on mountains; You raise me up, to walk on stormy seas; I am strong, when I am on your shoulders; You raise me up to more than I can be".

Das Leben hält noch soviel für uns bereit und ich bin dankbar es mit dir erleben zu dürfen! Ich liebe dich.



## Erklärung

Ich versichere, dass ich die von mir vorgelegte Dissertation selbständig angefertigt, die benutzten Quellen und Hilfsmittel vollständig angegeben und die Stellen der Arbeit – einschließlich Tabellen, Karten und Abbildungen -, die anderen Werken im Wortlaut oder dem Sinn nach entnommen sind, in jedem Einzelfall als Entlehnung kenntlich gemacht habe; dass diese Dissertation noch keiner anderen Fakultät oder Universität zur Prüfung vorgelegt worden ist, sowie, dass ich eine solche Veröffentlichung vor Abschluss des Promotionsverfahrens nicht vornehmen werde.

Die Bestimmungen dieser Promotionsordnung sind mir bekannt. Die von mir vorgelegte Dissertation ist von Prof. Dr. Paul Schulze-Lefert und Dr. Yusuke Saijo betreut worden.

Ich versichere, dass ich alle Angaben wahrheitsgemäß nach bestem Wissen und Gewissen gemacht habe und verpflichte mich, jedmögliche, die obigen Angaben betreffenden Veränderungen, dem Dekanat unverzüglich mitzuteilen

---

Ort, Datum

---

Unterschrift